Designed analogues of the aplyronines for use in antibody–drug conjugates

A thesis submitted for the degree of Doctor of Philosophy
at the University of Cambridge

Rachel Jayne Porter

Jesus College

Department of Chemistry

July 2019

Declaration

This dissertation is the result of my own work and includes nothing which is the outcome of work done in collaboration except as declared in the Preface and specified in the text.

It is not substantially the same as any that I have submitted, or, is being concurrently submitted for a degree or diploma or other qualification at the University of Cambridge or any other University or similar institution except as declared in the Preface and specified in the text. I further state that no substantial part of my dissertation has already been submitted, or, is being concurrently submitted for any such degree, diploma or other qualification at the University of Cambridge or any other University or similar institution except as declared in the Preface and specified in the text.

In accordance with the Board of Graduate studies guidelines, this document does not exceed 60,000 words.

Rachel Jayne Porter

July 2019

For Mum and Dad

Acknowledgements

This dissertation would not have been possible without the help, support and guidance of many important people in my life and I would like to extend my sincere thanks to all of them.

Above all, I am deeply grateful to Professor Ian Paterson for welcoming me into his group at Cambridge and giving me the opportunity to embark on a PhD within natural product synthesis. His guidance and unfailing support over the past four years has truly been invaluable. I must also extend my heartfelt thanks to Professor David Spring and Professor Jonathan Goodman for all their help and encouragement.

Lab 122 has been an irreplaceable part of my time at Cambridge and it has been a pleasure to work alongside such talented and inspirational people who I am delighted to call close friends. I am grateful to the NMR users, Simon Williams, Andrew Phillips, Bing Yuan Han, Talia Pettigrew and Nelson Lam and for all members of Team Aplyronine and Team ADC. Special thanks must go to Talia Pettigrew, my fume hood neighbour and constant companion on the aplyrologue project, for her friendship and exceptional proofreading of this document.

Nic Davies, Naomi Hobbs and Carlos Davies have provided outstanding technical support to always keep the lab running smoothly.

I am deeply indebted to Jeremy Parker at AstraZeneca as an industrial supervisor. From organising my placement in Macclesfield to guidance on the project, his advice and support has been invaluable. In addition, I am thankful to the EPSRC and AstraZeneca for providing generous financial support. For sparking my interest in organic chemistry and supporting my application to Cambridge I am extremely grateful to Dr Jonathan Burton and Dr Edward Anderson at Oxford, without whom I would not be where I am today.

A sincere thanks to my dear friend Nelson Lam who I have had the pleasure of sharing my PhD adventure with over the past four years. Thank you for keeping me going through the tough times and for always putting a smile on my face.

Thank you to Mum and Dad for your endless support, love and guidance in everything I do, I am eternally grateful for it all. Finally, to Harry, my best friend. Words cannot do justice to all that you do for me. Thank you for always believing in me and for your unwavering support, I could not have done this without you.

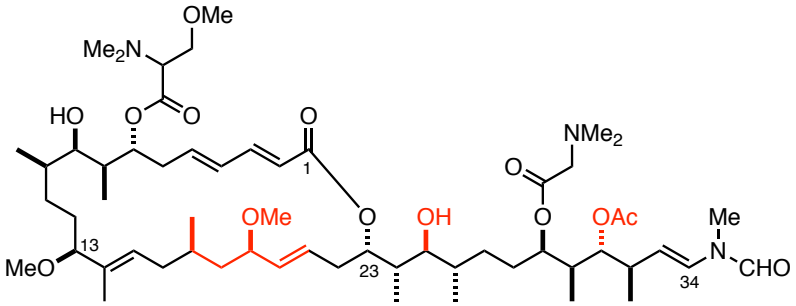

Aplyronine D

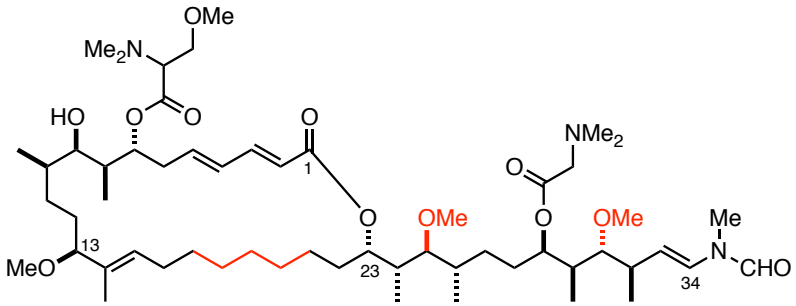

Aplyronine D analogue

Designed analogues of the aplyronines for use in antibody – drug conjugates

Rachel Jayne Porter

Summary

The aplyronines are a family of structurally complex marine macrolides, isolated from the sea hare *Aplysia kurodai,* that exhibit picomolar growth inhibitory activity in the NCI 60 cell line panel. An unprecedented heterotrimeric complex has been observed to form between aplyronine A and actin and tubulin together, resulting in disruption of cytoskeletal dynamics and subsequent cell death. This novel mode of action, coupled with their exquisite biological activity, renders the aplyronines compelling candidates for incorporation as payloads into antibody–drug conjugates provided the supply problem can be solved.

Guided by structure-activity relationship (SAR) studies, a highly convergent route towards novel and simplified aplyronine structures has been designed. Routes to these function-oriented analogues should be more streamlined and efficient due to judicious structural editing, whilst functionality and potency are retained.

Chapter 1 introduces marine natural products and illustrates their therapeutic potential alongside the challenges associated with these highly complex structures. The aplyronine family of natural products is introduced and a function-oriented approach towards analogue design is presented. The avenue of targeted therapies is discussed, with particular focus on the field of antibody–drug conjugates.

Chapter 2 outlines the synthesis of our key simplified fragments. Significant optimisation efforts towards the synthesis of the side chain ketone are discussed, together with the synthesis of the northern fragment. Chapter 3 outlines two complementary fragment coupling strategies to access our designed analogues. Contrasting to the established sequence, an alternate approach is examined in which the southern and side chain fragments are first connected before the northern piece is appended. The strengths and shortcomings of each route are reviewed.

Chapter 4 culminates in endgame manipulations to generate a range of simplified analogues and details their initial biological evaluation. Preliminary investigations into linker strategies using a quaternary amine approach are investigated. Chapter 5 summarises this work and presents suggestions for future directions of this research for the purpose of developing antibody–drug conjugates.

Contents

Nomenclature

Metal enolate stereochemistry

According to accepted convention, the two metal enolates **A** and **B** will be referred to as (*E*)- and (*Z*)-enolates respectively (**Figure 1**). The metal–oxygen substituent is considered to have higher priority than the R_1 substituent in all cases.

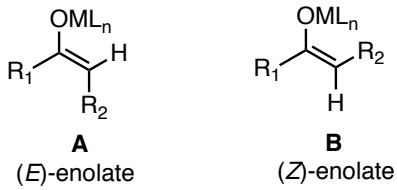

Figure 1 (*E*)- and (*Z*)-enolate naming convention

Syn- and *anti*-diastereoisomers

The *syn*- and *anti*-convention introduced by Masamune for assigning the relative stereochemistry of vicinal stereocentres is used in this dissertation.[1] A *syn*-relationship is defined by two substituents (R_1 and R_2) pointing in the same direction relative to the plane, defined by the main chain drawn in a zigzag confirmation, as shown in **Figure 2**. Conversely, an *anti*-relationship is defined by the two substituents occurring on opposite sides of the plane. Thus, the two diastereoisomers **C** and **D** are referred to as *syn*- and *anti*- respectively.

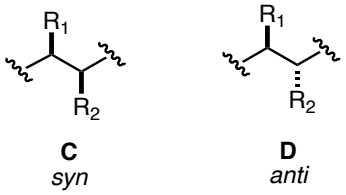

Figure 2 *Syn*- and *anti*-diastereoisomers

Aldol adduct stereochemistry

In aldol reactions where an α-chiral ketone directs the stereochemical outcome, the aldol adduct is referred to as shown in **Figure 3**. Here, the pre-existing ketone α-stereocentre is labelled as "1". This convention recognises the origin of the stereochemistry whilst also defining the relative stereochemistry between the substituents.

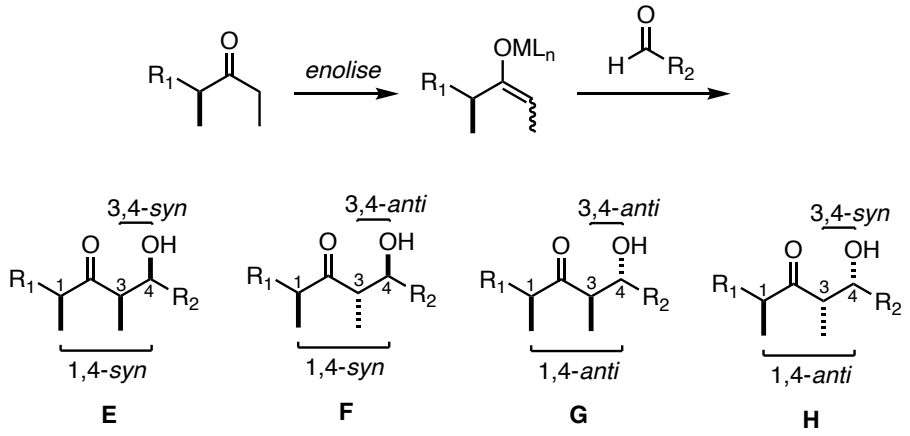

Figure 3 Aldol adduct stereochemistry

Compound numbering

The naming and numbering of compounds is in accordance with the priorities set out by IUPAC. The numbering system for aplyronine analogues and intermediates follows that of Yamada and co-workers in their original publication detailing the isolation and characterisation of the aplyronines.[2] It is used in the assignments of ^{1}H NMR spectra and is illustrated in **Figure 4**.

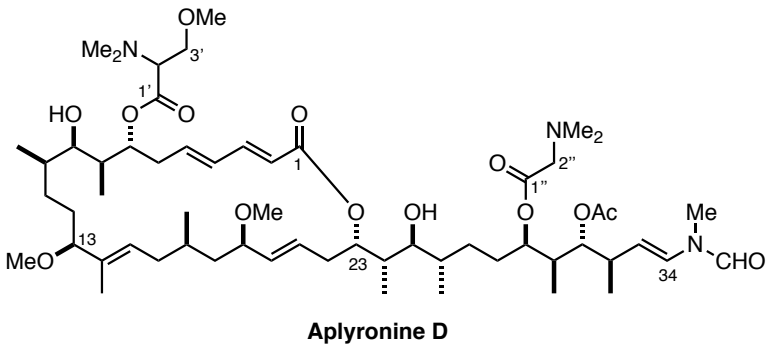

Figure 4 Compound numbering for the aplyronines

Abbreviations

$[\alpha]_D$	specific rotation
Ac	acetyl
ADC	antibody–drug conjugate
ADP	adenosine diphosphate
Alloc	alloxycarbonyl
ApA, ApB *etc*	aplyronine A, B *etc*
app	apparent
aq.	aqueous
Ar	aryl
ATP	adenosine triphosphate
Bn	benzyl
Boc	*tert*-butoxycarbonyl
bp	boiling point
br	broad
brsm	based on recovered starting material
n-Bu	*n*-butyl
Bz	benzoyl
c	concentration
ca.	circa
calc.	calculated
cat.	catalytic
CBS	Corey–Bakshi–Shibata
cm^{-1}	wavenumber(s)
COSY	^1H–^1H correlation spectroscopy
CSA	10-camphorsulfonic acid
Cy	cyclohexyl
cymene	4-isopropyltoluene
d	doublet
δ	chemical shift
DAR	drug–antibody ratio
DCC	*N*,*N'*-dicyclohexylcarbodiimide
DDQ	2,3-dichloro-5,6-dicyano-1,4-benzoquinone
DEAD	diethyl azodicarboxylate
DFT	density functional theory

DIAD	diisopropyl azodicarboxylate
DIBAL	diisobutylaluminium hydride
DMAla	*N*,*N*-dimethylalanine
DMAP	*N*,*N*-dimethylaminopyridine
DME	1,2-dimethoxyethane
DMF	*N*,*N*-dimethylformamide
DMGly	*N*,*N*-dimethylglycine
DMP	Dess−Martin periodinane
DMSer	*N*,*O*-dimethylserine
DMSO	dimethylsulfoxide
DPEN	diphenylethylenediamine
dr	diastereomeric ratio
ee	enantiomeric excess
ent	enantiomer
epi	epimer
eqv.	equivalent(s)
ESI	electrospray ionisation-method
Et	ethyl
EtOAc	ethyl acetate
FDA	Food and Drug Administration
Fmoc	fluorenylmethyloxycarbonyl
h	hour(s)
HeLa	human cervical adenocarcinoma cell line
HMBC	Heteronuclear multiple-bond correlation spectroscopy
HMDS	hexamethyldisilazane
HMPA	hexamethylphosphoramide
HPLC	high performance liquid chromatography
HRMS	high resolution mass spectrometry
HTS	high throughput screening
HWE	Horner−Wadsworth−Emmons
Hz	hertz
i-	*iso*-
i.p.	intraperitoneal
IC_{50}	half maximal inhibitory concentration
IgG	human immunoglobulin G
imid.	imidazole
IPA	isopropyl alcohol
IR	infrared

J	coupling constant
K_d	dissociation constant
L	ligand
LiHMDS	lithium hexamethyldisilazane
LLS	longest linear sequence
2,6-lut	2,6-lutidine
M	molar
m	multiplet
m-CPBA	*meta*-chloroperoxybenzoic acid
MHz	megahertz
mAB	monoclonal antibody
Me	methyl
min	minute(s)
mmol	millimole(s)
mol	mole(s)
m.p.	melting point
MS	mass spectrometry
Ms	methanesulfonyl (mesyl)
MTBE	methyl *tert*-butyl ether
MTPA	methoxy(trifluoromethyl)phenyl acetic acid
m/z	mass-to-charge ratio
n-	normal
n.d.	not determined
NCI	National Cancer Institute
NCS	*N*-chlorosuccinimide
NHK	Nozaki–Hiyama–Kishi
NMR	nuclear magnetic resonance
nOe	nuclear Overhauser effect
obs	obscured
PG	unspecified protecting group
PAB	*para*-aminobenzyl
PABC	*para*-aminobenzyl carbamate
PABQ	*para*-aminobenzyl quaternary ammonium
PE	petroleum ether, boiling point 40–60 °C
PEG	polyethyleneglycol
Ph	phenyl
PMB	*para*-methoxybenzyl
PMP	*para*-methoxyphenyl

ppm	parts per million
PPTS	pyridinium *para*-toluenesulfonate
Pr	propyl
py	pyridine
q	quartet
quint	quintet
R	unspecified substituent
R_f	retention factor
rt	room temperature
s	singlet
SAR	structure–activity relationship
sat.	saturated
SD	subdomain
SET	single electron transfer
SPR	surface plasmon resonance
t-	*tertiary*-
t	triplet
TAMRA	tetramethylrhodamine
TBAF	tetrabutylammonium fluoride
TBAI	tetrabutylammonium iodide
TBDPS	*tert*-butyldiphenylsilyl
TBS	*tert*-butyldimethylsilyl
TCA	2,2,2-trichloroacetimidate
TCBC	2,4,6-trichlorobenzoyl chloride
TES	triethylsilyl
Tf	trifluoromethanesulfonyl
THF	tetrahydrofuran
TIPS	triisopropylsilyl
TLC	thin layer chromatography
TMS	trimethylsilyl
TMSer	*N*,*N*,*O*-trimethylserine
TS	transition state
Ts	*para*-toluenesulfonyl
UV	ultraviolet

Chapter 1

Introduction

1.1 Bioactive natural products throughout history

Nature represents a vast, fertile source of structurally diverse biologically active compounds and offers inspiration for the development of novel therapeutic agents. Arising from secondary metabolite pathways, many natural products exhibit extremely high potencies and selectivities to ensure survival in extreme habitats and offer defence mechanisms against potential predators. Natural products, especially those from terrestrial origins, have historically been a source of drug molecules, with plants in particular forming the basis of these traditional medicines.[3,4]

The use of plant-based drugs, rich in bioactive natural products, has been well described throughout history in the form of oils, infusions, potions and remedies for the treatment of a range of diseases. Clay tablets from Mesopotamia (2600 B.C.) documented oils from *Cupressus sempervirens* (cypress) and *Commiphora* species (myrrh) for the treatment of coughs, colds and inflammation, which are still in use today. This is believed to depict the earliest record of natural products as therapeutic agents.[5] Several well-known milestones in drug discovery from natural products followed, including the isolation of morphine from *Papaver somniferum* (opium poppy) and the anti-inflammatory acetylsalicyclic acid (aspirin) from the bark of the willow tree *Salix alba* in the 1800s.[6,7] Their structural diversity and biological activity render natural products the most valuable source of new drugs and drug leads. In fact, over the last twenty years, more than one third of all FDA-approved therapeutic agents were derived from or inspired by natural products with more

than 50% of small molecule drugs originating from natural products and their mimics, during 1981 to 2014.[8]

1.1.1 Marine natural products

Despite covering more than 70% of the surface of the earth, the world's oceans remain a vastly underexplored resource. The flora and fauna within the marine environment are a rich and valuable source of biodiversity. Advancements in underwater exploration technology, enabling the improved collection of marine organisms and isolation of their metabolites, have fuelled the discovery of thousands of bioactive marine natural products.[8,9] The ocean is a biologically challenging environment, with many sedentary marine organisms (*e.g.* sponges) relying on chemical means of defence against predation and competition. To counteract dilution effects from the sea, these marine metabolites have evolved into exceptionally potent cytotoxic agents. Many of these compounds appear to show superior molecular diversity compared to their terrestrial counterparts and belong to completely novel chemical classes.[10]

Prized sources of natural products from the marine environment include algae, sponges, corals and molluscs. Algae alone account for a vast array of structurally diverse natural products, with over 30,000 algal species worldwide.[11] In particular, red algae are an unrivalled source of chemically unique halogenated sesquiterpenes and have been investigated since 1970.[12–14] Comprising approximately 60% of all marine animals, marine invertebrates are another highly valued source with over 11,000 novel natural product structures discovered between 1990 and 2014.[15,16] Finally, microorganisms such as marine cyanobacteria, fungi and bacteria have received increased attention as a fertile sources of bioactive metabolites, with many natural products originally isolated from marine macroorganisms having now been attributed to metabolic products of symbiotic microorganisms.[17–19]

Whilst exhibiting unique architectural complexity, many marine natural products also display novel modes of action in biochemical systems. These molecules have become validated starting points for the targeted development of drug-like molecules for the treatment of human diseases, especially in the field of cancer therapy.[20,21] Common strategies for the treatment of cancer involve the interference and disruption of cellular processes such as signal transduction, microtubule assembly and DNA interactions, ultimately leading to apoptosis of the proliferating cancer cells.[22]

The first FDA-approved marine derived anticancer drug was cytarabine (**1**) (**Figure 5**) in 1969. From the Caribbean sponge *Cryptotheca crypa*, Bergmann isolated and identified the nucleosides spongouridine (**2**) and spongothymidine (**3**).[23] These antiviral compounds guided the development of an analogue (Ara-C, **1**) as a clinical anticancer agent for the treatment of leukemia.[23]

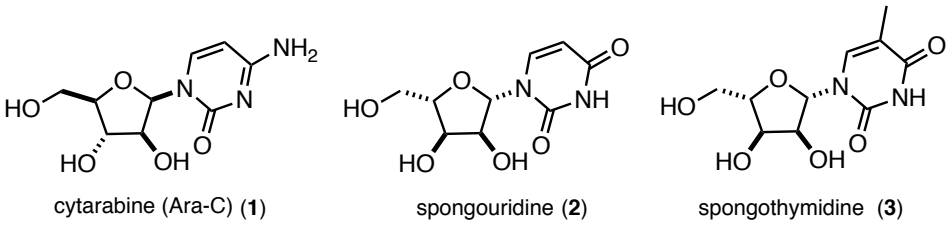

Figure 5 Structure of cytarabine (**1**) and related nucleosides

Today, several other notable anticancer drugs derived from marine origins are on the market (**Figure 6**), with many more undergoing clinical trials. Trabectedin (**4**, Yondelis®) is an anti-neoplastic marine alkaloid which was approved for the treatment of advanced soft tissue sarcoma in 2007. In 2010, the microtubule targeting agent eribulin mesylate (**5**, Halaven®) was approved for clinical use for the treatment of metastatic breast cancer.

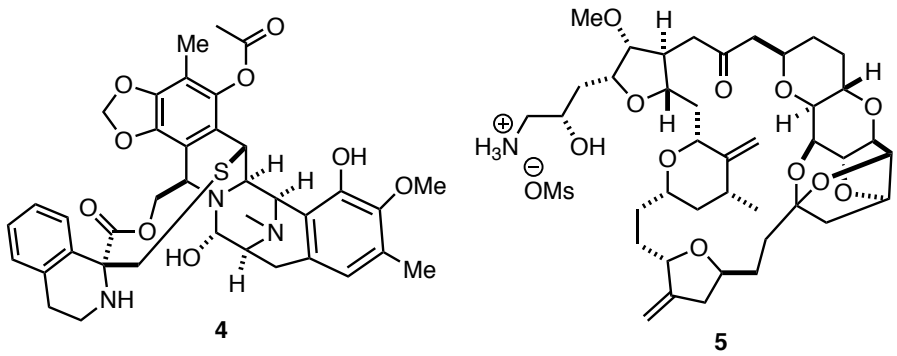

Figure 6 'Drugs from the sea', trabectedin (**4**) and eribulin mesylate (**5**)

A major obstacle in the evaluation and development of a natural product through to a viable drug candidate is the sustainable supply of highly precious material. The synthesis of these intricate structures is demanding and uncompromising, thus offering a tantalising challenge to the synthetic organic chemist. Consequently, elegant yet highly selective and stereocontrolled routes to these metabolites are required.[24,25]

Accessing multigram quantities of complex material exclusively through synthesis has been exemplified through the combined Novartis–Smith–Paterson synthesis of the anticancer agent discodermolide (**6, Figure 7**) on a 60 g scale.[26–30] This remarkable sequence illustrates the power of contemporary organic synthesis and the link between total synthesis in academia to the process chemistry field. Despite this synthetic success, Phase I clinical trials were halted due to issues with off-target toxicity and clinical development was ultimately discontinued, an all too common outcome in the case of highly cytotoxic natural product based therapeutics.[31]

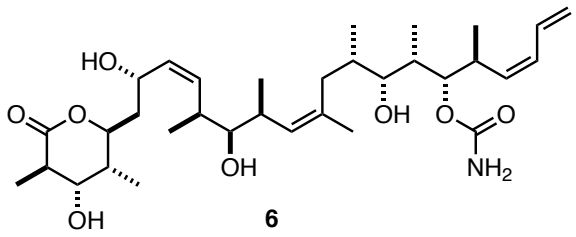

6

Figure 7 Marine natural product discodermolide (**6**)

1.1.2 Synthetic analogues of natural products

Total synthesis offers the opportunity to develop novel, simplified analogues or hybrids of natural products, with the anticipation of enhancing or maintaining biological activity, whilst greatly simplifying the synthesis. This tailored approach circumvents the low chemical tractability displayed by natural products as lead structures in drug development. These refined structures have also yielded crucial information on modes of action and biological activities.[32]

This "function-oriented" strategy[33] focusses on function by design with an emphasis on synthetic economy, and has been applied to numerous natural products.[34–36] In particular, the development of bryostatin 1 (**7**) analogues or "bryologs" by Wender and co-workers resulted in the generation of a range of simplified and clinically superior analogues (**Figure 8**).[37–39] In addition, fragment-oriented synthesis has been applied to the anticancer natural product families the migrastatins (**8**) and anguinomycins (**9**, **Figure 8**).[40,41] The potent biological activities of the natural products are retained in these structurally simplified analogues (as deemed by the reduction in molecular weight, MW), whilst the synthetic effort required is greatly reduced by the elimination of a number of non-essential stereocentres and functionalities.

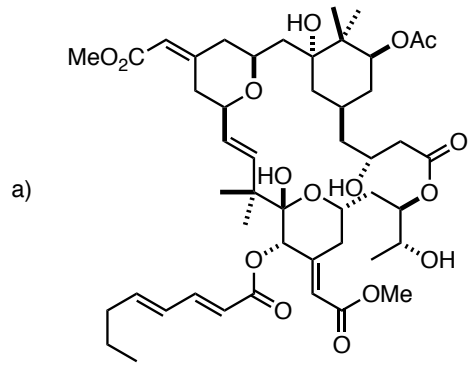

bryostatin 1 (**7**)
PKC K_i = 1.35 nM
~ 40–89 steps

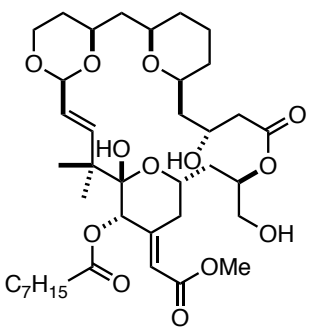

bryostatin 1 analogue (**10**)
PKC K_i = 0.25 nM
19 steps LLS
20% reduction in MW

a)

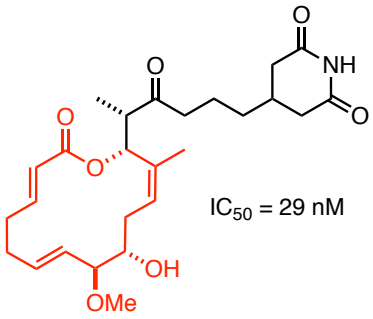

IC_{50} = 29 nM

Migrastatin (**8**)

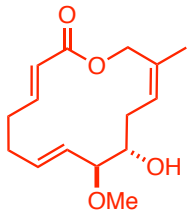

IC_{50} = 22 nM
43% reduction in MW
Saves 9 steps

Migrastatin core anaolgue (**11**)

b)

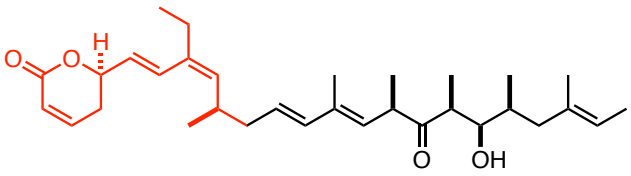

Anguinomycin D (**9**)

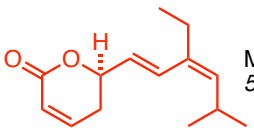

Maintains bioactivity
56% reduction in MW

Anguinomycin D analogue (**12**)

c)

Figure 8 Function-oriented synthesis of simplified analogues: a) bryostatin 1 (**7**) and "bryolog" (**10**) (PKC = protein kinase C); b) Migrastatin (**8**) and the core analogue (**11**) (IC_{50} values are for 4T1 murine breast cancer); c) Anguinomycin D (**9**) and analogue (**12**)

Perhaps the most notable example of truncating a highly complex natural product is represented by the anticancer drug eribulin mesylate (**5**), a simplified analogue of the marine natural product halichondrin B (**13**, **Figure 9)**. Scarce supply from the marine source necessitated formidable synthetic efforts and the first total synthesis of halichondrin B was reported by Kishi in 1992 in over 90 steps.[42] Biological testing on numerous intermediates and analogues from the synthesis revealed its activity hinged upon the macrocyclic lactone moiety alone.[43] This resulted in the development of a scalable 37-step industrial synthesis by Eisai of the structurally simpler analogue eribulin (**5**), which was approved in 2010 by the FDA.[44]

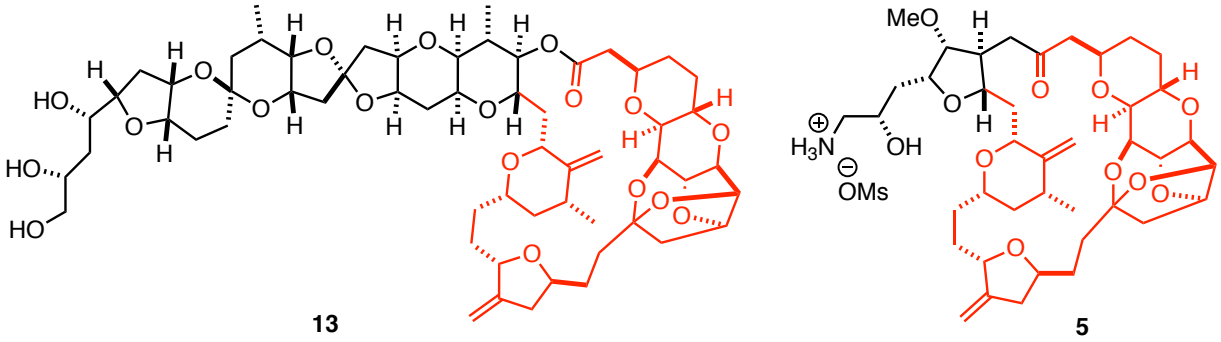

Figure 9 Halichondrin B (**13**) and its simplified analogue eribulin mesylate (**5**)

Overall, eribulin (**5**) represents a vast simplification in structure through the exclusion of the seven polyether rings, remarkably resulting in halving the number of synthetic steps, whilst conserving the potent anticancer activity exhibited by the parent compound.

1.2 Targeted cancer therapy

Traditional chemotherapeutic drugs primarily target and inhibit cell division. However, these cytotoxic agents affect not only proliferating cancer cells, but other rapidly dividing healthy cells and tissues. This off-target toxicity, stemming from a lack of specificity, results in many unpleasant and dangerous side effects such as hair loss, nausea and myeloid suppression.[45] The inherent toxicities of potent natural products at doses required for efficacy results in a narrow therapeutic index and limits their progress towards clinical use. Increasing potency, thereby decreasing the minimum effective dose, alongside improving the selectivity for neoplastic cells, can lead to a larger therapeutic window (**Figure 10**).[46]

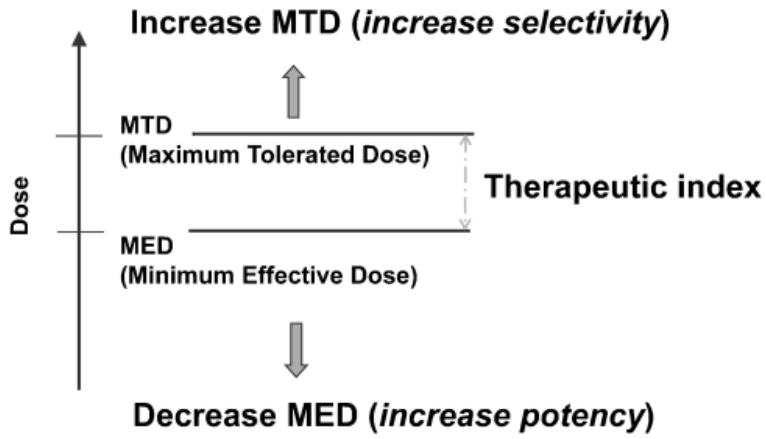

Figure 10 Maximising the therapeutic window of drugs [46]

More than one hundred years ago, Paul Ehrlich first articulated the notion of combining a toxic entity together with specific binding to a diseased cell or organism within a single molecule and coined the term "magic bullets" to describe molecules such as these. Targeted medicine which sets the goal of aiming precisely with highly potent drugs dominates contemporary drug discovery. Indeed, it could be said that the development of personalised and tailored drugs is the ultimate goal within modern oncology research.

The development of "magic bullet" therapeutics that selectively deliver cytotoxic agents to the tumour site has greatly progressed over the last few decades.[47,48] These revolutionary medicines aim to inhibit essential biochemical targets and molecular pathways that are critical for the growth and maintenance of cancer cells.[49] Targeting mutant kinases with small molecule tyrosine kinase inhibitors has seen success through the approval of Imatinib (**14**, **Figure 11**) for the treatment of chronic myeloid leukaemia by Novartis in 2001.[50]

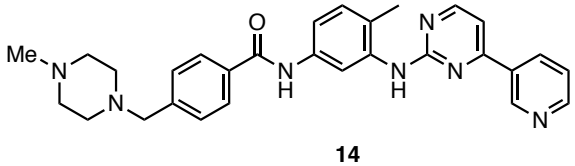

14

Figure 11 Imatinib (**14**), a small molecule tyrosine kinase inhibitor

Other approaches involve conjugated species consisting of cytotoxic effectors that are linked to small molecules, such as folic acid, that selectively bind to receptors on the surface of tumours.[51]

Monoclonal antibodies, which can specifically recognise antigens on the surface of cancer cells, offer another avenue for targeted therapy. In particular, antibody–drug conjugates (ADCs) have emerged as promising and clinically validated leads for the treatment of cancer.[52]

1.3 Antibody–drug conjugates

Antibodies, or immunoglobins, are large Y-shaped proteins produced by plasma cells and are utilised within the immune system to identify and neutralise pathogens such as bacteria and viruses. The antibody specifically recognises a unique antigen expressed on the surface of the pathogen and binds to it through non-covalent interactions. By exploiting their specific binding properties, monoclonal antibodies can act as a mechanism for the selective delivery of cytotoxic agents to cancer cells. This new frontier in cancer therapy has grown rapidly, with four commercial ADCs on the market and more than sixty under investigation in clinical trials.[53–57]

Antibody–drug conjugates consist of a cytotoxic drug (often referred to as the payload or warhead) linked to a monoclonal antibody, as illustrated in **Figure 12**. This linkage should mask the cytotoxicity of the drug during transport but effectively release it when the conjugate reaches its intended antigen binding target. These three components together give rise to a powerful therapeutic agent guided by the exquisitely selective antibody, capable of delivering traditionally intolerable cytotoxic drugs directly to cancer cells.

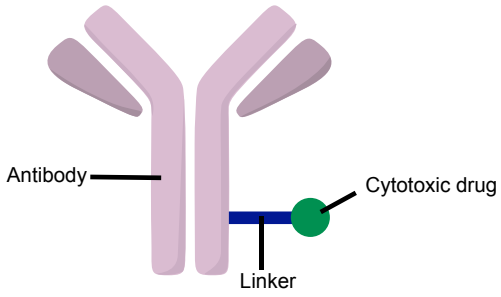

Figure 12 Generalised structure of an antibody–drug conjugate

Once bound, the conjugate is then internalised into the cell *via* endocytosis and undergoes chemical or enzymatic cleavage to release the therapeutic agent. The drug then enters the cytosol and reaches its cellular target, eventually resulting in apoptosis (**Figure 13**). Additionally, if the cytotoxic agent is released into the extracellular tumour environment before internalisation, there is potential for neighbouring cancer cells to be killed in a

process known as the "bystander effect". This effect could be significant in solid tumours where ADC penetration may be limited, or if the target antigen is expressed heterogeneously.[58]

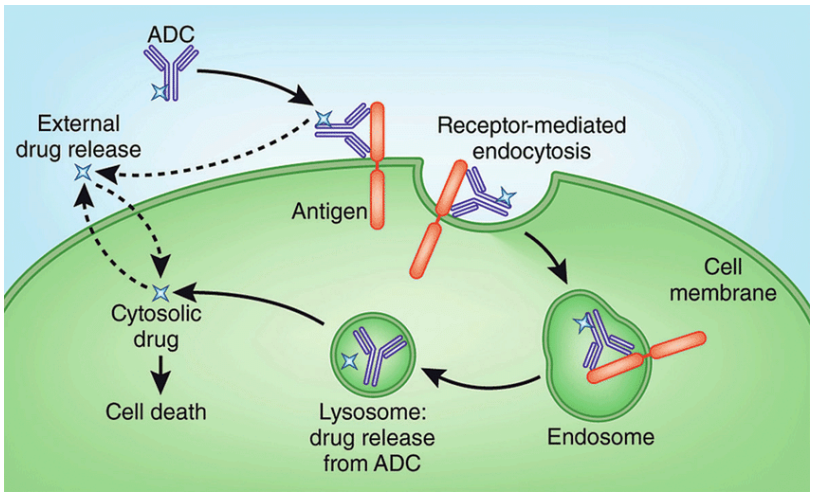

Figure 13 Mechanism of action of an ADC [59]

The use of antibody–drug conjugates brings with it many advantages due to the large contact surface area relative to small molecules. Humanised antibodies display long half-lives of up to three weeks in circulation and therefore are practical for clinical use.[46] The high affinity in antibody–antigen interactions should result in the accumulation of the antibody at the tumour site, avoiding delivery to healthy tissues. Wastage of the precious cytotoxic agent is also reduced through decreased metabolism and excretion. Highly potent warheads are required, meaning previously rejected natural products that displayed off-target toxicity can now be reconsidered. Antibody–drug conjugates can therefore offer a viable and prolonged treatment option in cancer therapy. However, numerous challenges remain in the design and production of these new modalities.

1.3.1 The antibody

The antibody must selectively bind to target antigens that are solely or overexpressed on the surface of tumour cells to convey the highest degree of targeted delivery.[60] This is achieved by capitalising on accessible tumour-associated markers and proteins which are abundantly expressed at the site of the disease in a homogeneous fashion but have little expression in normal cells. Alongside specificity for a target, the antibody should have sufficient binding affinity for retention and accumulation at the tumour site. However,

antibodies with extremely high antigen affinity can result in reduced efficiency for tumour penetration.[61–63] Thus, an ADC with high antigen affinity does not necessarily translate to a treatment with high clinical efficacy.

First generation ADCs made use of murine or chimeric antibody sequences, which elicited an immunological response to the foreign proteins and resulted in rapid clearing of the murine antibody from circulation.[46,64] This problem has since been overcome in current ADCs with the incorporation and development of fully human antibodies.[65]

1.3.2 The linker

The choice and design of linkers for immunoconjugates is paramount. The linker must remain stable in circulation, avoiding uncontrolled leakage of the precious cytotoxic agent, yet precisely release the drug upon delivery to the cell. Consequently, the linker can play a profound role in defining the selectivity, pharmacokinetics, therapeutic window and even the overall success of the ADC. There are two main types of linkers currently in use: cleavable and non-cleavable linkers.

Cleavable linkers contain labile functional groups that are easily broken down in the cell, such as hydrazones or disulfide and amide bonds (**Figure 14**). This process relies on the differences between the intracellular and plasma environments, such as acidic pH ranges and reduction potentials. However, these linkers have been observed to slowly release the drug into plasma, leading to systemic toxicity. A further cleavable linker strategy is to rely on intracellular proteases or esterases found in the lysosome to elicit hydrolytic enzymatic cleavage of peptide amide or ester bonds, typically used in combination with a self-immolating spacer unit. The dipeptide valine-citrulline (Val-Cit) motif is an example of this and undergoes specific cleavage upon exposure to the lysosomal protease cathepsin B.[66]

In most cases, these linkers are designed to release the parental toxin in a chemically unmodified, fully active form. This traceless approach is the main advantage of cleavable linkers and the cytotoxic potency of the conjugated payload can thus be estimated from the known pharmacological parameters of the free payload.

Conversely, non-cleavable linkers rely upon complete proteolytic degradation of the antibody component of the ADC within the lysosome. This liberates a modified payload containing the amino acid residue derived from the antibody, typically a cysteine or lysine motif. With these linkers, any differences in activity between parent drug and potential

ADC metabolites must therefore be considered. Structurally, these linkers are typically alkyl or polyethyleneglycol (PEG) chains terminally appended with functionality to facilitate conjugation to the toxin and antibody. Non-cleavable linkers therefore confer the advantage of enhanced plasma stability and thus avoid non-specific release of the drug. This stability, however, limits the propensity for bystander killing of neighbouring cells.

The linker is an integral structural aspect in designing a successful ADC therapeutic and current work in the field is largely focused on developing more sophisticated linker technologies for more effective and better tolerated ADCs.[66]

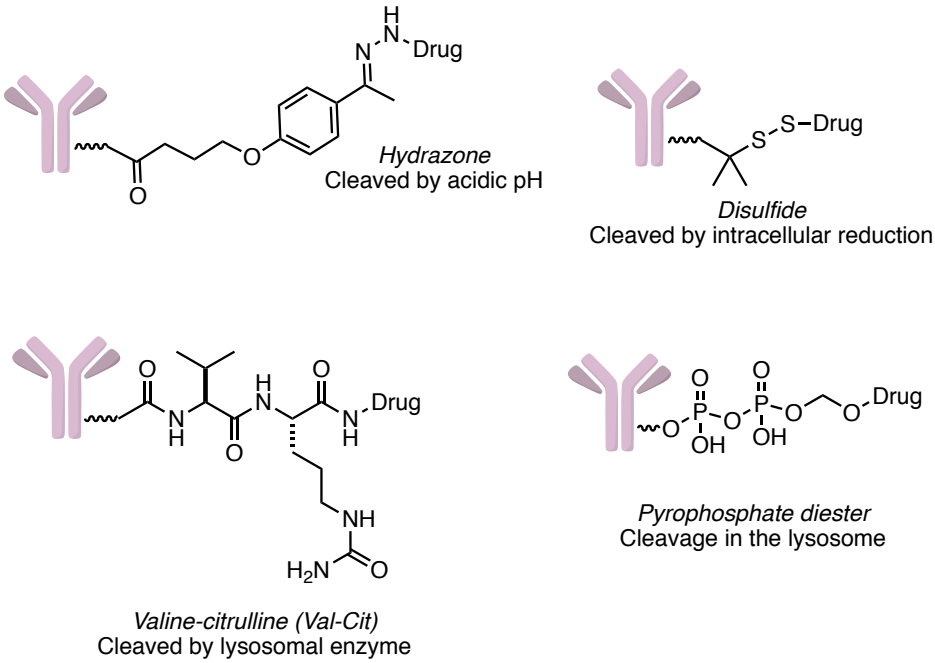

Figure 14 Cleavable linker strategies used in ADCs

1.3.3 Conjugation methods

One of the main difficulties associated with antibody–drug conjugates is achieving homogeneity through conjugation methods. Zero to eight drug molecules can typically be conjugated to an antibody and heterogeneous mixtures of species with varying drug to antibody ratios (DAR) have usually been produced.[67] Controlling the number and position of drug molecules attached to an antibody has important consequences for its pharmacokinetics. Unconjugated or poorly conjugated (*e.g.* with the payload localised in antigen binding sites) species can offset the benefit of drug-loaded ones, resulting in diminished activity. In addition, there is some evidence to suggest that a larger DAR leads to higher clearance rates from the system.[68] There is increased interest in overcoming

heterogeneity by utilising site specific conjugation through techniques such as bioorthogonal chemistry and protein engineering.[69] Conjugation can occur through native nucleophilic residues on the antibody scaffold or non-native functionality introduced through genetic engineering. In either case, these chemically reactive sites on the antibody surface must be utilised without impacting on the biophysical integrity of the antibody framework.[70,71]

Conventionally, the naturally occurring reactive lysine and cysteine residues on the antibody have been used as conjugation sites through acylation and alkylation reactions. These are an attractive option due to the ease of reactivity without any processing or modification of the antibody required. Most ADCs are built on immunoglobin scaffolds (IgG) possessing over 80 lysine residues, 20 of which are found at highly solvent accessible sites, resulting in products with greatly variable DARs. This non-specific conjugation results in heterogeneous mixtures that can be prone to aggregation.[72] Conversely, cysteine residues within an antibody exist as disulfide pairs and are more uniformly distributed with 4 inter-chain disulfides and 12 intra-chain pairs. Selective reduction of the inter-chain disulfides produces eight possible sites for bioconjugation, again leading to a mixture of products (**Figure 15**).

Modern advancements in genetic engineering have enabled site-selective antibody modification through artificially engineered cysteine residues on the antibody surface, *e.g*. Genentech's THIOMAB technology. Further methods of site specific linkage to produce ADCs with precise DAR include engineering to introduce unnatural amino acid residues for orthogonal bioconjugation, *e.g*. azide click chemistry.[73–75]

Cysteine conjugation takes advantage of fast Michael addition reactions with maleimides, resulting in succinimide thioethers. A major problem with this approach is the tendency of thiosuccinimide linkages to undergo a retro-Michael reaction, thereby resulting in non-specific deconjugation. However, it has been reported that hydrolysis of the thiosuccinimide ring can prevent this elimination from occurring, circumventing the loss of drug–linker unit from the ADC.[76] As disulfide bonds are an integral structural element of the antibody scaffold, techniques involving developing re-bridging linkers have evolved for ADC production. The idea is simple: a bis-reactive drug–linker moiety undergoes reaction with both thiol residues produced from disulfide cleavage, leading to covalent re-bridging of the protein in tandem with drug attachment (**Figure 16**).[77,78] Ultimately, the combination of conjugation and linker chemistry must be customised to the antibody, the cytotoxic molecule and the profile of the disease to be treated in order to create an effective ADC.

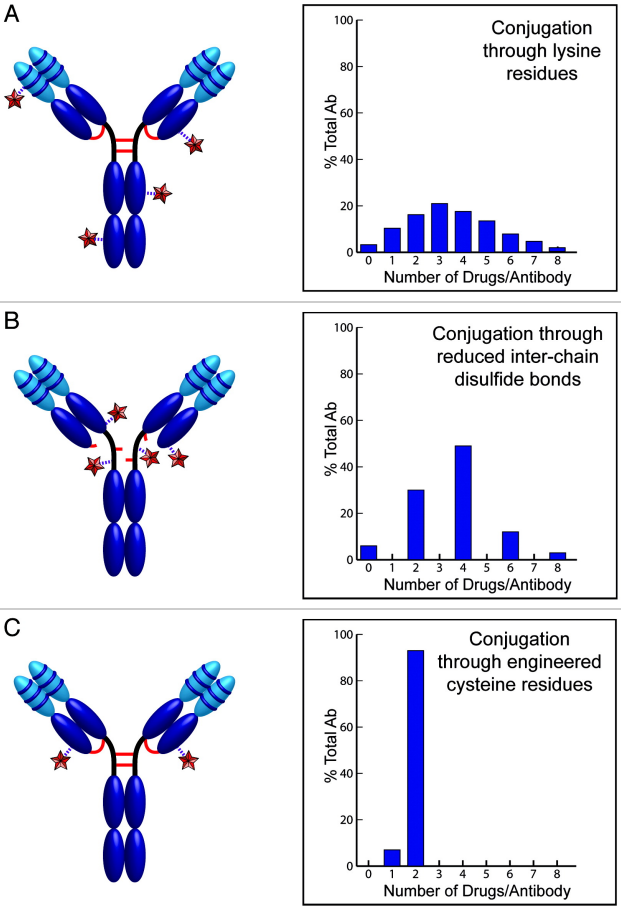

Figure 15 Antibody conjugation using native amino acid residues; A) lysine conjugation, B) cysteine conjugation from reduced disulfides, C) cysteine conjugation through engineered residues [72]

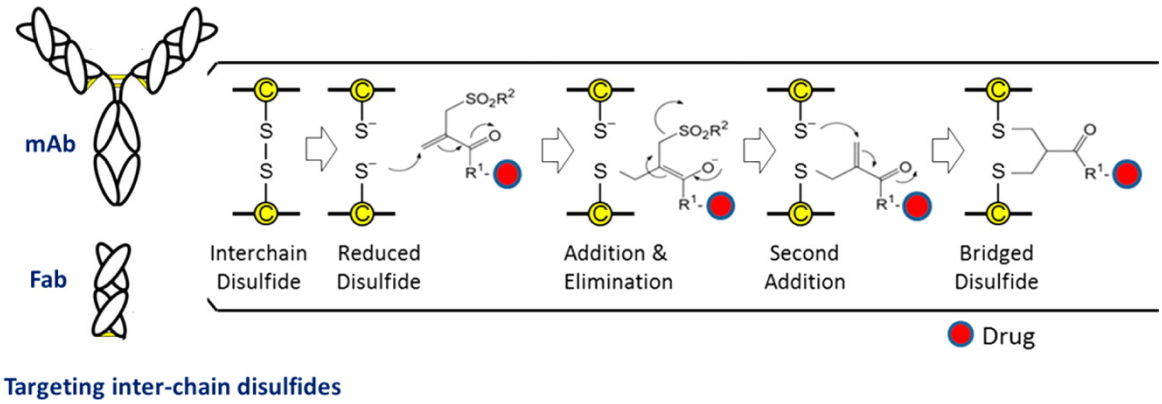

Figure 16 Conjugation of a payload to a disulfide bridge [78]

1.3.4 The payload

The core requirement for the payload is cytotoxicity. For an ADC to be therapeutically active, the number of drug molecules required to kill the cell should be well below the delivery threshold of the antibody. Combined with limited delivery of the cytotoxin caused by poor internalisation of the conjugate or inefficient payload release, the potency commanded is that of the sub-nanomolar range. Indeed, it has been reported that very few drug molecules actually reach the cell with studies suggesting only 0.01–0.1% per injected dose per gram of tumour mass is internalised.[79]

The drug has to be amenable to selective functionalisation and attachment to the linker under physiologically compatible conditions. These non-trivial modifications should not negatively affect the potency of the parent drug. The conjugate should also be stable and soluble enough to store in aqueous media and to allow for controlled reactions with antibodies.

Currently, the vast majority of ADCs in the clinic or in trials fall within two main categories: microtubule inhibitors (auristatins, tubulysins, maytansines) or DNA-damaging agents (calicheamicin, duocarmycin and pyrrolobenzodiazepine dimers). All these natural products were previously excluded as single use therapeutics due to the potential for off-target toxicities, but guided by the impeccable cell-targeting ability of an antibody they have resurfaced as viable drug candidates.[46] Arguably, these payloads are somewhat limited in their mechanisms of action and future advances in the field should gear towards novel payload classes with diverse mechanisms of action to help combat resistance.

The viability of antibody–drug conjugates as therapeutic agents has been clinically demonstrated through the approval of ADCs for cancer treatment. Adcetris (brentuximab vedotin **15**, **Figure 17**) is currently on the market for the treatment of Hodgkin lymphoma. This ADC features monomethyl auristatin E (MMAE), a microtubule inhibiting natural product derived from the marine natural product dolastatin 10, originally isolated from the sea hare *Dolabella auricularia*, as the cytotoxic warhead.[80,81] Conjugation occurs through a cysteine residue *via* a maleimide group attached to the peptide-cleavable valine–citrulline linker containing a self-immolative spacer. Kadcyla (ado-trastuzumab emtansine **16**, **Figure 17**), approved for the treatment of metastatic breast cancer, uses the plant-derived drug maytansine which also targets microtubule assembly.[82] This ADC contains a non-cleavable linker conjugated *via* a maleimide onto the antibody through lysine residues. Maytansine and MMAE were previously excluded as anticancer drugs due to unacceptably high toxicity in human trials but have now seen clinical success through incorporation into immunoconjugates.

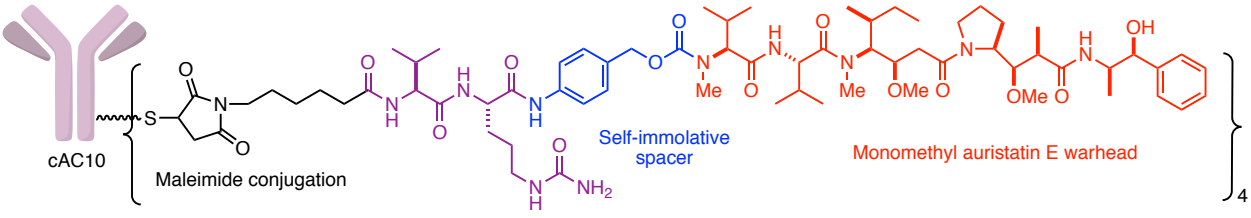

15
Adcetris (brentuximab vedotin)

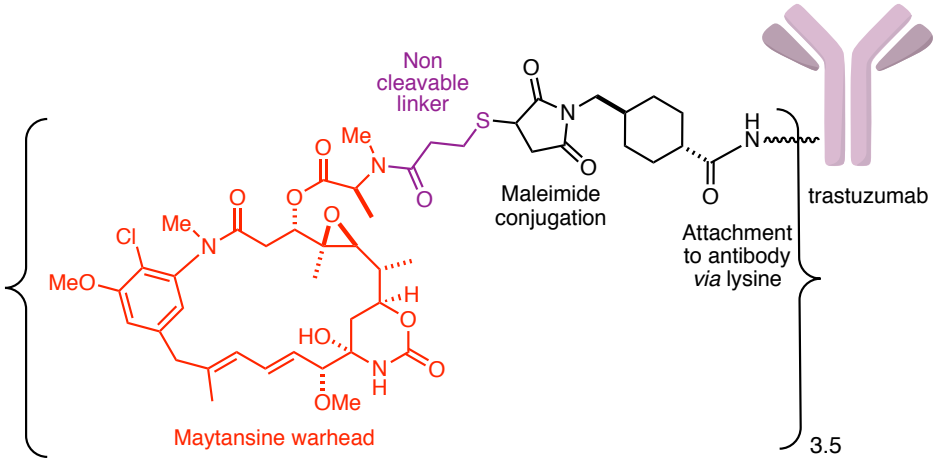

16
Kadcycla (ado-trastuzumab emtansine)

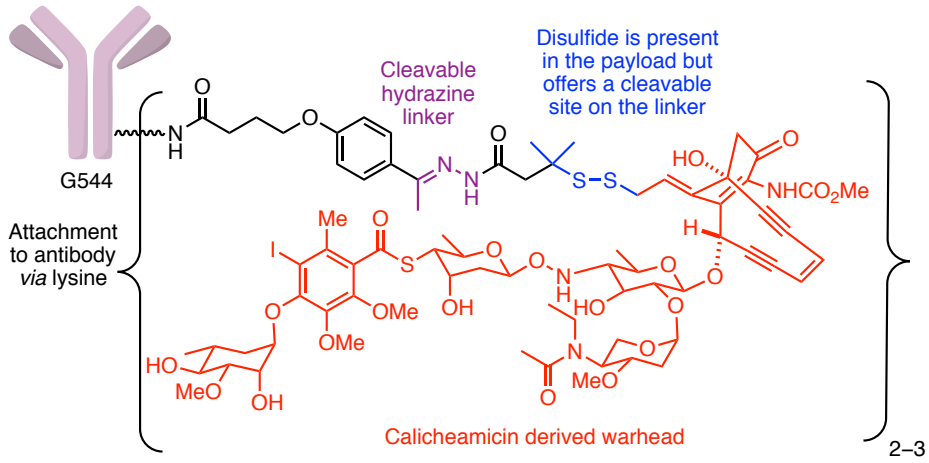

17
Besponsa (inotuzumab ozogamicin)

Figure 17 ADCs currently on the market

Derivatives of the calicheamicins, a family of bacterial-derived antitumour antibiotics, are prevalent in multiple ADCs.[83–85] Their biological activity is elicited through binding of DNA leading to strand scission and resulting in cell death. Besponsa (inotuzumab ozogamicin **17**, **Figure 17**) was approved in 2017 for the treatment of acute lymphoblastic leukaemia and contains a calicheamicin based payload. Mylotarg (gemtuzumab ozogamicin), also containing a calicheamicin payload, was re-introduced to the market for acute myeloid leukaemia in 2017 after previously being excluded due to issues surround toxicity.

1.3.5 Summary and outlook

ADCs have paved the way to revive highly potent compounds as cancer chemotherapeutic agents that were too toxic to be clinically useful on their own. Current conjugates make use of antibodies that are of human origin, and therefore not immunogenic, and linkers that are designed to be stable in circulation yet precisely release the toxin upon internalisation into the cell.

ADCs rank among the most actively pursued classes of therapeutics in oncology, yet many challenges still remain in their development. Low to moderate preferential accumulation of the antibody at the tumour site has been reported in a number of cases with wide variations in tumour uptake observed.[86] Processes such as antibody–tumour localisation *in vivo* also remain largely underexplored. Furthermore, the development of more homogeneous and stable conjugate systems is of paramount importance for the success of next-generation antibody therapeutics.

Additionally, the high cost of bringing an ADC to market must be considered. Many rounds of optimisation are usually required to deliver an effective therapeutic. Nevertheless, with many more ADCs currently in various stages of clinical testing, this is a field that is rapidly expanding and demonstrates the enormous potential of these targeted therapies.

1.4 The aplyronines

1.4.1 Isolation and structural determination

The aplyronines are a family of polyketide marine natural products isolated by Yamada and co-workers from the sea hare *Aplysia kurodai*, collected of the coast of the Mie prefecture in Japan. This marine mollusc has proven to be a fertile source of bioactive natural products including aplysin[87] (**18**), aplaminone[88] (**19**), aplysiasecosterol A[89] (**20**) and many others (**Figure 18**).

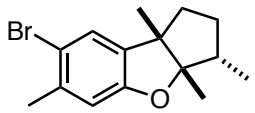

Aplysin (**18**)

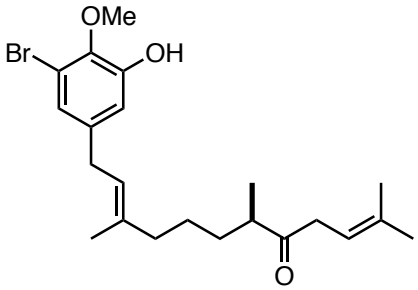

Aplaminone (**19**)

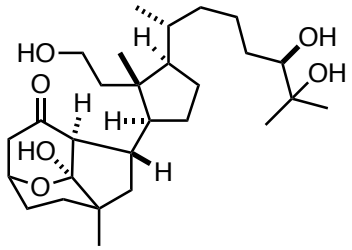

Aplysiasecosterol A (**20**)

Figure 18 Selected bioactive molecules isolated from *Aplysia kurodai*

Aplyronine A (**21**), together with its two congeners aplyronines B (**22**) and C (**23**), was originally isolated in 1993 through an eight-step chromatographic sequence guided by HeLa–S_3 cytotoxicity assays.[2] An improved isolation procedure led to the discovery in 2000 of the minor congeners aplyronines D–H.[90] Isolation yields remained prohibitively low however, with 300 kg of wet sea hare yielding only 75 mg (10^{-5} %) of aplyronine A and less than 1 mg of some of the minor congeners (**Table 1**).

Table 1 Structure and activity of the aplyronine family. [a] mg per 300 kg sea hare; [b] *in vitro* activity against HeLa–S_3 cells;[91] *1.1–3.1 *S*:*R*, **5:1 *S*:*R*

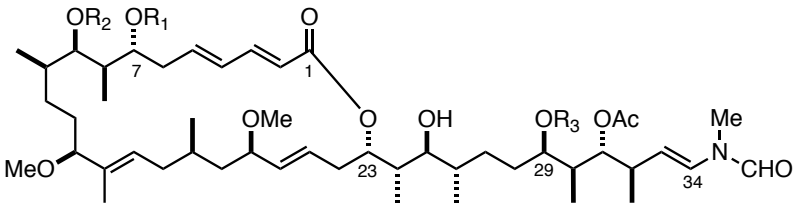

Congener	R_1	R_2	R_3	Isolation yield [a] / mg	IC_{50} [b] /nM
A **(21)**	TMSer	H	DMAla	75	0.45
B **(22)**	H	TMSer	DMAla	4.3	2.9
C **(23)**	H	H	DMAla	0.9	22
D **(24)**	TMSer	H	DMGly	2.6	0.071
E **(25)**	= 22-methylaplyronine A			4.0	0.18
F **(26)**	TMSer	H	MMAla	0.7	0.18
G **(27)**	DMSer	H	MMAla	1.6	0.12
H **(28)**	H	DMSer	DMAla	0.6	9.8

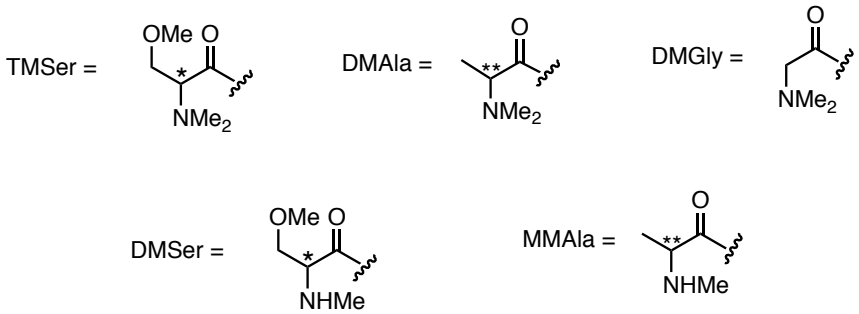

Elucidation of the key structural features was determined by analysis of IR, UV and 1D ^{1}H and ^{13}C NMR data. Each congener features a 24-membered macrolactone with an eleven-carbon side chain, terminating in an *N*-methyl-*N*-vinyl formamide moiety. Fifteen stereocentres append the carbon backbone, arranged in three stereotetrads (C_7–C_{10}, C_{23}–C_{26} and C_{29}–C_{32}) with three isolated stereocentres (C_{13}, C_{17} and C_{19}). The absolute and relative configuration of aplyronine A was determined by detailed 2D NMR studies and stereocontrolled synthesis of various degradative fragments. This assignment was further supported by the completion of the first total synthesis of aplyronine A by the Yamada group in 1994.[92–97]

The structural variation in the aplyronine congeners is chiefly seen in the identity and positioning of the amino acid residues between the C_7, C_9 or C_{29} hydroxyls. The configuration of the stereogenic amino acids is noteworthy, as they present as scalemic mixtures of the corresponding (*R*)- and (*S*)-epimers. These ratios seem to always favour the naturally occurring (*S*)-configuration. It is postulated that this stereocentre could undergo epimerisation in the biosynthesis of these molecules or during the isolation procedure.[2]

1.4.2 Biological activity

The cytotoxicity of the aplyronines in the HeLa–S_3 cell line is nothing short of exceptional, with IC_{50} values in the low to sub-nanomolar range across the family. Furthermore, on testing in the NCI human tumour 60 cell line primary screen, aplyronine A displayed excellent activity, with a GI_{50} of less than the 0.1 nM minimum threshold being observed across the majority of cell lines.[98,99]

The main difference between the congeners of the aplyronine family lies in the amino acid residues. It is notable that these seemingly small differences yield such strong variations in their biological activities (**Table 1**). For example, aplyronine A is approximately 50 times more cytotoxic than aplyronine C, which lacks the methylated serine ester group at C_7. Other congeners that contain this trimethyl serine residue in the same position also exhibit high toxicities, but their full biological evaluation has been hampered due to low isolation yields.

On top of this excellent *in vitro* activity, the most abundant congener, aplyronine A exhibits promising growth inhibitory activity *in vivo* against a range of implanted tumour types in mouse xenographs as summarised in **Table 2**. Remarkable dose-dependent antitumour activities and high survival rates were observed in the case of Lewis lung carcinoma and P388 leukaemia.[91]

Table 2 *In vivo* antitumor activity of aplyronine A in mice. [a] Schedule: intraperitoneally (i.p) days 1-5; aplyronine A was dissolved in DMSO (0.08 mg mL^{-1}) and then diluted with a physiological solution of NaCl

Tumour	Route[a]	Dose / mg kg^{-1} day^{-1}	Median survival time / days	Test/control / %	Survivors after 60 days
P388 leukaemia	i.p.	0.08	59.9	545	4/6
	Control	—	11.0		0/7
C26 colon carcinoma	i.p.	0.08	40.0	255	0/6
	Control	—	15.7		0/10
Lewis lung carcinoma	i.p	0.04	60.1	556	6/6
	Control	—	10.8		0/8
B16 melanoma	i.p.	0.04	46.8	201	0/6
	Control	—	23.3		1/9
Ehrlich carcinoma	i.p.	0.04	59.7	398	2/6
	Control	—	15.0		0/8

These results are extremely promising and have propelled the aplyronines into serious contention as potential preclinical candidates.[100]

1.4.3 Interaction with actin

Actin was identified as the target biomolecule of the aplyronines by fluorescence-based measurements by Karaki and co-workers in 1996. Aplyronine A was observed to bind to G-actin in a 1:1 ratio.[101] Actin is an extremely important and abundant protein, found in almost all eukaryotic cells, and is one of the main classes of cytoskeletal proteins within the cytoplasm. Actin is involved in the regulation of a variety of cellular processes including cytokinesis, muscle contraction, signalling and the formation of cell junctions.[102,103]

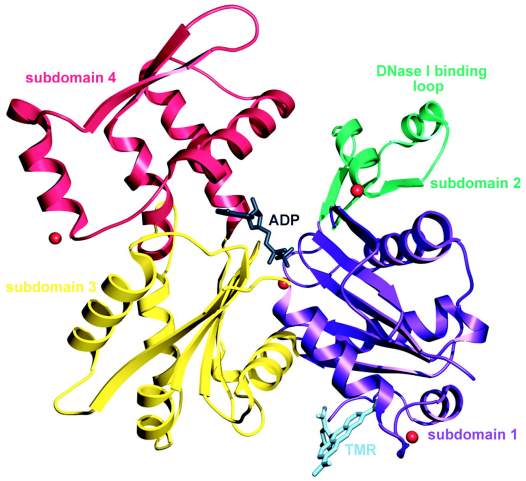

Figure 19 Structure of uncomplexed actin in the ADP state[104]

Actin exists in two forms: monomeric G-actin (globular) and in the form of microfilaments in polymeric F-actin (filamentous). Polymerisation of G-actin to F-actin can occur under physiological conditions and it is this dynamic equilibrium which is essential for actin to exert its cellular function. The unidirectional process of filament growth takes place in a head-to-tail manner at the barbed ends of G-actin and is mediated by the interconversion of ATP and ADP (**Figure 20**).[105]

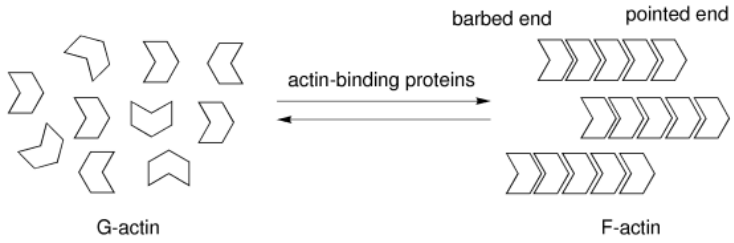

Figure 20 Dynamic equilibration between G- and F-actin and the actin treadmilling process[106,107]

Aplyronine A has been found to intercalate *via* its side chain into a narrow hydrophobic cleft of G-actin. This complex causes sequestering of G-actin monomers and thus inhibition of treadmilling and polymerisation to F-actin. Additionally, rapid depolymerisation of F-actin can occur through capping and resulting severing of the actin filaments.[101,108] Disruption of this normal actin modulation pathway can lead to accelerated depolymerisation and apoptosis. The aplyronine binding mode described has subsequently been confirmed by X-ray analysis (**Figure 21**).[108] This side chain binding occurs between subdomains 1 and 3, with the amino acid residues in actin participating in hydrophobic interactions with the aliphatic tail regions, ensuring the extended conformation. The macrolide core also forms important contacts with a large hydrophobic area on the surface of actin. In contrast, the polar terminus is located in a hydrophilic environment and forms key stabilising contacts in this region.

A striking structural resemblance is borne between the aplyronine side chain and other actin binding natural products. A highly conserved motif terminating in the same *N*-methyl-*N*-vinyl formamide moiety is present many actin binding natural products including reidispongiolide A (**29**), mycalolide B (**30**), scytophycin C (**31**) and rhizopodin (**32**) (**Figure 22**).[109–112] Interestingly, the 80 known actin-binding natural products encompass just 8 major skeletal types. The aplyronines, possessing an 11-carbon aliphatic side chain coupled with the hydrophobic macrolide core, represent one class of such compounds.[113]

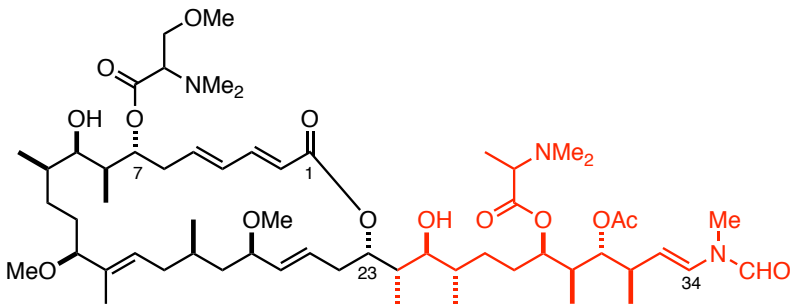

Aplyronine A (**21**)

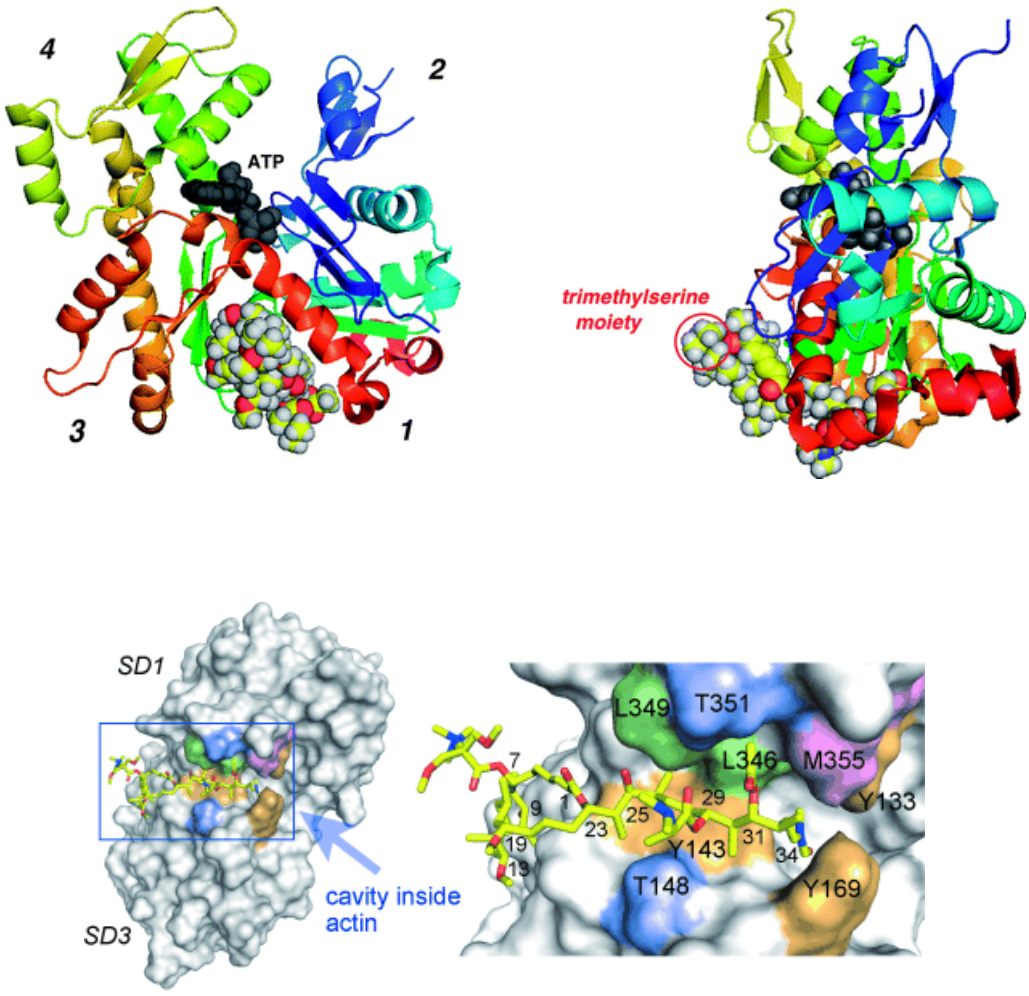

Figure 21 X-ray crystal structure of the aplyronine A:actin complex[108,114]

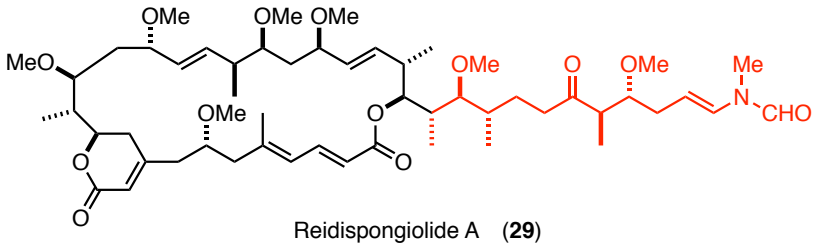

Reidispongiolide A (**29**)

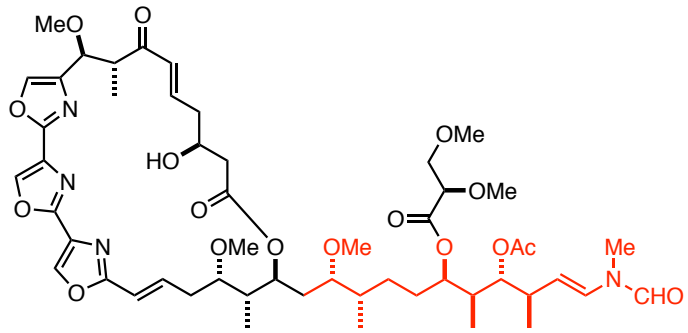

Mycalolide B (**30**)

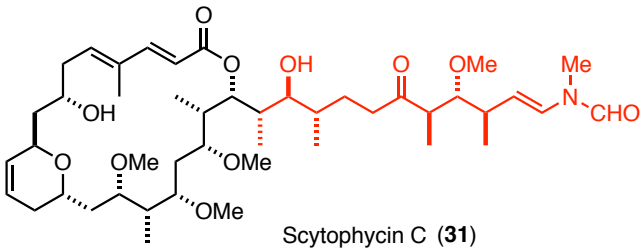

Scytophycin C (**31**)

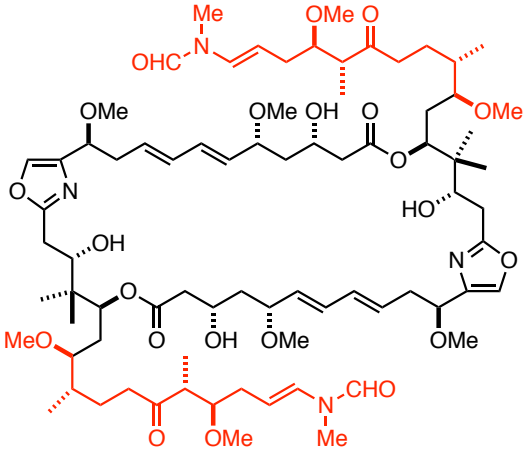

Rhizopodin (**32**)

Figure 22 Related actin binding natural products with the highly conserved side chain

1.4.4 Structure–activity relationship studies

It has been well established that the side chain motif in the aplyronines is crucial for actin binding. A wide range of side chain analogues, based on the aplyronines or the related reidispongiolide A (**29**), have been prepared by the Yamada[115–117] and Paterson[118–121] groups to investigate this effect.

However, actin binding alone cannot account for the variance in biological activity displayed by the aplyronine family. It is evident that actin depolymerising ability does not mirror the cytotoxicity of the aplyronines. For example, aplyronine A possesses an actin depolymerising IC_{50} value of 31 μM, whereas cytoxicity towards HeLa–S_3 cells occurs with an IC_{50} of 0.45 nM.[116] Furthermore, aplyronines A and C have identical side chains and bind actin with equal affinity, yet aplyronine A is 50 times more cytotoxic, confirming that actin depolymerisation alone is not sufficient to confer cytotoxicity. An early insight into the structure–activity relationships at play can thus be gleaned from this observation; the only difference between these congeners is the presence of the trimethyl serine residue at C_7 in aplyronine A. This C_7 trimethyl serine residue must therefore be profoundly important in conveying strong levels of cytotoxicity.

Extensive structure–activity relationship studies have been carried out on aplyronine A and derivatives to gain a better understanding of the structural features which are necessary to confer biological activity (**Figure 23**).[117,122,123]

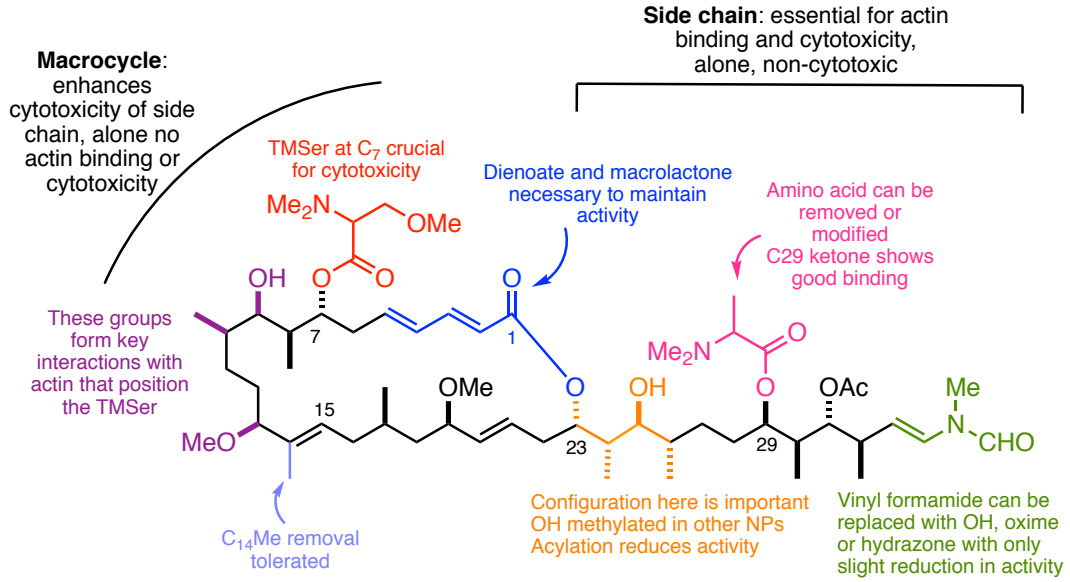

Figure 23 Summary of SAR studies on aplyronine A

The presence of the C_7 trimethylserine residue, the conjugated diene moiety and hydroxyl groups at C_9 and C_{29} are features necessary to impart toxicity and very little variation is tolerated with regards to cytotoxicity compared with actin binding. Actin depolymerisation is strongly associated with the side chain, and is enhanced when combined with the macrocycle. From all this, we see that the parameters of actin depolymerisation ability and cytotoxicity are not always correlated. From crystal structures of the aplyronine–actin complex, it is evident that the trimethylserine residue protrudes solely into the surrounding bulk solvent. This indicates that its critical influence on cytotoxicity is not due to interactions with actin and suggests the possibility of binding to another protein target.

Kigoshi and co-workers have invoked tubulin binding as an additional mode of action and reported that aplyronine A forms an unprecedented 1:1:1 heterotrimeric complex with actin and tubulin (**Figure 24**).[124] Tubulin is another abundant cell protein and its monomers polymerise to form microtubules, which are important components of the cytoskeleton, especially during cell division. Aplyronine A therefore appears able to mediate a protein–protein interaction (PPI) between these significant biomacromolecules.

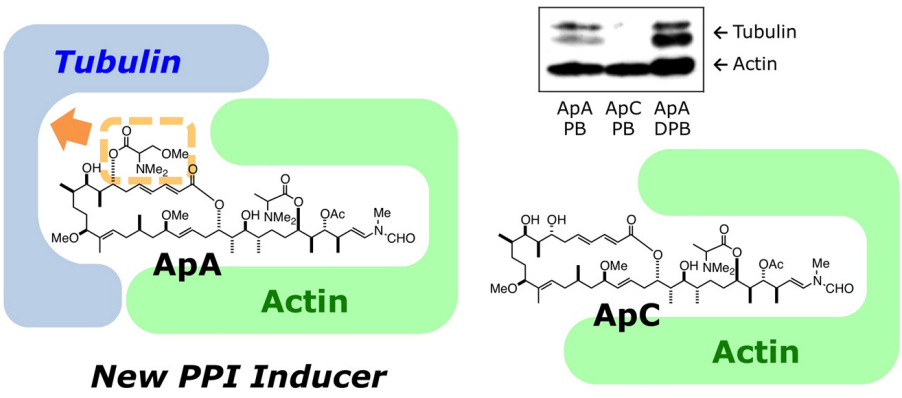

Figure 24 Proposed 1:1:1 heterotrimeric complex between aplyronine A, actin and tubulin; PB = protein binding, DPB = duel protein binding [124]

Through photoaffinity labelling and fluorescence microscopy measurements, the actin–aplyronine A complex was found to synergistically bind to tubulin. Interestingly, without actin, no binding to tubulin was observed. This suggests actin binding may induce a conformational change to create a new tubulin binding site, possibly mediated by the trimethylserine residue on the aplyronine molecule. Aplyronine C, in the presence of actin, did not bind to tubulin at all, further cementing the importance of the trimethylserine ester moiety for interactions with tubulin.[124] Kigoshi has further studied these proposed interactions and binding affinities using surface plasmon resonance (SPR).[125]

It is unclear exactly how this ternary complex induces cytotoxicity. Consistent with other antimitotic agents, such as vinblastine or paclitaxel, the mechanism of action may be disruption or blocking of the microtubule spindle organisation and dynamics during mitosis, ultimately leading to apoptosis.[126,127]

Synergistic binding to two biomacromolecules is rarely seen in natural products and could offer enormous therapeutic potential.[128,129] Furthermore, with this completely novel mechanism of action, there is the possibly of overcoming drug resistance pathways.

Returning to the numerous criteria for a suitable ADC payload, we see that the aplyronines meet many of the fundamental requirements and as such are compelling candidates for this targeted therapy. Firstly, they exhibit exquisite cytoxicity in the sub-nanomolar range across a range of cell lines, and have even proven to be remarkably effective *in vivo*. Through extensive SAR studies and analysis of the aplyronine pharmacophore, suitable sites for functional handles can be identified to facilitate linker attachment. A highly promising feature of these bioactive natural products is their exciting and unique unprecedented mechanism of action, lending support to the aplyronines tremendous promise as an anticancer therapeutic. Antibody conjugation would not only limit off-target toxicity issues that could be associated with these highly potent molecules, but also reduce the amount of these scarce natural products required for clinical development.

The realisation of the incorporation of the aplyronines and their analogues into antibody–drug conjugates hinges upon the supply issue being solved. The current supply of these highly precious natural products is minute and thus ADC development is reliant on total synthesis to deliver an efficient and scalable route.

1.5 Synthetic efforts

Due to their structural complexity, the aplyronines represent an impressive synthetic target and have garnered the interest of a number of research groups. To date, three total syntheses have been reported, beginning with the pioneering work of Yamada and co-workers. In 1994, Yamada reported the first total synthesis of aplyronine A (**21**) in 98 steps (47 LLS) with an overall yield of 0.39%. This lengthy route was justified given the need for flexibility within the synthesis to rigorously confirm the structure and absolute configuration of aplyronine A (**21**).[92] The synthesis of aplyronines B (**22**) and C (**23**) quickly followed, along with simplified fragments for SAR studies.[97,130] More recently, Kigoshi has reported a second-generation synthesis of aplyronine A (**21**) in 38 steps LLS and an improved 1.4% overall yield.[131] Fragments have additionally been synthesised by Calter, Marshall and

Fuchs, generally following the main disconnections used by Yamada and Paterson.[132–136] The Paterson group has had a longstanding interest in the aplyronine family and synthetic efforts are summarised below.

1.5.1 Paterson approach to the aplyronines

Efforts towards the total synthesis of the aplyronines in the Paterson group first began in 1995. Notable highlights of this ongoing work include the total synthesis of aplyronine C and novel tail analogues in 2013, and the completion of aplyronines A and D in 2015.[137,138] Refined coupling strategies and revised synthetic steps have led to improved routes to advanced fragments and deeper knowledge about the chemistry of the aplyronines. The highly stereocontrolled and convergent route offers the opportunity to access multiple congeners of the aplyronine family through late-stage functionalisation with the appropriate amino acid residues.

Controlled installation of the dimethylalanine residue at C_{29} can be achieved through a selective Keck esterification at this position. Subsequent esterification at C_7 over C_9 is dependent on the less hindered hydroxyl conferring increased reactivity at this position. Common intermediate **33** (**Scheme 1**) therefore represents a diversification point, allowing access to multiple analogues. The C_{28}–C_{34} region could be disconnected from the main chain through a sequence of aldol–dehydration–reduction steps starting from ketone **34** and C_1–C_{27} aldehyde **35**. The (*E*)-trisubstituted olefin could be installed through a Horner–Wadsworth–Emmons (HWE) reaction and Yamaguchi macrolactonisation would assemble the macrocycle from two advanced fragments: the northern C_1–C_{14} phosphonate **36** and the southern C_{15}–C_{27} aldehyde **37**.

In the forward synthesis, a series of substrate-controlled aldol reactions and diastereoselective 1,3-*anti* reductions were used to efficiently construct the C_7–C_{10}, C_{23}–C_{26} and C_{29}–C_{32} stereotetrads. Reagent-controlled reduction was responsible for installing the isolated C_{13} and C_{19} stereocentres. A key step in the Paterson approach was the strategic installation of the *N*-methyl-*N*-vinyl formamide side chain terminus. A modified Wittig reaction, using methodology developed within the group, proved successful in introducing this delicate moiety.[139] Overall this route gave aplyronine C (**23**) in 28 steps LLS (47 total steps) in an overall yield of 3.6%.

Further improvements were implemented in the group's synthesis of aplyronines A and D and include a more streamlined protecting group strategy to deliver a route more amenable to scale up.[138]

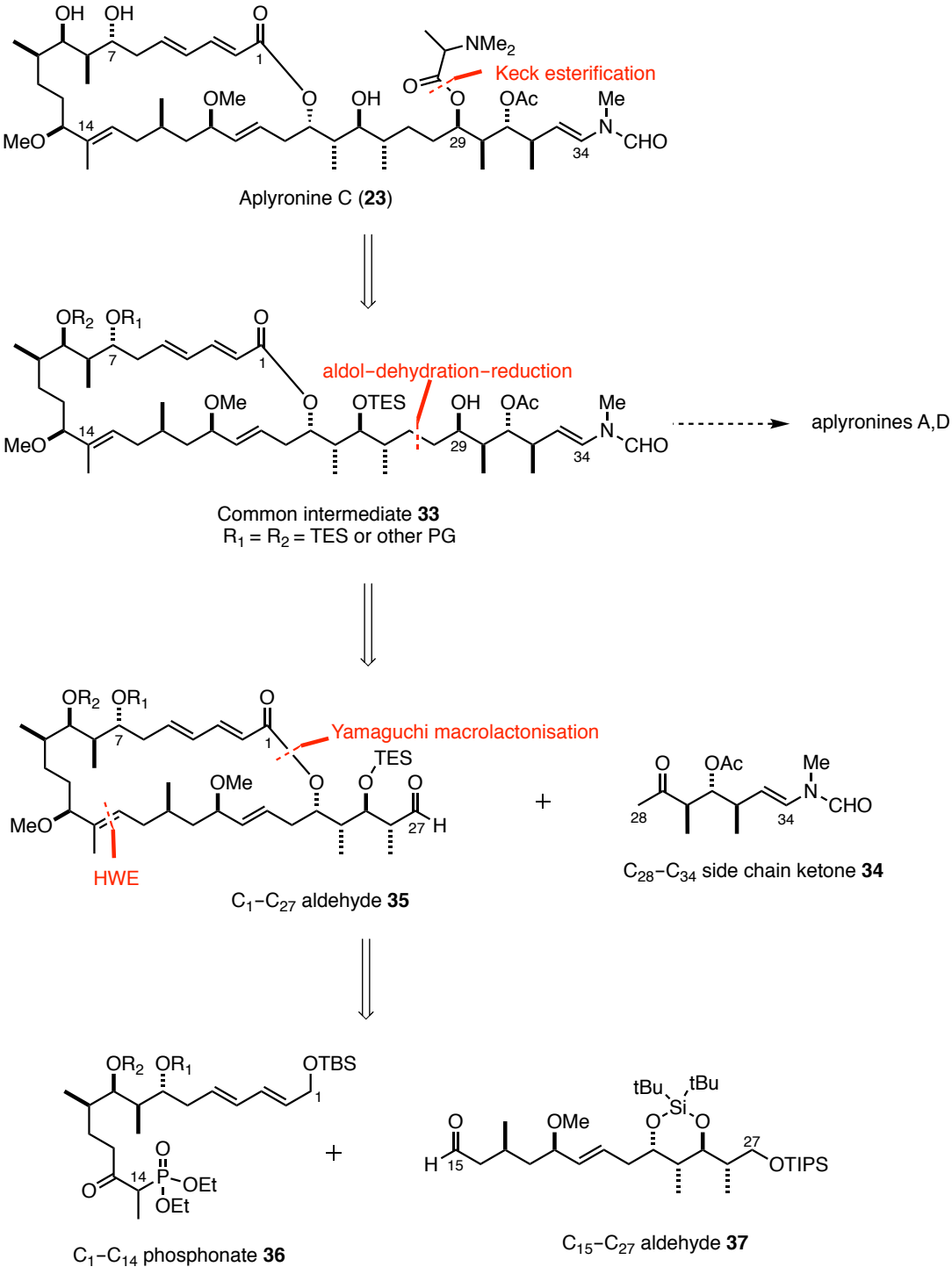

Scheme 1 Paterson approach to the total synthesis of the aplyronines

1.5.2 Aldol methodology

The stereotetrads found within the aplyronines are a common motif found in polyketide natural products. Biosynthetically, under the control of polyketide synthase enzymes, these originate from iterative addition of malonyl CoA or methylmalonyl CoA to the growing carbon chain. Depending on the type of condensation, one or two stereocentres can be introduced per cycle and the resulting β-hydroxy ketone unit can be further manipulated through reduction or dehydration reactions. This process is the source of the 1,3-oxygenation pattern ubiquitously found in polyketides.[140]

The Paterson approach to the aplyronines calls for construction of the stereotetrads using powerful boron aldol methodology largely developed in our laboratory. Enolisation of methyl (acetate type) or ethyl ketones (propionate type) and subsequent reaction with aldehydes can generate β-hydroxy ketones in a regio-, stereo- and enantioselective fashion (**Figure 25**). Comprehensive understanding of this aldol chemistry coupled with stereoselective reductions allows access to every possible permutation of stereotetrad pattern.

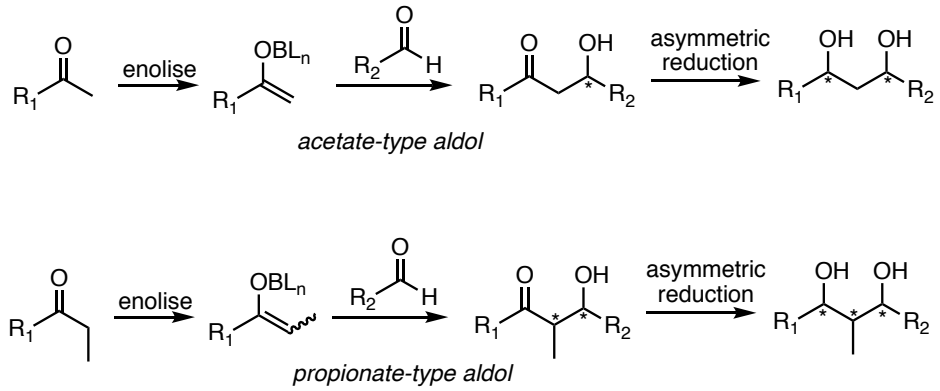

Figure 25 General acetate- and propionate-aldol reactions using methyl or ethyl ketones

The relative configuration of the adducts arising from aldol reactions with boron enolates can be reliably predicted from inspection of the Zimmerman–Traxler transition state models (**Figure 26**).[141] These chair-like transition structures are energetically favourable through minimisation of unfavourable 1,3-diaxial interactions. For this reason, (*E*)-enolates typically proceed to give 1,2-*anti* aldols, whereas (*Z*)-enolates produce 1,2-*syn* products.

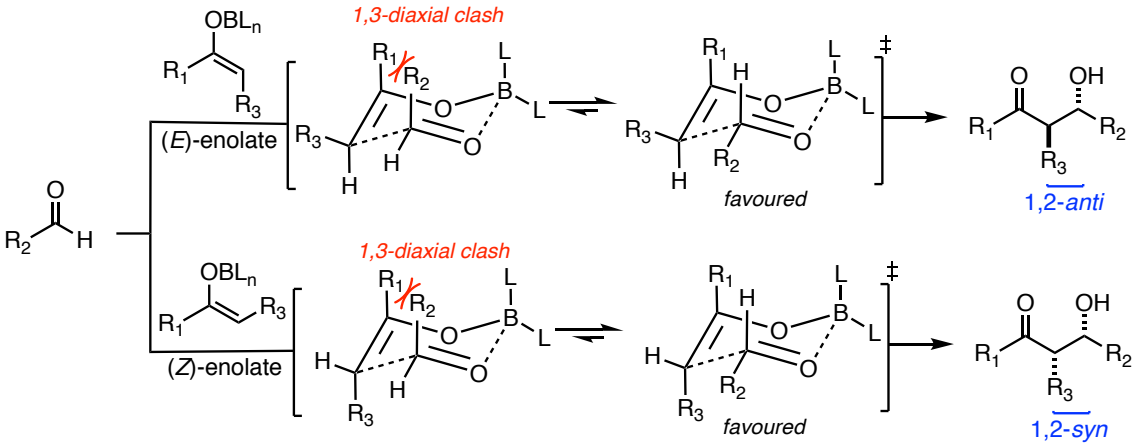

Figure 26 Zimmerman–Traxler transition state models for (*E*)- and (*Z*)-boron enolates[141]

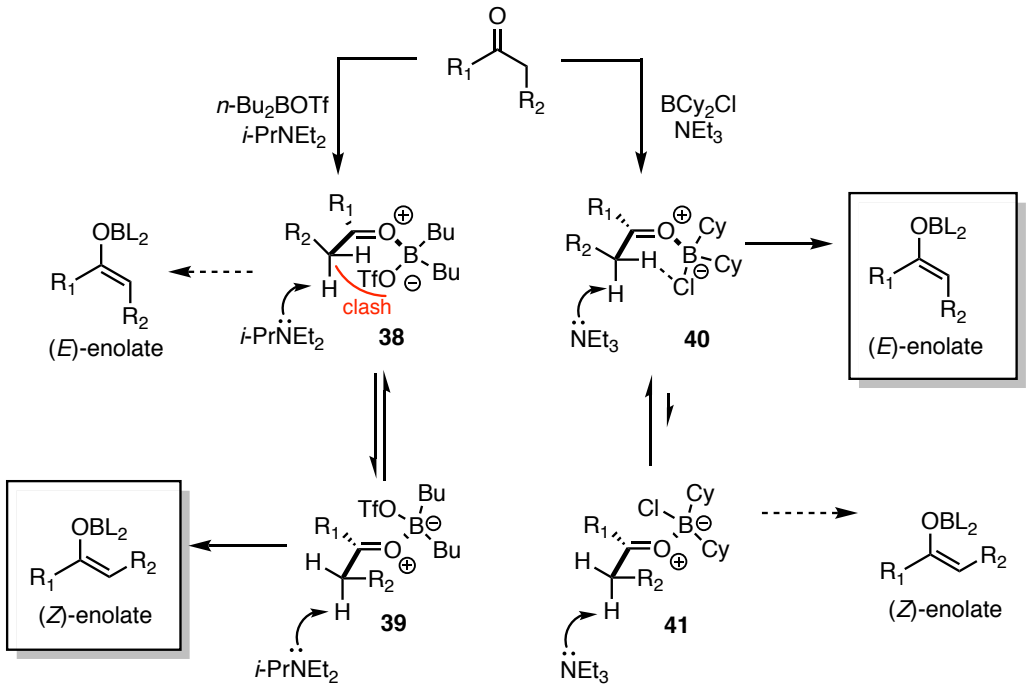

Scheme 2 Rationale for stereocontrolled formation of (*E*)- and (*Z*)-boron enolates[142]

High levels of stereoinduction are observed in boron-mediated aldol reactions. This can be attributed to short boron-oxygen bond lengths, ensuring the formation of tight, cyclic transition states that exacerbate the effects of unfavourable 1,3-diaxial interactions.[143] Thus, the formation of geometrically pure enolates is of paramount importance to control the stereochemical outcome of these reactions. Numerous powerful methods have therefore been developed to enable the stereoselective formation of boron enolates.[145–148]

Enolisation at low temperatures (*e.g.* –78 °C) with dialkyl boron triflates (*e.g.* *n*-Bu_2BOTf) and a sterically demanding tertiary amine base (*e.g.* *i*-Pr_2NEt) results in the selective formation of (*Z*)-enolates. Conversely, a combination of bulky ligands (*e.g.* cyclohexyl), a poor leaving group (*e.g.* chloride) and a small amine base (*e.g.* NEt_3) favours the formation of (*E*)-enolates (**Scheme 2**).[148] Formation of (*Z*)-enolates with dialkyl boron triflates is primarily governed by sterics, with both complexes **38** and **39** theoretically possible. Ultimately, the steric clash arising from the large triflate substituent and the incoming bulky base disfavours the formation of **38**, resulting in the generation of the (*Z*)-enolate. However, for (*E*)-enolates the formation of complex **40**, with boron directed towards the less substituted side of the carbonyl group, is favoured for both steric and electronic reasons. An energetically favourable interaction has been found to exist between the chlorine atom and the hydrogen *cis* to the carbonyl lone pair. This induces a partial negative charge on the adjacent carbon and thus activates the *cis*-hydrogen for deprotonation, selectively generating the (*E*)-enolate.

Enolate geometry dictates the required relative stereochemistry of an aldol adduct. However, there is inherently no control of absolute stereochemistry unless a chiral element is present on either the enolate or aldehyde substrate. In particular, chiral ketones are able to furnish aldol adducts with high stereeocontrol through control of π-facial selectivity. Within our laboratory, Roche ester derived ethyl ketones **42** and **43** are frequently used to induce the desired absolute stereochemistry through boron and titanium-mediated aldol reactions (**Figure 27**). The selectivity in these cases will be discussed as they are encountered in the text.

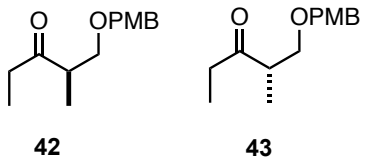

42 **43**

Figure 27 Roche ester derived ethyl ketones **42** and **43**

1.6 Analogue design and project aims

1.6.1 Analogue design

The aplyronines, through their exquisite potency and novel biological activity, have surfaced as a compelling candidate for incorporation into antibody–drug conjugates. As discussed previously, truncating complex natural products whilst retaining their pharmacophore brings with it many advantages. Developing simpler analogues that preserve the aplyronines' function and potency, whilst greatly shortening the synthesis of these complex structures, allows for investigations towards a viable and accessible ADC payload. Generating structurally simplified analogues also offers the opportunity to create more efficient and streamlined syntheses.

A proposed function-oriented analogue scaffold is illustrated in **Figure 28**. Structure–activity relationship studies of the aplyronines have indicated that the southern region of the macrocycle does not make any significant contact interactions for actin binding or cytotoxicity, other than conferring overall shape (**Figure 28**). Therefore, we propose that modifications in this area should not detrimentally affect bioactivity and offers potential to simplify the synthesis. Replacing the C_{17}–C_{21} chain with a simple hydrocarbon backbone removes two stereocentres and an olefin, drastically shortening the synthesis of this fragment.

Additional modifications include the replacement of the C_{31} acetoxy group with a methyl ether, thereby reducing the potential for elimination and the need to manipulate protecting groups in subsequent steps. The substitution of the C_{25} hydroxyl by a methoxy group would ensure selective macrolactonisation at C_{23}, avoiding the need to isomerise the undesired 26-membered ring formed through reaction at C_{25} that had previously caused difficulties within the synthesis.[149] Methoxy groups in these positions are present in other natural products that exhibit comparable binding affinity to actin and so these modifications are anticipated to be well tolerated in analogue **44**. With modifications predominantly located in the southern fragment, the route towards these simplified analogues intersects well with the established Paterson synthesis.

The Paterson group is not alone in our attempts to truncate the aplyronines to produce novel analogues or hybrids. Kigoshi and co-workers have reported the synthesis of hybrid structures with the aim of enhancing actin-depolymerising activity or cytotoxicity.

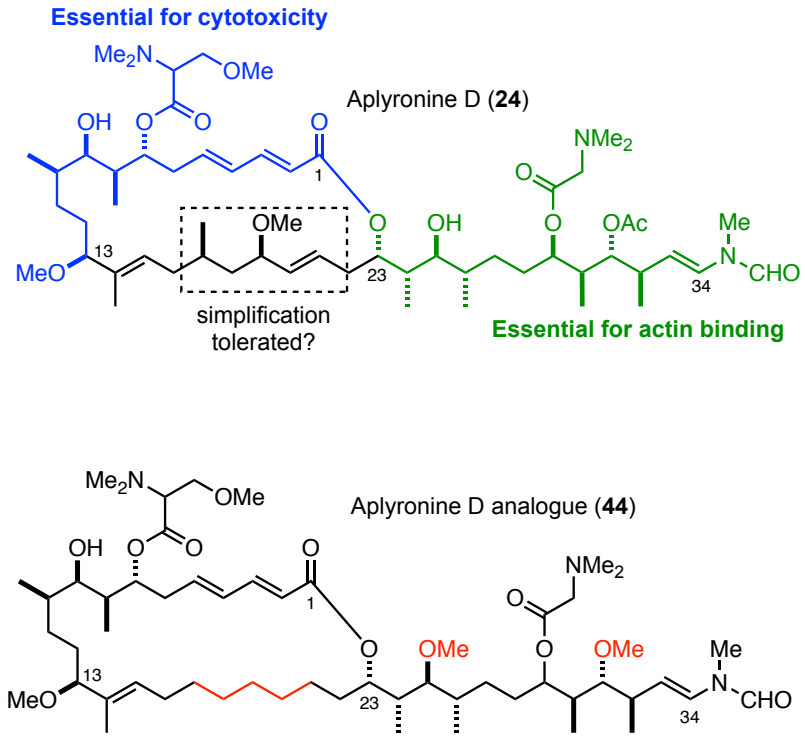

Figure 28 Function-oriented aplyronine D analogue (**44**)

The first hybrid compound (**45**, **Figure 29**) was reported by Kigoshi in 2012. Here, the macrolactone core of aplyronine A was appended with the side chain of mycalolide B (**30**, **Section 1.4.3**, **Figure 22**), a macrolide natural product isolated from a Japanese sea sponge.[110,123] Whilst this hybrid compound showed somewhat more potent actin-depolymerising activity than aplyronine A, the cytotoxicity towards HeLa–S_3 cells was disappointingly around 1000-fold lower. This result served to once again confirm that there is no direct correlation between actin-depolymerizing activity and cell growth inhibitory activity. The researches postulated that inversion in configuration at C_{25} causes a change in the conformational relationship between the macrolactone and side chain, as seen from the X-ray crystal structure (**Figure 29**) between the actin–aplyronine A complex and an actin–karbiramide C (a mycalolide B related compound) complex. Whilst both compounds bind readily with actin, the change in angle and thus directional orientation of the macrolactone means that hybrid **45** cannot maintain a strong interaction to tubulin to confer cytotoxicity.

In an effort to create a hybrid that is able to induce the desired protein–protein interaction, the Kigoshi group subsequently reported the synthesis of an aplyronine A–swinholide hybrid. In this case, the macrolide core of aplyronine A was combined with the side chain of the marine macrolide swinholide A (**Figure 29**).[150,151]

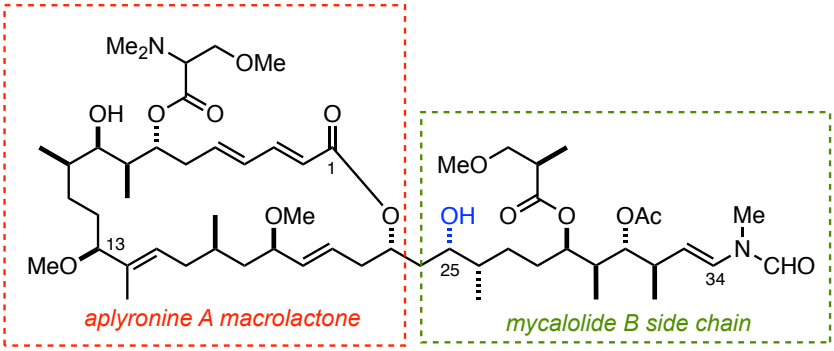

Aplyronine A–mycalolide B hybrid **45**

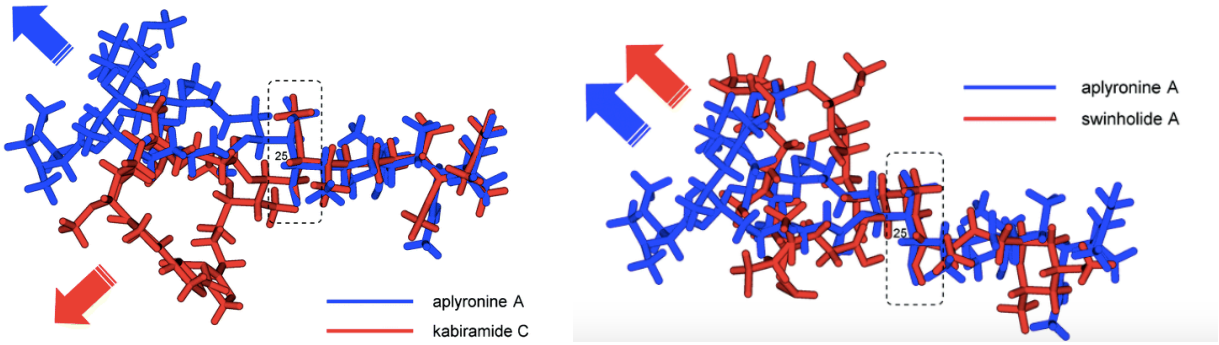

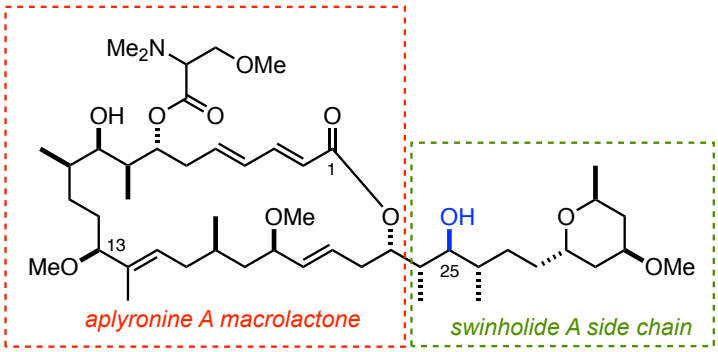

Aplyronine A–swinholide A hybrid **46**

Figure 29 Aplyronine hybrid compounds. Superimposed conformations of actin–aplyronine A and –kabiramide C or –swinholide A complexes based on X-ray analyses are shown. The arrows indicate the directional orientation of the macrolactone part in the corresponding complexes.[151]

This new hybrid **46** retained sub-nanomolar cytotoxicity towards HeLa–S_3 cells. Inspection of the X-ray crystal structure confirms that this compound adopts a similar actin-binding conformation to the parent aplyronine A, and thus may be inferred to induce the postulated PPI between actin and tubulin.

Guided by molecular modelling studies, the Kigoshi group have recently reported the synthesis of vastly simplified aplyronine analogues **47**–**49** (**Figure 30**).[152] This bold approach consists of only the C_1–C_9 northern region coupled with the C_{23}–C_{34} side chain. Perhaps unsurprisingly, these heavily truncated structures do not show sufficient PPI inducing effects or cytotoxicity. These oversimplified analogues demonstrate that the macrolactone portion of the aplyronines is indeed necessary to confer rigidity to fix the overall conformation to interact with tubulin.

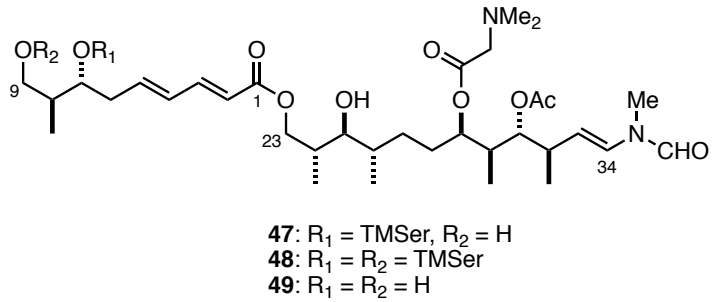

47: R_1 = TMSer, R_2 = H
48: R_1 = R_2 = TMSer
49: R_1 = R_2 = H

Figure 30 Kigoshi's simplified aplyronine analogues[152]

Together, these results from Kigoshi and co-workers demonstrate that simplified hybrid aplyronine structures that retain biological activity are synthetically tractable, yet also serve as a stark warning that over-simplification can lead to serious deleterious effects on cytotoxicity.

1.6.3 Project aims

The overall goal of this work is to develop novel bioactive analogues of the aplyronine family of natural products that can be incorporated into antibody–drug conjugates. The intention is to design and synthesise unique, yet simplified hybrid structures that are more accessible than the current routes to the aplyronines but retain the functionality and potency of the parent molecules. These streamlined and more efficient syntheses ideally would be amenable to large scale production and industrial development, thus saving overall time, resources and energy.

Importantly, this work also allows for investigation into an alternative coupling strategy. Typically, the macrocycle is constructed before attachment of the side chain to limit the risk of any degradation of the delicate *N*-vinyl formamide moiety. A complementary approach would be to couple the southern C_{15}–C_{27} aldehyde fragment **50** with the side chain moiety **51**, before addition of northern fragment **36** and finally macrolactonisation. These coupling strategies are outlined in **Scheme 3**. We therefore set the aim of bolstering the efficiency of the Paterson synthetic route through this alternative coupling strategy.

The flexibility of this approach allows for the construction of numerous different analogues and hybrids. The option to vary amino acid residues and modify functionality on the side chain opens up avenues for diversification. By fine-tuning these parameters, it is anticipated that a superior warhead for an ADC can be produced, with the potential for diversity in linker design and attachment.

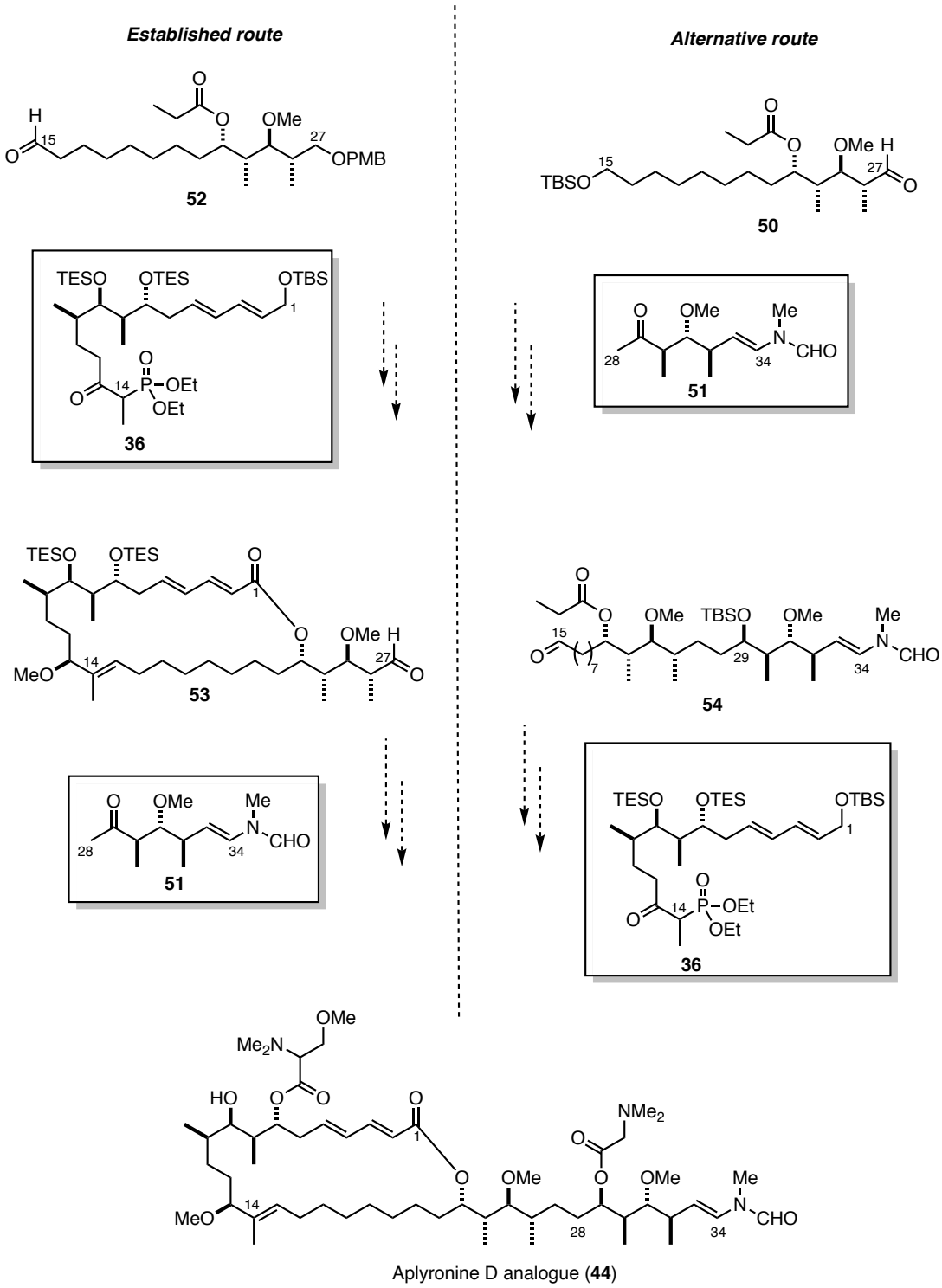

Scheme 3 Overview of coupling strategies towards aplyronine analogues

Chapter 2

Synthesis of advanced fragments

2.1 C_1–C_{14} northern phosphonate 36

As discussed in **Section 1.6.1**, the northern fragment **36** for analogue synthesis is equivalent to that used in the synthesis of the parent natural products. This reflects the importance of this region in governing the exquisite cytoxicity displayed by the aplyronines. The dienoate moiety and the C_7 trimethyl serine ester form key interactions and are crucial for promoting tubulin binding, with their removal leading to detrimental effects on the potency of these compounds.[153]

This fragment features a 1,4-*syn*-3,4-*anti* stereotetrad and a (2*E*,4*E*)-diene, terminating in a phosphonate moiety to facilitate a Horner–Wadsworth–Emmons olefination for extension of the carbon skeleton. The potentially sensitive dienoate is initially masked as an alkynoate and exposed through a triphenylphosphine-promoted isomerisation. A substrate-controlled boron-mediated aldol reaction and 1,3-*anti* reduction sequence sets the configuration of the stereotetrad, revealing Roche ester-derived ethyl ketone **42** and aldehyde **55** as key fragments (**Scheme 4**).

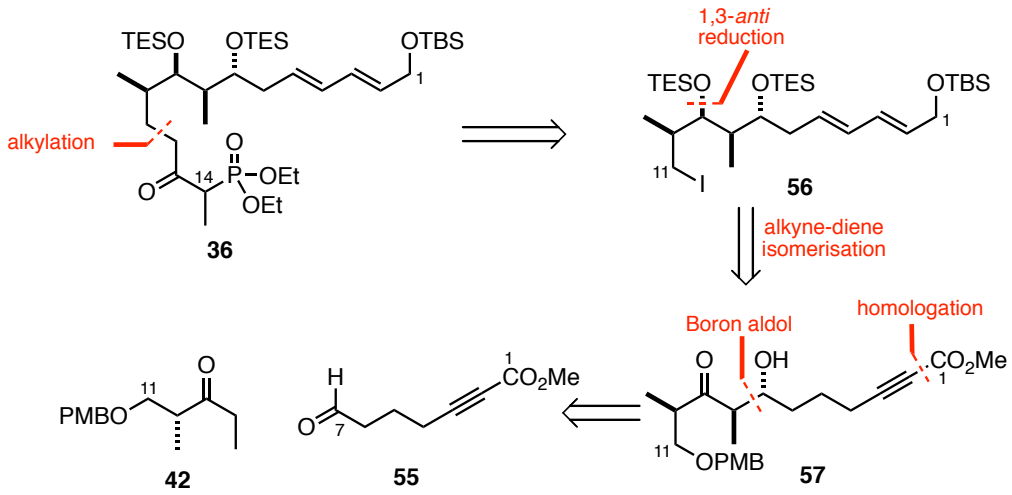

Scheme 4 Retrosynthetic analysis of the C_1–C_{14} northern fragment **36**

2.1.1 *Anti*–aldol coupling

The synthesis of the C_1–C_{14} northern fragment **36** commences with a selective boron aldol reaction that is utilised to set the required 1,4-*syn*-3,4-*anti* relationship within the stereotetrad. The required ethyl ketone coupling partner **42** was easily accessed in three steps from commercially available (*R*)-Roche ester **58**. Following PMB protection, ester **59** was converted to the corresponding Weinreb amide **60** and subjected to ethylmagnesium bromide. After initial attack of the Grignard reagent, the stability of the resulting metal-chelated intermediate prevents further addition, thereby minimising the formation of the tertiary alcohol byproduct. Chiral ethyl ketone **42** could reliably be produced in good yields on multigram scale by this route (65% over three steps, **Scheme 5**).

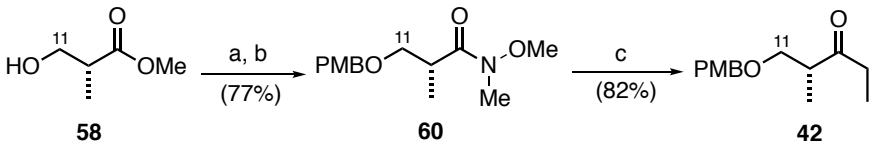

(a) PMBTCA, PPTS, CH_2Cl_2; (b) Me(OMe)NH · HCl, *i*-PrMgCl, THF, —20 °C; (c) EtMgBr, Et_2O

Scheme 5 Synthesis of ethyl ketone **42**

Aldehyde **55** was prepared *via* Parikh–Doering oxidation of the corresponding alcohol precursor which had been synthesised in four steps from 5-hexyn-1-ol by Dr Mike Housden (**Scheme 6**). With the requisite aldol coupling partners in hand, ketone **42** could be treated with dicyclohexylboron chloride and triethylamine to selectively form the desired (*E*)-

enolate **62** (**Scheme 7**). Subsequent addition of aldehyde **55** afforded aldol adduct **57**, following oxidative workup, in excellent yield and diastereoselectivity on multigram scale (88%, >95:5 *dr*).

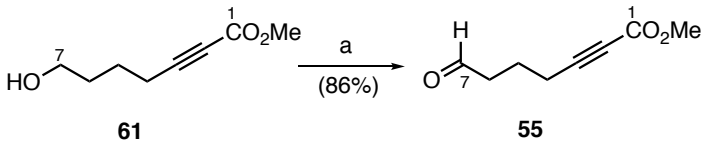

61 **55**

(a) SO_3·py, DMSO, NEt_3, CH_2Cl_2, 0 °C

Scheme 6 Oxidation of alcohol **61** to aldehyde **55**

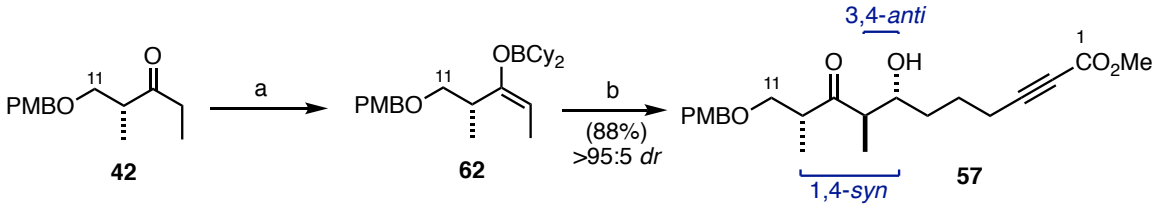

42 **62** **57**

(a) BCy_2Cl, NEt_3, Et_2O, 0 °C; (b) **55**, −78 °C → −20 °C *then* MeOH, H_2O_2, pH 7.0 buffer

Scheme 7 Boron mediated aldol coupling of ketone **42** with aldehyde **55**

The stereochemical outcome of this reaction can be rationalised by the control of enolate geometry and consideration of the competing transition states as illustrated in **Scheme 8**. The hydroxyl configuration ultimately derives from the facial selectivity of the α-chiral enolate while the 3,4-*anti* geometry can be ascribed to the (*E*)-enolate (**Section 1.5.2**). Through density functional theory studies (DFT), the high levels of stereoinduction observed in aldol reactions of β-alkoxy borinates has been rationalised by Paton and Goodman where reactions with (*Z*)-enol borinates proceed through chair transition states, whilst (*E*)-enol borinates proceed *via* boats.[148,154] These boat like transition structures are energetically more favourable and relieve the unfavourable 1,3-diaxial interactions between the ligand on boron and the side chain of the enolate. Notably, the boat conformation is stabilised by a formyl hydrogen bond between the aldehydic proton and the electron rich alkoxy oxygen substituent. Although this necessitates folding the alkyl chain towards the incoming aldehyde, which would appear to be a sterically unfavourable situation, the stabilising C-H-O interaction more than compensates for this.[155] The facial preference of enolate attack is therefore controlled by the minimisation of 1,3-allylic strain ($A_{1,3}$) between the α-methyl group and the enolate substituent. Consequently, *Re*-face attack, leading to the 1,4-*anti* product *via* **TS-2**, is disfavoured due to destabilising

interactions whilst *Si*-face attack, *via* **TS-1**, is more energetically favoured, leading to the observed 1,4-*syn*-3,4-*anti* product with high selectivity.

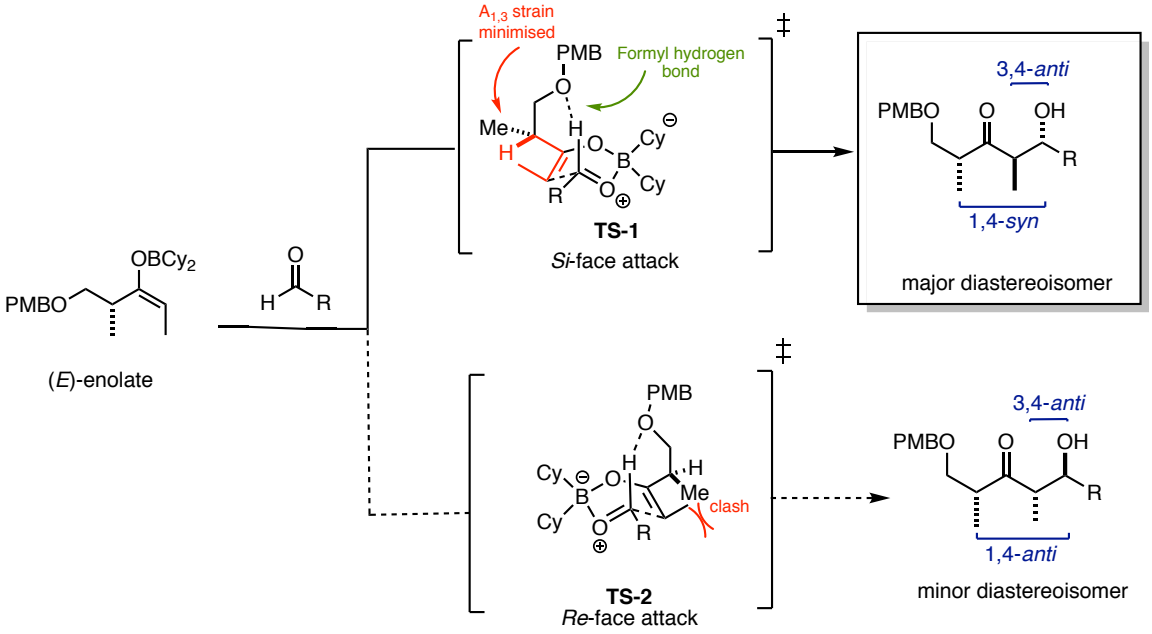

Scheme 8 Competing transition states for aldehyde addition of the (*E*)-enol borinate derived from Roche ester ethyl ketone **42**

2.1.2 1,3–*Anti* reduction and alkynoate isomerisation

An Evans–Tishchenko reduction was successfully employed to install the required 1,3-*anti* relationship, setting the configuration of the full C_7–C_{10} stereotetrad (**Scheme 9**).[156] This hydroxyl-directed reduction of ketone **57** utilising SmI_2 proceeded in excellent yield (98%) and diastereoselectivity (>95:5 *dr*).

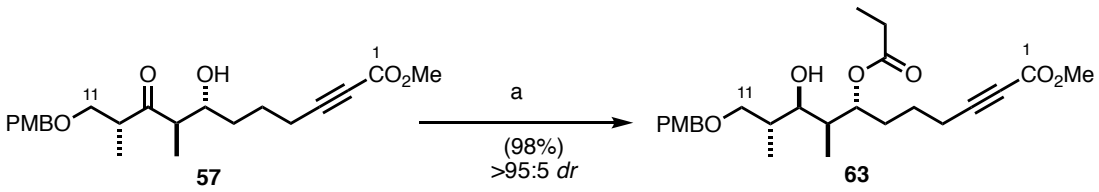

(a) SmI_2, EtCHO, THF, 0 °C

Scheme 9 Evans–Tishchenko reduction of ketone **57**

Mechanistically, this transformation is thought to involve the generation of a catalytically active samarium (III) pinacolate **64**, *via* reductive homocoupling of the excess aldehyde (**Scheme 10**).[156] This is evidenced by the colour change of the reaction from dark blue-green Sm(II) to yellow Sm(III) upon addition of the aldehyde.

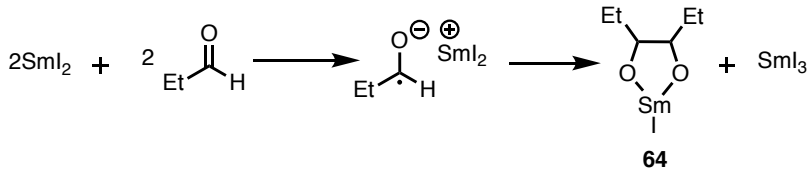

Scheme 10 SmI_2 mediated pinacol coupling of EtCHO

This species acts as a Lewis acid, promoting hemiacetal formation followed by intramolecular hydride transfer *via* a 6,6-chair transition state. High levels of diastereoselectivity are observed due to the coordinating ability of the oxophilic samarium, leading to conformational rigidity in this tight, bicyclic transition structure (**Scheme 11**).

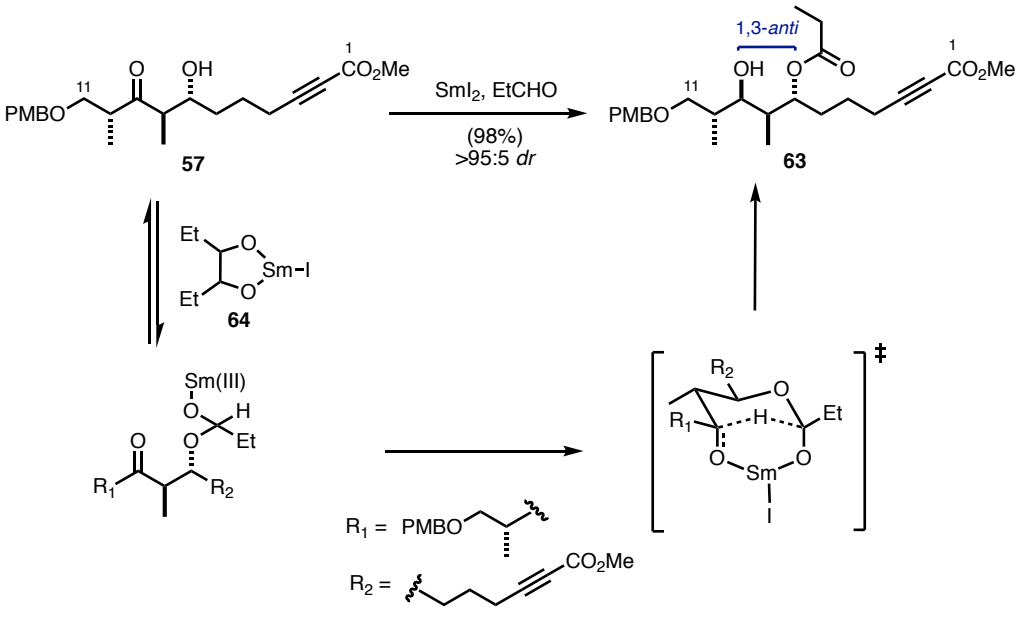

Scheme 11 Proposed mechanism for the Evans–Tischenko 1,3-*anti* reduction of ketone **57**

Due to the extreme sensitivity of SmI_2, this reagent was always freshly prepared by sonicating a mixture of samarium metal and 1,2-diiodoethane in THF, taking care to rigorously exclude air and moisture. This method reliably produced a deep blue solution of SmI_2 for use in reduction reactions with a 10 mol% loading and excess of propionaldehyde. The ^{1}H NMR spectrum of **63** was identical to that previously reported, with the *anti*-configuration between C_7 and C_9 having previously been confirmed using the Rychnovsky ^{13}C NMR method following acetonide formation.[157]

Following Evans–Tishchenko reduction, ester **63** was then submitted to alkynoate isomerisation. Utilising conditions reported by Rychnovsky,[158] exposure to triphenylphosphine and phenol for a prolonged period of time (48 h) cleanly afforded the desired (2*E*,4*E*) diene **65** in 93% yield (**Scheme 12**). Diagnostically large coupling constants between the olefinic protons ($^3J_{H–H}$ = 15.2–15.7 Hz) confirmed the presence of the thermodynamic, all-*trans* diene product.

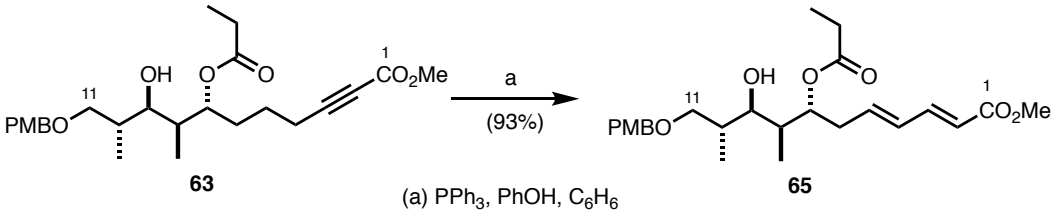

Scheme 12 Isomerisation of alkynoate **63**

A mechanistic description for this thermodynamically driven transformation is outlined in **Scheme 13**. Nucleophilic attack of triphenylphosphine onto alkynoate **63** results in an allenic enolate which can be protonated by phenol at the α-position to yield conjugated olefin **66**. Subsequent proton transfer and isomerisation of the olefin yields **67** which is additionally stabilised as a phosphorus ylid. Protonation of the ylid intermediate followed by E1cB elimination furnishes the thermodynamically favoured (*E*,*E*) diene. The use of phenol as a cocatalyst is crucial in this reaction; its inherent acidity facilitates the initial addition of triphenylphosphine to the alkyne, whilst its strong conjugate base (PhO^-) can promote the subsequent proton transfer steps.

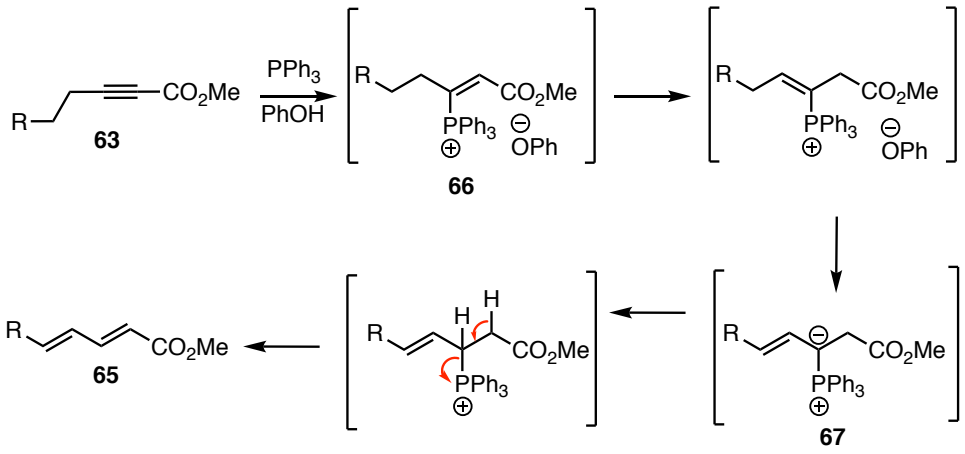

Scheme 13 Mechanistic rationale for the triphenylphosphine promoted isomerisation of alkynoates

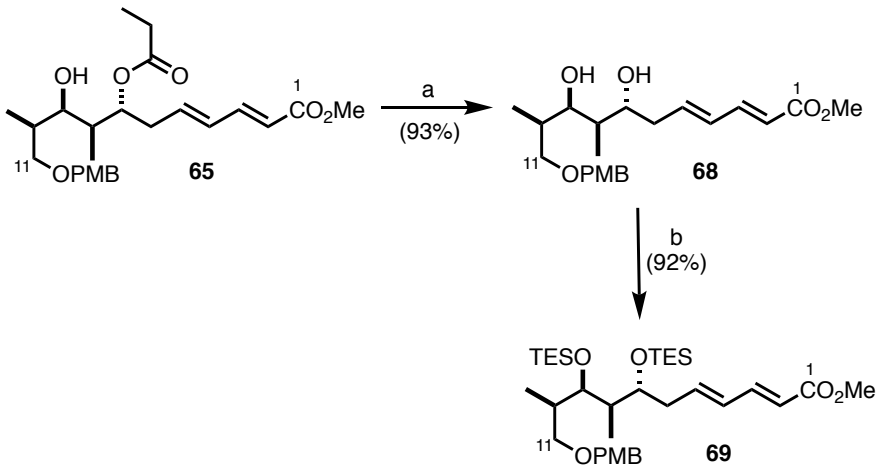

(a) K_2CO_3, MeOH; (b) TESOTf, 2,6-lutidine, −78 °C

Scheme 14 Methanolysis of ester **65** and subsequent *bis*-TES protection of diol **68**

As differential protection of the C_7 and C_9 hydroxyl groups was not required, methanolysis of ester **65** (K_2CO_3, MeOH) yielded diol **68** as a single diastereoisomer in 93% yield (**Scheme 14**). At this point, it was necessary to decide on a suitable protecting group strategy to advance material towards our aplyronine analogues. In the first generation Paterson approach to the aplyronines, a cyclic *para*-methoxyphenyl (PMP) acetal had been used, in anticipation of the increased conformational rigidity associated with this group biasing the macrolactonisation to favour the desired 24-membered macrocycle.[159] Alongside this, a more recent strategy had been developed in the group involving a *bis*-TES ether protection of the hydroxyl groups.

Whilst both protecting group strategies on this fragment were initially investigated by the author, informative results came from Talia Pettigrew which indicated that *bis*-TES protection would ultimately be superior to the PMP route. Pettigrew had advanced material with both protecting groups to the macrolactone core and found that the PMP variant encountered more problems and complications compared to the *bis*-TES version. Consistently lower yields plagued the PMP route, together with purification difficulties at the HWE coupling stage.[158] Based on these observations it was ultimately decided to move forward with the *bis*-TES approach for continued work towards analogue development.

An additional advantage of this route is the early installation of the TES ethers which are utilised in the endgame of the aplyronine total synthesis. With only one site for macrolactonisation in our analogues, this circumvents the need for a more rigid protecting group and ultimately avoids a now unnecessary protecting group swap, streamlining the route overall.

Resultingly, treatment of diol **68** with an excess of TESOTf afforded **69** in 92% yield (**Scheme 14**). Overall this fully protected northern fragment precursor **69** could be accessed in 9 steps and 37% yield from (*R*)-Roche ester. Additional plentiful stocks of this fragment were generously supplied by Dr Mike Housden for studies towards the aplyronine total synthesis and analogue development. With this key intermediate in hand, attention then turned to elaborating this material into the required northern phosphonate **36** for advanced fragment coupling.

2.1.3 Elaboration into C_1–C_{11} iodide 56

From **69**, the required northern fragment **36** could be accessed in a further 5 steps. In preparation for the subsequent alkylation step (*vide infra*, **Section 2.1.4**), the terminal C_{11} PMB ether would need to be elaborated to a primary iodide and the C_1 ester reduced and protected as a TBS ether.

The C_{11} alcohol could be revealed by a DDQ mediated, oxidative cleavage of the PMB group. Mechanistically the deprotection proceeds *via* initial formation of a charge transfer complex through a series of single electron transfer (SET) steps between the electron rich PMB aromatic ring and the electron accepting DDQ. This is followed by benzylic dehydrogenation, affording the desired deprotected alcohol and PMB aldehyde as illustrated in **Scheme 15**.[160]

Pleasingly, this transformation proceeded smoothly under neutral conditions (pH 7.0 buffer) to afford alcohol **70** in 89% yield with no identifiable byproducts detected or migration of the silyl groups observed. In the analogous transformation, carried out by the author, with C_7 and C_9 protected as a PMP acetal the yield was significantly lower at 67%. This drop in yield can be attributed to migration of the acetal group to the terminal position and overoxidation of the PMP group leading to benzoate byproducts.[159] These side reactions were thought to be promoted by the production of the weakly acidic DDQH (**Scheme 15**) and could not be fully suppressed, even with the use of pH 9.2 buffer. This outcome further cemented the choice of the *bis*-TES protection strategy moving forward.

At this stage, alcohol **70** represented a stable intermediate that could be safely stored at –20 °C for prolonged periods of time with no obvious degradation. Therefore, major stocks of material were stored at this point as the ensuing intermediates containing the primary iodide or phosphonate moiety were observed to degrade over time and were best used immediately.

Alcohol **70** could then be converted to iodide **71** under standard Appel-like conditions (PPh_3, imidazole, I_2) in good yield (**Scheme 16**).[161,162] Due to the potential for interference in the subsequent alkylation step, the carbonyl moiety at the C_1 ester was reduced to the primary alcohol and masked as a TBS ether. Treatment of ester **71** with excess DIBAL, followed by protection with TBSCl afforded **56** in 96% yield over two steps (**Scheme 16**). This completed the synthesis of the full C_1–C_{11} iodide segment **56** and set the stage for the final alkylation step and completion of the northern fragment.

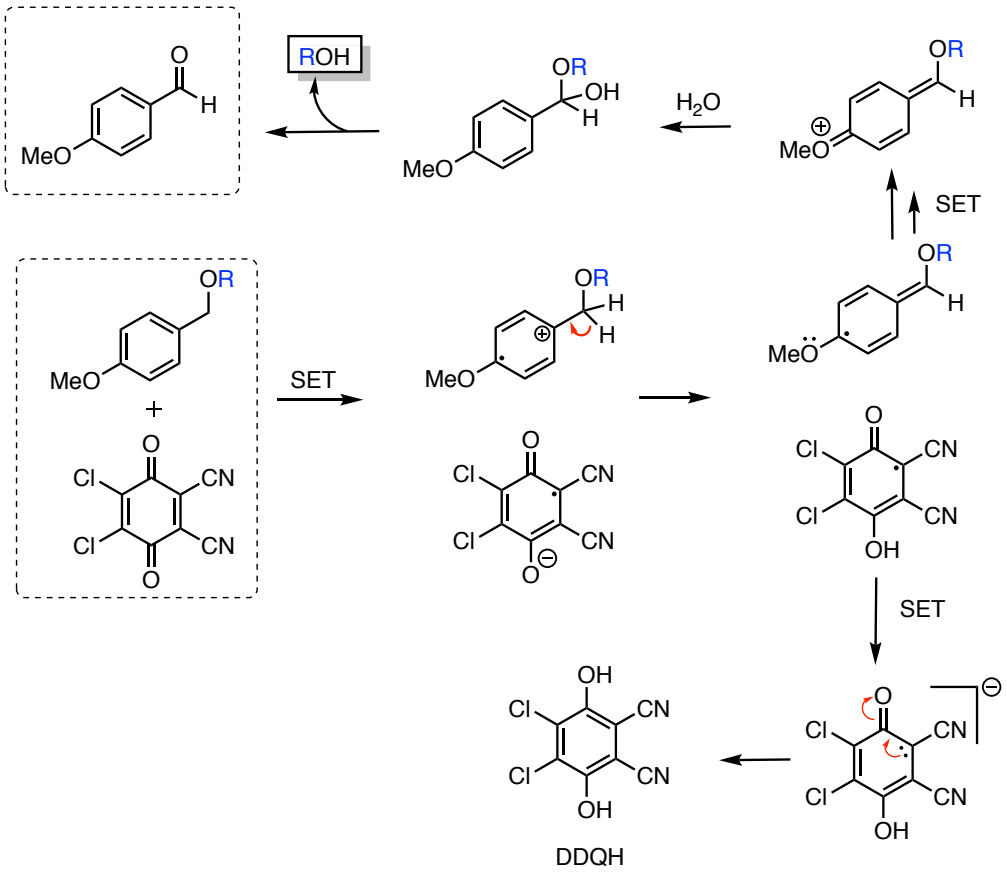

Scheme 15 Proposed mechanism for DDQ mediated deprotection of a PMB ether

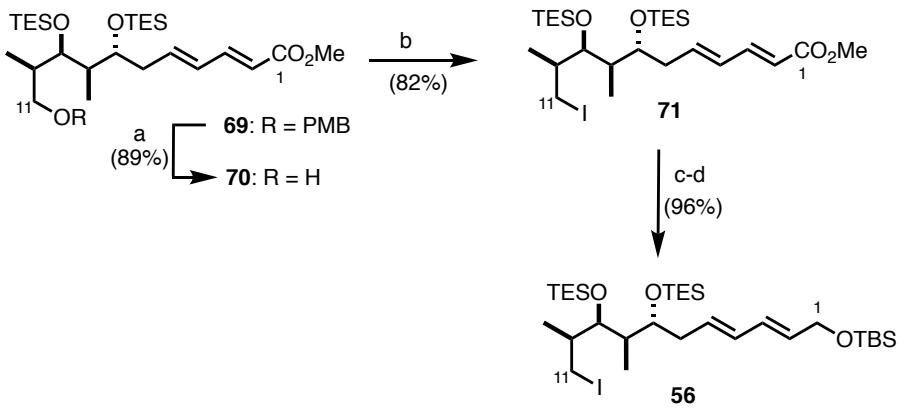

(a) DDQ, CH_2Cl_2/pH 7.0 buffer (2:1); (b) PPh_3, imidazole, I_2, MeCN/Et_2O (1:1), 0 °C → rt; (c) DIBAL, CH_2Cl_2, −78 °C; (d) TBSCl, imidazole, CH_2Cl_2

Scheme 16 Deprotection and elaboration of **69** to iodide **56**

2.1.4 Alkylation to C_1–C_{14} phosphonate 36

The Paterson approach for advanced fragment coupling necessitates the installation of a β-ketophosphonate moiety to engage in an HWE reaction to forge the C_{14}–C_{15} trisubstituted olefin. Homologation of the carbon chain of iodide **56** can be accomplished by a chain extension alkylation with **72**, utilising conditions developed by Grieco and Pogonowski.[163]

Synthesis of the C_{12}–C_{14} β-ketophosphonate linker **72** can be achieved through deprotonation of commercially available diethyl ethylphosphonate with *n*-BuLi, followed by quenching with ethyl acetate (**Scheme 17)**. This process is amenable to large scale; the product **72** can be isolated cleanly *via* distillation under reduced pressure in good yield. Additionally, this product can be stored at –20 °C for prolonged periods of time with no obvious degradation.

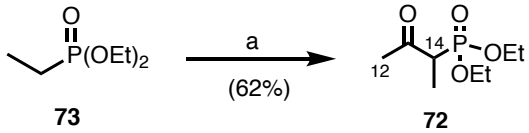

73 **72**

(a) *n*-BuLi, THF, −78 °C, 1h; *then* EtOAc

Scheme 17 Synthesis of linker phosphonate **72**

Sequential deprotonation of **72** with sodium hydride followed by *n*-BuLi generated a pale-yellow solution of the required dianion for alkylation with iodide **56**. Under kinetic control at low temperatures, dianions derived from β-ketophosphonates have been found to react at the less hindered and more basic γ-position as illustrated by Grieco (**Scheme 18**).

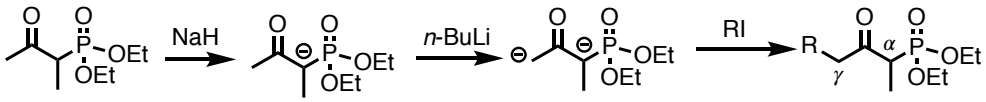

Scheme 18 Regioselective alkylation of dianions derived from β-ketophosphonates

However, the selectivity of this reaction proved challenging to control. As expected, there is to be no stereoselectivity at C_{14}, with a 1:1 mixture of diastereoisomers formed at this position. Additionally, Dr Lydia Lee discovered that the undesired regioisomer stemming

from reaction at the α-position was a significant constituent of the isolated material (*ca*. 20-30%).[157] This branched regioisomer is inseparable from the desired product by column chromatography, but fortunately does not engage in the subsequent HWE reaction and can be readily separated after that stage.

The regioselectivity of the alkylation shows marked differences depending on the identity of the iodide electrophile. Reaction with PMP protected iodide **74** at −50 °C resulted in the formation of desired phosphonate **75** alongside the undesired regioisomer **76** in a 6:1 ratio. Conversely, with the more hindered *bis*-TES protected iodide **56** no reactivity was observed below 0 °C and as a result the regiomeric ratio was a disappointing 3:1 (**Scheme 19**). Interestingly, the addition of HMPA to encourage deaggregation of the dianion did not appear to affect the outcome.

Significant optimisation studies on this challenging reaction were first undertaken by Lee (on the PMP system) and more recently by Anžiček and Pettigrew (on the *bis*-TES variant).[157,164,165] A wide variety of conditions were trialled, including choice of solvent, order of addition of reagents, the influence of HMPA, concentration and scale. However, the reaction remained capricious and no significantly improved conditions were ultimately found. The best results for the *bis*-TES system moving forward seemed to be an approximately 3:1 ratio of regioisomers and a modest yield (60-70%) on multigram scale. This outcome was considered reasonable and, for the purposes of advancing material towards our designed aplyronine analogues, no additional time was spent in further optimisation of this reaction.

This alkylation step concludes the synthesis of the C_1–C_{14} northern phosphonate **36** which overall was accessed in 14 steps and in 18% yield from commercially available (*R*)-Roche ester.

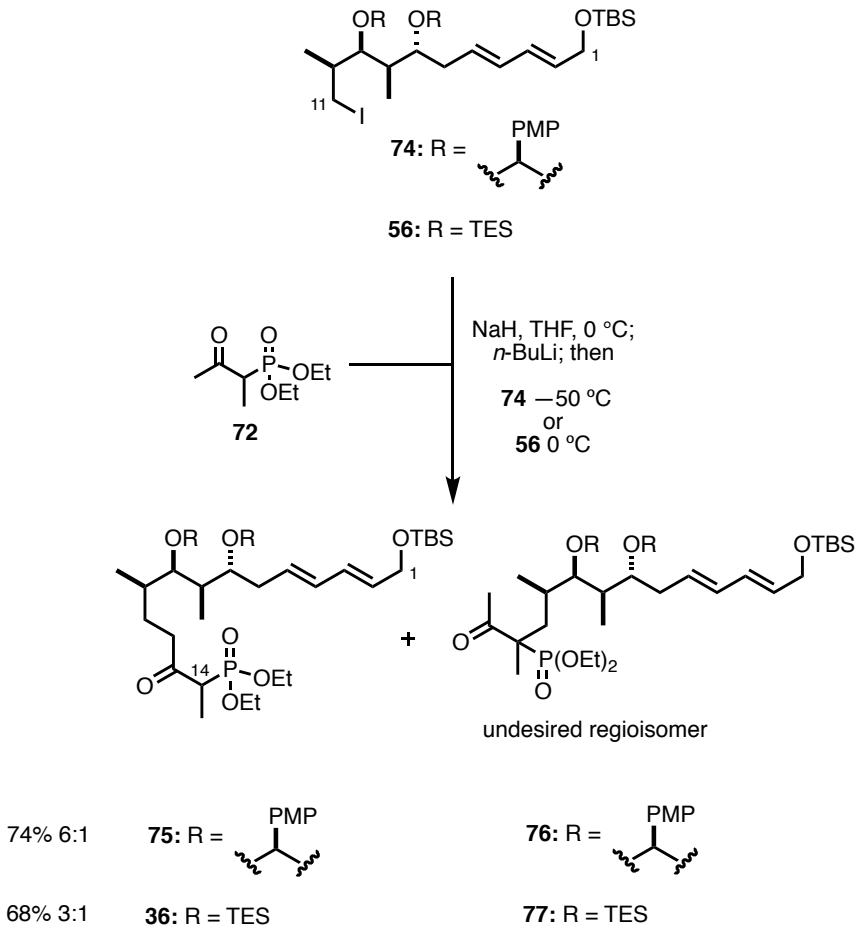

Scheme 19 Contrasting results for the alkylation of PMP and *bis*-TES protected iodides **74** and **56** in the alkylation reaction with phosphonate **72**

2.2 C_{28}–C_{34} side chain ketone 51

The necessary side chain fragment **51** for our designed aplyronine analogues possesses one modification: replacement of the C_{29} acetoxy by a methyl ether moiety. A third-generation approach to access a variant of this ketone coupling partner was developed by Dr Sarah Fink in the synthesis of aplyronine C and is outlined in **Scheme 20** below.[137] Our planned modification lends itself well to incorporation *via* this route.

Key structural features of this fragment include the terminal *N*-vinyl formamide functionality, which can be installed from aldehyde **78** under modified Wittig conditions with subsequent isomerisation to the (*E*)-olefin. The 1,3,4-*syn* stereotetrad is set in a diastereoselective aldol reaction of (*R*)-Roche ester derived ethyl ketone **42** and acetaldehyde.

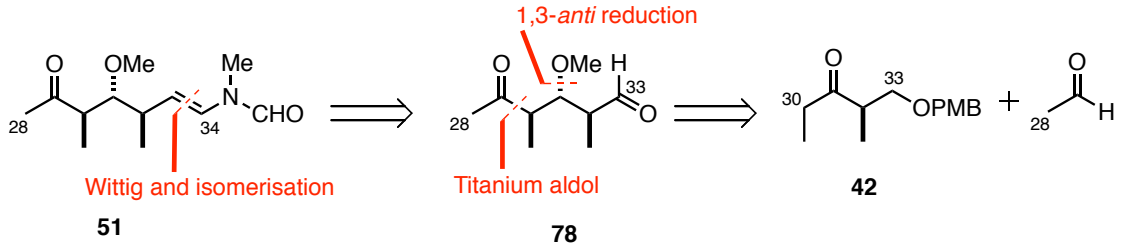

Scheme 20 Retrosynthetic analysis of the C_{28}–C_{34} side chain ketone fragment **51**

The groundwork on this fragment was undertaken by Talia Pettigrew, who proved the validity of Fink's route for incorporation of the methyl ether functionality. Initial work by Pettigrew bore out a titanium-mediated aldol coupling to set the requisite *syn* stereochemistry. Preliminary investigations into *N*-vinyl formamide installation *via* a double Swern oxidation and Wittig reaction sequence was met with reasonable success, albeit on small scale (9 mg, 21% yield). For completeness, Fink and Pettigrew's work is summarised in **Scheme 21**.

The aim of the author was therefore to build on Pettigrew's initial results and access multigram quantities of key intermediates to deliver a sizeable stockpile of side chain ketone **51** for advanced fragment coupling. In particular, the modified Wittig approach was targeted as a step that required optimisation and further investigation. Synthetic efforts reported hereupon are those of the author.

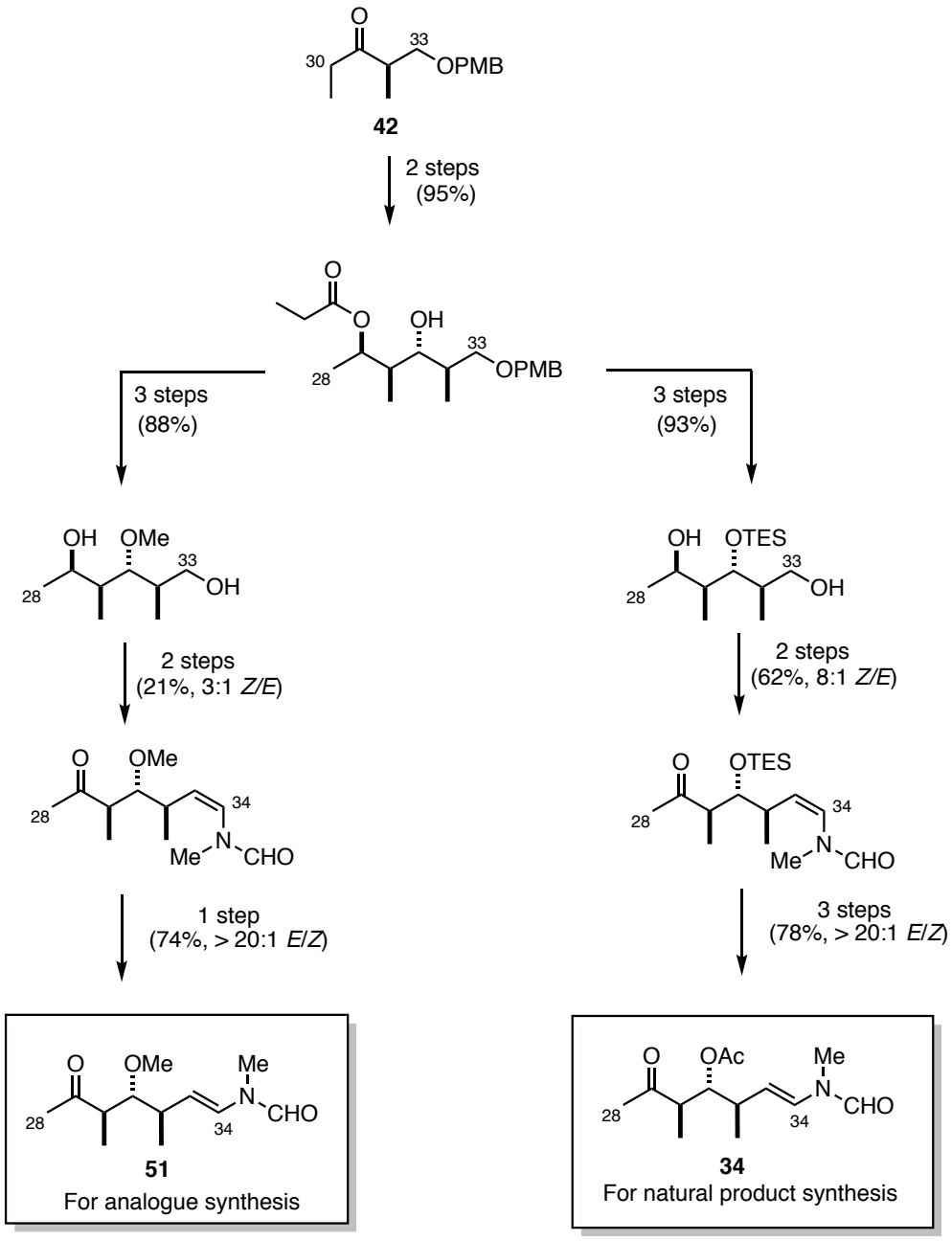

Scheme 21 Fink and Pettigrew's work on synthesising side chain ketone fragments **34** and **51**

2.2.1 Titanium-mediated aldol coupling

Fink's original protocol to construct the C_{29}–C_{30} bond relied upon a tin (II) triflate mediated aldol reaction to set the desired *syn* stereochemistry. However, recent work within the Paterson group on titanium-mediated aldol methodology has superseded this approach.[164,165] Compared to their tin counterparts, titanium-mediated aldol reactions convey a number of advantages. For example, asymmetric aldols utilising tin Lewis acids appear to be highly dependent on reagent quality.[120] Additionally, the preparation of these reagents is often lengthy and necessitates the use of hazardous materials, ultimately generating a significant amount of toxic tin waste.

Urpí and Romea have demonstrated the feasibility of titanium (IV) enolates in asymmetric aldol reactions to assemble polypropionate motifs in polyketide natural products.[166,167] Titanium Lewis acids such as $TiCl_4$ and the softer Ti(*i*-PrO)Cl_3 have been found to selectively generate (*Z*)-enolates, which upon addition of an aldehyde result in the formation of the *syn*-product. Based on this discovery, this methodology has been incorporated into the aplyronine project as a desirable alternative to tin mediated aldol reactions.

Attractively, the required ethyl ketone **42** required for the side chain fragment is identical to that utilised previously in the northern fragment synthesis (**Section 2.1.1**). In this case ketone **42** could be enolised upon treatment with Ti(*i*-PrO)Cl_3 and diisopropylethylamine at −78 °C to afford the desired (*Z*)-enolate **79** (**Scheme 22**). Treatment with excess acetaldehyde forged aldol adduct **80** in 77% yield and 17:1 *dr*. This reaction was extremely amenable to scale up and was reliably reproducible, which was exemplified with a 12 g batch yielding 77% of **80** in 14:1 *dr* in a single manipulation. This further highlights the robustness and operational ease of the titanium aldol method.

The reaction between titanium enolates and aldehydes is understood to proceed *via* a chelated Zimmerman–Traxler transition state as illustrated in **Scheme 23**.[168] This chair-like conformation is facilitated by strong titanium-oxygen interactions between the electron-rich PMB group and the highly oxophilic titanium centre. The stereoselectivity is conveyed from the stereogenic centre on the enolate, with the major all-*syn* aldol product arising from the less sterically crowded transition structure **TS-3.**

Pleasingly, upon inspection, NMR comparisons between the titanium (IV) and tin (II) aldol products were identical.[137]

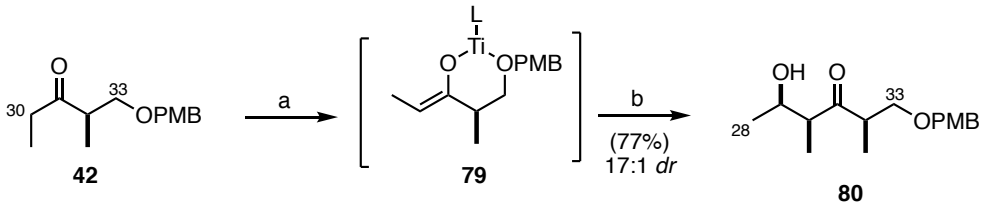

Scheme 22 Titanium mediated aldol reaction of ethyl ketone **42** and acetaldehyde

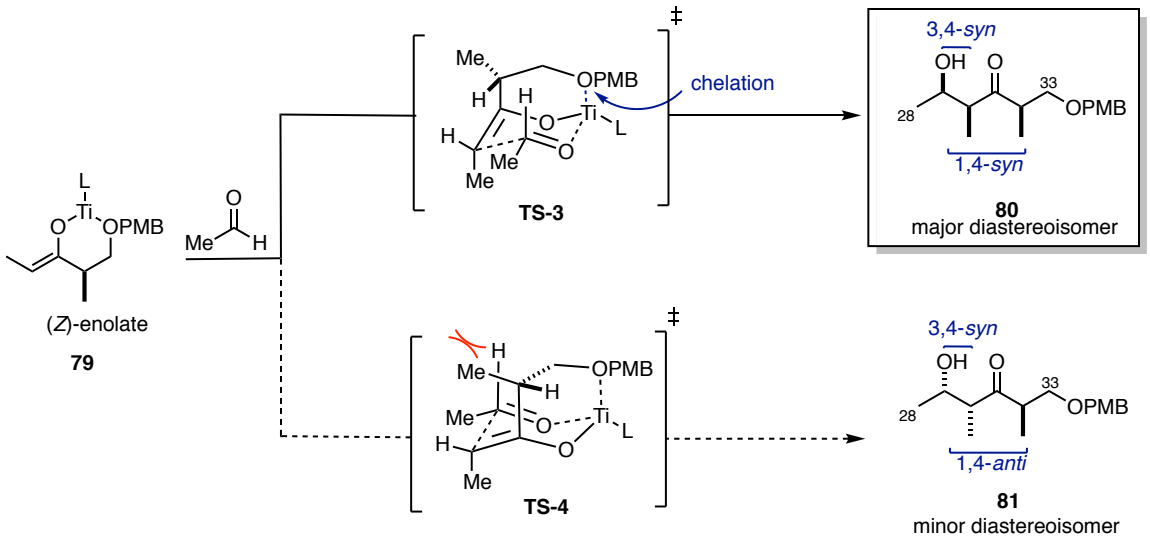

Scheme 23 Models for competing transition states in the titanium (IV) mediated aldol reaction of ketone **42**

Subsequent Evans–Tishchenko reduction of aldol adduct **80** yielded ester **82** and set the configuration across the full stereotetrad. This reaction again exhibited very high yields and excellent diastereoselectivity (97%, >95:5 *dr*) for the 1,3-*anti* product with no appreciable loss of selectivity on multigram scale (**Scheme 24**). Ultimately, through this aldol reaction and reduction sequence, over 12 g of intermediate **82** was efficiently prepared in a single batch.

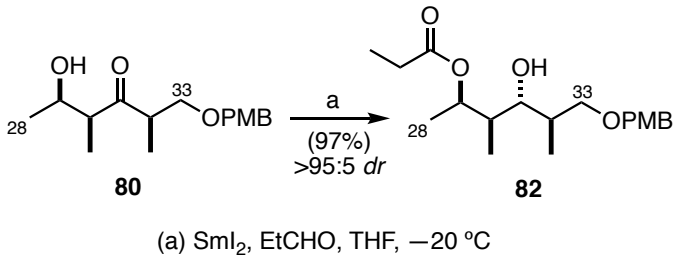

Scheme 24 Evans–Tishchenko reduction of aldol adduct **80**

2.2.2 Elaboration to diol 83

Alcohol **82** represents the point of divergence between the natural product and the analogue aplyronine projects (**Scheme 21**). Protection of the C_{31} hydroxyl with a TES ether, before a protecting group swap after the Wittig reaction, ultimately leads to the natural product fragment with the acetoxy functionality. This switch was necessary as the acetate group was found to be prone to elimination in the subsequent Wittig step. For analogue development, the desired methyl ether moiety could instead be installed at this point as we anticipated that it would be more robust and less susceptible to elimination. This tactic would save us two synthetic steps and the associated processing time and effort by avoiding the protecting group exchange.

Methylation could be achieved by treatment of alcohol **82** with Meerwein salt (Me_3OBF_4) and proton sponge which proceeded smoothly. Cleavage of the PMB ether with DDQ, followed by DIBAL reduction revealed diol **83**, as illustrated in **Scheme 25**. This set the stage to begin investigations into the challenging Swern oxidation and Wittig sequence to append the delicate *N*-vinyl formamide moiety.

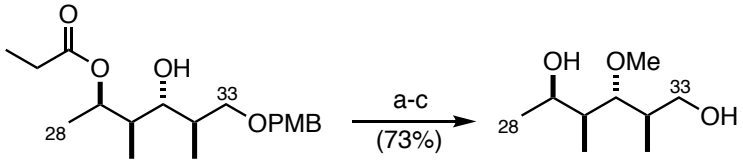

82 **83**

(a) Meerwein salt, proton sponge, CH_2Cl_2; (b) DDQ, CH_2Cl_2/pH 7.0 buffer (2:1), 0 °C; (c) DIBAL, CH_2Cl_2 −78 °C

Scheme 25 Synthesis of diol **83**

2.2.3 *N*-vinyl formamide installation

With diol **83** in hand, the two termini could be concurrently advanced to their desired oxidised forms. Kinetically, oxidation at C_{33} is expected to be more rapid, risking the formation of a cyclic byproduct through intramolecular hemiacetal formation through the C_{29} hydroxyl group. This issue could be circumvented by the use of a double Swern oxidation, as demonstrated by Fink.[120] Mechanistically, this activates both hydroxyls as the corresponding alkoxysulfonium salts before the addition of triethylamine triggers carbonyl formation, thus limiting the potential for nucleophilic attack. Resultingly, formation of the sensitive keto-aldehyde **78** could be achieved under these conditions, with no discernible epimerisation of the α-stereocentres observed (**Scheme 27**). This material was found to be extremely unstable on silica and was therefore best used crude with minimal purification. During work-up, the combined organics could be washed carefully with dilute acid (0.5 M HCl), base ($NaHCO_3$) and finally brine to successfully remove the triethylamine hydrochloride salt produced in the Swern oxidation, which would inevitably quench the ylid formed in the following Wittig olefination. Additionally, aldehyde **78** was always cautiously concentrated *in vacuo* to minimise losses due to volatility.

With aldehyde **78** in hand, attention turned to the installation of the sensitive *N*-vinyl formamide subunit. The modified Wittig protocol discussed here was developed within the Paterson group in earlier studies towards aplyronine A (**21**)[139] and has since been employed in our total synthesis of reidispongiolide A (**29**).[169] The necessary phosphonium salt **84** could easily be prepared in a two-step sequence. Following the protocol of Couture,[170] *N*-methyl formamide and paraformaldehyde were reacted with TMSCl in refluxing chloroform to give *N*-(chloromethyl)-*N*-methylformamide **85**, which could be treated with triphenylphosphine to precipitate phosphonium salt **84** in 32% yield. Despite the low yield, this method is very amenable to scale-up to produce large quantities of the solid Wittig

reagent, which could be stored at –20 °C indefinitely with no obvious degradation. To access this fragment Fink utilised an alternative protocol which employed thionyl chloride as the chlorinating agent.[171] However, this has the disadvantage of producing large volumes of hydrochloric acid and sulfur dioxide as gaseous byproducts on scale and necessitates the distillation of **85**. Couture's procedure is therefore operationally simpler and delivers **84** in a comparable yield to that of Fink.

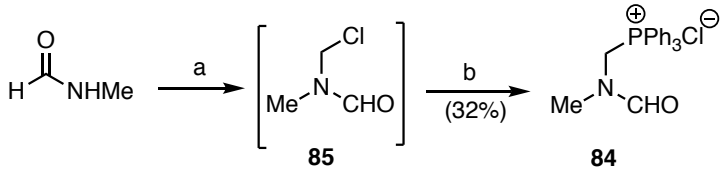

(a) $(CH_2O)_n$, TMSCl, $CHCl_3$, 60 ºC; (b) PPh_3, Et_2O

Scheme 26 Synthesis of phosphonium salt **84**

Treatment of phosphonium salt **84** with LiHMDS generated the required ylid. However, upon addition of keto-aldehyde **78**, the desired enamide **86** was formed in a disappointing 30% yield (3:1 *Z*/*E*) over the two steps (**Scheme 27**). Whilst this represents an improvement on Pettigrew's preliminary results, this was in stark contrast to Fink's outcome with the C_{31} TES protected variant (75% over two steps, 8:1 *Z*/*E*).[120] Despite numerous attempts, the poor result could not initially be improved upon, with yields consistently in the range of 25-35%.

No identifiable byproducts could be detected by TLC, nor isolated *via* column chromatography of the crude material. The Wittig olefination was judged to be the problem step, with the oxidation apparently proceeding reasonably well (80-90%) as judged by the crude ^{1}H NMR, with good mass recovery of aldehyde **78**. Interestingly, no elimination products were ever observed in this reaction, lending a degree of confidence to our initial hypothesis that the methyl ether is indeed more robust in this sense than the acetoxy moiety.

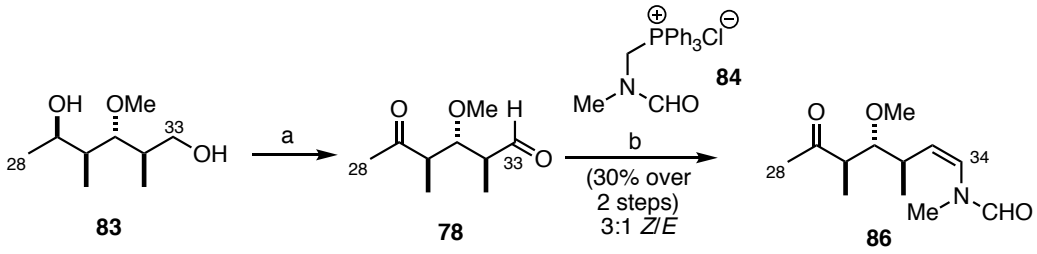

(a) $(COCl)_2$, DMSO, NEt_3, CH_2Cl_2, −78 ºC → 0 ºC; (b) LiHMDS, **84**, THF, −78 ºC → 0 ºC, 45 min; then **78**, −78 ºC

Scheme 27 Swern oxidation and Wittig olefination sequence to access enamide **86**

Frustratingly, the low mass balance after the Wittig reaction could not be accounted for and an alternative approach was therefore sought. An examination of the literature, particularly within the syntheses of related natural products possessing this *N*-vinyl formamide terminus, revealed varying approaches for incorporation of this challenging subunit. In Yamada's total syntheses of aplyronines A, B and C (**21**-**23**), this moiety is installed classically *via* the condensation of aldehyde **87** with *N*-methyl formamide under mildly acidic conditions. The thermodynamic (*E*)-olefin was formed in a modest 48% yield (**Scheme 28**).[92,97]

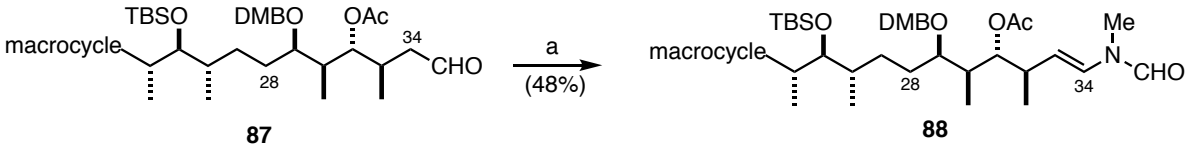

87 **88**

(a) MeNHCHO, PPTS, hydroquinone, benzene, 80 ºC

Scheme 28 Yamada's condensation approach to install the terminal *N*-vinyl formamide[97]

Paterson's alternative protocol utilises P_2O_5 to promote the condensation and act as dehydrating agent. This was successfully implemented in the total synthesis of scytophycin C (**31**, **Scheme 29**) from aldehyde **89**.[139,172]

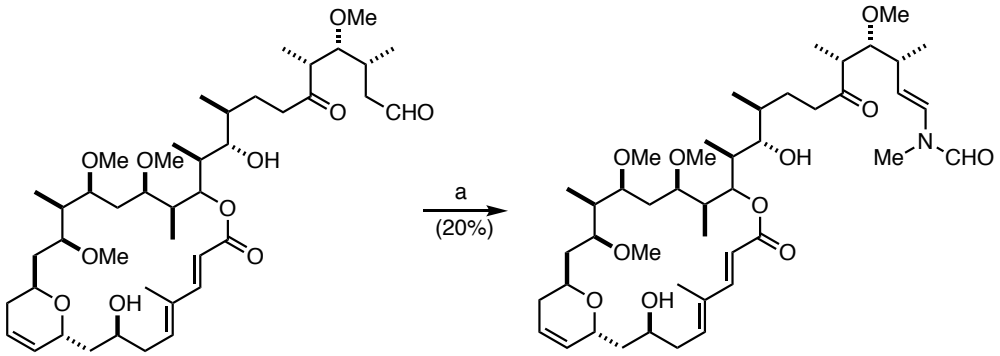

89 **31**

(a) P_2O_5, MeNHCHO, CH_2Cl_2

Scheme 29 Paterson's P_2O_5 mediated condensation reaction to install the *N*-vinyl formamide functionality[172]

However, these condensation reactions require the preparation of a homologated aldehyde, which would require significant synthetic effort with a new retrosynthetic approach. Thus, this methodology was judged not to be viable at this time.

Advances in metal-catalysed *N*-alkenylation reactions have expanded the chemist's toolbox and can be useful for installing *N*-vinyl formamide moieties. Takai olefination of an aldehyde or hydrozirconation of a terminal alkyne can generate (*E*)-vinyl halides with good levels of stereoocontrol.[173,174] With the desired (*E*)-geometry pre-installed, a metal-catalysed cross coupling can then deliver the required *N*-vinyl formamide.[175]

In particular, Miyashita and co-workers applied a Takai olefination and Buchwald amidation sequence to great success in their synthesis of scytophycin C (**31**, **Scheme 30**).[176,177] Importantly, scytophycin C (**31**) bears a remarkably similar side chain to that of our designed aplyronine analogues. The *N*-vinyl formamide terminus was introduced in 59% yield over the two steps from aldehyde **90** – a marked improvement on Paterson's 20% yield for the condensation reaction (**Scheme 29**). Notably, Miyashita additionally reported extreme difficulties in utilising the Wittig method to complete this transformation, with elimination of methanol being the predominant outcome and no desired product detected.

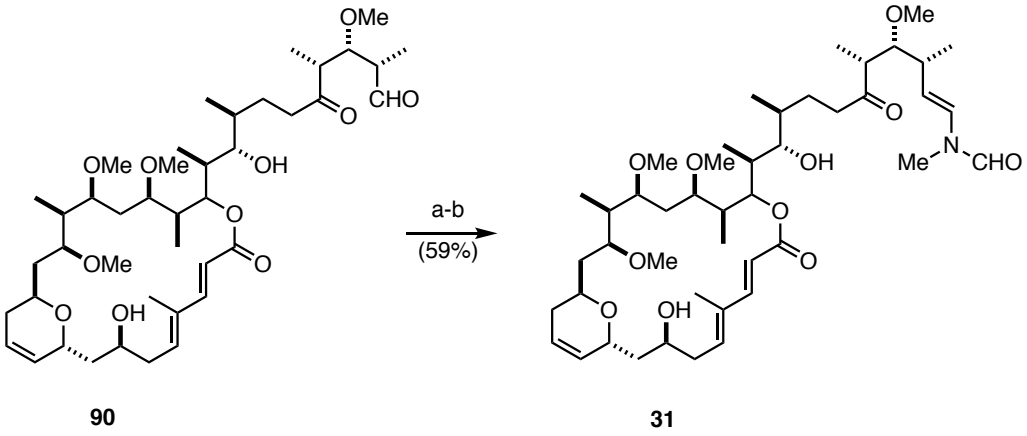

90 **31**

(a) $CrCl_2$, CHI_3, THF, 0 ºC; (b) *trans*-1,2-cyclohexanediamine, CuI, K_3PO_4, MeNHCHO, dioxane

Scheme 30 Miyashita's Takai–Buchwald sequence for terminal amidation of aldehyde **90** [177]

Encouraged by this successful example and noting that this sequence conveniently intersected our developed route well, the Takai olefination–Buchwald amidation approach was investigated as a potential solution to the difficulties previously encountered. However, disappointingly this was not to be the case. Attempted Takai olefination of aldehyde **78** led to a mixture of elimination products whilst the desired (*E*)-vinyl iodide **91** was not detected (**Scheme 31**). Further optimisation of this reaction was not undertaken.

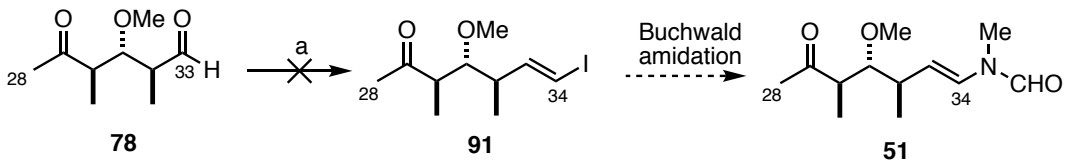

(a) $CrCl_2$, CHI_3, THF, 0 ºC

Scheme 31 Attempted Takai olefination to produce (*E*)-vinyl iodide **91**

On balance, it was decided to follow Fink's original protocol with a TES ether in place at C_{31}, and to undertake a protecting group swap to install the new methoxy group after the Wittig reaction, thus mirroring the approach used to construct the natural products. Whilst this route would not save any synthetic steps in this sequence, it should result in a greater overall yield and allow for a smoother and higher throughput of material. This strategy would be dependent on the resulting methylation proceeding efficiently and without elimination, nor degradation of the *N*-vinyl formamide. The viability of this approach was investigated and is outlined in **Scheme 32**.

Returning to intermediate **82** at the diversification point (**Scheme 21**), TES protection could be cleanly accomplished by exposing alcohol **82** to TESOTf and 2,6-lutidine at –78 °C to furnish TES ether **92**. DDQ mediated PMB cleavage and deprotection of the propionate ester with DIBAL furnished diol **93** in 74% yield over two steps (**Scheme 32**).

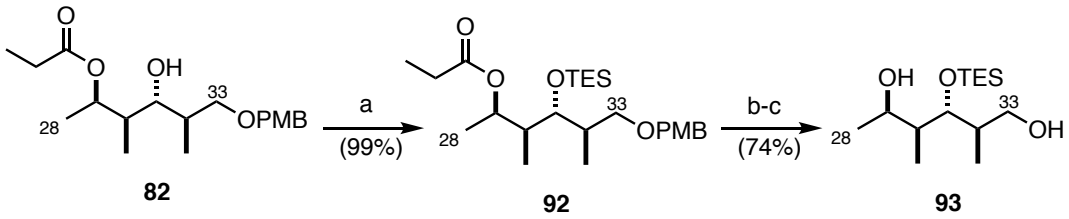

(a) TESOTf, 2,6-lutidine, CH_2Cl_2, —78 ºC; (b) DDQ, CH_2Cl_2/pH 9.2 buffer (4:1); (c) DIBAL, CH_2Cl_2, —78 ºC

Scheme 32 Elaboration of alcohol **82** to TES protected intermediate **93**

Gratifyingly on this TES substrate, the double Swern oxidation and Wittig olefination protocol following the previously utilised sequence delivered formamide **94** in a much-improved yield of 71% on multigram scale. Subsequent TES deprotection under neutral conditions using AcOH-buffered TBAF yielded alcohol **95** in 99% yield (**Scheme 33**). With intermediate **95** in hand, attention turned to the methylation to yield our desired methyl ether-containing fragment.

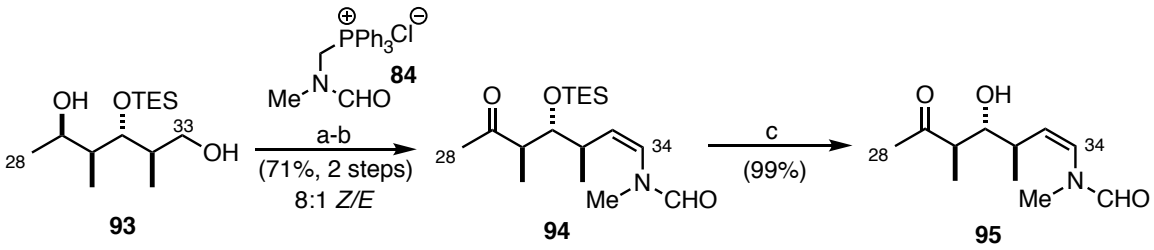

(a) $(COCl)_2$, DMSO, NEt_3, CH_2Cl_2, −78 °C → 0 °C; LiHMDS, **84**, THF, −78 °C → 0 °C, *then* −78 °C; (c) TBAF, AcOH

Scheme 33 Swern–Wittig sequence on TES protected diol **93**

In the event, this seemingly trivial transformation on alcohol **95** proved to be highly troublesome. Initial results using our previous conditions (Meerwein salt and proton sponge) were tantalisingly promising, with the methylation apparently proceeding smoothly on test reaction scale (10 mg, 64%, **Table 3**, entry 1). However, attempts to replicate this result on a preparative scale revealed significant reactivity problems, with minimal conversion observed in all attempts. Further optimisation efforts for this step are outlined in **Table 3**.

Increasing the equivalents of Meerwein salt and proton sponge in an attempt to promote the conversion to methylated product **86** was unsuccessful. Significant starting material remained, combined with a variety of spots on TLC and a complex crude ^{1}H NMR (**Table 3**, entry 3). On the other hand, decreasing the equivalents of reagents, in order to combat unwanted side reactions potentially inhibiting the reaction, again led to no reactivity (**Table 3**, entry 4).

Moving away from the Meerwein system, the classical Williamson ether synthesis (NaH, MeI) was trialled (**Table 3**, entry 5).[178] Perhaps unsurprisingly, significant decomposition was observed during this reaction, presumably *via* a retro aldol-type mechanism. Late stage methylation utilising methyl triflate and 2,6-di-*tert*-butylpyridine has seen some success within complex natural product syntheses, as demonstrated by Evans and co-workers in their synthesis of ionomycin A. However, the authors do report that this reaction can be "quite substrate dependant." [179] Nevertheless, these conditions were applied to our *N*-vinyl formamide system but returned poor results (**Table 3**, entry 6). No discernible product (or byproduct) could be isolated from the complex mixture.

A survey of the literature directed us towards the avenue of carbohydrate methodology and revealed the silver (II) oxide–methyl iodide methylation system, originally developed by

Kuhn.[180,181] Standard procedures called for the use of a polar solvent and 3 equivalent of MeI and 2 equivalents of Ag_2O per alcohol to be methylated. Application of this protocol in acetonitrile at room temperature yielded only starting material as judged by TLC analysis. Upon gradual warming of the reaction to 80 °C, trace amounts of desired methylated product were observed (**Table 3**, entry 7). Encouraged by this result, the material was re-submitted and reacted at 80 °C from the beginning. Puzzlingly, despite refluxing for a prolonged period of time, no methylated product **86** was detected and starting material was returned quantitively upon work-up (**Table 3**, entry 8). Switching the reaction solvent to DMF at 80 °C was destructive and led to a mixture of elimination products (**Table 3**, entry 9).

Table 3 Screen of methylation conditions on alcohol **95**

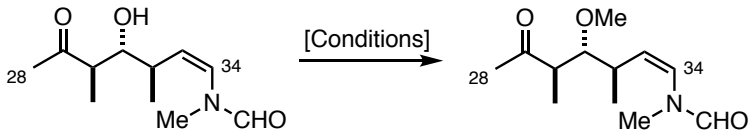

95 **86**

Entry	Scale / mg	Conditions	Result	Comment
1	10	Me_3OBF_4 (4 eqv.) proton sponge (5 eqv.)	64% **86**	
2	50	Me_3OBF_4 (4 eqv.) proton sponge (5 eqv.)	Starting material	Faint by-products on TLC
3	50	Me_3OBF_4 (10 eqv.) proton sponge (12 eqv.)	Starting material	Messy TLC and crude NMR
4	50	Me_3OBF_4 (2 eqv.) proton sponge (3 eqv.)	Starting material	
5	10	MeI NaH	Decomposition	Assumed retro aldol
6	25	MeOTf (10 eqv.) 2,6-di-*tert*-butylpyridine (20 eqv.)	Decomposition	No byproducts isolated
7	50	MeI, Ag_2O, MeCN rt $\rightarrow$ 80 °C	Trace product	Mainly starting material
8	50	MeI, Ag_2O, MeCN 80 °C	Starting material	
9	50	MeI, Ag_2O, DMF 80 °C	Elimination	

Based on these vexing results, it was clear that this post-Wittig methylation strategy was not a viable route to access our desired fragment. In the end, with limited options available, attention returned to the originally planned Wittig olefination on aldehyde **78** with the C_{31} methyl ether already installed.

The nature of the alcohol protecting group at C_{31} appears to have a significant effect on the outcome of the Wittig olefination, with drastic differences in yield observed under identical conditions (**Table 4**).

Table 4 Variations in yield observed in the modified Wittig reaction

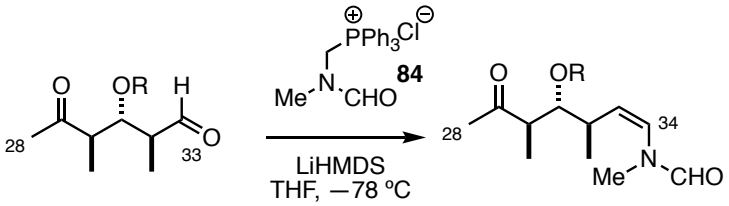

Entry	R	Yield (over two steps)
1	TES	71% (8:1 *Z/E*)
2	Me	35% (3:1 *Z/E*)
3	PMB[a]	43 % (5:1 *Z/E*)

[a] Reaction performed by Dr Sarah Fink [120]

Elimination tends to be the main reported problem and seems to account for the reduction in yield, especially for the PMB variant (**Table 4**, entry 3). Fink noted that PMBOH made up 25% of the crude material, presumably caused by the excess ylid competitively acting as a base in an E2 or E_1cB reaction.[120] As previously discussed, no elimination products were ever observed by this author in the methyl ether system.

Reidispongiolide A (**29**) possess a very similar side chain to our targeted analogues. During their total synthesis, Paterson and co-workers applied this modified Wittig olefination to deliver enamide **96** in a respectable 52% yield (**Scheme 34**).[169] This result further highlights that the methyl ether system does appear to suffer from reduced yields compared to the TES equivalent. Aldehyde **97** is almost identical to our substrate: the only difference is the lack of a methyl group at C_{32}, therefore rendering it not α-chiral. This could explain the greater efficiency of the reaction on this less delicate substrate. In an effort to optimise this challenging reaction, we returned to our initial protocol for the Wittig olefination.

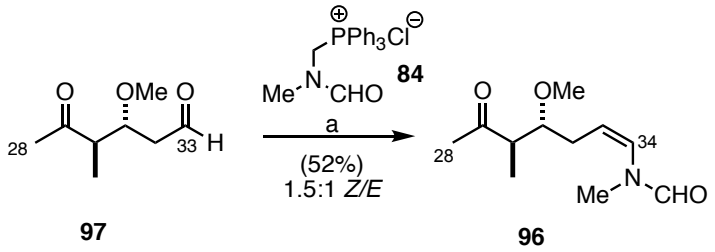

97 **96**

(a) LiHMDS, **84**, THF, −78 ºC → 0 ºC, *then* **97**, −78 ºC

Scheme 34 Installation of the enamide functionality in reidispongiolide A (**29**)

The procedure reported in the original publication shows marked differences to that used in recent syntheses within the group.[139] The aplyronine and reidispongiolide systems both make use of a slight excess of both phosphonium salt **84** and LiHMDS (1.5 and 1.4 equivalents respectively), with the excess base ensuring full deprotonation of the salt. Upon addition of the base to generate the ylid, the system is warmed from −78 °C to 0 °C over 30 min, during which time the white suspension turns bright yellow, before being re-cooled to −78 °C for the addition of the aldehyde. Contrastingly, Paterson's original protocol calls for a much higher excess of reagents (2 equivalents of phosphonium salt **84** and 3 equivalents of base). An additional difference between the two procedures is the work-up protocol. Initially this made use of a neutral quench (pH 7.0 buffer) which had been replaced to by acidic quench (NH_4Cl) in the aplyronine project.

With some trepidation, we returned to original protocol. Fearing that 3.0 equivalents of LiHMDS might promote unwanted side reactions, the loading was dropped to 2.1 equivalents in conjunction with 2.0 equivalents of phosphonium salt **84**. Progressively warming the system from −78 °C to 0 °C over 2 h, instead of only 30 min, was also introduced. A much slower generation of ylid was observed, as evidenced by a very gradual change in reaction colour from white to bright yellow over this warming period. Pleasingly, initial results from quenching with pH 7.0 buffer were good, with the reaction delivering much improved yields on scale (**Table 5**). Ultimately, this reaction could reliably deliver enamide **86** in 50-60% yield over two steps. This was evidently a drastic improvement on previous results for this difficult transformation.

Upon close inspection, the ^{1}H NMR spectrum revealed that this reaction delivered enamide **86** as an inseparable mixture of (*Z*)- and (*E*)-isomers in a 3:1 ratio. The spectrum is further complicated by the presence of rotamers within each isomer (7:1 and 2:1 respectively), arising from the restricted rotation around the *N*-vinyl formamide bond (**Figure 31**, distinguishable resonances of the minor rotamers are denoted with an asterisk).

Table 5 Optimisation of the Wittig olefination on aldehyde **78**

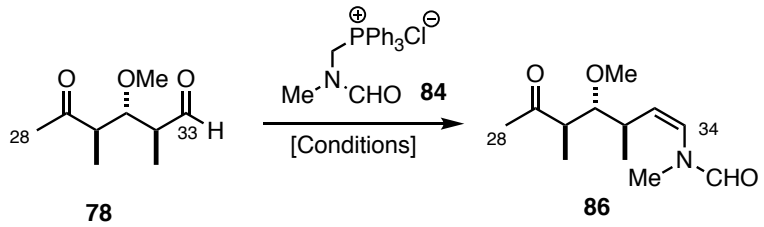

Entry	Scale / mg	Equivalents	Ylid generation conditions (temperature range and time)	Yield (over two steps)
1	100	1.5 LiHMDS 1.4 salt **84**	–78 °C → 0 °C 30 min	35%
2	200	2.1 LiHMDS 2.0 salt **84**	–78 °C → –40 °C → –20 °C → 0 °C 2 h	52%
3	450	2.1 LiHMDS 2.0 salt **84**	–78 °C → –40 °C → –20 °C → 0 °C 2 h	46%
4	1000	2.1 LiHMDS 2.0 salt **84**	–78 °C → –40 °C → –20 °C → 0 °C 2 h	62%

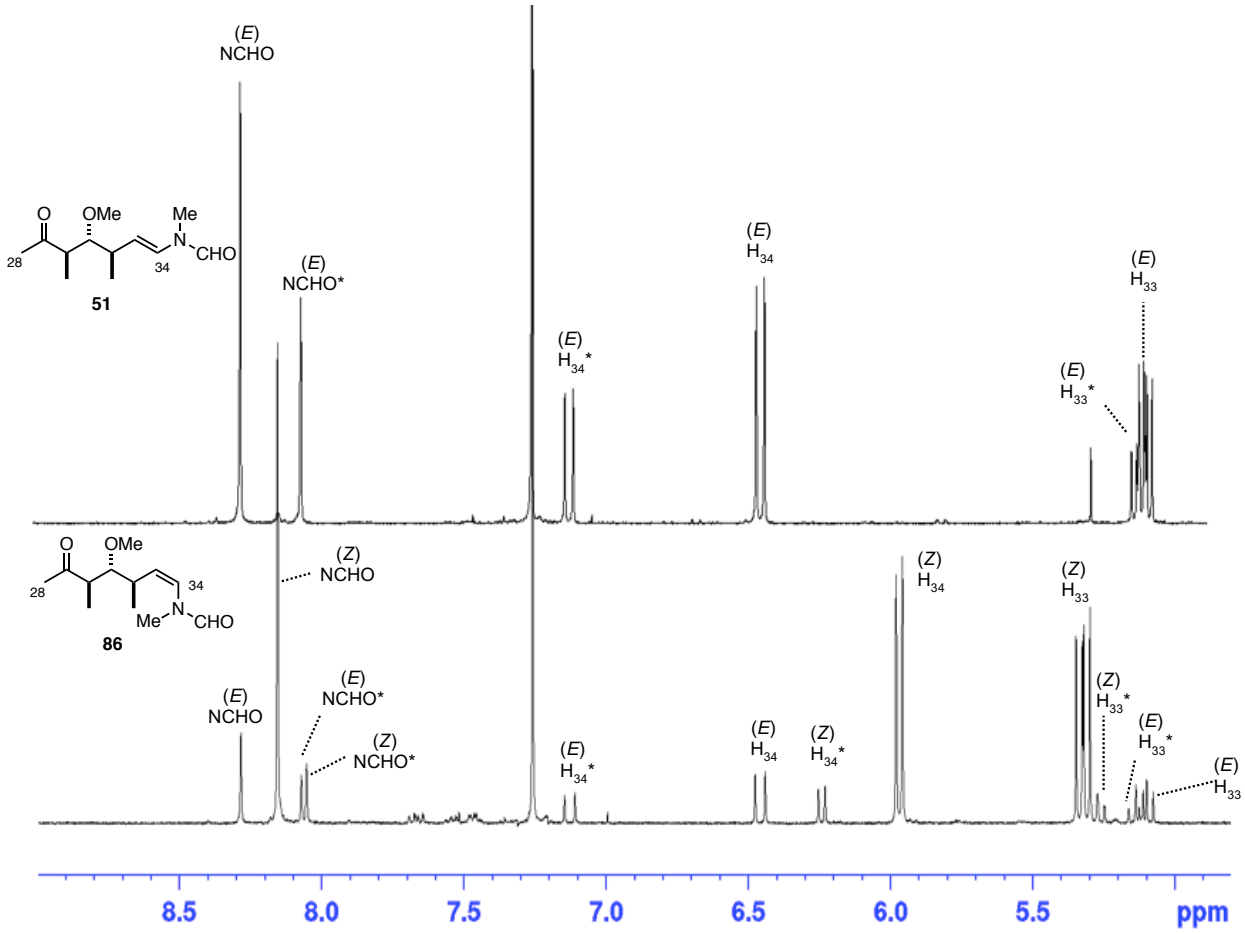

Figure 31 ^{1}H NMR resonances within the olefinic region of enamides **86** and **51**

The ratio of double bond isomers was inconsequential as the mixture was to be isomerised to the required (*E*)-geometry in the next step. Consequently, enamide **86** could be converted into the thermodynamically favoured (*E*)-olefin **51** *via* treatment with molecular iodine in CH_2Cl_2 for 24 h.[139,169,182] This reaction was carried out in the absence of light and is thought to proceed *via* an ionic mechanism under these conditions (**Scheme 35**). The proposed mechanism involves electrophilic attack of iodide at C_{33}, followed by rotation about the C_{33}–C_{34} bond and subsequent elimination to furnish the desired (*E*)-isomer.

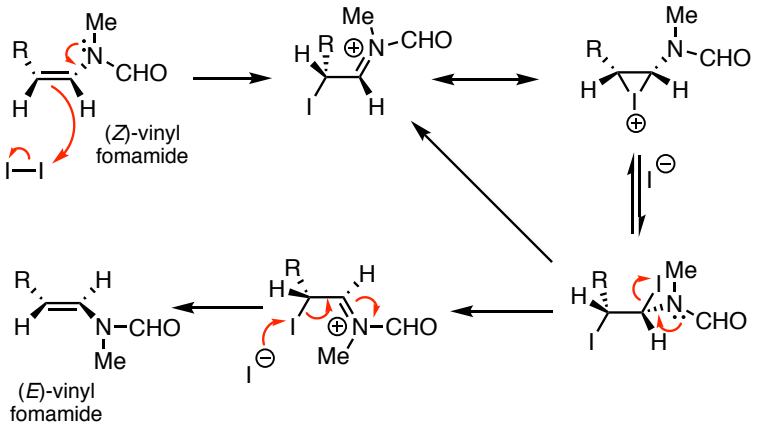

Scheme 35 Mechanistic proposal for the iodine mediated (*Z*)- to (*E*)-enamide isomerisation

Gratifyingly, 5 mol% of iodine could be used to deliver (*E*)-enamide **51** as a single geometric isomer and as a 2:1 mixture of rotamers about the amide bond (**Scheme 36**).

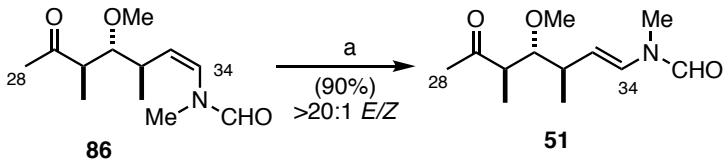

Scheme 36 Iodine mediated (*Z*)- to (*E*)-isomerisation of enamide **86**

This completes the synthesis of our modified side chain ketone **51**. Overall, more than 1g of this fragment was synthesised in 8 steps and 30% yield from ethyl ketone **42**. This fragment brought unanticipated challenges in the Swern–Wittig sequence, but careful optimisation has rendered these conditions experimentally reproducible and reliable.

2.3 C_{15}–C_{27} southern fragment 98

The simplified southern fragment **98** contains two of our planned modifications for designed aplyronine analogues: the C_{17}–C_{21} hydrocarbon chain and the C_{25} methyl ether. Synthetic work on this fragment was exclusively undertaken by Talia Pettigrew and, for completeness, her work is summarised in **Scheme 37**.[165]

Pettigrew further extended the applications of titanium (IV) mediated aldol methodology to construct the C_{23}–C_{26} stereotetrad in this fragment. The simplified aldehyde **99** for aldol coupling could be accessed in two steps from 1,9-nonanediol and the ketone partner **43** was derived from (*S*)-Roche ester. Compared to the tin variant, the titanium approach was again found to be more favourable and provided the aldol adduct **100** in good yield and diastereoselectivity (85%, 17:1 *dr*) on multigram scale. The fully protected southern fragment **98** was delivered after a further two steps: an Evans–Tishchenko reduction and subsequent methylation.

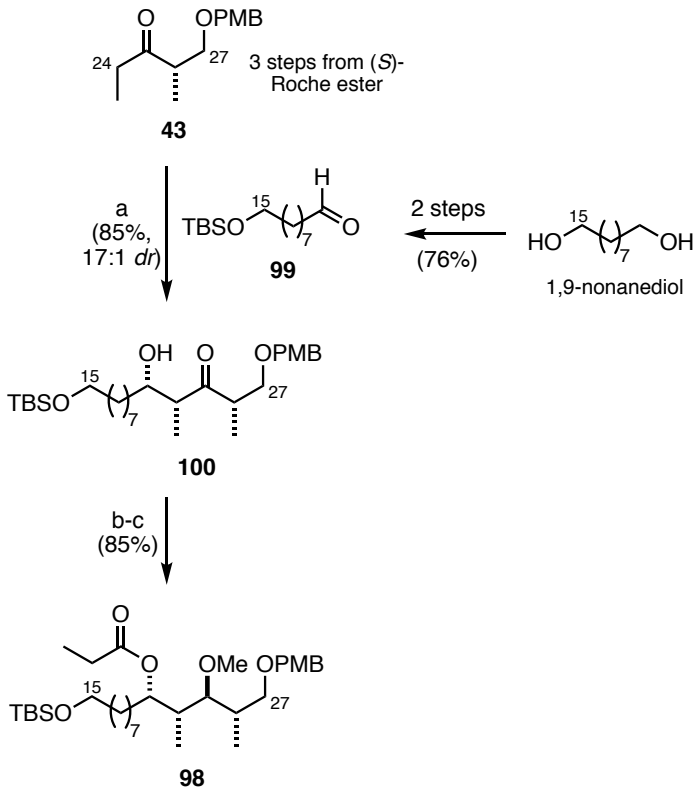

(a) (*i*-PrO)$TiCl_3$, (*i*-Pr)$_2$NEt, CH_2Cl_2, −78 °C; (b) SmI_2, EtCHO, THF, −20 °C;
(c) Meerwein salt, proton sponge, CH_2Cl_2

Scheme 37 Outline of Pettigrew's route to access the simplified southern fragment **98** [165]

Pettigrew's simplified fragment **98** was synthesised in 8 steps and 20% yield from (*S*)-Roche ester. Compared to the equivalent fragment in the group's synthesis of aplyronines A and D, this represents a considerable saving of 8 synthetic steps.[138] Pettigrew estimated that to make 1 g of this fragment *via* this route would take 8 working days, compared to approximately 16 days for the full natural product fragment. This further demonstrates the reliability and efficiency of Pettigrew's synthetic approach.

2.4 Summary

This chapter has outlined the synthesis of our advanced modified fragments for incorporation into our designed 'aplyrologues'. The northern phosphonate **36** has been synthesised in 14 steps and 18% yield from (*R*)-Roche ester (**Scheme 38**). In advancing this material, the *bis*-TES protected variant was selected to move forward in place of the PMP acetal, due to advantages gained in later steps of the synthesis.

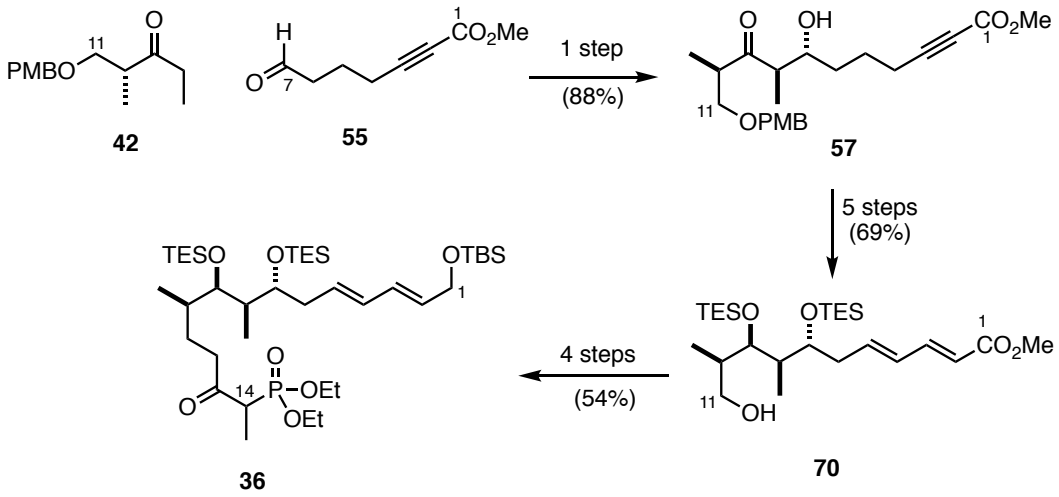

Scheme 38 Summary of northern phosphonate **36** synthesis

Titanium (IV) Lewis acid aldol methodology was used with great success in the side chain synthesis, providing multigram quantities of the required aldol adduct with the correct all *syn*-stereochemistry. This is an operationally easier procedure than the corresponding tin aldol route which was used in earlier iterations of the aplyronine synthesis.[120] Overall, side chain ketone **51** with the necessary C_{31} methyl ether moiety, has been synthesised in 8 steps and 30% yield from ethyl ketone **42 (Scheme 39)**. This represents a saving of two steps by circumventing the protecting group swap in the synthesis of the natural products.

Significant optimisation of the challenging Swern–Wittig sequence was carried out to successfully deliver reliable experimental conditions for this reaction. Additionally, this work has provided insight into the stability of the methyl ether moiety; it has demonstrated its robustness towards elimination, thus validating the incorporation of this functionality into advanced fragments.

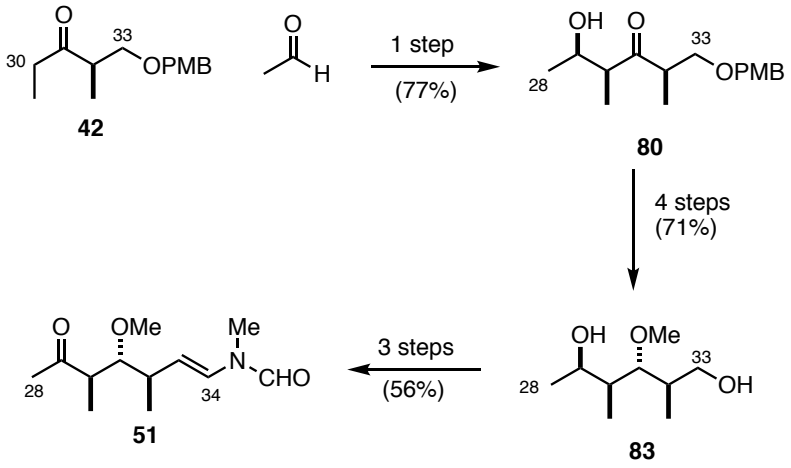

Scheme 39 Summary of side chain ketone **51** synthesis

With plentiful stocks of all three advanced fragments, attention now turned to exploring strategies for fragment coupling to advance material towards our desired aplyronine analogues.

Chapter 3

Fragment coupling strategies

The southern fragment **98** is orthogonally protected at each terminus: C_{15} bears a silyl ether whereas a benzylic ether lies at C_{27}. This differentiation allows for selective removal of each protecting group to allow for fragment coupling to either the northern or side chain fragments after oxidation to the aldehyde. A Horner–Wadsworth–Emmons olefination forges the C_{14}–C_{15} northern-southern connection, whilst an aldol reaction unites the southern and side chain fragments across the C_{27}–C_{28} bond (**Scheme 40**).[138]

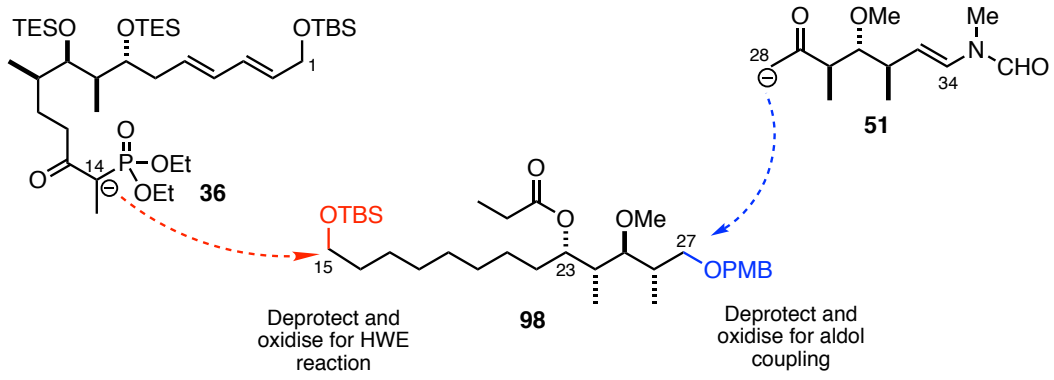

Scheme 40 Fragment coupling connection points at each end of the C_{15}–C_{27} southern fragment

Traditionally, the aplyronine scaffolds have been constructed by first connecting the northern and southern fragments *via* a HWE reaction, then closing of the macrolactone at C_{23}, before the side chain is finally appended using an aldol coupling.[137,138,149] This strategy was deliberately designed for late stage introduction of the sensitive *N*-vinyl formamide moiety. Within the natural product system, with the acetoxy substitution at C_{31}, the formamide was prone to decomposition through hydrolysis or elimination pathways under a variety of conditions.[120] Thus, careful handling of all late stage intermediates was required after the installation of this delicate functionality. Furthermore, compounds containing the *N*-vinyl formamide exists as stable rotamers, leading to complications in purification and NMR analysis of all subsequent intermediates.

Encouraged by our results during the synthesis of side chain ketone **51**, we were optimistic that our methyl ether variant would not exhibit the same sensitivity issues as its acetoxy counterpart. Therefore, we could consider exploring an alternative coupling strategy to offer more flexibility in the synthesis of our designed aplyronine analogues and expand the range of analogues generated *via* late-stage transformations.

3.1 Alternative coupling strategy

Based on previous observations, early introduction of the *N*-vinyl formamide moiety could be tenable. This opens up the possibility for a reversed coupling sequence where the southern and side chain fragments are first connected, before the northern portion is joined. This would complete the full C_1–C_{34} backbone before macrolactonisation.

This approach would convey a number of advantages. Firstly, the chemistry used to attach the side chain ketone usually is carried out on highly precious, late stage intermediates thus limiting optimisation efforts. For example, in the synthesis of aplyronines A and D, the aldol coupling sequence to connect the C_{27}–C_{28} bond was found to occur in a moderate 65% yield by Dr Simon Williams.[121,138] Williams' optimisation efforts were frustrated by a lack of material given the valuable nature of the intermediates. Similarly, the zinc borohydride reduction to set the configuration at C_{29} has been afflicted by highly variable yields and *dr*. Improvements have analogously been prohibited by the limited quantity of substrate available. Furthermore, this alternative sequence opens up the possibility of new sites of linkage for ADC development. Hence, by coupling the side chain and southern fragments together at an earlier stage, we gain the opportunity to undertake optimisation studies on these challenging reactions to potentially deliver a more efficient route to our designed analogues.

3.1.1 Aldol–dehydration–reduction sequence

With side chain ketone **51** in hand, the required aldehyde coupling partner was revealed in two steps. Deprotection of PMB ether **98** with DDQ proceeded smoothly, followed by Swern oxidation delivered aldehyde **50** in 88% yield over two steps (**Scheme 41**).

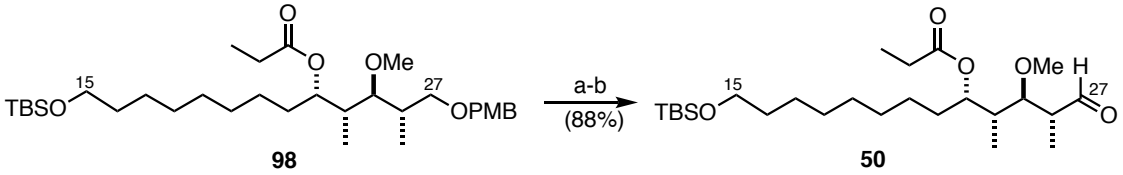

(a) DDQ, CH_2Cl_2/pH 7.0 buffer (2:1); (b) $(COCl)_2$, DMSO, NEt_3, −78 °C → 0 °C

Scheme 41 Deprotection and oxidation sequence to aldehyde **50**

A boron-mediated aldol reaction had previously been successful in joining analogous fragments together in the aplyronine natural product syntheses.[138] Williams and Fink had both noted that an excess of enolate is required to push the reaction to completion, coupled with a mild non-oxidative work-up procedure.

Ketone **51** was therefore enolised with dicyclohexylboron chloride and triethylamine at 0 °C, before the addition of aldehyde **50** at −78 °C. Aldol adduct **101** was obtained after a non-oxidative work up (MeOH, pH 7.0 buffer) as an inconsequential mixture of diastereoisomers, along with excess ketone **51**. This mixture was directly subjected to a Burgess dehydration protocol, at which point the diastereoisomers converged to enone **102**. At this point ketone **51** could be separated more easily *via* column chromatography.[183] Initial results using these standard conditions yielded a result comparable to that of Williams (**Table 6**, entry 1).

Theorising that incomplete breakdown of the boronate species under the non-oxidative conditions could be responsible for the relatively low yield, an oxidative work up using hydrogen peroxide was trialled. However, under the harsher conditions, complete decomposition of the product was observed (**Table 6**, entry 2). This stands in contrast to results obtained during our group's synthesis of reidispongiolide and rhizopodin. Both routes employed a hydrogen peroxide oxidative work-up with great success on arguably more delicate substrates.[169,184]

Hence, a milder work up procedure was sought. Taking inspiration from the group's work on spongistatin, a silica gel work-up surfaced as a viable candidate to break down the

intermediate boron aldolate.[185] Pleasingly, an improved yield of 70% was achieved using this procedure (**Table 6**, entry 3), further highlighting the mild nature of boron-mediated aldol reactions within complex natural product synthesis.

Whilst the majority of the excess ketone can be easily recycled after the Burgess elimination step, it would be preferable to lower the number of equivalents if possible. Gratifyingly, employing only 1.5 equivalents of ketone **51**, enone **102** could be isolated in an excellent 90% yield over three steps (**Table 6**, entry 4). On scale this could be further reduced to just a slight excess of 1.2 equivalents without appreciable loss in efficiency (**Table 6**, entries 5 and 6).

Table 6 Optimisation efforts for the aldol coupling between ketone **51** and aldehyde **50**

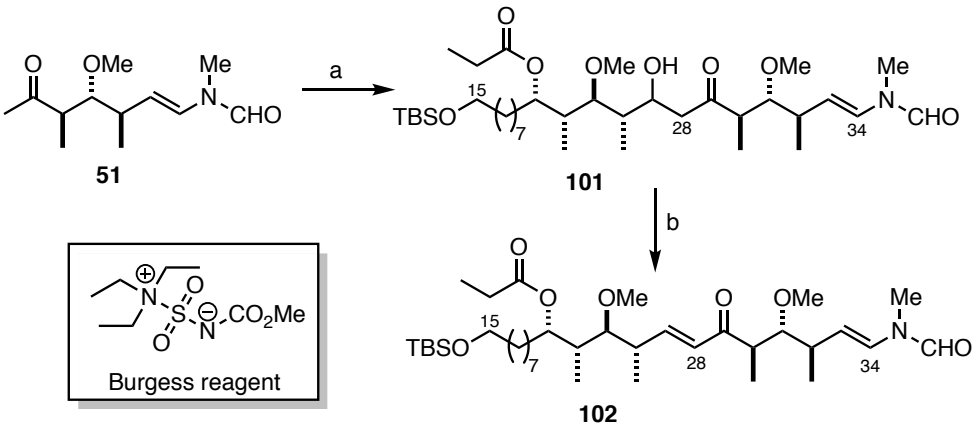

(a) BCy_2Cl, NEt_3, Et_2O, 0 ºC, *then* **50**, −78 ºC → −10 ºC; (b) Burgess reagent, THF

Entry	Scale / mg	Ketone eqv.	Work-up	Yield (over 3 steps)
1	60	2	Non-oxidative (MeOH, pH 7 buffer)	58%
2	40	2	Oxidative (H_2O_2)	0%
3	35	2	Non-oxidative (SiO_2)	70%
4	40	1.5	Non-oxidative (SiO_2)	90%
5	300	1.2	Non-oxidative (SiO_2)	85%
6	1000	1.2	Non-oxidative (SiO_2)	84%

The second key step of this fragment coupling sequence is elimination of the newly formed C_{27} hydroxyl. This relies on the extremely mild and selective nature of the Burgess reagent, which exists as the inner salt. Mechanistically, initial formation of the sulfamate ester is followed by an E_i-type elimination. Intramolecular *syn*-elimination of the β-hydrogen occurs *via* a cyclic six-membered transition state to generate the olefin product with high stereoselectivity.[183,186] As illustrated in **Scheme 42**, the (*E*)-selectivity stems from the preference for the large groups (R_1 and R_2) to minimise unfavourable steric interactions in the transition state. The Burgess reaction has therefore found widespread use as a mild and selective method to dehydrate secondary and tertiary alcohols within complex natural product syntheses.[187–190]

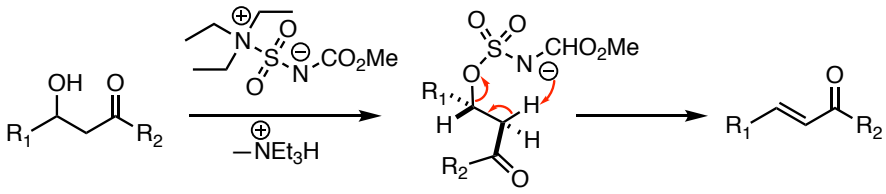

Scheme 42 Mechanism for dehydration reactions using the Burgess reagent

The reaction was operationally simple and generally proceeded well at room temperature. Aldol adduct **101** was simply added to a slight excess of Burgess reagent in THF and the reaction left to stir for 16 h. Monitoring by TLC analysis was straightforward due to the large differences in polarity of the starting alcohol and product enone. However, on larger scales it became apparent that the reaction was sluggish, and a considerable amount of starting material would remain, even with warming to 40 °C. In these cases, it was best to work-up and purify the product, before re-submitting the recovered starting material. Interestingly, within the field of natural product synthesis, there are instances where the Burgess dehydration has been successfully carried out in refluxing toluene, with no degradation products observed.[190,191] Although these conditions were not trialled on our system, this might represent a possible solution for future optimisation of this reaction.

Conjugate reduction of enone **102** was achieved through treatment with Stryker's reagent: triphenylphosphine copper hydride hexamer.[192] For the purpose of the Paterson group's studies into the aplyronines, Dr Simon Williams developed a convenient method to freshly prepare a solution of Stryker's reagent for use in conjugate reduction reactions.[138] This solution is operationally much simpler to use than the solid reagent which is highly air sensitive, laborious to prepare and must be stored and manipulated within a glovebox.[193] To render the reaction catalytic in copper, several methods have been developed using

organosilanes, designed to produce copper hydride species *in situ*.[194–197] Following the procedure of Yun, a solution of Stryker's reagent in toluene could be prepared from copper (II) acetate, triphenylphosphine and an excess of tetramethyldisiloxane (TMDS). A characteristic colour change from blue-green to bright red over 8-10 h signifies the formation of the desired copper hydride species.[198] Conveniently, the solution was amenable to storage at –20 °C for up to a month.

Mechanistically, conjugate addition of the soft hydride nucleophile produces copper enolate **103** which can react with the excess organosilane to regenerate the active catalyst. In this step, the product becomes masked as the silyl enol ether **104**, which upon protonation furnishes ketone **105** (**Scheme 43**). Employing a catalyst loading of 20 mol% copper, ketone **105** could be delivered in excellent yield (93%), as evidenced by the loss of the characteristic enone signals by ^{1}H NMR analysis. No extra precautions such as solvent degassing were necessary. Due to the similarities in retention factor between enone **102** and ketone **105** on TLC, the reaction mixture was often left overnight (16-24 h) to ensure full conversion to the product. Once complete, the mixture was simply applied directly to a silica gel column and the product eluted cleanly.

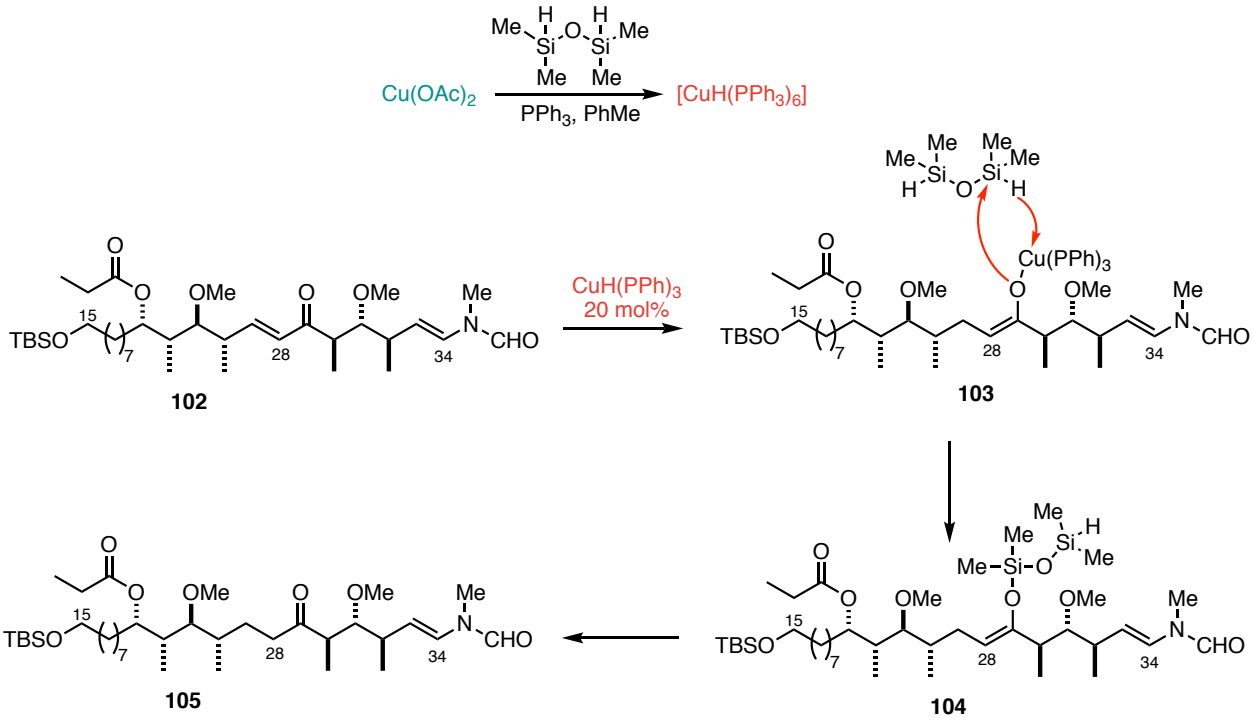

Scheme 43 Stryker's reduction of enone **102** to ketone **105**

With this sequence thoroughly optimised, and the first goal within our alternative coupling sequence met, attention turned to the diastereoselective reduction of ketone **105**.

3.1.2 Reduction of ketone 105

The final step to construct the stereotetrad within the side chain required the diastereoselective reduction of ketone **105**. Previous work had identified zinc borohydride as a useful reducing agent for this transformation. However, yields and *dr* had been found to vary significantly (50–90%, 3:1–10:1 *dr*) and were seemingly dependent on the quality of the reagent and scale of the reaction.[120,138] Fink's best result on the natural aplyronine side chain was a promising 90% yield and 10:1 *dr*, albeit this was an isolated result on small scale. The diastereoselectivity has been proposed to arise from an eight membered, zinc-chelated transition state involving the ketone and acetyl carbonyl groups.[199]

This transformation was first trialled on side chain ketone **51** as a simpler model system. In this trial, reduction of ketone **51** with freshly prepared zinc borohydride solution yielded a mixture of diastereoisomers (1.5:1 *dr*) in a moderate 70% yield (**Scheme 44**). Gratifyingly, the diastereoisomers were separable through careful column chromatography.

A Mosher ester analysis was carried out to determine the absolute configuration of C_{29} in the major diastereoisomer of **106**.[200,201] Esterification with (*R*)- and (*S*)-α-methoxy-α-(trifluoromethyl)phenyl acetic acid (MTPA-OH) under Keck conditions (DCC, DMAP, DMAP·HCl) afforded the (*R*)- and (*S*)-Mosher ester derivatives **107** and **108** in 81% and 76% yield respectively (**Scheme 45**).[202] The Mosher method relies on the assumption that the ester derivatives predominantly adopt the conformation in which the methine proton, ester carbonyl and trifluoromethyl group are coplanar, as depicted in **Figure 32**. The presence of a phenyl ring results in diamagnetic shielding of the protons that reside on the same side of the plane as the ring (*i.e.* H_a, H_b and H_c). These proton signals in the (*R*)-MTPA ester will be therefore shifted upfield relative to the analogous set of protons in the (*S*)-MTPA ester. The reverse is true for protons H_x, H_y and H_z. By analysing the difference in chemical shifts $\Delta\delta = \delta_S - \delta_R$ for as many protons as possible, it is possible to determine the absolute configuration of the carbinol centre. The sign of this difference is expected to be negative for protons on one side of the hydroxyl and positive for those on the other.[203]

Analysis of ^{1}H NMR spectra for both compounds showed that the $\Delta\delta_{S-R}$ signs for protons in the vicinity of the carbinol centre corresponded to the pattern, in agreement with the (*R*)-configuration at C_{29} (**Scheme 45**).

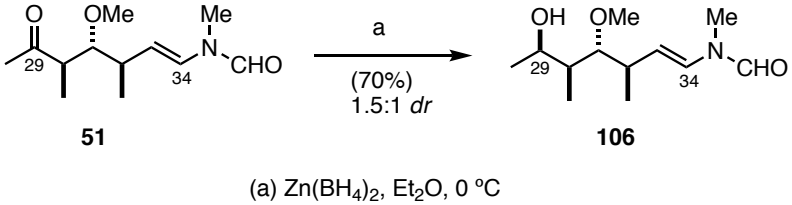

51 **106**

(a) $Zn(BH_4)_2$, Et_2O, 0 °C

Scheme 44 Zinc borohydride reduction of side chain ketone **51**

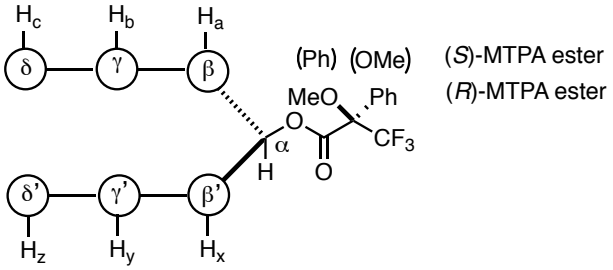

Figure 32 Model representation for Mosher ester analysis of absolute configuration of a carbon stereocentre

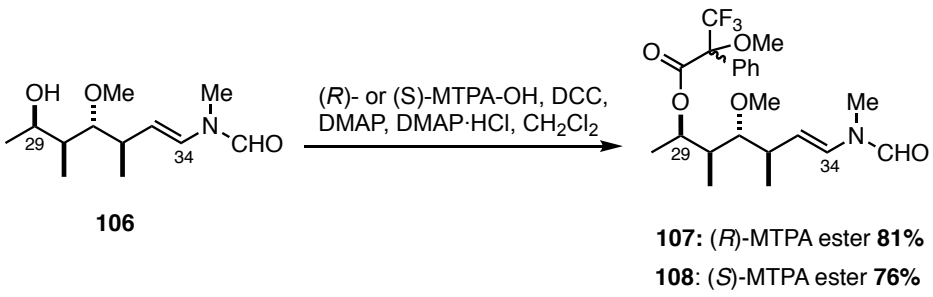

106

107: (*R*)-MTPA ester **81%**

108: (*S*)-MTPA ester **76%**

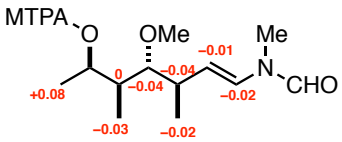

Scheme 45 Preparation and analysis of Mosher ester derivatives **107** and **108**

With these results to support our assignment of the major diastereomer as the desired (*R*)-configuration, these conditions were next investigated on our real system, ketone **105**.

Initial results to generate alcohol **109** were pleasing with a reasonable yield of 68% together with an increase in stereoinduction to 6:1 *dr* (**Scheme 46**). However, this result was not always reproducible, and we were troubled with variations in yield and *dr* similar to those observed by Williams. Puzzlingly, each batch of reagent was prepared in an identical manner, but there appeared to be no consistency of results between each reaction with different batches yielding different results. Lowering the temperature to –10 °C, in the hope of improving the *dr*, led to the reaction stalling. This reaction currently remains capricious with yields varying between 55–70% and stereoinduction fluctuating between 1.5:1–6:1 *dr*.

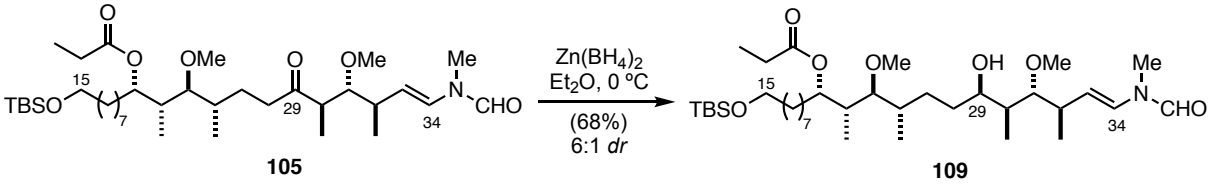

Scheme 46 Zinc borohydride reduction of ketone **105**

Again, the diastereoisomers were separable *via* column chromatography. This fortunately permitted recycling of unwanted diastereoisomer **110** by oxidising back to starting material ketone **105** and re-subjecting this to the reduction conditions (**Scheme 47**). This provided a fairly effective working solution for advancing material through this sequence.

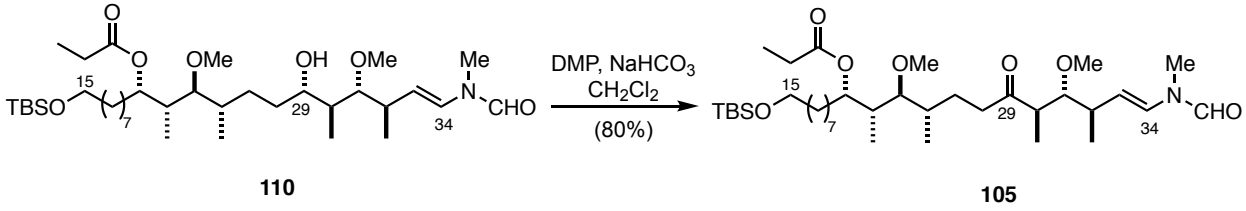

Scheme 47 Re-oxidation of unwanted diastereoisomer **110**

The stereochemical outcome of this reduction is noteworthy. Due to the superior coordinating ability of Zn^{2+}, high levels of stereoinduction have been observed in zinc borohydride mediated reductions.[199,204] Dr Sarah Fink had screened a variety of reducing agents to effect this transformation and zinc borohydride surfaced as the only reagent capable of overturning the Felkin–Anh bias to favour the desired 1,3-*anti* (*R*)-configuration.[120]

As our compounds differ sufficiently from the natural product to make stereochemical comparisons difficult, once again a Mosher ester analysis was carried out to rigorously confirm the (*R*)-configuration at the newly formed hydroxyl (**Scheme 48**).

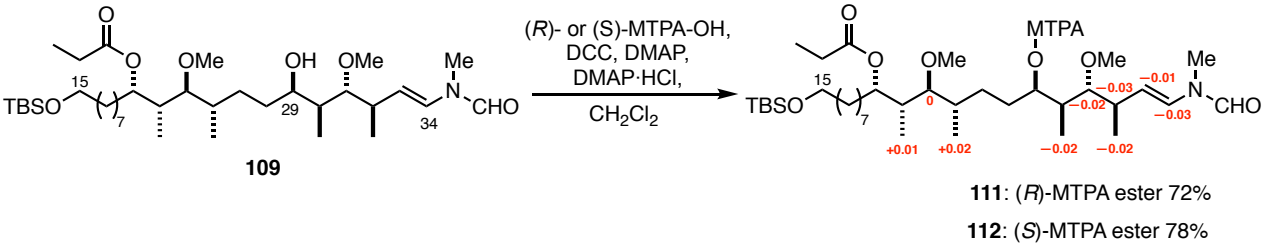

Scheme 48 Formation and analysis of Mosher esters **111** and **112**

Further optimisation of this reduction reaction is ultimately required; however, it was deemed prudent at this stage to continue to push forward towards coupling the northern fragment to construct our designed analogues.

3.1.3 Elaboration to aldehyde 54

To assemble the full carbon skeleton *via* HWE coupling to the northern C_1–C_{14} phosphonate **36** (**Section 2.1**), the aldehyde functionality had to be revealed at C_{15} (**Scheme 49**). To avoid undesired oxidation, the newly formed hydroxyl at C_{29} was masked as a TBS ether (TBSOTf, 2,6-lutidine) in good yield. Gratifyingly, the potentially sensitive *N*-methyl-*N*-vinyl formamide moiety remained untouched under these Lewis acidic conditions. Contrary to the established coupling sequence, where the C_{29} hydroxyl is revealed at a late-stage and directly esterified, alcohol protection is necessary at this earlier point in the synthetic route.

Removal of the primary TBS ether at C_{15}, in the presence of the more sterically hindered secondary centre, could be achieved through treatment of **113** with TBAF. Careful monitoring of the reaction by TLC analysis ensured clean conversion to the desired primary alcohol **114**, with no doubly deprotected byproduct observed. Subsequent DMP oxidation of alcohol **114** proceeded smoothly to generate aldehyde **54** which was used crude in the ensuing HWE olefination reaction. Thus, with the required aldehyde in hand, our focus turned to the pivotal HWE coupling to furnish the complete aplyronine carbon backbone.

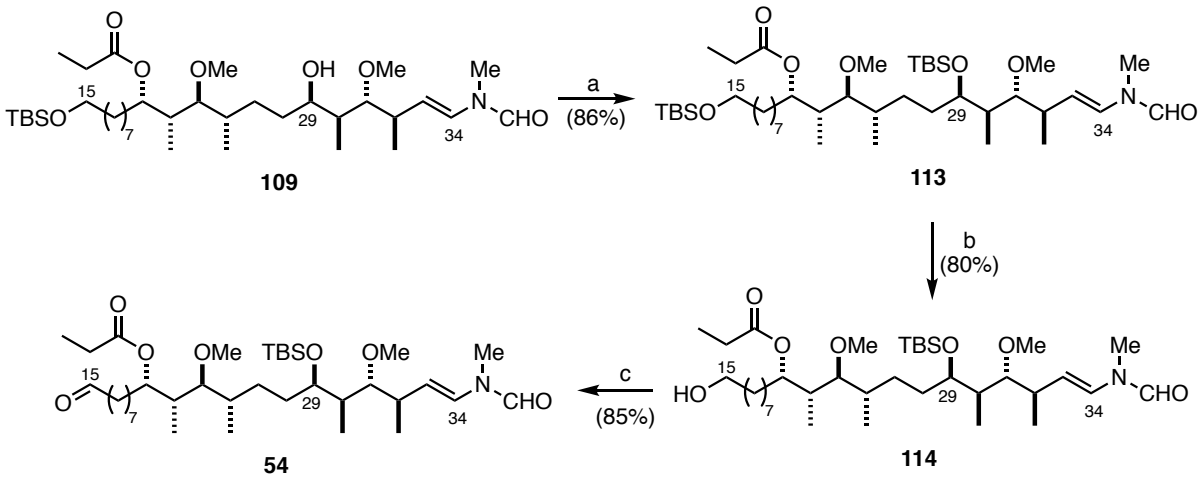

(a) TBSOTf, 2,6-lutidine, CH_2Cl_2, −78 °C; (b) TBAF, THF; (c) DMP, $NaHCO_3$, CH_2Cl_2

Scheme 49 Elaboration of C_{15}–C_{34} fragment **109** to aldehyde **54**

3.1.4 HWE coupling and C_{13} reduction

The Horner–Wadsworth–Emmons olefination is a powerful method for the stereoselective olefination of aldehydes and ketones with stabilised phosphonate carbanions leading to products with high (*E*)-selectivity.[205,206] A variant on the Wittig reaction, the use of phosphoryl-stabilised carbanions has many advantages over the traditional triphenyl-phosphorous ylids and offers great synthetic utility.[207,208]

Mechanistically, deprotonation of β-ketophosphonate **36** leads to the stabilized phosphonate carbanion **115 (Scheme 50)**. This can reversibly add into aldehyde **54** to form an oxaphosphetane intermediate that irreversibly decomposes to generate the enone product **116**. The thermodynamic driving force for this reaction is the loss of the phosphate ester moiety.

The stereoselectivity of the Horner–Wadsworth–Emmons olefination derives from both kinetic and thermodynamic control through the reversible addition of the phosphonate carbanion to the carbonyl group.[208–210] Although minimisation of steric interactions between the aldehyde proton and bulky phosphonate is preferred (**Scheme 50**, **TS-5**), this ultimately leads to an oxaphosphetane intermediate that places the aldehyde R group and the β-carbonyl in a *syn*-arrangement. Hence, the collapse of this adduct towards the (*Z*)-

enone is slow. Contrastingly, whilst reaction through **TS-6** is initially less favourable due to destabilising steric interactions, this pathway eventually leads to the corresponding *anti*-oxaphosphetane intermediate. Resultingly, collapse of this adduct is fast to generate the thermodynamically favoured (*E*)-olefin through stereoselective carbon–carbon bond formation.

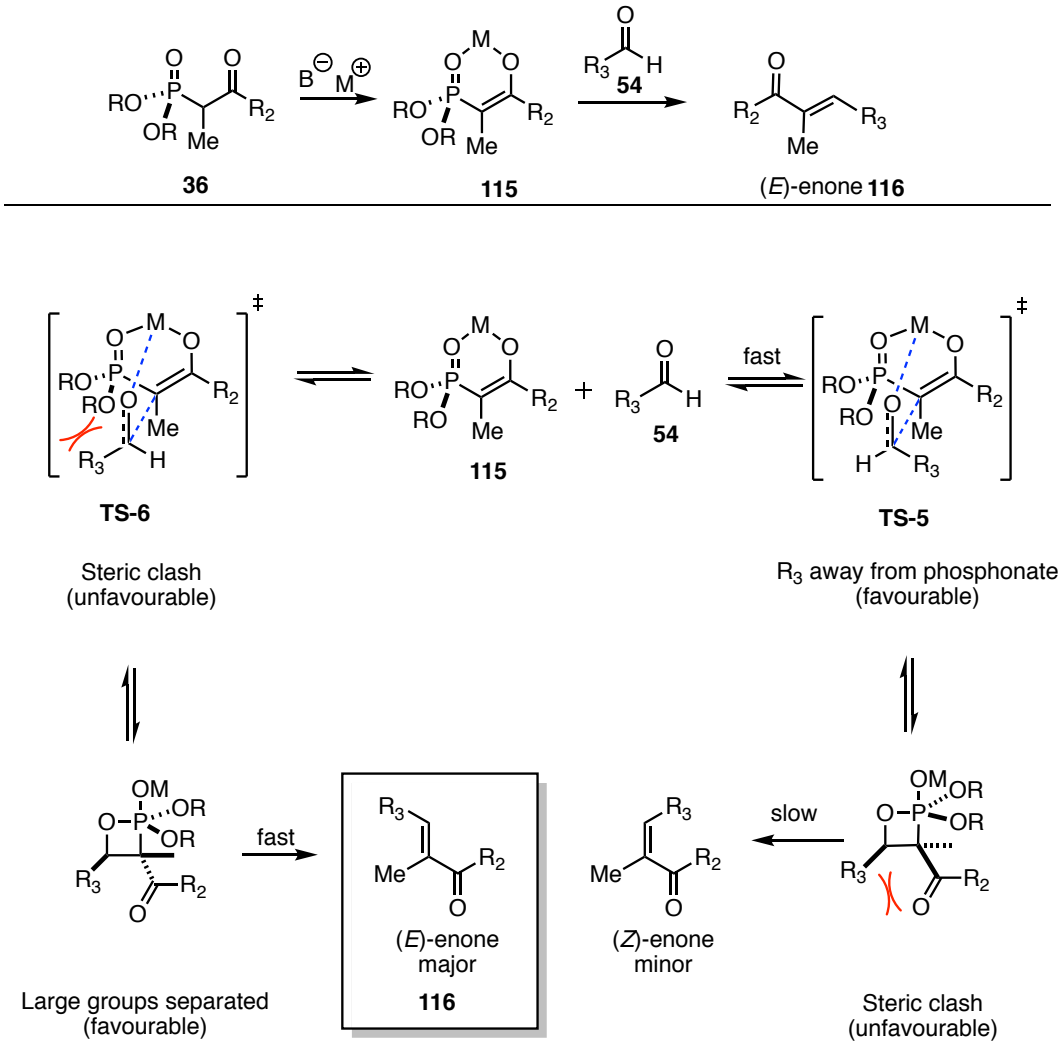

Scheme 50 The origin of selectivity in the Horner–Wadsworth–Emmons olefination

As β-ketophosphonate **36** was more readily accessible (10 steps) than aldehyde **54** (15 steps) it was used in slight excess (1.1 equivalents) and as a mixture of regiosiomers (**Section 2.1.4**). Deprotonation of **36** with $Ba(OH)_2$ in anhydrous THF, followed by the addition of aldehyde **54** in wet THF (THF/H_2O, 40:1) generated enone **116** in 85% yield (**Scheme 51**). Analysis of the ^1H NMR confirmed the excellent *E*/*Z* selectivity (>20:1) with none of the undesired (*Z*)-isomer detected in the crude mixture. The unreacted regioisomer

77 could easily be separated from the product *via* column chromatography. Conveniently, this extremely mild reaction could be left to run for an extended period of time (*i.e.* > 72 h) without detrimental effects.

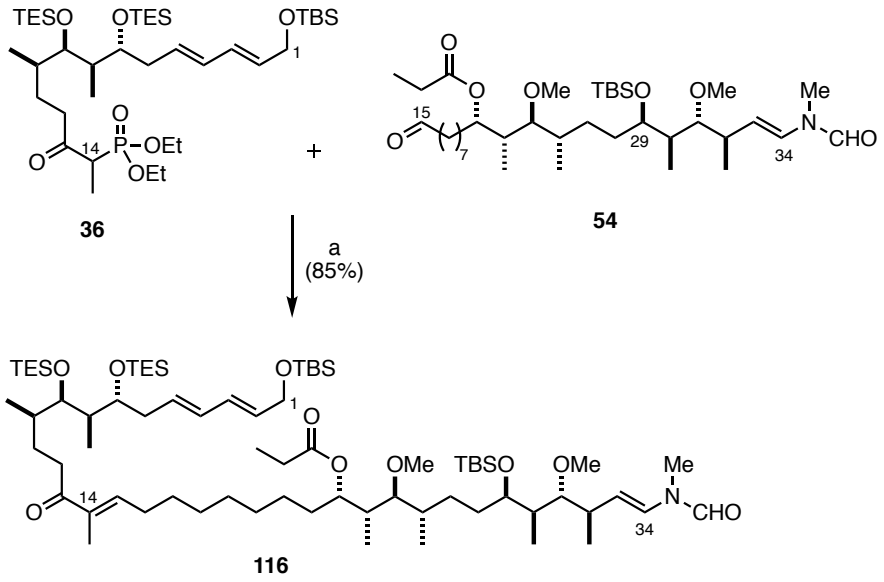

(a) $Ba(OH)_2$, THF, *then* **54**, THF/H_2O (40:1)

Scheme 51 Horner–Wadsworth–Emmons olefination of β-ketophosphonate **36** and aldehyde **54**

The construction of the trisubstituted olefin in this complex intermediate is noteworthy. This class of olefins represents a challenging target to build *via* the HWE reaction, but the unique barium hydroxide variant of this methodology has proved to be extremely efficient in this regard. Our group demonstrated that barium hydroxide could be utilised under very mild conditions (wet THF, rt) to efficiently furnish substituted olefins from base-sensitive and structurally complex aldehydes.[211] This methodology has since been successfully applied to highly functionalised substrates in complex natural product syntheses.[212–214]

Having successfully completed our final fragment coupling and forged the full carbon skeleton of our analogues, the next step was the installation of the final stereocentre at C_{13}. A chiral reducing agent is necessary for this transformation due to the lack of inherent substrate bias in **116** for installation of this isolated carbinol stereocentre. The Corey–Bakshi–Shibata (CBS) reduction is able to circumvent this issue by utilising a chiral catalyst to sterically differentiate between the substituents on a carbonyl group. Mechanistically, the CBS reduction commences with the Lewis basic nitrogen on the

proline derived oxazaborolidine coordinating with the Lewis acidic borane reducing agent. This coordination forms a well-defined chiral complex between the reactants and activates borane as a hydride donor for intramolecular hydride transfer to the carbonyl. Additionally, the Lewis acidity of the endocyclic boron is enhanced, thus promoting ketone coordination *via* the sterically more accessible oxygen lone pair. The face-selective hydride transfer is thought to proceed through a boat-like transition structure in which the large substituent (R_L) is orientated pseudo-equatorially away from the methyl group on boron to minimise unfavourable steric interactions.

The absolute stereochemistry of the newly formed carbinol can thus be predicted from the transition state structure **TS-7** illustrated in **Scheme 52**. In this particular case, the 'large' group is represented by the olefin and the 'small' group by the alkyl chain.

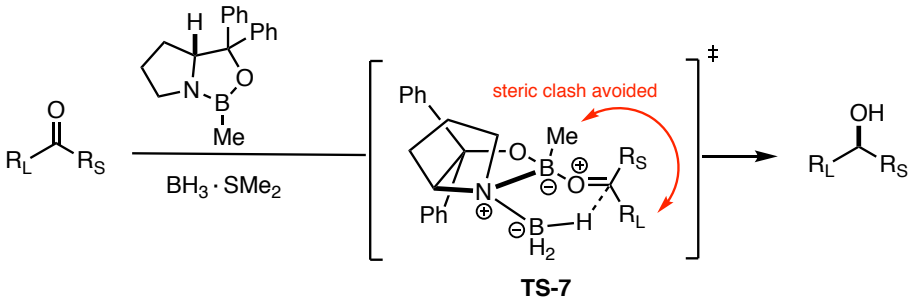

Scheme 52 Transition state model for ketone reduction with (*R*)-CBS catalyst

Enone **116** was subjected to standard CBS reduction conditions ((*R*)-Me-CBS catalyst, $BH_3{\cdot}SMe_2$, −10 °C) and delivered alcohol **117** in 30% yield on small scale. Despite employing stoichiometric amounts of 'catalyst' the reaction would not go to completion, with mostly starting material returned upon work up. Initially, this was taken as a positive sign: whilst conversion was low, no byproducts were detected and it was hoped that with optimisation the yield would improve. However, despite multiple attempts, this reaction remained troublesome (**Table 7**, entries 1–2). On larger scales, it became apparent that side reactions were occurring, as evidenced by the disappearance of the *N*-vinyl formamide signals in the ^{1}H NMR of the crude material. These byproducts were tentatively attributed to the catalyst or reductant interacting with the *N*-vinyl formamide moiety, leading to hydrolysis or reduction byproducts. The reaction remained puzzlingly unreliable and irreproducible, with seemingly identical conditions returning any combination of starting material enone **116**, trace amounts of desired product **117** or a number of unidentified byproducts.

Table 7 Screening of conditions for the asymmetric reduction of enone **116**

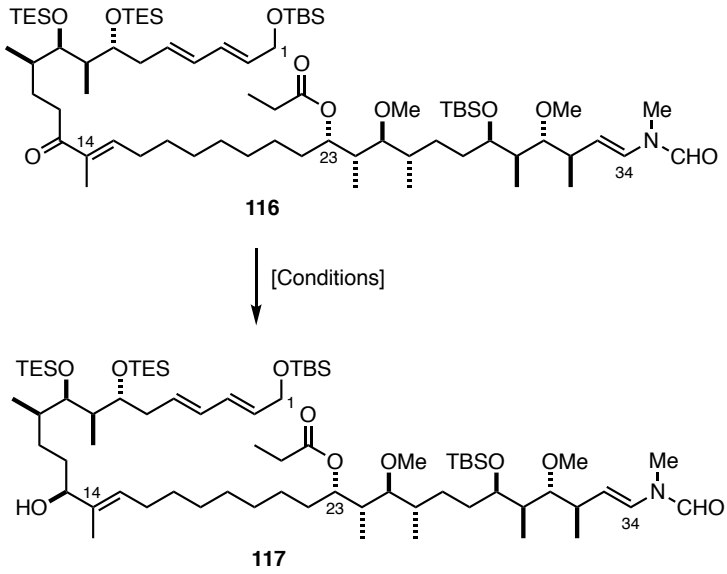

Entry	Scale / mg	Conditions	Result
1	10	(*R*)-Me-CBS catalyst (1.3 eqv.), $BH_3 \cdot SMe_2$ (1.2 eqv.), −10 °C	30% **117**
2	35	(*R*)-Me-CBS catalyst (1.3 eqv.), $BH_3 \cdot SMe_2$ (1.2 eqv.), −10 °C	**116** or unidentified byproducts or trace **117**
3	10	(*R*)-Me-CBS catalyst (2 eqv.), catecholborane (2 eqv.), −78 °C → 0 °C	**116**
4	10	(*R*)-Me-CBS catalyst (2 eqv.), catecholborane (2 eqv.), −20 °C → rt	Trace **117**
5	30	(*R*)-Me-CBS catalyst (2 eqv.), Catechol borane (2 eqv.), −10 → rt	Unidentified byproduct *N*-vinyl formamide signals lost
6	15	RuCl(η^6-cymene)[(*S,S*)-(Ts-DPEN)] 40 °C	Unidentified byproduct

It is noteworthy to mention that in all previous CBS reductions within the aplyronine projects in our group, none had been attempted on a substrate containing the *N*-vinyl formamide functionality, perhaps foreshadowing these observed disappointing results. In the hope of gaining a reproducible result, varying the hydride source from borane to catechol borane[215,216] at a range of temperatures was investigated. These attempts were not successful, and we were plagued by similar reactivity problems (**Table 7**, entries 3–5).

Given the failure of the CBS reaction, a Noyori asymmetric transfer hydrogenation reaction was next investigated (**Table 7**, entry 6). This approach utilises a chiral ruthenium catalyst together with either 2-propanol or formic acid as the hydrogen source to enact the asymmetric reduction.[217,218] In our case, formic acid was avoided as it was expected this would promote the hydrolysis of the sensitive *N*-vinyl formamide moiety. Interestingly, the product isolated from this reaction showed the characteristic downshift of H_{15} expected upon reduction of the carbonyl, but curiously no corresponding signal for H_{13} could be detected. Mass spectrometry results additionally provided no insight into the identity of this byproduct.

These results reveal a serious disadvantage in this alternative coupling approach and it soon became apparent that gambling on the outcome of this reaction was not the best use of material or a reliable way to enact this transformation.

Consequently, we decided to continue our synthesis with the enone functionality in place. The C_{13} methoxy has proved to be crucial to help anchor and position the trimethyl serine moiety as required for interaction with tubulin. Whilst the carbonyl moiety could still conceivably pick up these interactions (*e.g.* through hydrogen bonding), it is unclear if changing the hybridisation state from sp^3 to sp^2, and thus changing the angle of the interaction, would have detrimental effects on the cytotoxicity. An analogue containing the enone moiety would therefore allow for further probing of the protein binding interactions and could deliver crucial SAR data. Thus, we decided to move forward towards closing the macrocycle to access our analogues.

3.1.5 Removal of the propionate ester

The propionate moiety in **116** had proved to be a judicious and robust choice of protecting group, demonstrating stability under a variety of conditions. However, the stage was now set for its removal and to reveal the C_{23} hydroxyl group for subsequent macrolactonisation. Due to the delicate nature and limited stocks of our advanced intermediate **116**, this transformation was first investigated on a model system. The undesired minor diastereomer **110** from the zinc borohydride reaction seemed an ideal choice, as our main concern was once again side reactivity of the *N*-vinyl formamide terminus.

A metal hydride reduction approach using DIBAL was employed by Pettigrew to effect this transformation in the established coupling sequence.[165] Theorising that DIBAL could readily cause reductive cleavage of the *N*-vinyl formamide moiety, these conditions were first investigated without anticipation of success. As expected, cleavage occurred even at low temperatures and the *N*-vinyl formamide signals disappeared from the crude ^{1}H NMR (**Table 8**, entry 1). Use of lithium borohydride or lithium tri-*tert*-butoxyaluminium hydride as alternative hydride sources led to similarly poor results (**Table 8**, entries 2 and 3). New mild and selective deprotection conditions were therefore sought.

Precluding the use of metal hydrides and acidic conditions, due to the instability of the *N*-vinyl formamide, we were left with only one approach – hydrolysis under basic conditions. A variety of bases were screened with very little success. Methanolysis under standard conditions (K_2CO_3, MeOH) returned starting material, even with prolonged stirring at elevated temperatures (**Table 8**, entries 4 and 5). Frustratingly, this result turned out to be a common occurrence in this reaction screen. Despite the use of seemingly harsh conditions, the propionate ester remained stubbornly intact and starting material was returned quantitively each time under various conditions (**Table 8**, entries 6–10). Within our group, barium hydroxide had proven to be an effective reagent to enact ester hydrolysis under mild conditions and was next trialled (**Table 8**, entry 11).[219,220] Whilst some reactivity was observed, no desired product could be isolated. Intriguingly, an unidentified byproduct was produced, containing ^{1}H NMR signals corresponding to both the propionate ester and the *N*-vinyl formamide moieties. The use of a Grignard reagent also failed to produce any desired product (**Table 8**, entry 12).

It was clear from these discouraging results that a more forceful approach was necessary. Remarkably, treatment with sodium hydroxide in refluxing methanol resulted in the desired hydrolysed product **118** in moderate yield (**Table 8**, entry 13). The production of a lower polarity spot was evident after a few hours and it was best to stop the reaction before starting material was completely consumed to avoid this.

Table 8 Investigation into the deprotection of model propionate ester **110**

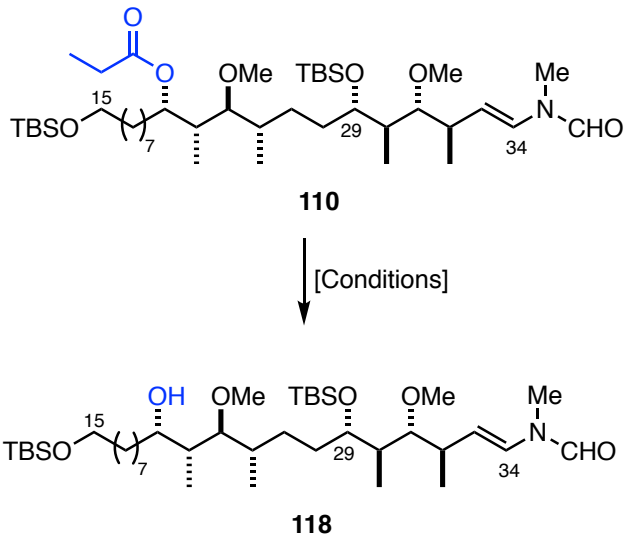

Entry	Conditions	Result
1	DIBAL, –78 °C	Hydrolysis of *N*-vinyl formamide
2	$LiBH_4$, 0 °C	Hydrolysis of *N*-vinyl formamide
3	$LiAlH(O\textit{t}\text{-}Bu)_3$, 0 °C	Hydrolysis of *N*-vinyl formamide
4	K_2CO_3, MeOH, rt	**110**
5	K_2CO_3, MeOH, 65 °C	**110**
6	LiOH, THF	**110**
7	NEt_3, MeOH	**110**
8	NaOMe, MeOH	**110**
9	KOH, THF	**110**
10	Me_3SnOH, CH_2Cl_2	**110**
11	$Ba(OH)_2$, MeOH	Unidentified product
12	MeMgBr (3 eqv.)	**110**
13	NaOH, MeOH, 65 °C	**118** (50%)

Before moving to the real system, these conditions were trialled on northern iodide **56** and gratifyingly, no elimination or deprotection reactions were observed at the silyl ethers. Pleasingly, these conditions translated well into the real system. The modest result of 55% yield (87% yield brsm) was deemed reasonable with the majority of unreacted starting material recovered (**Scheme 53**). Hence, a sufficient quantity of advanced material could be produced to continue work towards the macrocycle.

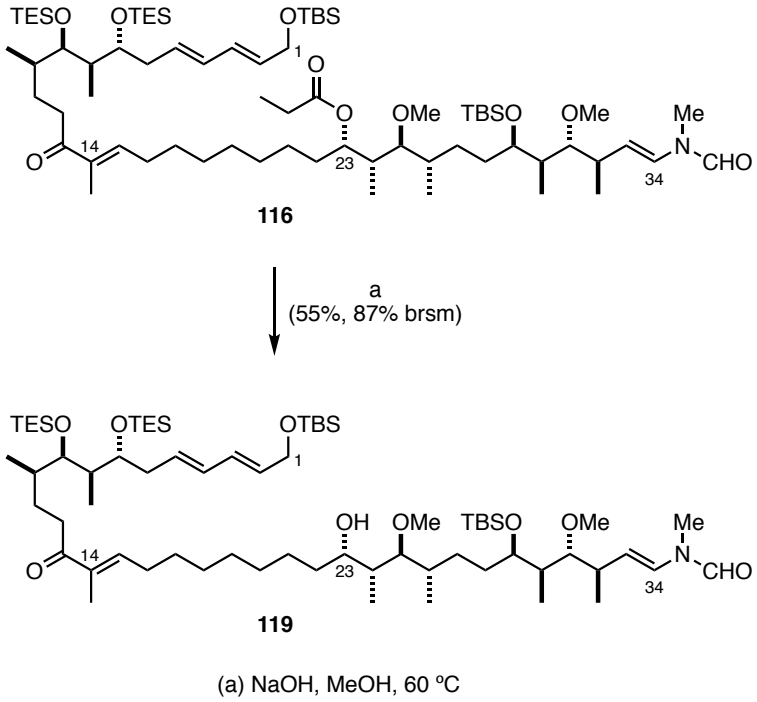

Scheme 53 Propionate ester cleavage in advanced fragment **116** to form C_{23} alcohol **119**

3.1.6 Advancement towards the macrocycle

Successful cleavage of the propionate left us two oxidation steps away from accessing the necessary *seco*-acid **120** for macrolactonisation. A serendipitous discovery during our group's studies towards the aplyronines was the concomitant deprotection and oxidation of an allylic silyl ether to the corresponding aldehyde upon exposure to DDQ.[159] The proposed mechanism commences with oxidation at the allylic position and hydride transfer from the activated methylene through single electron transfer steps. The aldehyde is then subsequently exposed through loss of the silyl group (**Scheme 54**).[221]

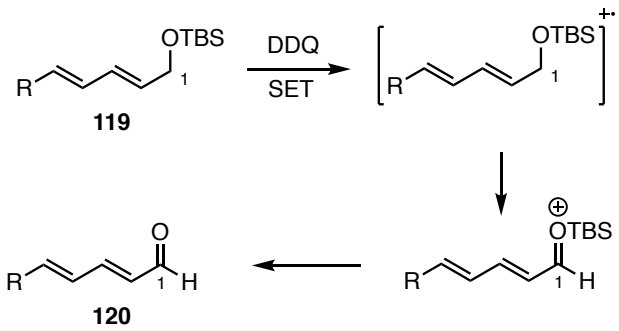

Scheme 54 DDQ mediated allylic oxidation of TBS ether **119**

Silyl ether **119** was therefore treated with DDQ in biphasic CH_2Cl_2/pH 7.0 buffer (1:1) solution at 0 °C to generate aldehyde **120** in 74% yield (**Scheme 55**). Oxidation to the required *seco*-acid followed by macrolactonisation would then furnish our fully protected aplyronine analogue precursor. This sequence was to be completed through a Pinnick oxidation and Yamaguchi esterification, analogous to the real aplyronine system.[222,223] Preliminary results indicated that macrolactonisation had occurred on test reaction scale (2 mg), however this result could not be replicated, and all subsequent attempts resulted in destruction of the material to unidentifiable byproducts (**Scheme 55**). Due to the small scale of these reactions, it is unclear which of the two steps proved incompatible with our substrate but, once again, the ^{1}H NMR signals from the *N*-vinyl formamide moiety had disappeared.

At this stage of the project, stocks of advanced intermediates were low. In the course of this route, we had faced unforeseen difficulties and encountered challenging reactions with poor yields. Furthermore, the crucial macrolactonisation had failed and the path towards successful optimisation was unclear. Hence, it was decided to abandon this alternative coupling strategy and revert to the well-established chemistry within the original coupling sequence.

3.2 Established coupling sequence

Whilst the alternate coupling sequence was under investigation by the author, Pettigrew was simultaneously advancing material towards analogues through the route borne out in the natural product synthesis. With plentiful stocks of northern and southern fragments to hand, the goal was therefore to obtain a sizeable stockpile of macrocyclic intermediate through this established route for advancement towards a library of analogues.

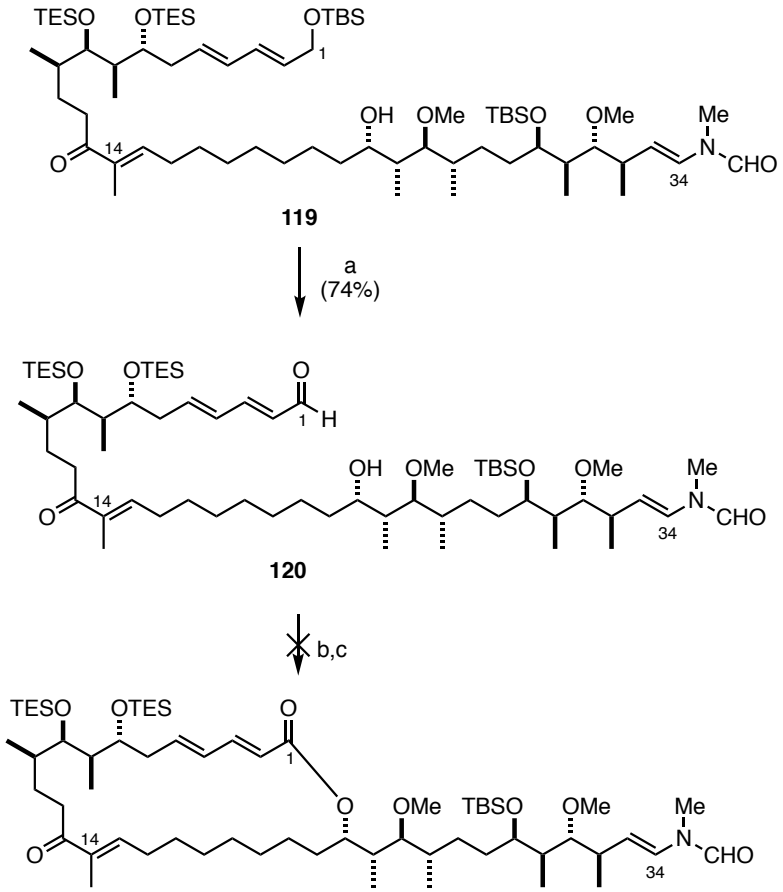

(a) DDQ, CH_2Cl_2/pH 7.0 buffer (1:1), 0 °C; (b) $NaClO_2$, NaH_2PO_4, *t*-BuOH, 2-methyl-2-butene, H_2O; (c)TCBC, NEt_3, THF; *then* PhMe, addition into DMAP, PhMe

Scheme 55 Oxidation of allylic TBS ether **119** to aldehyde **120** and attempted Pinnick and macrolactonisation reactions

3.2.1 Coupling of northern and southern fragments

This well precedented coupling strategy commences with the Horner–Wadsworth–Emmons reaction of β-ketophosphonate **36** and aldehyde **52**. The required aldehyde could be accessed through selective deprotection of the TBS ether at C_{15} under acidic conditions, followed by Swern oxidation of the resulting alcohol (**Scheme 56**).

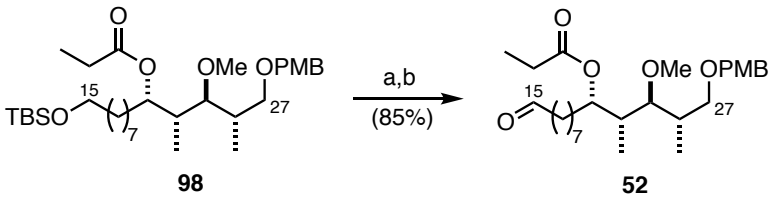

98 **52**

(a)THF/H_2O/HCl 3M aq. (5:2:1); (b) $(COCl)_2$, DMSO, NEt_3, CH_2Cl_2, −78 °C → rt

Scheme 56 Deprotection and oxidation of southern fragment **98** to aldehyde **52**

By an analogous procedure (**Section 3.1.4**), the HWE reaction proceeded smoothly to generate enone **121** in 85% yield (**Scheme 57**). In this case, aldehyde **52** was viewed as the less precious fragment (accessible in 5 steps) compared to phosphonate **36** (10 steps) and thus was used in slight excess (1.05 equivalents). Again, the phosphonate minor regioisomer **77** could be separated cleanly at this stage. With the two fragments coupled, the next step was the introduction of the allylic alcohol through asymmetric reduction of the C_{13} ketone. Pleasingly, without the *N*-vinyl formamide moiety present, the CBS reduction proceeded smoothly to generate alcohol **122** in excellent yield (93%) as a single diastereoisomer. The stereocontrol can be rationalised by inspection of the transition state as previously discussed (**Section 3.1.4**, **Scheme 52**). Stoichiometric quantities of the CBS 'catalyst' were employed to ensure high reaction rates and selectivity. The 13*S* alcohol was assigned by comparison to Pettigrew's analysis, wherein the configuration was determined through Mosher ester analysis.[165] Ensuing methylation with Meerwein salt (Me_3OBF_4) and proton sponge proceeded smoothly in 87% yield. The propionate ester cleavage, which had caused such difficulties in the presence of the *N*-vinyl formamide could now simply be achieved through treatment with DIBAL at low temperature. Alcohol **123** could be quickly and efficiently formed in this way in almost quantitative yield (**Scheme 57**).

This sequence of steps could reliably be carried out on larger quantities of material and delivered over 2 g of alcohol **123** for further studies, further highlighting the efficiency of this route. Pleasingly, all of the steps displayed equal or improved yields on larger scales.

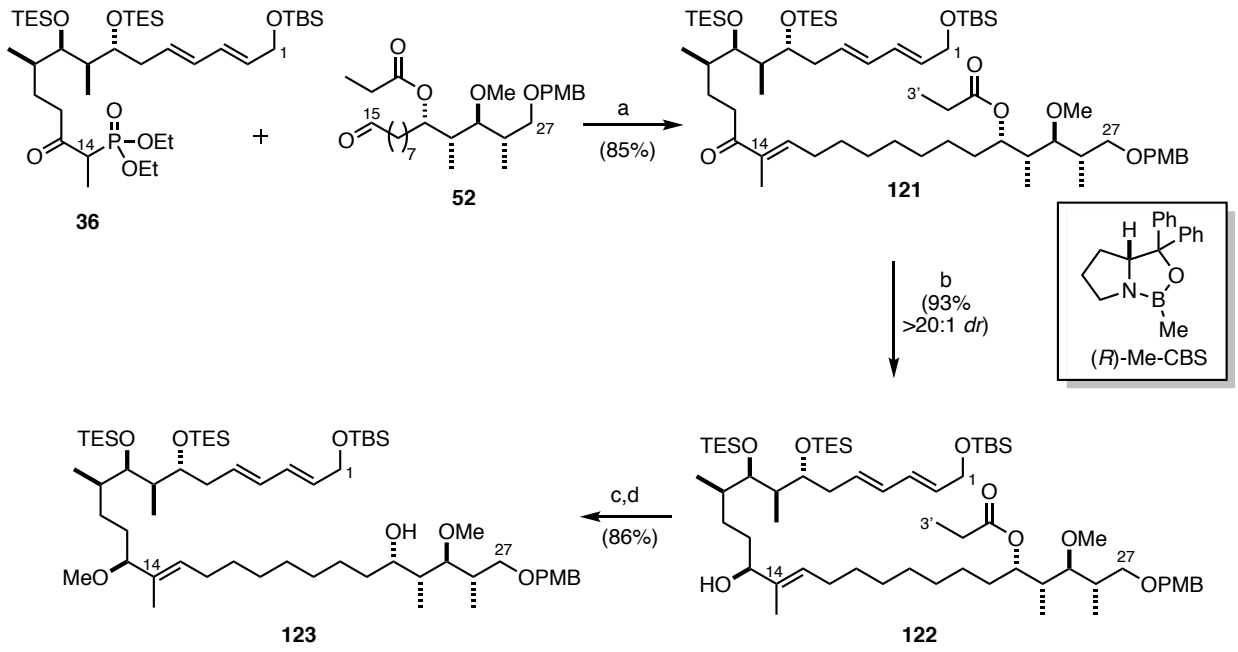

(a) $Ba(OH)_2$, THF, *then* **52**, THF/H_2O (40:1); (b) (*R*)-Me-CBS, $BH_3 \cdot SMe_2$, THF, −10 °C; (c) Me_3OBF_4, proton sponge, CH_2Cl_2; (d) DIBAL, CH_2Cl_2, −78 °C

Scheme 57 Northern and southern fragment coupling and elaboration to generate alcohol **123**

3.2.2 Towards the macrocycle

As previously discussed in **Section 3.1.6**, the 24-membered macrolactone could be accessed through oxidation at C_1 to expose the carboxylic acid for subsequent esterification. This sequence begins with the elegant DDQ mediated deprotection and oxidation of the allylic TBS ether **123**. However, careful handling was required for this compound. Unlike the previous DDQ substrate **119**, our current intermediate possesses a PMB ether at C_{27} which is usually labile under the oxidative DDQ conditions. Preferential macrolactonisation to forge the undesired 26-membered macrolactone had been observed to occur on material with the C_{27} alcohol, hence its protection remained essential at this stage.[165] Woodrow observed that the allylic oxidation occurred faster than PMB cleavage to deliver the desired kinetic aldehyde product.[221] Pettigrew witnessed similar results and delivered optimised conditions for this transformation.

Moving forward, TBS ether **123** was exposed to solid DDQ in biphasic CH_2Cl_2 and aqueous buffer solution at 0 °C. The reaction was strictly quenched after 15 min to avoid

chemoselectivity issues with the PMB ether. In this way, aldehyde **124** could be formed in a respectable 75% yield and unreacted starting material could easily be recovered and resubmitted. Pettigrew reported optimum results with the use of pH 9.2 buffer solution. It was surmised that under neutral conditions (pH 7.0 buffer), the acidic DDQH generated during the reaction was promoting undesired protecting group migrations, leading to apparent recovered 'starting material' that was not synthetically useful. Gratifying, under the basic buffered conditions, the recovered material proved to be spectroscopically identical to the starting material. Overall, aldehyde **124** could reliably be produced with a best result of 75% yield (91% brsm) on a scale of 800 mg.

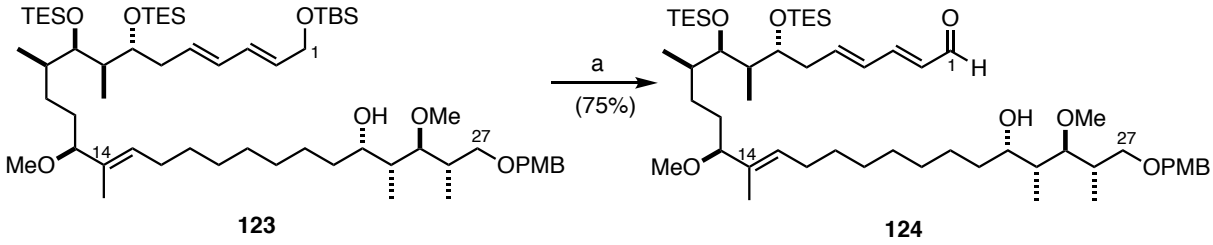

(a) DDQ, CH_2Cl_2/pH 9.2 buffer (4:1), 0 ºC

Scheme 58 DDQ mediated allylic TBS deprotection and oxidation sequence to form aldehyde **124**

The *seco*-acid for macrolactonisation can be obtained through a chemoselective Pinnick oxidation of the aldehyde at C_1. The strengths of the Pinnick oxidation lies in the mild reaction conditions, rendering it applicable for use on complex substrates with a broad range of sensitive functional groups. Under conditions of sodium chlorite in combination with hypochlorous acid and scavengers, Lindgren and Nilsson first reported the oxidation of aldehydes to carboxylic acids.[223] Kraus and co-workers developed the methodology further by introducing 2-methyl-2-butene as the scavenger under buffered conditions.[224,225] Pinnick successfully generalised this process and demonstrated its application to a wide range of α,β-unsaturated aldehydes.[226]

The active oxidant in this transformation is believed to be chlorous acid ($HClO_2$), produced from sodium chlorite under the mildly acidic dihydrogenphosphate-buffered conditions. Addition of this species into the aldehyde produces an adduct that undergoes hydride abstraction through a pericyclic transition state. In this process, the carboxylic acid product and hypochlorous acid (HOCl) are produced (**Scheme 59**). This HOCl byproduct is a highly

reactive species and can react with the starting sodium chlorite to generate chlorine dioxide (ClO_2), thus inhibiting the reaction. Additionally, any olefins present in the aldehyde substrate risk reaction with electrophilic HOCl, resulting in the creation of unwanted halohydrins. Consequently, a sacrificial additive, such as 2-methyl-2-butene, is added in large excess to act as a HOCl scavenger and prevent byproduct formation.

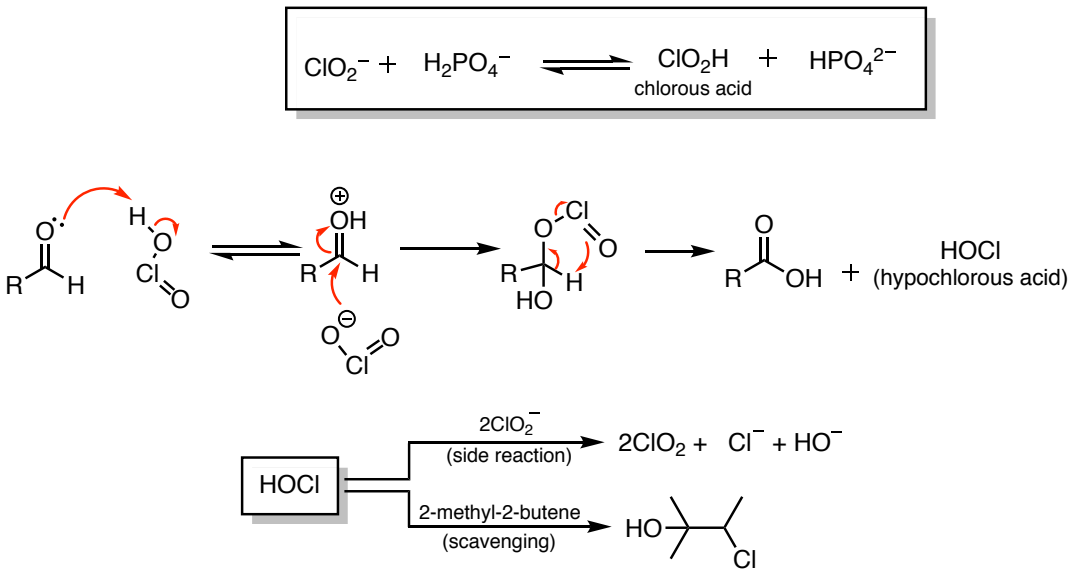

Scheme 59 Mechanism for the Pinnick oxidation of an aldehyde

In this case, Pinnick oxidation of aldehyde **124** proceeded smoothly upon exposure to a large excess of reagents, to yield *seco*-acid **125** after a simple aqueous workup (**Scheme 60**). Typically, the material was clean enough to be subjected directly to the esterification reaction in crude form and thus column chromatography was not performed on the highly polar acid.

3.2.3 Macrolactonisation

With the required *seco*-acid **125** in hand, attention turned to the pivotal macrolactonisation step. The method of choice was the Yamaguchi protocol as this had been successfully implemented in the aplyronine natural product synthesis to form the C_1–C_{27} macrocycle. In the method developed by Yamaguchi, upon treatment with 2,4,6-trichlorobenzoyl chloride and triethylamine, the carboxylic acid functionality is first converted to the reactive mixed anhydride species (**Scheme 61**). The mixed anhydride solution is then diluted and added slowly (*e.g. via* syringe pump) to a solution of DMAP which acts as a nucleophilic catalyst

to promote the intramolecular condensation. Classically, the reaction is conducted under conditions of high dilution and slow addition to minimise intermolecular coupling and suppress the formation of oligomers.[222] Investigations by Dhimitruka and SantaLucia have suggested the formation of a symmetrical aliphatic anhydride, contrasting with the mixed anhydride view.[227,228]

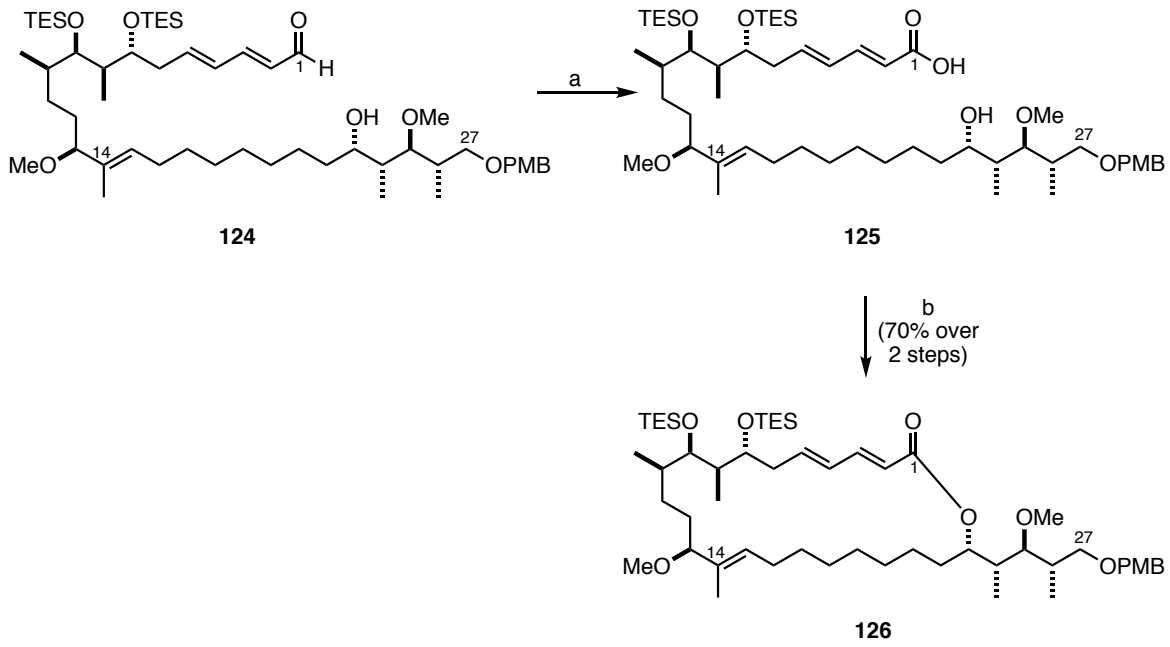

(a) $NaClO_2$, $NaH_2PO_4 \cdot 2H_2O$, *t*-BuOH, 2-methyl-2-butene, H_2O; (b) TCBC, NEt_3, THF; *then* PhMe, addition into DMAP, PhMe

Scheme 60 Pinnick oxidation and Yamaguchi macrolactonisation sequence to form the fully protected C_1–C_{27} macrocyclic intermediate **126**

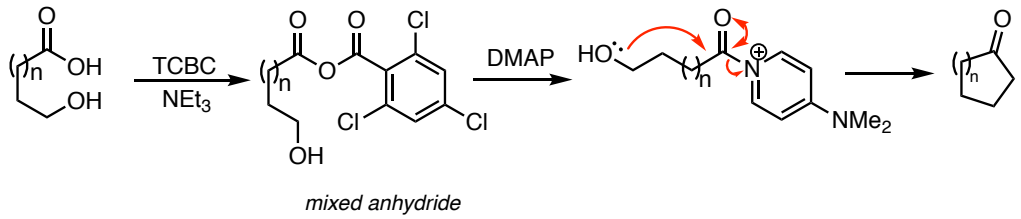

Scheme 61 Mechanism for the Yamaguchi macrolactonisation

Seco-acid **125** was treated with TCBC and NEt_3 before the mixed anhydride solution was diluted with toluene and added to a large excess of DMAP over 2-12 h *via* syringe pump. This delivered macrolactone **126** in good yield (70% yield over two steps, **Scheme 60**) on a 500 mg batch. Through this procedure, over 1 g of key macrocyclic intermediate **126** was generated. The fully protected macrocycle was a convenient point to store advanced stocks, as this material proved amenable to long term storage at –20 °C.

3.3 Side chain installation

With plentiful stocks of protected macrocycle **126**, the planned sequence to construct our aplyronine analogues could continue with the final fragment coupling to attach the side chain. Having fully optimised this reaction in the alternative coupling sequence, we were optimistic that these conditions would translate well into our current system.

3.3.1 Aldol coupling

Deprotection of PMB protected macrocycle **126** could be achieved under standard conditions (DDQ, CH_2Cl_2, pH 7.0 buffer), and the resulting alcohol **127** was oxidised with DMP. This delivered the macrocyclic aldehyde **53** necessary for subsequent aldol coupling (**Scheme 62**).

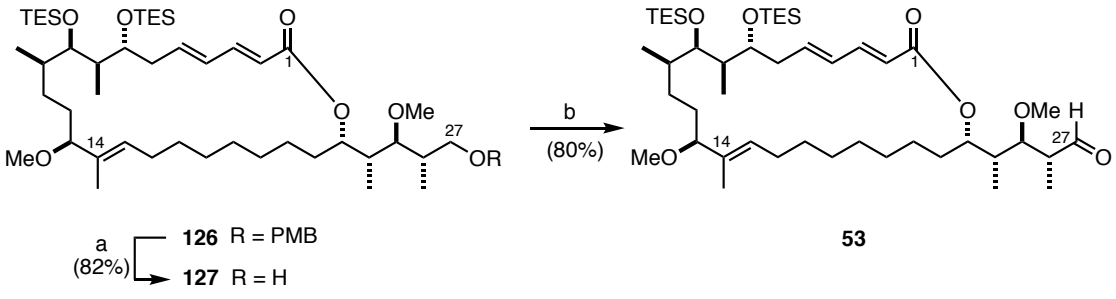

(a) DDQ, CH_2Cl_2/pH 7.0 buffer; (b) DMP, $NaHCO_3$, CH_2Cl_2

Scheme 62 Synthesis of aldehyde **53** from PMB protected macrocycle **126**

Due to the highly precious nature of the intermediates, we proceeded with caution for this final fragment coupling. Frustratingly, the previously developed conditions (1.5 equivalents of enolate, silica gel work-up) did not translate well into these more advanced substrates. All initial attempts at the boron-mediated aldol reaction failed, with starting material aldehyde **53** and ketone **51** returned quantitatively. Reflecting that poor-quality reagents might have caused the reaction to fail, fresh dicyclohexylboron chloride was prepared, but to no avail. The reaction remained troublesome. Puzzlingly, Pettigrew reported no similar difficulties at this stage and successfully forged the coupled product.

In an attempt to encourage conversion, the excess of side chain ketone **51** was vastly increased to 6 equivalents, alongside a change in experimental procedure. Previously, the Lewis acid and triethylamine base had been added neat to a solution of ketone **51** in diethyl ether. Contrastingly, in this case it was found that pre-mixing the BCy_2Cl and NEt_3 and generating a 1 M solution of 'enolising reagent' was crucial for a successful reaction. Whilst the high loading of ketone is not ideal, the differences in molecular weight between this small fragment and the larger macrocycle render this manageable. Additionally, excess enolate would regenerate ketone **51** upon workup and the surplus could be recovered almost quantitatively after the Burgess elimination. Pleasingly, it was found that on larger scales, the ketone loading could be reduced to 2 equivalents.

To this end, the enolate derived from ketone **51** was added to aldehyde **53** at −78 °C and the reaction was slowly warmed to −20 °C over 1 h. Progression could be monitored by TLC analysis and once complete, the reaction was quenched by addition of silica gel and stirring with exposure to air. As before, incorporation of the *N*-vinyl formamide moiety results in a large increase in polarity of the aldol adduct product **128**, rendering it inseparable from excess ketone at this stage.

The Burgess elimination was employed once again to eliminate the newly formed C_{27} hydroxyl to forge enone **129**. As previously observed, the reaction was prone to stalling and best practice was to halt, work-up and resubmit the material to ensure full conversion. Through this aldol–dehydration sequence, the full C_1–C_{34} aplyronine carbon skeleton was assembled in a good 65% yield over 3 steps from alcohol **127** (**Scheme 63**).

3.3.2 Conjugate reduction of enone 129

With the full carbon backbone in place, the final step in this sequence is the conjugate reduction of enone **129** to form ketone **130**. This transformation is precedented within the aplyronine natural product synthesis and can be accomplished by treatment with Stryker's

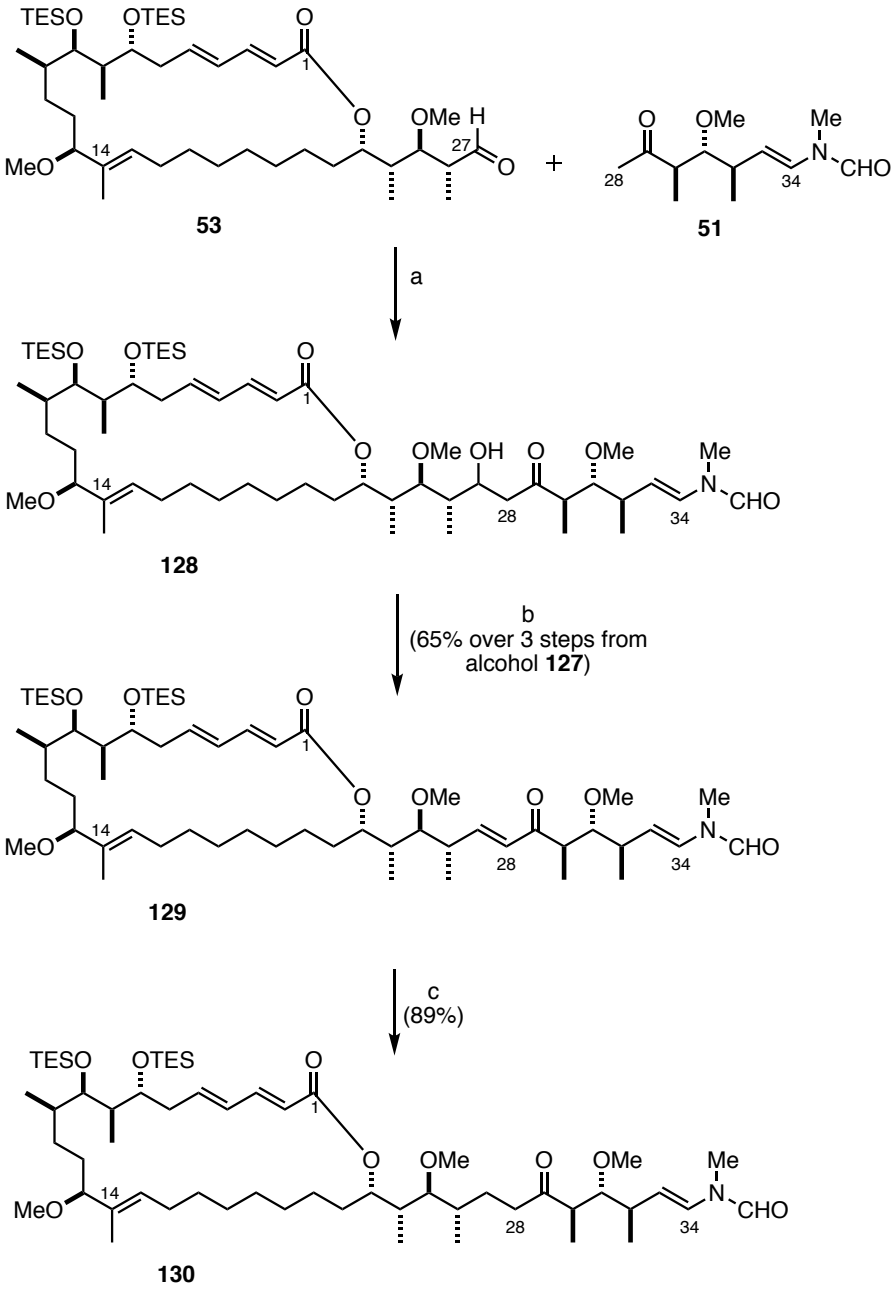

(a) **51**, $BCy_2Cl \cdot NEt_3$ (1M in Et_2O), 0 ºC, then **53**, −78 ºC; (b) Burgess reagent, THF; (c) $[CuH(PPh_3)]_6$ (5 mol%), PhMe

Scheme 63 Synthesis of advanced ketone **130** with the full C_1–C_{34} aplyronine carbon skeleton

reagent. The reagent was prepared and used in an analogous manner to that previously discussed (**Section 3.1.1**). Notably, in this case, it is imperative to achieve chemoselectivity for the enone over the pentadienoate moiety. For this purpose, triphenylphosphine was crucially employed as a ligand to form a less active reagent through a modified Lipshutz protocol.[229]

Treatment of enone **129** under standard conditions of 20 mol% of Stryker's reagent solution led to a product initially identified as ketone **130 (Scheme 63)**. However, upon closer inspection of the ^{1}H NMR it soon transpired that another component was present in the reaction mixture (*ca*. 50%). Significantly reduced integration values of the dienoate protons (H_2–H_5) indicated that side reactivity of the pentadienoate moiety was occurring alongside enone reduction. Byproduct **131** is surmised to have the structure shown in **Figure 33**, although this has not been rigorously confirmed through purification and full structural elucidation as the byproduct is inseparable from ketone **130**.

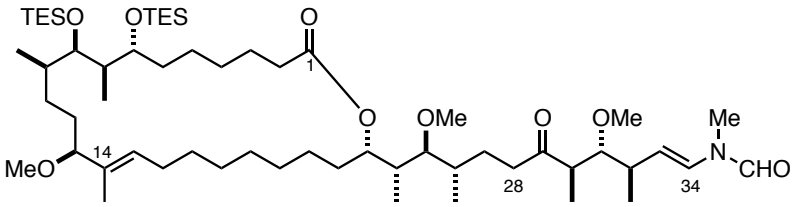

131

Figure 33 Hypothesised reduced dienoate product from Stryker's reduction of enone **129**

Williams reported no evidence of this byproduct forming on the real aplyronine system and surprisingly, the reaction had to be pushed to completion with further aliquots of Stryker's reagent solution needed.[121] It therefore seems that on our simplified substrate, the pentadienoate moiety is much more susceptible to conjugate reduction. Re-examination of Pettigrew's results indicate that **131** was also observed in this case.

Optimisation of this reaction was carried out in an effort to suppress the formation of this unwanted byproduct (**Table 9**). Running the reaction at a lower temperature or in the dark did not improve the result (**Table 9**, entries 1–2). Lowering the loading required us to balance the reactivity with selectivity (**Table 9**, entries 3–4) with 5 mol% loading ultimately providing pleasing results.

Table 9 Optimisation of the conjugate reduction of enone **129** using Stryker's reagent

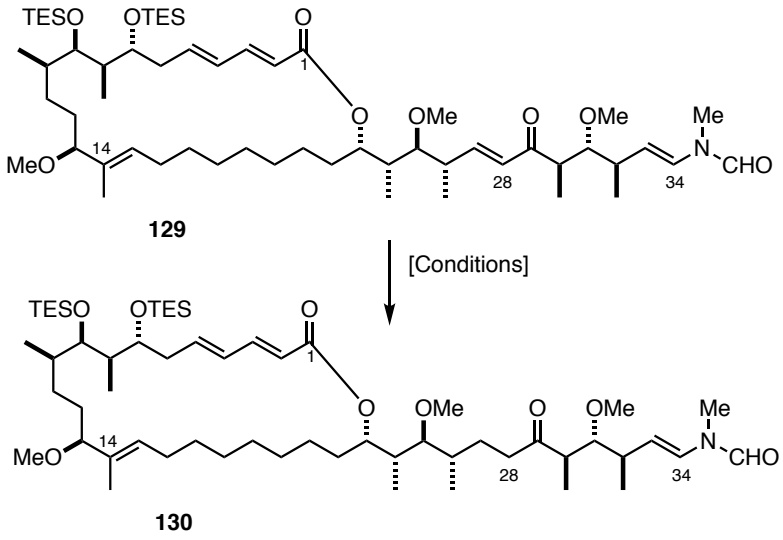

Entry	Conditions	Result
1	20 mol% → 40 mol% $[CuH(PPh_3)]_6$, TMDS, 0 °C	Significant over-reduction
2	20 mol% $[CuH(PPh_3)]_6$, rt, TMDS, dark	Significant over-reduction
3	1 mol% $[CuH(PPh_3)]_6$, TMDS, rt	No conversion
4	5 mol% → 20 mol% $[CuH(PPh_3)]_6$, TMDS, rt	89% **130**

With careful monitoring of the reaction together with the reduced catalyst loading, ketone **130** could be cleanly furnished in a few hours in an excellent and reliable 89% yield, with no over-reduction observed (**Scheme 63**). Monitoring conversion by TLC analysis was futile since starting material enone **129**, ketone **130** and byproduct **131** all possess the same retention factor on silica in a variety of solvent systems. Hence aliquots were taken every hour, filtered through a small plug of silica and analysed by ^{1}H NMR spectroscopy. By this method it was possible to follow the disappearance of enone signals to judge when the reaction was complete, whilst minimising the formation of byproduct **131**. At this point, the full carbon skeleton of our designed analogues was in place and the stage was set for late stage diversification to deliver a library of analogues for biological evaluation.

3.4 Summary

This chapter has outlined endeavours towards two complementary methods for advanced fragment coupling. Firstly, we focused on connecting the southern and side chain fragments before the addition of the northern fragment (**Scheme 64**). Whilst this approach ultimately failed to deliver a reliable and efficient route towards analogues, its advantage lay in the early entry of the boron-mediated aldol reaction. Significant optimisation of this reaction was carried out with a noteworthy improvement in yield obtained. Furthermore, this route taught us much about the side chain chemistry and revealed the truly remarkable and impressive stability of *N*-vinyl formamide moiety to a variety of conditions. However, given the difficulties of the CBS reduction associated with the *N*-vinyl formamide and failures in macrolactonisation, efforts towards this route were deprioritised in favour of the established approach.

The previously published Paterson strategy once again served well and proved to be a reliable method to unite complex fragments to assemble the C_1–C_{27} macrolactone. Elaboration of the macrolactone to the full carbon skeleton was achieved through appendage of the side chain moiety. The late stage boron-aldol coupling in this route proved challenging to implement on more complex substrates but ultimately delivered the desired coupled product. Optimisation of the Stryker's reduction yielded a reliable protocol to furnish ketone **130** efficiently (**Scheme 65**).

Following this sequence, ketone **130** was prepared in 14 steps and 17% yield from southern fragment **98**. The highly anticipated conversion of ketone **130** into designed aplyronine analogues will be presented in the next chapter.

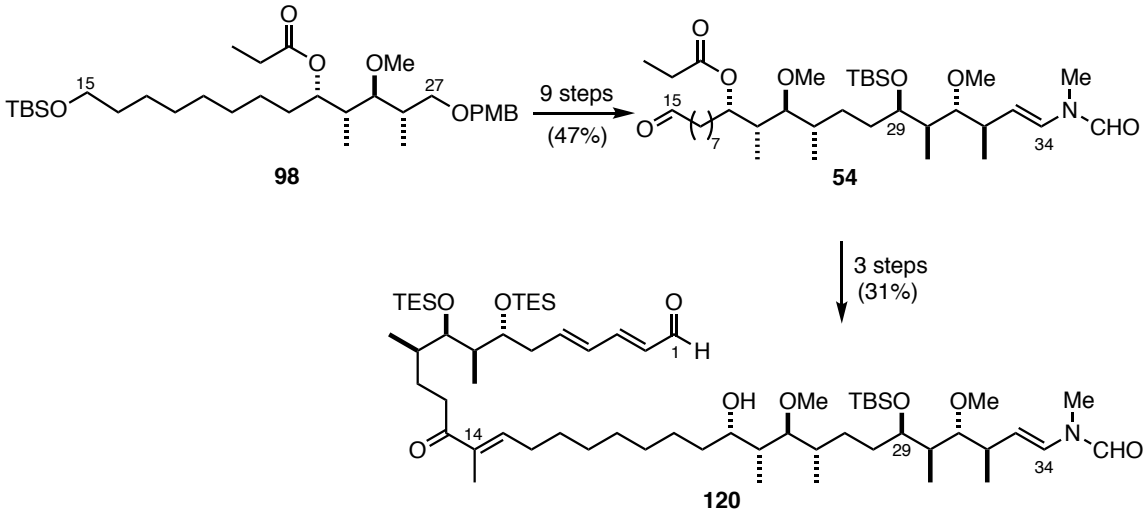

Scheme 64 Summary of the alternative coupling approach

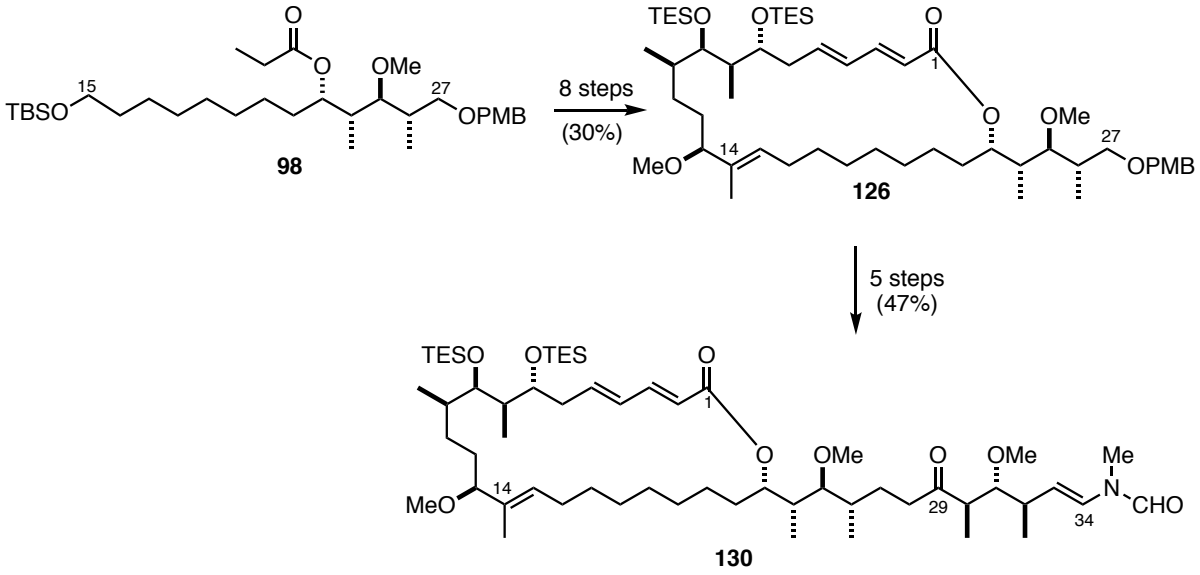

Scheme 65 Summary of the established coupling strategy to ketone **130**

Chapter 4

Towards antibody–drug conjugates

Our ultimate goal is to develop structurally simplified analogues of the aplyronines, that retain the exquisite potency of the corresponding natural products, to incorporate into next generation antibody–drug conjugates. At this point, in order to achieve this aim, three outcomes needed to be accomplished: (1) completion of the synthesis of these highly complex molecules through a late stage diversification strategy, thus generating a small library of analogues, (2) biological testing of our analogues to critically assess the effects of our structural modifications, and (3) investigations into suitable linker chemistry for bioconjugation to an antibody. Each of these efforts will now be described.

4.1 Completion of analogue synthesis

With ketone **130** in hand, the full analogue skeleton was in place and only few modifications were needed to complete the synthesis of these designed compounds. A late stage diversification strategy was envisaged to ultimately generate a focused library of analogues. With the C_{29} ketone in place, those analogues contain a side chain similar to that of scytophycin C (**Figure 22, Section 1.4.3**) and in the first instance these hybrid structures were targeted.

4.1.1 Scytophycin-type hybrid analogues

Ketone **130** could be transformed into aplyronine–scytophycin hybrid analogues in two steps, deprotection and esterification. Esterification at C_7 with *N*,*N*,*O*-trimethylserine (TMSer) is pivotally important for cytotoxicity and our attention turned to installing this crucial functionality. As previously discussed, this amino acid residue exists as a scalemic mixture of epimers (*ca.* 1:1) and it is unclear if this is a natural feature of these compounds, or an artefact of the isolation procedure. Due to subtle differences in the pharmacophore, each diastereoisomer could have a unique biological profile as one of the serine enantiomers could potentially promote stronger interactions with tubulin than the other. Hence, appending enantiomerically pure amino acids was a deliberate strategy designed to examine these effects.

Towards this end, Pettigrew made significant progress, delivering two aplyronine–scytophycin analogues (**Figure 34**). The first of these was the aplyronine C-like hybrid **132**, bearing two free hydroxyl groups in the northern region. The second analogue **133** contains the naturally occurring (*S*)-TMSer amino acid group at C_7.[165] Close inspection of the ^{1}H NMR spectrum, however, revealed that the over reduced dienoate byproduct **131** (**Section 3.3.2**) was a significant contaminant of this material and thus could have consequences in modifying the biological activity of these compounds (*vide infra*, **Section 4.2**). Following this discovery, the goal of the author was therefore to re-synthesise these analogues to cleanly deliver the separate (*R*)- and (*S*)-trimethyl serine esters.

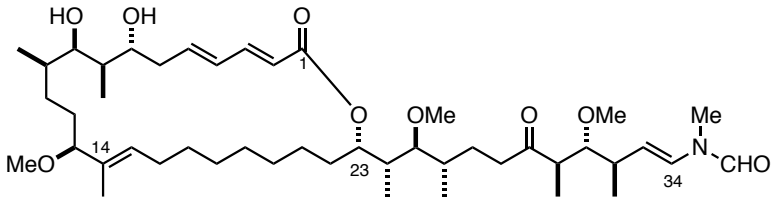

132

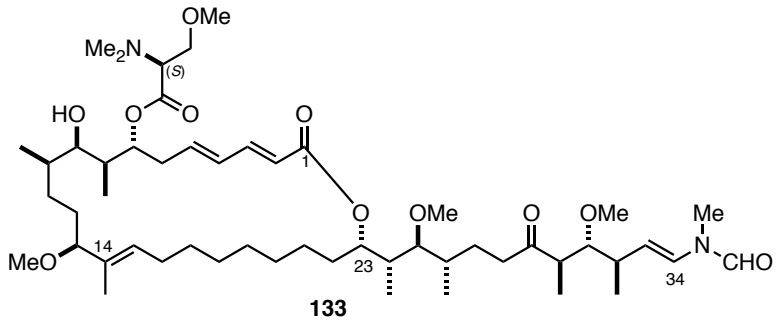

133

Figure 34 Aplyronine–scytophycin hybrid analogues synthesised by Pettigrew

Exposure of *bis*-TES protected **130** to conditions of buffered HF·pyridine resulted in the formation of diol **132** in 85% yield (**Scheme 66**). Dr Simon Williams had prepared each enantiomer of TMSer for use in the aplyronine projects and had successfully demonstrated that acylation could be achieved site-selectively at C_7 over the more hindered C_9 position.[121] Yonemitsu esterification conditions proved to be the most reliable way to achieve this transformation. These conditions are a variant of the Yamaguchi method whereby all the reagents are combined simultaneously, bypassing the pre-formation of the mixed anhydride species.[230]

Careful monitoring of the progress of the reaction was necessary to avoid *bis*-acylation, and by cautiously adding aliquots of reagent from a stock solution it was possible to push the reaction to an acceptable conversion. In this way, the (*S*)-epimer **133** was prepared in 62% yield and the analogous (*R*)-epimer **134** in 73% yield (**Scheme 66**).

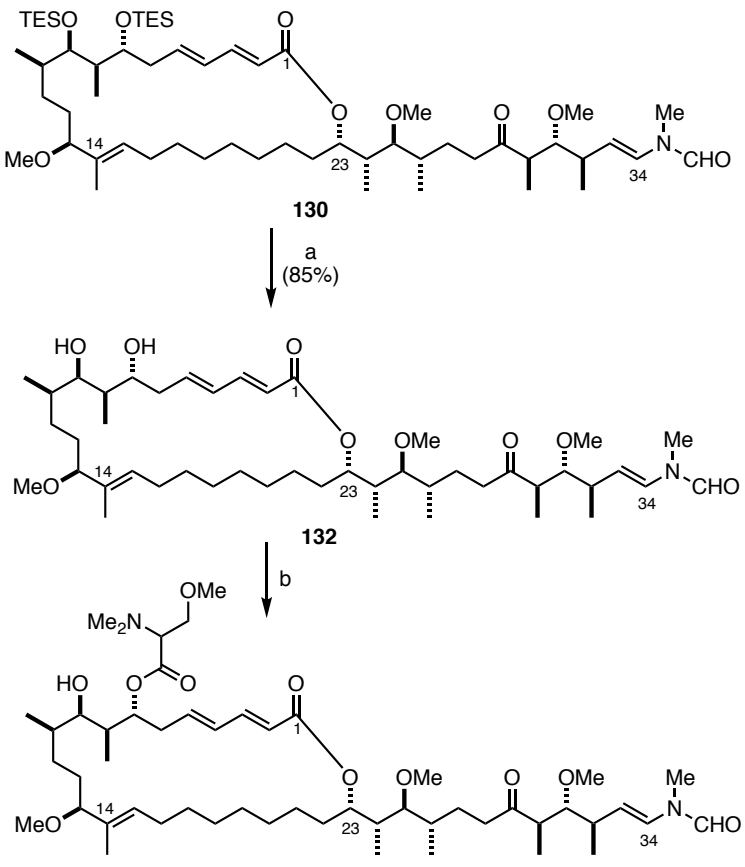

(a) HF·py, py, THF, 0 ºC → rt; (b) (*S*)- or (*R*)-TMSer, DMAP, TCBC, NEt_3, CH_2Cl_2/benzene, 0 ºC

Scheme 66 Synthesis of scytophycin-type analogues **133** and **134**

4.1.2 Aplyronine D analogue 44

With the C_{29} ketone analogues in hand, the next stage of our project was to investigate the installation of the ester moiety at this position. As in the alternative fragment coupling sequence (**Section 3.1.2**), diastereoselective reduction of the ketone functionality would be necessary. Initial testing of the zinc borohydride reduction on highly advanced ketone **130** once again highlighted the challenges associated with this reaction. In this case, ^{11}B NMR analysis confirmed the zinc borohydride reagent had successfully formed ($Zn(BH_4)_2$ ^{11}B: – 45 ppm).[204]

As previously experienced, yields and *dr* were highly variable. Furthermore, on these more complex substrates, TLC analysis and column chromatography were more difficult. The compounds appear as two spots due to the stable *N*-vinyl formamide rotamers and have a tendency to streak due to their high polarity. Moderate yields of 50-60% were typically observed with a *dr* of 2:1 (**Scheme 67**). Interestingly, an attempt to carry out the reaction using sodium borohydride seemed to yield the undesired (*S*)-diastereoisomer exclusively, although due to the small scale of the reaction this product was not fully characterised. The (*R*)-configuration at C_{29} was unambiguously determined by Mosher ester analysis. Thus, the (*R*)- and (*S*)-MTPA esters **136** and **137** were formed, and the sign of $\Delta\delta_{S-R}$ for protons on each side of the derivatised alcohol was consistent with the (*R*)-configuration as shown (**Scheme 67**).

We first targeted an aplyronine D analogue with the *N*,*N*-dimethyl glycine residue in the side chain. Based on Yamada's initial biological testing, aplyronine D exhibits greater cytotoxicity than aplyronine A and so was prioritised for analogue development. Additionally, the lack of stereogenicity in the amino acid somewhat simplifies the analysis of the products.

Dimethyl glycine esterification of C_{29} in **130** could be achieved under Keck conditions, and the crude material immediately subjected to buffered HF·pyridine to enact the *bis*-TES deprotection. Through this sequence, diol **138** was formed in 69% yield over the two steps. Finally, esterification at C_7 using the naturally occurring (*S*)-trimethyl serine residue under the previously discussed Yonemitsu conditions afforded aplyronine D analogue **44** in 65% yield (**Scheme 68**). This analogue was now ready to be submitted for biological evaluation (*vide infra*, **Section 4.2**), alongside our scytophycin hybrid analogues **133** and **134,** to provide an insight into the effects of our modifications on cytotoxicity. Notably, these analogues have been designed to allow for a direct comparison of each epimer of TMSer, together with the effect of the ketone moiety at C_{29}, thus providing valuable SAR data.

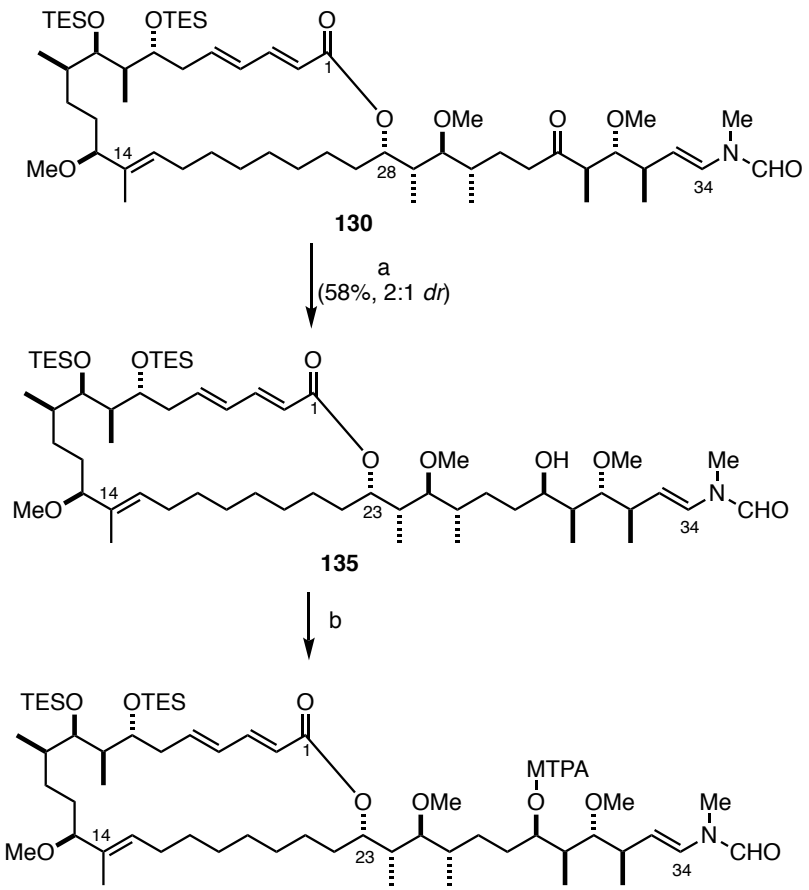

136 (*R*)-MTPA ester (63%)

137 (*S*)-MTPA ester (72%)

(a) $Zn(BH_4)_2$, Et_2O, 0 °C; (b) (*S*)- or (*R*)-MTPA-OH, DCC, DMAP, DMAP · HCl, CH_2Cl_2

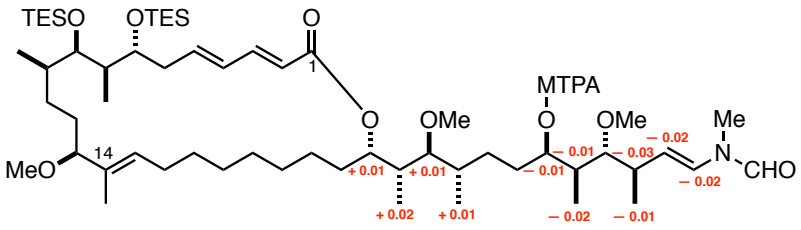

Scheme 67 Diastereoselective reduction of ketone **130** and Mosher ester analysis of alcohol **135**

Due to time pressures, the corresponding aplyronine A analogue containing a DMAla residue at C_{29} was not synthesised, but could easily be made *via* an analogous procedure in the future. With a small set of analogues in hand, the much-anticipated biological testing could now be undertaken. Details of this will follow in the next section.

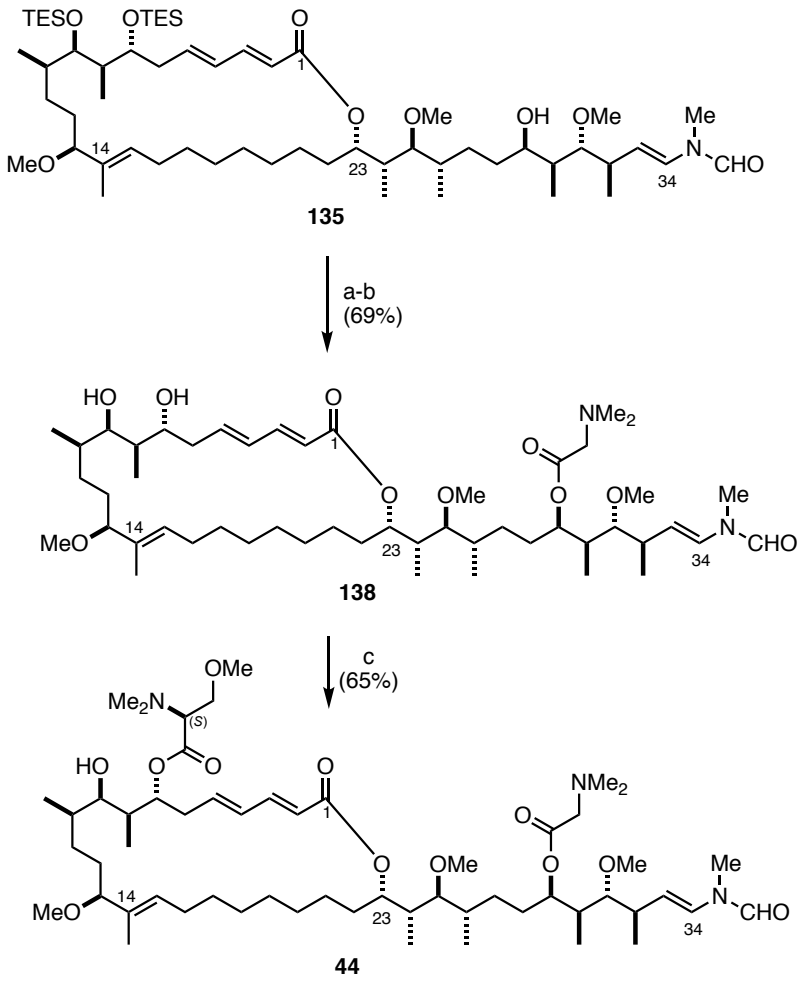

(a) DMGly, DCC, DMAP, DMAP·HCl, CH_2,Cl_2; (b) HF·py, py, THF, 0 ºC → rt;
(c) (*S*)-TMSer, DMAP, TCBC, NEt_3, CH_2Cl_2/benzene, 0 ºC

Scheme 68 Synthesis of aplyronine D analogue **44**

4.2 Biological testing

Biological testing of our aplyronine analogues was carried out by Steve Walsh in collaboration with the David Spring group from the Department of Chemistry and the Jay Carroll lab at Cancer Research UK Cambridge Research Institute. To allow for comparisons with Yamada's original biological data for the natural products, the HeLa cell line was initially chosen with a view to expanding our testing to other cell lines after these initial studies.

4.2.1 First phase

The first round of biological testing was carried out using the material prepared by Talia Pettigrew.[165] These constitute our scytophycin–aplyronine hybrid analogues with the C_{29} ketone functionality (**Figure 35**, compounds **132** and **133**). Alongside these simplified structures, synthetic samples of the aplyronines (**Figure 35**, compounds **21, 23** and **24**) prepared by Williams were submitted to the cytotoxicity assay to provide a means of directly evaluating and assessing the outcome of our structural modifications. The microtubule stabilising marine natural product discodermolide (**6, Figure 7, Section 1.1.1**) was additionally included as a control across separate assays.

The results of this assay are summarised in **Table 10**. Compounds were tested in three independent experiments, each consisting of three replicates of the same concentration of each drug. As anticipated, synthetic aplyronine A, C and D samples showed the expected picomolar antiproliferative activity. These results independently agree with earlier biological results obtained by Williams in collaboration with Professor Fernando Diaz in Madrid (Ap A 0.30 nM, ApD 0.40 nM, HeLa cell line).[121] Interestingly, the activities of aplyronine A and aplyronine D appear to be approximately equal in this HeLa cell line. This is in contrast to Yamada's findings (ApA 0.45 nM, ApD 0.071 nM, HeLa–S_3 cell line).[2,90] HeLa cells are heterogeneous and contain more than one type of mutant cells, one of which is HeLa–S_3.[231–234] It is possible that aplyronine D is more selective for these cells, which could account for the stark difference in IC_{50} values. However, it is worth mentioning that Yamada's 2012 paper disclosing the minor aplyronines contains no experimental procedures for the measurement of cytotoxicity. Alongside this, it is not clear if the cytotoxicity values quoted for aplyronines A-C were obtained in parallel assays alongside aplyronines D-H or if they are merely those measured upon their isolation in 1993. If the latter is true, it is reasonable to assume a degree of discrepancy between experiments run 19 years apart.

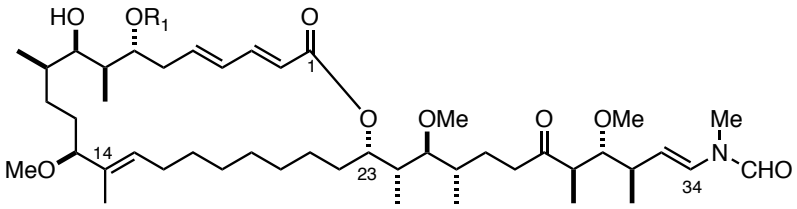

	R_1
TP01 **133**	(*S*)-TMSer
TP02 **132**	H

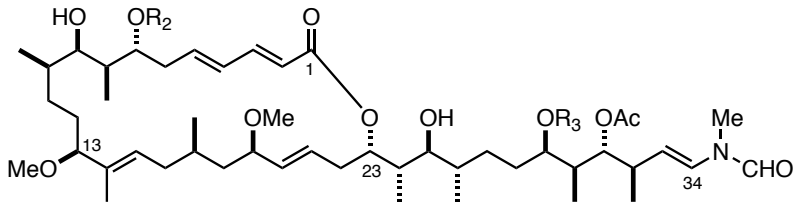

	R_2	**R_3**
Ap A **21**	TMSer (*S*:*R*, 1:1)	(*S*)-DMAla
Ap C **23**	H	(*S*)-DMAla
Ap D **24**	TMSer (*S*:*R*, 1:1)	DMGly

Figure 35 Aplyronine samples for first round of biological testing

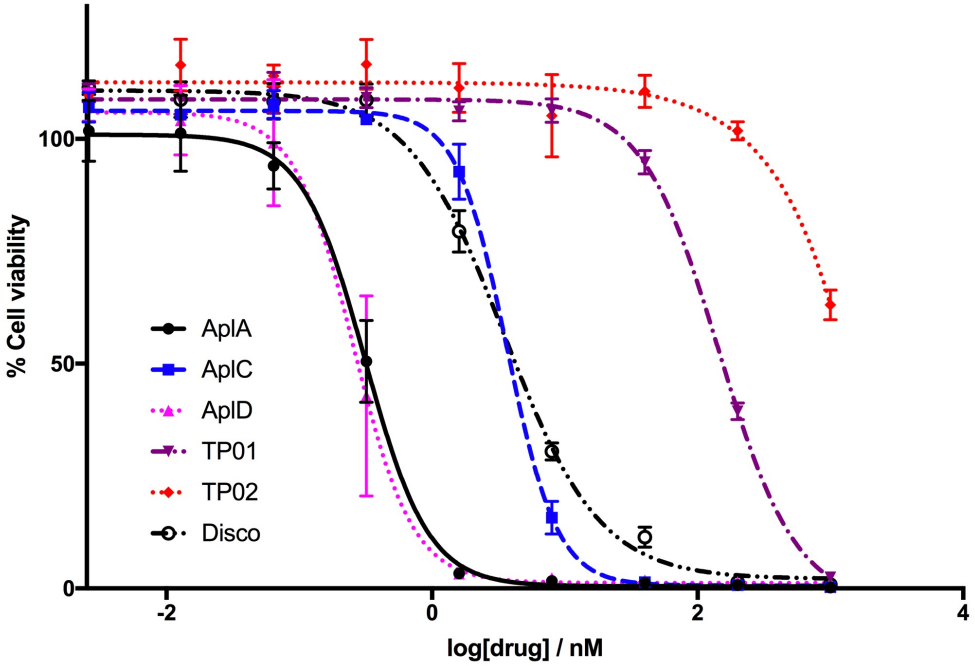

Figure 36 Cell viability graph for first phase of compounds in biological testing

Table 10 Antiproliferative activity of synthetic aplyronines and analogue samples against HeLa cells

Compound	IC_{50} / nM
Ap A **21**	0.31
Ap C **23**	3.67
Ap D **24**	0.26
TP01 **133**	146
TP02 **132**	n.d.
Discodermolide **6**	3.49

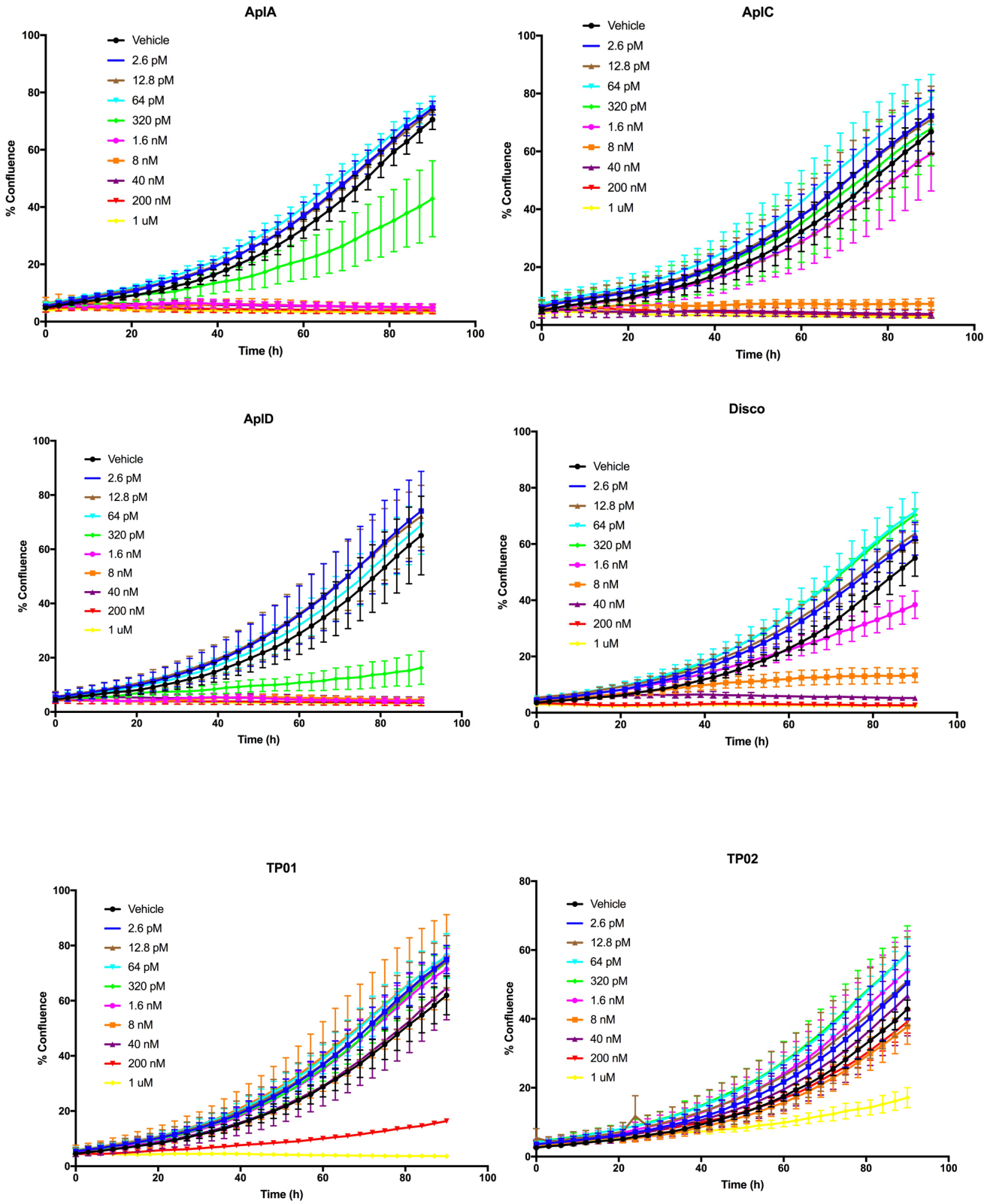

Figure 37 Cell growth over 4 days for first phase compounds. Vehicle refers to 0.1% DMSO in DMEM (Dulbecco's modified Eagle's medium)

Two types of data are illustrated in **Figures 36** and **37**. Percentage viability illustrates the number of cells alive at a fixed point in time, in this case after 96 h. Alongside this, cell growth was monitored over the same time period. Our scytophycin hybrid analogues do not appear to mirror the picomolar antiproliferative activity of the parent natural products, with IC_{50} values over 100 nM. However, the differences observed between TP01 **133** and TP02 **132** serve as further proof of the necessity for the C_7 trimethyl serine residue to promote increased cytotoxicity.

As previously discussed (**Section 3.2.3**), the reduced dienoate product **131** is a constituent in Pettigrew's material and it is possible that some of the reduced activity observed for TP01 **133** stems from this byproduct either competitively binding or inhibiting the binding of the true analogue to actin and tubulin. Additionally, the amount and concentration of 'true' analogue is reduced, leading to errors in obtaining an accurate value. Previous SAR studies from the Yamada and Kigoshi groups have confirmed that the fully saturated dienoate results in a significant loss of activity.[108] Hence it was necessary to re-synthesise analogue **133** as detailed in **Section 4.1.1** and re-submit the pure sample for re-testing.

4.2.2 Second phase

Once our re-synthesised aplyronine–scytophycin analogues **133** and **134** and the aplyronine D analogue **44** were in hand, these compounds were submitted to a second round of biological testing against HeLa cells (**Figure 38**). These results would allow us to directly compare the importance of the configuration of TMSer at C_7 and the ketone functionality at C_{29}. Alongside these analogues, the actin-binding reidispongiolide A (**29**) and tubulin-binding discodermolide (**6**) were submitted for control and comparison purposes.

The results of this assay are summarised in **Table 11**. Compounds were tested in triplicate at the same concentration of each drug. The three analogue samples tested exhibit IC_{50}'s greater than 100 nM, whilst discodermolide displayed an analogous value to that of our first assay (**Figure 39**). Disappointingly, our analogues do not appear to possess the sub-nanomolar potency exhibited by the parent natural product. There could be a number of reasons for this. Firstly, loss of the pharmacophore could stem from our analogues biding to actin or tubulin in an altered conformation compared to the natural products. Removal of the olefin and the two stereocentres in the southern region may change the binding mode or binding direction. This could also alter the protruding conformation of the trimethyl serine residue for tubulin binding, thus negatively impacting the activity. Additionally, the increased conformational flexibility in the macrolide ring in our analogues may also contribute to this effect. All previous evidence suggests that the C_{13} methoxy, the C_{10}

methyl and the C_9 hydroxyl groups have important roles and function as anchors to retain the protrusive trimethylserine moiety.[108] Perhaps one of the removed stereocentres forms an additional crucial interaction and its removal could be significant enough to change the binding mode of our analogues. Finally, an important consideration is the potential impact our alterations have on cell permeability. It may be that the modifications have rendered these molecules less permeable *via* the cell membrane than their natural counterparts. A surprising outcome of these results is the apparent lack of importance in the configuration of the trimethyl serine residue at C_7 (compare RP-1 **133** and RP-2 **134**). This effect would be valuable to explore in more detail, possibly with the parent aplyronine D structures.

We had indeed hoped to see equal or higher potency in the analogues to further their potential for inclusion in ADCs. These biological results were therefore disappointing. One encouraging prospect is that whilst the native aplyronines are too toxic to be administrated as a standalone chemotherapeutic, the reduced potency of our analogues opens up the possibility of their usage in chemotherapy.

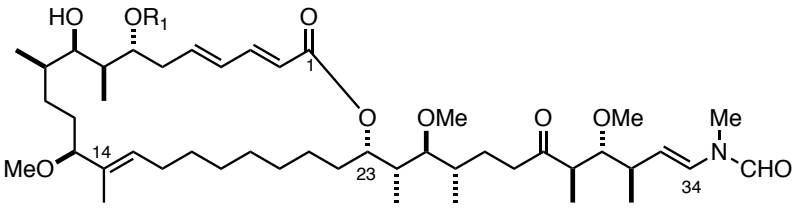

	$\mathbf{R_1}$
RP-1 **133**	(*S*)-TMSer
RP-2 **134**	(*R*)-TMSer

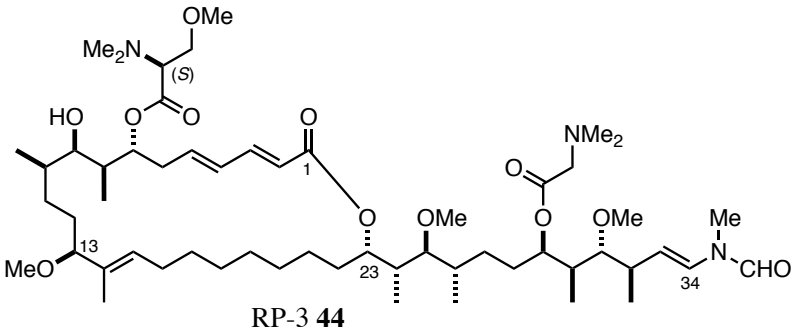

RP-3 **44**

Figure 38 Aplyronine analogue samples for second phase of biological testing

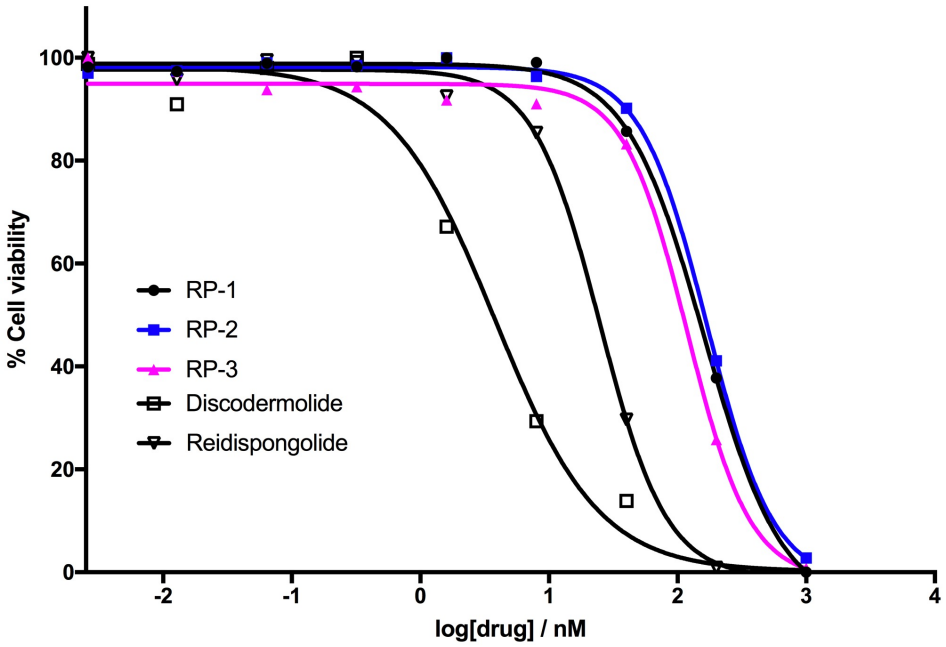

Figure 39 Cell viability graph for second phase compounds in biological testing

Table 11 Antiproliferative activity of second phase aplyronine analogue samples against HeLa cells

Compound	IC_{50} / nM
RP-1 **133**	164
RP-2 **134**	192
RP-3 **44**	125
Discodermolide **6**	3.4
Reidispongiolide A **29**	21

Despite these initially disappointing results, there is still a lot of underexplored potential for the development of aplyronine analogues for ADC development. Diversification of this preliminary small library would generate more 'aplyrologues' and we can make use of the SAR and protein binding knowledge that this gives us to find the best possible combination of activity and simplicity. Once an appropriate analogue is in hand, attention can turn to ADC construction where linker chemistry is of paramount importance.

4.3 Linker strategies

Since the ultimate goal of this work is to develop novel ADCs, it would also be necessary to develop chemistry to link our eventual warhead of choice to an antibody. To this end, in parallel with the ongoing aplyrologue synthesis, we set out to develop an aplyronine derivative suitable for bioconjugation to an antibody. This section will concentrate on identifying a suitable modification site within our analogues to which a linker could be attached. A discussion on possible bioconjugation strategies to antibodies will be presented in the next chapter.

In identifying optimal linker attachment points, it is necessary to consider the effect the linkage may have on biological activity if a non-cleavable variant is used. Additionally, another important consideration is that the chemistry used to install the linker must be compatible with the wide range of functional groups present in our compounds.

Kigoshi has demonstrated that the *N*-vinyl formamide terminus can serve as an attachment point to a variety of biological probes.[114,124,235,236] SAR studies showed that replacement of this moiety with other polar functional groups such as alcohols, oximes, or hydrazones could be well tolerated with respect to cytotoxicity.[116,117] Various derivatives could therefore be introduced through deliberate hydrolysis of the *N*-vinyl formamide moiety and subsequent condensation with a substituted hydroxylamine (**Figure 40**). Importantly, this work illustrated that biological activity could be retained upon installation of large groups containing both hydrophobic and hydrophilic parts into the aplyronine tail region.

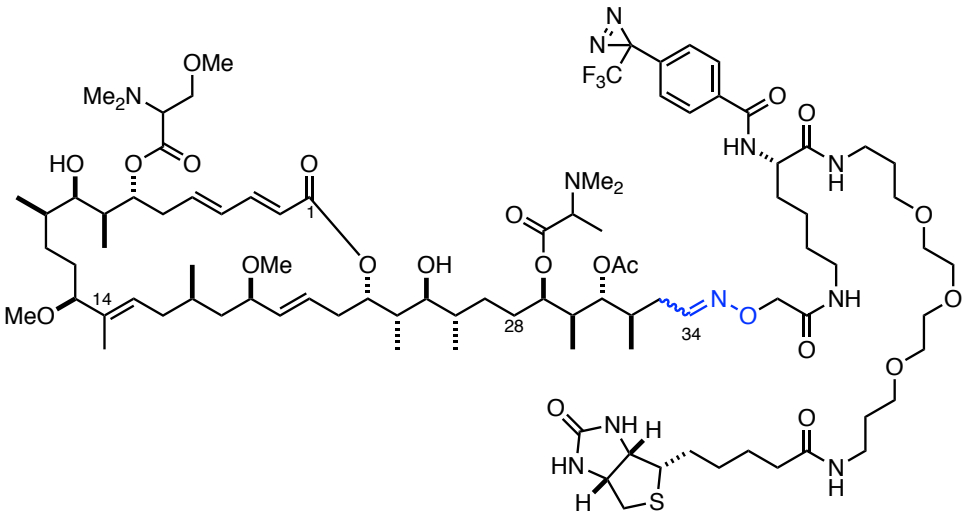

Figure 40 Photoaffinity derivative of aplyronine A through an oxime linkage, synthesised by Kigoshi[114]

This approach initially seemed an attractive prospect: it was well precedented and signified a late stage modification so fitted in well with our synthetic route. However, we had spent considerable time and effort optimising the installation of the *N*-vinyl formamide moiety and to simply replace it at this stage seemed counterintuitive. Additionally, oxime linkages can be labile under physiological conditions, leading to reduced ADC stability in plasma and the possibility of issues due to off-target toxicity. As such, a focus on more stable linkers was deemed appropriate at this stage.

Many methods have been reported in the literature for conjugation strategies of complex natural products.[237–240] For our purposes, late stage approaches using functionality already in place within our analogues was highly desirable. To this end, our initial focus was conjugating through the pendant amino acid residues as these represent the final steps in our analogue synthesis.

Williams validated this tactic through the synthesis of linker-modified derivative **139**, extending from the dimethylglycine residue at C_{29} (**Figure 41**).[121,138] The basis of this approach can be explained with the aid of the crystal structure of the 1:1 aplyronine A-actin complex, in which the C_{29} DMGly residue appears to protrude into the surrounding bulk solvent.[108] Hence, elaboration of the amino acid moiety should not significantly impact the key ligand–protein binding interactions. Williams' designed substrate **139** contains an Fmoc-protected primary amine group for non-cleavable bioconjugation to an antibody through a maleimide or amide functionalisation strategy.[237,241]

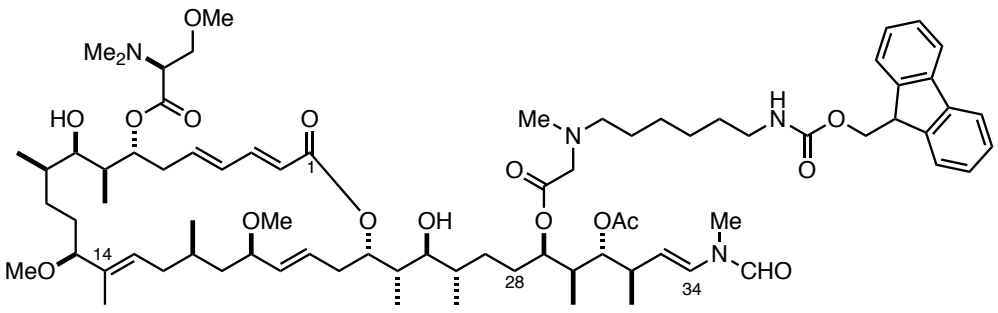

139

Figure 41 Aplyronine derivative synthesised by Williams for antibody conjugation extending through the dimethyl glycine ester residue[121]

The disadvantages of non-cleavable linkers, namely the liberation of an unknown linker modified payload, led us to shift to a cleavable approach. Cleavable linkers are designed to release parental payload compounds in a traceless manner after the bond cleavage event.

Hence, the well-characterised chemical entity with known potency is released through this more defined method.

The field of cleavable linkers commonly encompasses hydrazones, disulfides, phosphate diesters and enzyme-cleavable dipeptides.[108] Of these, the enzyme-cleavable dipeptide motif surfaced as a compelling candidate for use in our aplyronine analogues. Specifically, our system could be compatible with the elegant linker technology reported by Seattle Genetics[242] and Pillow and co-workers at Genentech.[243] The Genentech protocol converts tertiary amine residues found in drug molecules to the corresponding *para*-aminobenzyl quaternary ammonium salts (PABQs, **Scheme 69**). This is in combination with a protease cleavable valine-citrulline (Val-Cit) dipeptide unit to promote the intracellular cleavage. Upon exposure to the protease cathepsin B, the Val-Cit component is recognised and the aniline amide is cleaved. This triggers the self-immolating 1,6-elimination sequence of the PAB moiety, leading to traceless drug release.

This methodology is an extension to the well-established para-aminobenzyl carbamate (PABC) self-immolating chemistry utilised in the clinically approved ADC Adcetris (**Figure 17, Section 1.3.4**) which contains a monomethyl auristatin E (MMAE) payload.[81,244,245] The limitations to this chemistry are substrate specific in that the drug molecule must contain either a primary or secondary amine residue that is capable of forming a carbamate or amide connection. Auristatin E **140** (**Figure 42**) was initially not amenable to this protocol due to the terminal tertiary amine, prompting the synthesis of the desmethyl analogue, monomethyl auristatin E **141**.[81] In this example the biological activity was not detrimentally affected by this minor change. However, maintaining potency after small alterations is not always trivial, as demonstrated by the tubulysins. Here, the removal of a methyl group from tubulysin analogue **142** resulted in a greater than 40-fold drop in potency (**Figure 42**).[81] The PABQ strategy is therefore a helpful extension of this methodology to allow us to derivatise tertiary amines directly.

The quaternary amine approach conveys an additional benefit through the introduction of the charged species, leading to improved physicochemical properties of the corresponding conjugates through reduced ADC aggregation.[246,247] Aggregation has been shown to decrease the therapeutic activity of the antibody and can elicit an immunological response.[248]

Importantly, this class of linkers displayed remarkable stability *in vivo* with no loss of small molecule observed after seven days of ADC circulation in mice. The Genentech ADC conjugates are constructed in three efficient steps. Starting with valine-citrulline linker **144** appended with a maleimide handle, the benzylic alcohol is first chlorinated, before S_N2

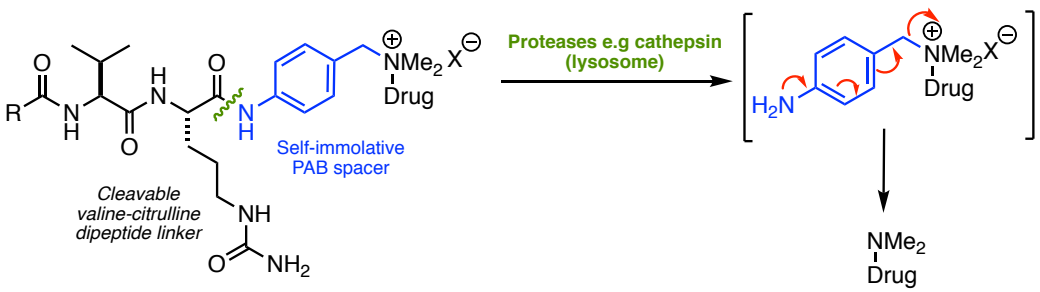

Scheme 69 Cleavable quaternary amine strategy and mechanism of intracellular cleavage

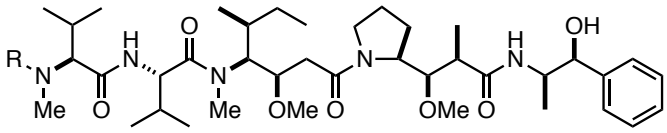

140 R = Me, auristatin E
141 R = H, monomethyl auristatin E (MMAE)

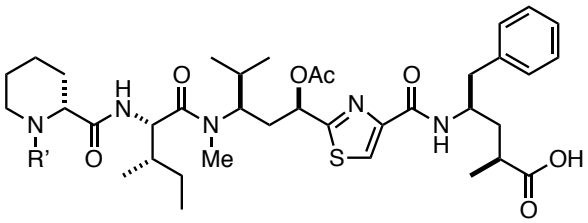

142 R' = Me, tubulysin analogue IC_{50} 0.8 μM (1A9 ovarian cancer cells)
143 R' = H, tubulysin analogue IC_{50} > 33 μM (1A9 ovarian cancer cells)

Figure 42 Structures of auristatin and tubulysin analogues

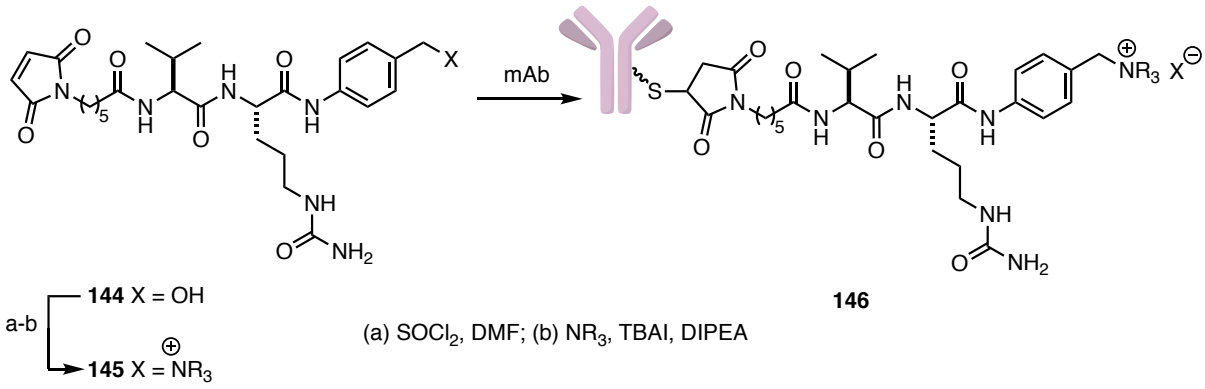

Scheme 70 Construction of ADCs using Genentech linker technology[243]

displacement of the halide by a tertiary amine on the payload delivers the quaternised product **145**. Ensuing bioconjugation through cysteine residues on the antibody affords the ADC (**146**, **Scheme 70**). Preliminary efforts toward the development of this linker strategy in the context of our aplyronine analogues will be now discussed.

Although linker **144** is commercially available, the exceedingly high cost of this material (*ca*. £2500/g) precluded its use as a starting material for our synthesis. Consequently, we set out to synthesise a sizeable quantity of this key intermediate for use towards developing linker chemistry for our analogues. This work was carried out in the AstraZeneca laboratories in Macclesfield, UK.

4.3.1 Synthesis of valine-citrulline linker 144

The use of valine-citrulline linker **144** is extremely well documented in the literature for ADC design.[249–251] Contrary to this, there is a distinct lack of publications that provide a detailed experimental procedure for the isolation and synthesis of this important linker motif.[252–254] The original report was provided by Dubowchik and co-workers, who accessed linker **144** through a series of amide bond couplings, starting from the parent amino acid residues (**Scheme 71**).[252] This approach is prevalent within the patent literature, but again, comprehensive experimental details remain sparse.

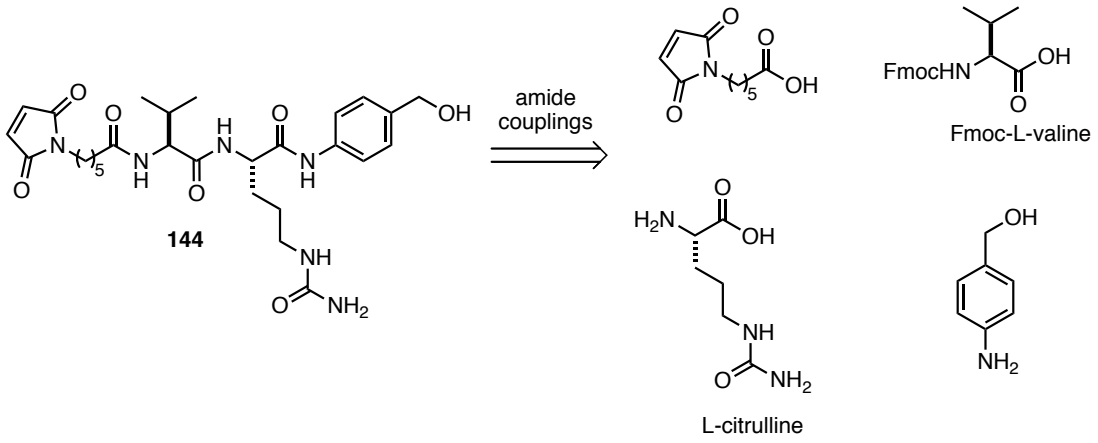

Scheme 71 Retrosynthesis of valine-citrulline linker **144**

Moving forward, this protocol was selected as the route to access linker **144**, due to its apparent chemical simplicity and anticipated ease of scale-up. However, this deceptively straightforward chemistry was to bring many unexpected challenges.

The synthesis commenced with conversion of commercially available Fmoc-protected-L-valine **147** into the corresponding *N*-hydroxysuccinimide activated ester **148**. Promoted by DCC, this transformation proceeded smoothly to deliver ester **148** in 90% yield (**Scheme 72**). Pleasingly, this transformation could be scaled up to produce decagram quantities of intermediate **148**.

Investigations then began on the subsequent coupling reaction to install the citrulline residue. Following the literature protocol, simple addition of L-citrulline to a basic solution of ester **148** yielded the desired dipeptide **149** in a promising 78% yield on 500 mg scale (**Scheme 72**). Stirring for prolonged periods (*ca.* 48-72h) was necessary to achieve good conversion. The work-up procedure for this reaction involved a citric acid quench followed by an organic extraction. The highly polar nature of these intermediates prohibits the use of column chromatography for purification and necessitates isolation *via* crystallisation.

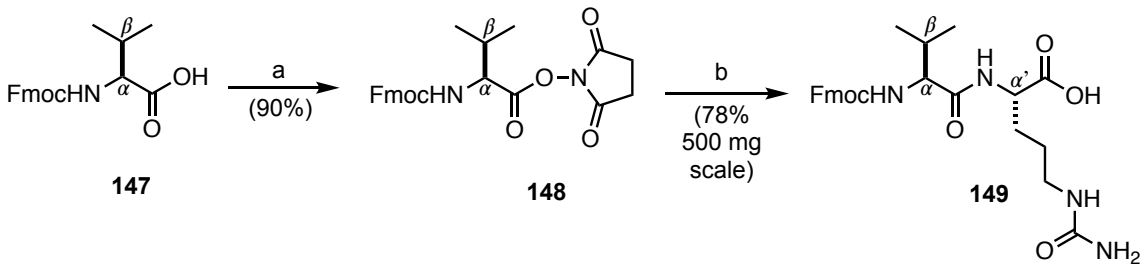

(a) *N*-hydroxysuccinimide, DCC, THF, 0 ºC; (b) L-Citrulline, $NaHCO_3$, DME/H_2O/THF (2:2:1)

Scheme 72 Synthesis of Fmoc-Val-Cit-OH **149**

Upon application of this protocol to a preparative scale reaction (*ca*. 5 to 10 g), several unexpected problems arose. Firstly, on scale the material appeared to be highly hygroscopic and as a result had to be dried in a vacuum oven for extended periods of time (72-96 h) in order to drive off the excess water present. Additionally, close examination of the ^{1}H NMR spectrum revealed that a significant quantity of citric acid, stemming from the work-up conditions, was contaminating the isolated material. All efforts to separate the citric acid from desired product **149** failed due to similarities in polarity and solubility. Alongside this, unreacted starting material Fmoc-Val-OSuc **148** had not been successfully removed and was present within the isolated material in meaningful quantities (*ca.* 5-10%). Hence, a new work-up procedure was developed to circumvent these issues.

This new work-up procedure was designed to allow for easy removal of unreacted starting material. To this end, the reaction was quenched with aqueous potassium carbonate solution before extraction with ethyl acetate. The dipeptide product **149** is initially masked as the

potassium carboxylate and thus remains in the aqueous phase, allowing clean removal of the organic starting material. Next, acidification of the basic media was required for extraction of the product. Citric acid was completely removed from the procedure and replaced by hydrochloric acid, which can be easily removed *in vacuo*. Whilst the formation of the byproduct was alleviated, this improvement was compounded with a further operational issue. Upon acidification, a large volume of thick, gelatinous material was formed that was exceedingly difficult to manipulate. Best practice was to extract this 'jelly' material with large volumes of polar solvents (EtOAc and IPA), which upon concentration and drying yielded the desired product **149**. Whilst the use of excessive volumes of solvent is not ideal, this sequence eventually proved reliable on scale (80-90% yield) and for the first time we had access to multigram quantities of pure dipeptide product **149** (**Scheme 73**).

The next step in this series was the installation of the self-immolating 'trigger', and the success of this reaction was found to hinge upon the quality of the 4-aminobenzyl alcohol (PABOH) reagent. This reaction was mediated by 2-ethoxy-1-ethoxycarbonyl-1,2-dihydroquinoline (EEDQ), a well-known coupling agent in peptide synthesis.[255–257] EEDQ allows the coupling of amino acids in a single operation with little or no racemisation. Mechanistically, activation of a carboxylic acid occurs *via* the formation of a mixed anhydride species **150** (**Scheme 74**). Displacement of the ethoxy group on EEDQ yields intermediate **151**, which decomposes through a 6-membered transition state to generate the mixed anhydride **150** which acts as the acyl transfer agent. Amide **152** is subsequently furnished after nucleophilic attack of the amine moiety from the second amino acid. Anhydride formation is believed to be slow, but once formed is consumed very rapidly hence reducing the susceptibility for racemisation.

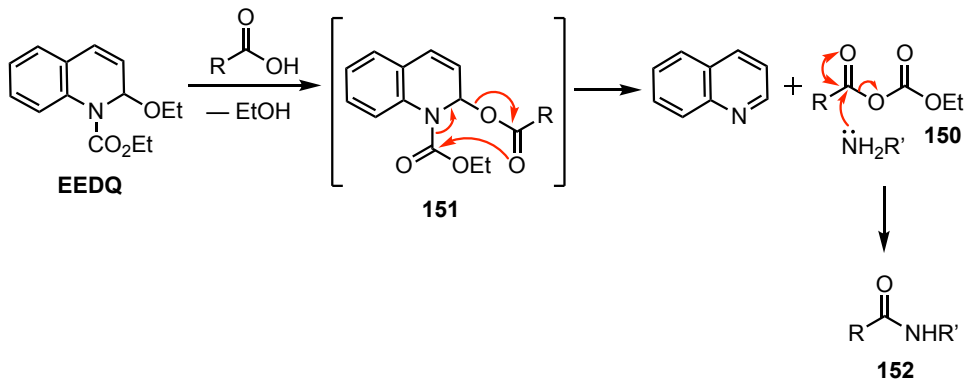

Scheme 74 EEDQ mediated amide coupling mechanism

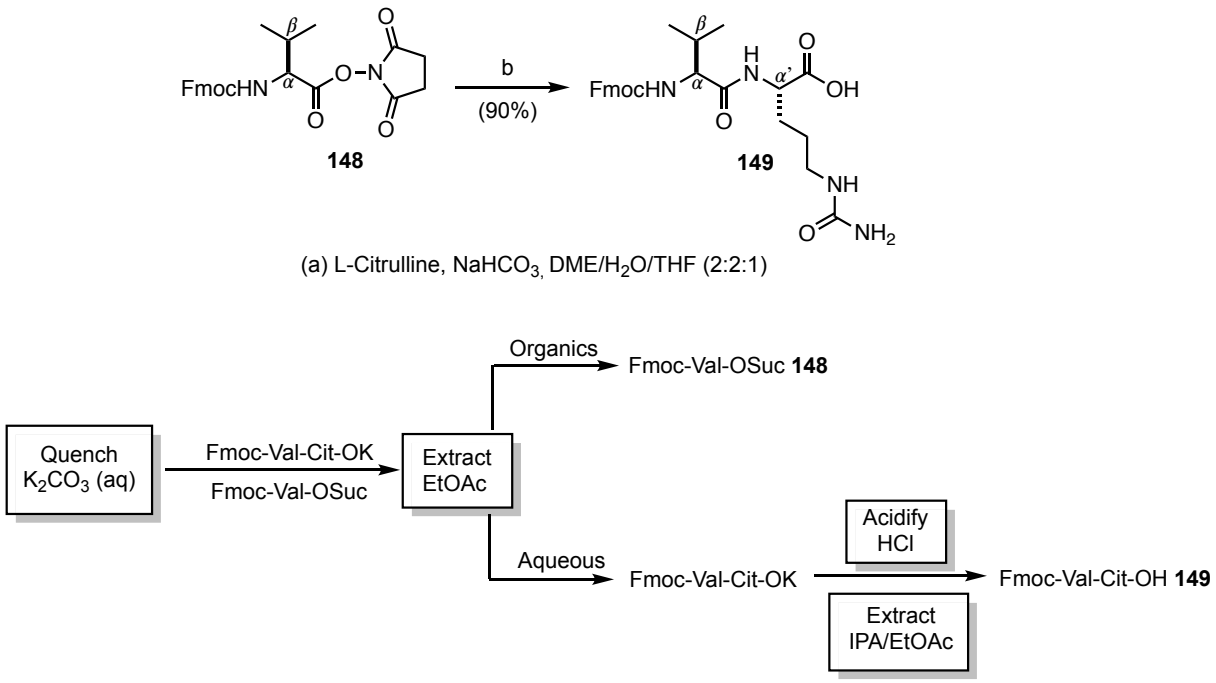

Scheme 73 Large scale (*ca*. 10 g) synthesis of **149** and improved work-up procedure

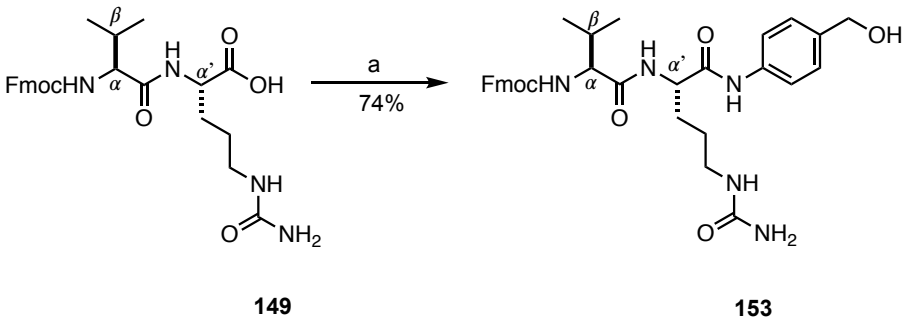

Scheme 75 Formation of valine-citrulline linker **153**

In this case, exposure of acid **149** to EEDQ and *para*-aminobenzyl alcohol yielded the coupled product after 72 h. Purification *via* filtration of the crystallised product yielded **153** in 74% yield (**Scheme 75**).

Overall, this protected valine-citrulline linker **153** was synthesised in 3 steps and 59% yield from **147**. With the Fmoc protecting group in place, this represented a convenient point to stockpile material and over 15 g of this intermediate was generated *via* this route. There is great potential for flexibility in advancing this material towards an ADC linker; the Fmoc group can simply be deprotected and a carboxylic acid-modified bioconjugation handle appended through a final amide coupling.

4.3.2 Valine-alanine linker 154 and quaternisation studies

Whilst the synthesis of Val-Cit linker **153** was explored and optimised, parallel investigations into quaternisation strategies were undertaken. For this purpose, we made use of the analogous Alloc-protected valine-alanine (Val-Ala) linker **154** which was kindly provided in house by AstraZeneca (**Figure 43**).

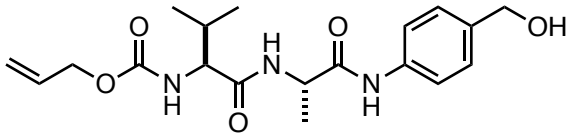

154

Figure 43 Valine-alanine linker **154** supplied by AstraZeneca

The valine-alanine linker system is an alternative substrate for cathepsin B cleavage and has recently seen incorporation into antibody–drug conjugates.[258,259] Compared to its Val-Cit counterpart, the Val-Ala system may offer benefits of reduced hydrophobicity and therefore lower potential for aggregation.[260,261]

Alloc deprotection was initially trialled using Pd(0) and pyrrolidine to act as the allyl scavenger.[262] However, the pyrrolidine byproduct could not be separated from the desired amine product, and so an alternative approach was sought. Pleasingly, treatment of **154** with catalytic tetrakis(triphenylphosphine)palladium(0) ($Pd(PPh_3)_4$) in combination with potassium carbonate in methanol delivered the deprotected amine **155** in 74% yield (**Scheme 76**). The lower than anticipated yield can be attributed to the highly polar nature of the product, leading to difficulties in work-up and isolation.

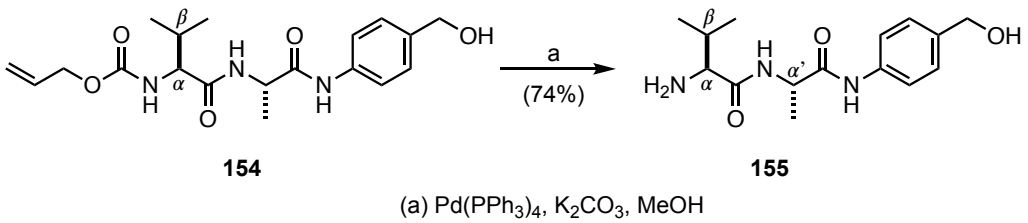

Scheme 76 Alloc deprotection of **154** with catalytic Pd(0)

Mechanistically, this transformation proceeds *via* oxidative addition of Pd(0) into the allylic carbonate to form a Pd(II) π-allyl complex. The resulting carbonate anion can undergo spontaneous decarboxylation to reveal the primary amine (**Scheme 77**). Pd(II) is reduced by attack of the scavenger species, presumed to be the methoxide anion in this case, which closes the catalytic cycle by regenerating Pd(0).

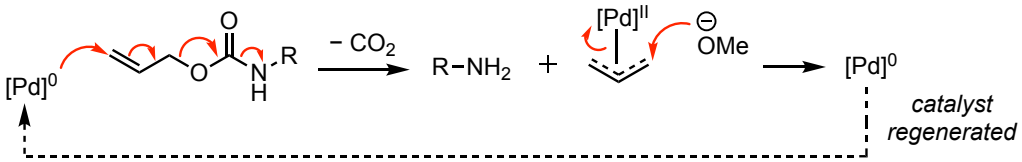

Scheme 77 Mechanism for Alloc deprotection using Pd(0)

With the free amine in hand, the bioconjugation handle could now be connected. For our purposes, the maleimide functionality was initially selected to align with the Pillow approach for reaction with a thiol-containing carrier. In principle, any antibody conjugation motif could be coupled at this point, provided it is appropriately substituted with a carboxylic acid to facilitate amide bond formation.

Coupling of 6-maleimidohexanoic acid and amine **155** could be achieved under standard conditions by exposure to HATU and diisopropylethylamine (DIPEA) overnight. At this point, the polarity of the product was sufficiently reduced so that purification could be performed *via* column chromatography to deliver amide **156** in 70% yield (**Scheme 78**). Subsequent chlorination of **156** could be achieved through treatment with thionyl chloride according to the protocol developed by Pillow.[243]

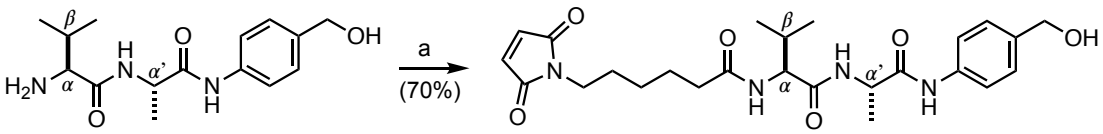

155 **156**

(a) 6-maleimidohexanoic acid, HATU, DIPEA, DMF, 1h, *then* **155**, DMF

Scheme 78 Amide coupling between amine **155** and 6-maleimidohexanoic acid

This method generated the required benzyl chloride **156** in a reasonable 61% yield (**Table 12**, entry 1). In an effort to improve the yield, additional chlorination conditions were screened. Limited optimisation was carried out due to the highly reactive nature of the intermediates and the potential for product degradation. We were further prohibited by the low organic solubility of the peptide linker and were limited to polar solvents such as DMF or DMSO. Attempted mesylation of the primary alcohol for subsequent substitution led to complete destruction of material (**Table 12**, entry 2). Chlorination using *N*-chlorosuccinimide (NCS) led to the production of an unknown intermediate that was not characterised (**Table 12**, entry 3).

Table 12 Efforts towards the chlorination of **156**

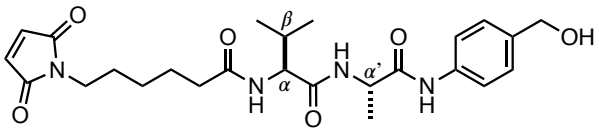

156

[Conditions]

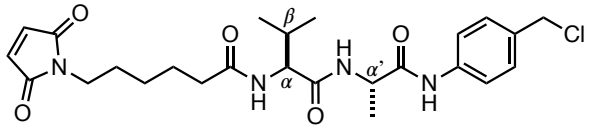

157

Entry	Conditions	Result
1	$SOCl_2$, DMF 0°C	61% **157**
2	MsCl, NEt_3, DMF 0°C	Decomposition
3	NCS, PPh_3, $NaHCO_3$, DMF	Unidentified product

Thionyl chloride was thus selected moving forward. This reaction was strictly quenched after 5 min to suppress unwanted side reactions stemming from the highly reactive species in solution. Chloride **157** precipitated from the aqueous quench and was isolated by a simple filtration. This provided linker model **157** to act as a screening platform for quaternisation strategies. Quaternisation was initially trialled with *N*,*N*-dimethylbenzylamine **158** or modified side chain fragment **159** as model systems for our aplyronine conjugation partners (**Figure 44**).

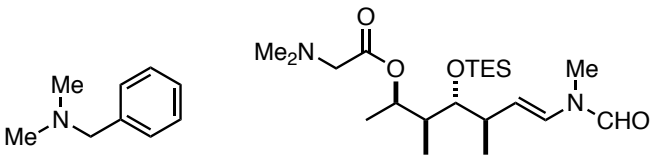

158 **159**

Figure 44 Model tertiary amines used for quaternisation reactions

Increasing the reactivity of the benzyl chloride was found to be necessary and this could be achieved through a Finkelstein reaction with an iodide salt such as KI or TBAI.[243] Preliminary results for the quaternisation reaction are presented in **Table 13**. Ultimately, within this first screen of conditions, no quaternised product was observed. The reaction proved difficult to follow by TLC analysis due to the high polarity of intermediates and the tendency for compounds to streak on silica. Time constraints precluded optimisation efforts for this reaction, which will therefore be a focus for further studies in the future.

4.4 Summary

This chapter has outlined our efforts towards constructing an antibody–drug conjugate based on an aplyronine payload. Completion of the synthesis of a small library of simplified analogues has been achieved and biological studies have been undertaken. The outcomes of the biological results indicate that this first round of analogues does not mirror the potent cytoxicities in the parent natural products. This reflects that our efforts to maximise both structural simplicity and cytotoxic potency have not yet come to fruition. However, these studies have delivered valuable information as to the necessity of certain functionalities for the activity of these compounds. In future studies, it will be possible to build on this knowledge to create compounds which do find the optimum point between complexity and activity.

Linker strategies have been discussed with a focus on the quaternary amine approach, and preliminary investigations into this chemistry have been undertaken. The future directions of this work and potential for developing ADCs will be presented in the next chapter.

Table 13 Quaternisation studies with chloride linker **157**

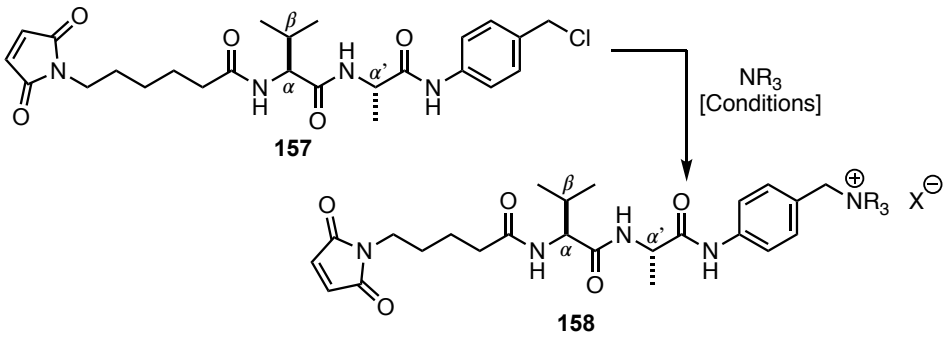

Entry	NR_3	Conditions	Result
1	**158**	KI, DMSO	No reaction
2	**158**	KI, DMSO, DIPEA	No reaction
3	**159**	KI, DMSO, DIPEA	No reaction
4	**159**	TBAI, DMF, DIPEA, 40 °C	No reaction

Chapter 5

Conclusions and future work

5.1 Future work

5.1.1 Evaluation and second-generation analogues

Although our initial simplified analogues have not demonstrated the excellent cytotoxicity exhibited by the parent aplyronines, there is scope to probe the underlying reasons for this and utilise this information to glean further valuable insight into the structure–activity relationships of the aplyronines and their protein targets. To this end, additional data could come from actin binding studies of our analogues alongside aplyronine D. This would validate whether actin is still indeed a target of our analogues and allow us to critically assess the effect our modifications have on protein binding. Alongside this, if a crystal structure of our analogues bound to actin could be obtained, we could examine the directional binding mode of the simplified macrocycle and its resulting impact on tubulin binding through the positioning of the critical trimethyl serine residue. Based on this information, we could rationally design a new range of simplified analogues that are able to promote the desired PPI to impart cytotoxicity.

Moreover, it would be necessary to explore the limit of structural simplicity whilst maintaining biological activity. Further modifications could be guided by computational

methods, especially if the crystal structure of the actin–aplyronine –tubulin ternary complex can be obtained.

Our simplified analogues are synthetically more tractable than the natural products and as such could be useful candidates to undertake further studies to probe fine details related to protein binding.

The late stage functionalisation strategy employed in our synthesis could deliver a second round of analogues possessing relatively minor modifications with ease. To this end, varying the pendant amino acid residues at C_7 and C_{29} offers an attractive and simple means of diversification. At the C_{29} position we can take inspiration from other actin binding natural products such as mycalolide B, which exhibits stronger actin-depolymerising activity and possesses an *O,O*-dimethylglycerate ester at this position. Additionally, the degree of *N*-methylation at the amino acid residues at both C_7 and C_{29} would be interesting to explore. To achieve this, several *N*-substituted variants of glycine and alanine could be appended at C_{29} in the side chain. Furthermore, the nature of the nitrogen atom could be also considered (*e.g.* basic, non-basic or absent altogether) by appending molecules such as *N*-acetyl-*N*-methylglycine or isovaleric acid. A schematic representing some of these proposed analogues is presented in **Figure 45**.

With regards to tubulin binding, varying the pattern of *N*-methylation in the serine residue at C_7 could offer insight into this interaction, which to date has not yet been fully elucidated. Each variant is expected to have a unique biological profile due to subtle differences in the pharmacophore in the northern portion of the macrocycle. Hence, dimethyl, monomethyl and unmodified serine motifs could be appended to probe this effect (**Figure 45**). Further biological testing of these analogues in assays against multiple cell lines will further guide the development of aplyronine derivatives as payloads in ADCs.

5.1.2 Improvements to the synthesis

The Paterson strategy to construct the aplyronines and their analogues has been designed to be highly efficient. Late stage diversification, through a common intermediate, allows access to multiple aplyronine congeners with relative ease. A streamlined protecting group strategy is in place alongside a comparatively simple endgame – all the relevant functional groups within the aplyronines are present once the side chain has been appended, apart from the pendant amino acids. Whilst many improvements have been made, there remain several steps which would benefit from further optimisation. This is especially true if the aplyronines and their analogues are to fulfil their potential as payloads for antibody–drug conjugates. Structurally simplified candidates ought to be amenable to large scale

manufacture to provide enough material for a clinical campaign. The most pressing matters to be examined for improvement in further studies are briefly discussed below.

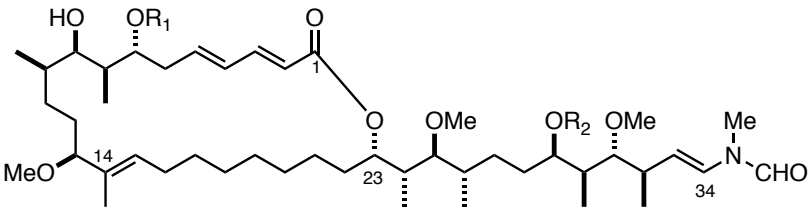

	—OR1
TMSer	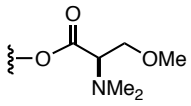
DMSer	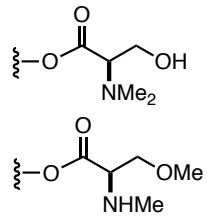
MMSer	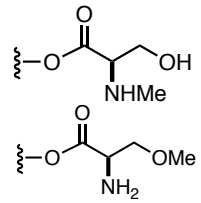
Ser	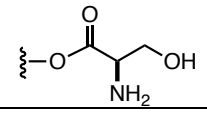
iso-Ser	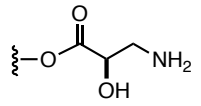

	—OR2
O,*O*-dimethylglycerate	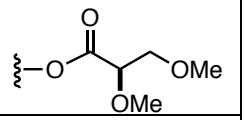
DMGly	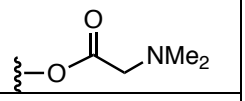
MMGly	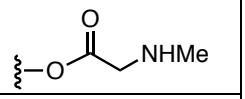
Gly	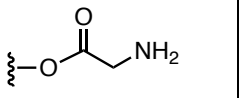
DMAla	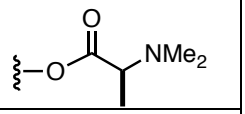
MMAla	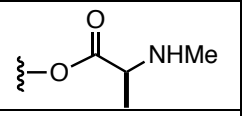
Ala	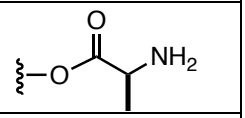
N-acetyl-*N*-methylglycine	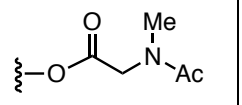
Isovaleric acid	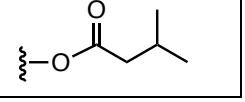

Figure 45 Proposed library of second-generation analogues

Firstly, within the northern fragment synthesis, the alkylation of iodide **56** remains a frustrating bottleneck (**Scheme 79**). Typically, on medium scale at least 25% of material, corresponding to several hundred milligrams, is lost at this stage in a single operation due to the undesired formation of the unproductive regioisomer **77 (Scheme 19, Section 2.1.4)**. Notably, this route contributes to the longest linear sequence of our synthesis. Significant further optimisation of this challenging reaction is thus required as a matter of priority. Removal of the C_{14} methyl group has been shown to be tolerable through SAR studies and so there is scope to potentially redesign this disconnection in the future.[117]

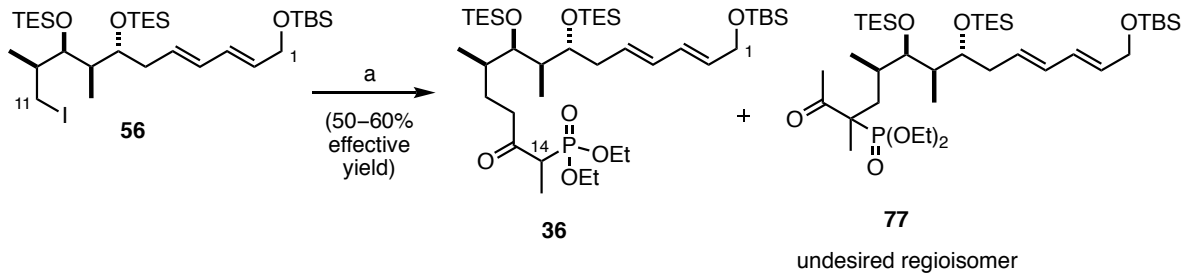

(a) **72**, NaH, THF, 0 ºC, *then n*-BuLi, *then* **56**, 0 ºC

Scheme 79 Alkylation of iodide **56** is a focus for optimisation efforts

The second reaction requiring extensive optimisation is the reduction to set the desired (*R*)-configuration at C_{29} (**Scheme 80**). In this work, this reaction is mediated by zinc borohydride and is plagued by inconsistency in yields and *dr* (55–65% yield, 1:1–6:1 *dr*). In the author's hands, the best result on advanced ketone **130** was a modest 58% yield and 2:1 *dr*. These results are especially concerning given the position of this reaction in the overall synthetic route. With only three further synthetic manipulations required to reach our complete analogues, this serious hit in yield and efficiency is further compounded due to the wastage of highly precious material which has already passed through many previous steps. Efforts to improve this reaction could focus on a screen of alternative reducing agents. For example, if sodium borohydride was able to enact this transformation to deliver the unwanted (*S*)-diastereoisomer in good yield and *dr*, a Mitsunobu esterification could be employed to ultimately set the desired configuration.[120,263] Additionally, reagent-controlled methods could be investigated, although efforts to develop the alternative coupling strategy during this work highlighted the incompatibility of the *N*-vinyl formamide moiety to CBS reduction conditions.

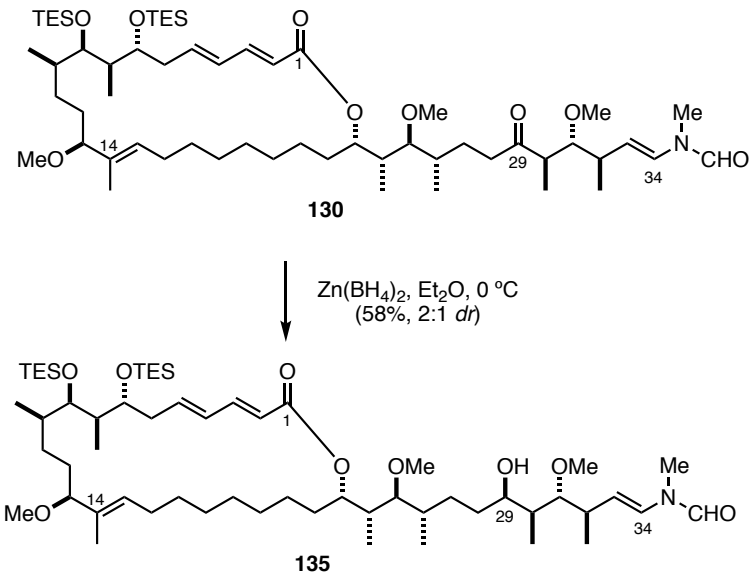

Scheme 80 Reduction of ketone **130** requires further optimisation

If optimisation of these challenging reactions can be accomplished, the efficiency and scalability of the route to the aplyronines and analogues will be boosted, thereby increasing the likelihood of success in future scale up efforts.

5.1.3 ADC development

The continuation of this work constitutes further studies towards our ultimate goal of incorporating the aplyronines into antibody–drug conjugates. To this end, the immediate focus should be to build upon the preliminary linker chemistry discussed in Chapter 4. The quaternary amine method is an attractive approach to release the free unmodified payload in a traceless fashion. Optimisation of the quaternisation reaction following the Genentech protocol should provide conditions to efficiently deliver an aplyronine-linker species for subsequent bioconjugation to an antibody.[243] The chemistry towards this linker species has been successfully optimised and large stockpiles of dipeptide material are in hand to facilitate these further studies.

Alongside developing the chemistry for a suitable linker species, reliable chemical means of bioconjugation that are compatible with our aplyronine payloads need to be realised. These challenges have been tackled by colleagues in Prof. David Spring's research group.

An elegant cysteine re-bridging approach (*vide supra*, **Section 1.3.3**) has been realised through the development of a novel divinylpyrimidine linker platform, and has been validated through the generation of highly plasma stable antibody constructs.[77] This technology has proven to be site-selective with predictable control over the drug to antibody ratio (DAR), without relying on antibody engineering. Further bioconjugation methods developed by the Spring group include novel enzymatically-cleavable linker methodologies and sequence-dependent bioconjugation.[264,265]

Our goal is thus to construct an ADC derivative of the aplyronines based on a quaternary amine linkage in tandem with a site-selective bioconjugation method, to deliver homogeneous ADCs with controlled DAR (**Figure 46**). These could be based on a simplified aplyronine scaffold, which has been the focus of this work, or the parent natural product structures. Generally, a spacer unit is employed between the linker–payload and bioconjugation site, and this can be utilised to improve the pharmacokinetics of the conjugate. These spacers typically incorporate a hydrophilic element such as the uncharged polyethyleneglycol (PEG) unit. This brings the advantage of increased aqueous solubility and decreased hydrophobicity, thereby reducing the potential for aggregation.

Ultimately, by this approach, we hope to accomplish our ambitious goal to create an effective targeted therapy based on the aplyronine family of natural products.

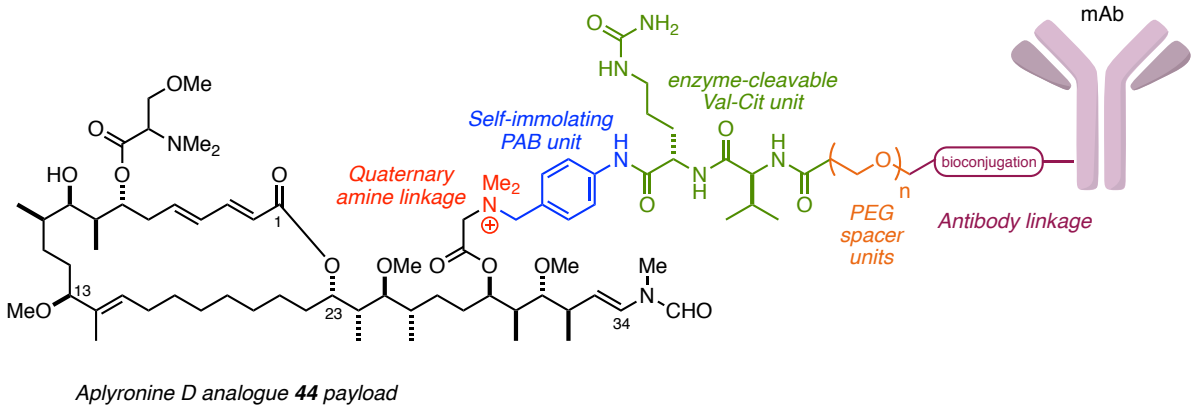

Figure 46 A possible form for our aplyronine antibody–drug conjugates

5.2 Overall conclusions

In this work, a function-oriented total synthesis of a small library of simplified aplyronine analogues has been developed. This achievement signifies the endpoint of this work by meeting one of the key goals set out at the beginning of this work.

The approach previously described by Paterson and colleagues is a highly efficient and convergent route to access these aplyronine derivatives and has been validated once again in the work detailed here. Through our late stage diversification strategy several congeners of the aplyronine family can be accessed with relative ease. This modular approach also paves the way for the creation of novel aplyronine hybrid structures which borrow elements from other natural products.

In Chapter one, the potential for marine natural products to provide inspiration for the design of clinically relevant molecules was introduced. The function-by-design approach of truncating natural products was discussed, and this concept was applied to the aplyronine family. Antibody–drug conjugates are emerging as a highly promising class of anticancer agents and the aplyronines have resurfaced as compelling candidates for incorporation into these targeted therapeutics.

Chapter two presented the synthesis of three key fragments, two of which contained modifications for construction of our simplified aplyronine scaffolds. Chapter three subsequently outlined two complementary coupling strategies to access complex advanced intermediates.

In Chapter four, efforts towards crafting an antibody–drug conjugate were discussed. Completion of a small library of analogues and their biological evaluation was accomplished, alongside preliminary studies into linker strategies. In contrast to our hopes and predictions for these molecules, it was demonstrated that our analogues in fact showed reduced potency compared to the natural products. Further exploration of these effects will uncover additional SAR data to guide the re-design of future simplified analogues.

Simplified aplyronine D analogue **44** has been synthesised in 1.7% overall yield and in 25 steps LLS (40 steps total) from Roche ester derived ethyl ketone **42**. For the purposes of applying this synthetic route to a promising scale up campaign, it compares favourably with the industrial manufacture of Halaven (eribulin mesylate **5**, **Section 1.1.1**), a marine natural product inspired drug. The current route used in production by Eisai requires 30 steps LLS

with 62 steps in total, demonstrating a high-profile success story in the combined efforts of both academia and industry to generate a viable solution to the supply problem purely by synthesis.

Our future goal of combining the exquisite biological activity of the aplyronines with the impeccable targeting ability of an antibody could have tremendous potential for the treatment of a variety of cancers. This brings us one step closer to realising the hope of Ehrlich's fabled magic bullet within modern medicine.

Chapter 6

Experimental

6.1 General procedures

All experiments were performed under anhydrous conditions and under an atmosphere of argon in oven dried glassware, employing standard techniques for handling air-sensitive materials, unless otherwise stated or when aqueous reagents were used.

Reagents and solvents were purified according to standard procedures.[266] Acetonitrile (MeCN), benzene (C_6H_6), dichloromethane (CH_2Cl_2) and dimethyl sulfoxide (DMSO) were distilled from calcium hydride (CaH_2) and stored under an argon atmosphere. Tetrahydrofuran (THF) and diethyl ether (Et_2O) were distilled from benzophenone ketyl radical and sodium or potassium wire, respectively, under an argon atmosphere. Triethylamine (NEt_3), 2,6-lutidine and hexamethyldisilazane (HMDS) were distilled from and stored over CaH_2. Diisopropylethylamine (*i*-Pr_2NEt) was distilled from ninhydrin, then redistilled from and stored over CaH_2. Oxalyl chloride ($(COCl)_2$) and titanium tetrachloride ($TiCl_4$) were distilled and stored at −20 °C under an atmosphere of argon. Propionaldehyde was distilled from calcium chloride ($CaCl_2$) immediately prior to use. DDQ was recrystallised from chloroform, and proton sponge was recrystallised from methanol. Barium hydroxide ($Ba(OH)_2$) was dried under high vacuum at 130 °C and stored under argon. 1,2-diiodoethane was washed with $Na_2S_2O_3$ solution and stored at −20 °C under argon.

All other chemicals were used as received from the manufacturer unless otherwise stated.

Solvents used in workup, extractions and flash column chromatography were distilled prior to use. Aqueous solutions of ammonium chloride (NH_4Cl), brine (NaCl), sodium bicarbonate ($NaHCO_3$), sodium thiosulfate ($Na_2S_2O_3$) and sodium / potassium (Na^+/K^+) tartrate were saturated. Buffer solutions were prepared from stock tablets as directed.

Purification by flash column chromatography was carried out using Merck Kieselgel 60 (230-400 mesh) silica gel under a positive pressure of regulated compressed air. All solvent mixtures are reported as volume mixtures. Preparative thin layer chromatography was carried out using Merck Kieselgel 60 F_{254} plates.

6.1.1 Biological studies

Cell Line

HeLa cells were obtained from the American Type Culture Collection (ATCC) and were maintained in Dulbecco's Modified Eagle Medium (DMEM) supplemented with 10% heat-inactivated FBS and 2 mM L-glutamine.

Cell Viability

Cells were seeded at 2,000 cells/well in 96-well plates for 24 h at 37 °C with 5% CO_2. Serial dilutions of aplyronine samples were added to the cells in complete growth medium and incubated at 37 °C with 5% CO_2 for 96 h. Cell viability was measured using CellTiter-Glo viability assay (Promega) according to the manufacturer's instructions. Cell viability was plotted as a percentage of untreated cells. Each measurement was taken in triplicate and three independent repeats were performed from different cell passages.

6.2 Analytical procedures

Analytical thin layer chromatography (TLC) was carried out using Merck Kieselgel 60 F_{254} plates which were visualised using UV light (254 nm) and stained with potassium permanganate, vanillin, anisaldehyde or phosphomolybdic acid / cerium (III) sulfate $Ce_2(SO_4)_3$ dips.

Proton nuclear magnetic resonance (NMR) spectra were recorded using an internal deuterium lock at ambient probe temperature (298 K) on the following instruments: Bruker Avance BB, or Bruker Avance TCI (500 MHzand Bruker DPX400 (400 MHz). An internal reference of δ_H = 7.26 ppm was used for residual solvent protons in $CDCl_3$ and δ_H = 7.26 2.50 ppm for DMSO. All ^{1}H NMR data are represented as: chemical shift (in ppm on the δ scale relative to δ_{TMS} = 0 ppm), integration, multiplicity (s = singlet, d = doublet, t = triplet, q = quartet, m = multiplet, br = broad, obs = obscured, app = apparent), coupling constant (*J* in Hz), and assignment. Assignments were determined on the basis of unambiguous chemical shift or coupling pattern, ^{1}H-^{1}H COSY, HSQC and HMBC experiments, or by analogy to fully interpreted data for related compounds.

Proton-decoupled ^{13}C NMR spectra were recorded using an internal deuterium lock at ambient probe temperature (298K) on the following instruments: Bruker Avance BB and Bruker Avance TCI (125 MHz). An internal reference of δ_C = 77.0 ppm was used for carbons in $CDCl_3$ and δ_C = 79.5 ppm for DMSO. All chemical shift values are reported in ppm on the δ scale relative to δ_{TMS} = 0 ppm.

Infrared spectra were recorded on a Perkin-Elmer Spectrum One FT-IR spectrometer. Absorbance frequencies (ν_{max}) are reported in cm^{-1}.

Optical rotations were measured on an Anton Parr MCP100 polarimeter at 589 nm and are reported as follows: $[\boldsymbol{\alpha}]_{\boldsymbol{D}}^{\boldsymbol{20}}$ at 20 °C (unless otherwise noted), concentration (*c* in g dL^{-1}) and solvent.

Melting points are uncorrected.

High resolution mass spectra (HRMS) were recorded at the EPSRC Mass Spectrometry Service (Swansea, UK) or at the departmental mass spectrometry service (University Chemical Laboratories, Cambridge) using electron impact (EI) and electrospray ionization (ESI) techniques. The parent ion is quoted with the indicated cation: $[M+H]^+$, $[M+Na]^+$ or $[M+NH_4]^+$.

6.3 Preparation of reagents

Dicyclohexylboron chloride (BCy_2Cl)

Cyclohexene (40 mL, 400 mmol, distilled from CaH_2) was dissolved in Et_2O (200 mL) and cooled to −10 °C. Monochloroborane methyl sulfide complex ($BH_2Cl{\cdot}SMe_2$, 20 mL, 200 mmol) was added dropwise over 15 min, and the solution was stirred at 0 °C for 1 h, then at rt for 1 h. The solvent was removed by distillation at ambient pressure (35 °C) under argon. Distillation under reduced pressure (0.3 mBar, 89−92 °C) gave BCy_2Cl as a colourless liquid, which was stored under argon at −20 °C.

Samarium (II) iodide (0.1 M in THF)

To samarium powder (108 mg, 0.72 mmol) and 1,2-diiodoethane (169 mg, 0.60 mmol) was added THF (6 mL). The mixture was sonicated for 1 h until a deep blue colour had developed. The resulting SmI_2 solution was used immediately.

Zinc borohydride ($Zn(BH_4)_2$, 0.175 M in Et_2O)

Zinc (II) chloride (1.49 g, 10.9 mmol) was dried under vacuum at 150 °C for 2 h then suspended in Et_2O (50 mL) and refluxed for 2 h until all the solids had dissolved. The resulting solution was cooled to rt and transferred to a flask containing sodium borohydride (0.817 g, 21.6 mmol) suspended in Et_2O (12 mL). The reaction was stirred vigorously for 16 h and the supernatant solution of $Zn(BH_4)_2$ (0.175 M) removed *via* cannula.

Stryker's reagent ($[CuH(PPh_3)]_6$)

Copper (II) acetate (25 mg, 0.125 mmol) and triphenylphosphine (66.0 mg, 0.25 mmol) were suspended in toluene (4.66 mL) under an argon atmosphere. Tetramethyldisiloxane (0.330 mL, 2.43 mmol) was added and the bright blue mixture stirred for 16 h to produce a deep red solution which was used directly in conjugate reduction reactions.

***i*-PrMgCl (2.0 M in THF)**

To magnesium turnings (3.74 g, 154 mmol) in THF (70 mL) was added a portion of *i*-PrCl (2.00 mL, 21.9 mmol) and one bead of iodine. The brown reaction mixture turned colourless and the temperature rose as the reaction initiated. A further quantity of *i*-PrCl (10.8 mL, 118 mmol) was added dropwise over 1 h. The dark grey solution of *i*-PrMgCl was cooled to rt and used immediately.

EtMgBr (3.0 M in Et_2O)

EtBr (11.2 mL, 150 mL) was added slowly to a suspension of magnesium turnings (4.01 g, 165 mmol) in Et_2O (50 mL) over 1 h. The dark grey solution of EtMgBr was used immediately.

Lithium hexamethyldisilazide (LiHMDS, 1.0 M in THF)

To a solution of HMDS (0.576 mL, 2.75 mmol) in THF (0.94 mL) at 0 °C was added *n*-BuLi (1.56 mL, 1.6 M in hexane, 2.5 mmol). The mixture was stirred for 1 h at 0 °C before being used immediately.

4-Methoxybenzyl-2,2,2-trichloroacetimidate (PMBTCA)

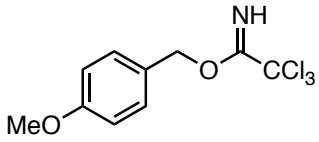

To a solution of 4-methoxybenzyl alcohol (5.00 g, 36.2 mmol) and tetrabutylammonium hydrogensulfate (123 mg, 0.362 mmol) in CH_2Cl_2 (50 mL) at −10 °C was added 50% aqueous KOH solution (50 mL). Trichloroacetonitrile (3.99 mL, 39.8 mmol) was added dropwise over 20 min and the biphasic mixture was rapidly stirred for 1 h whilst warming to rt and stirred further 2 h. The organic phase was separated, and the aqueous phase was extracted with Et_2O (3 × 100 mL). The combined organic phases were dried ($MgSO_4$) and concentrated *in vacuo.* Purification by flash chromatography on neutral alumina (1:19 EtOAc/PE) yielded PMBTCA as a colourless oil (9.35 g, 92%).

R_f 0.33 (1:19 EtOAc/PE, alumina plate); **^{1}H NMR** (500MHz, $CDCl_3$) δ_H 8.36 (1H, br s, NH), 7.37 (2H, d, J = 8.5 Hz, ArH), 6.91 (2H, d, J = 8.6 Hz, ArH), 5.28 (2H, s, OCH_2Ar), 3.82 (3H, s, OMe).

These data are in agreement with those previously reported.[267]

_N_-(chloromethyl)-_N_-methylformamide, 85

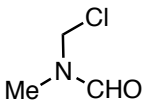

To a stirred solution of paraformaldehyde (1.65 g, 55.0 mmol) in $CHCl_3$ (150 mL) was added *N*-methylformamide (2.92 mL, 50.0 mmol) and TMSCl (19.0 mL, 150 mmol). The mixture was heated to reflux for 2 h then cooled to rt and concentrated *in vacuo* to give crude **85** as a pale yellow oil. The crude material was used directly in the next reaction.

^{1}H NMR (400 MHz, $CDCl_3$) δ_H 8.29 (0.67H, s, NCHO), [8.07] (0.33H, s, NCHO*), 5.25 (1.33H, s, CH_2Cl), [5.24] (0.67H, s, CH_2Cl*), [3.08] (1H, s, NMe*), 2.98 (2H, s, NMe).

Distinguishable resonances of the minor rotamer (2:1 ratio) are given in brackets and assignments denoted with an asterisk.

(_N_-methylformamido)methyl)triphenylphosphonium chloride, 84

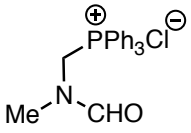

Crude *N*-chloromethyl-*N*-methylformamide **85** was added to a stirred solution of triphenylphosphine (14.4 g, 55.0 mmol) in Et_2O (100 mL) and stirred at rt for 24 h. The resulting slurry was filtered and washed with anhydrous Et_2O (3 × 15 mL), then dried under high vacuum to give a white solid (6.03 g, 32% over 2 steps).

^{1}H NMR (500 MHz, $CDCl_3$) δ_H 8.16–7.64 (16H, m, NCHO, NCHO*, ArH), [6.60] (0.30H, d, J = 2.4 Hz, NCH_2P*), 6.22 (1.60H, d, J = 4.1 Hz, NCH_2P), 3.20 (2H, s, NMe), [2.80] (1H, s, NMe*).

Distinguishable resonances of the minor rotamer (4:1 ratio) are given in brackets and assignments denoted with an asterisk.

These data are in agreement with those previously reported.[139,268]

Diethyl (3-oxobutan-2-yl)phosphonate, 72

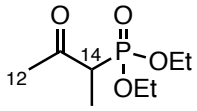

To a solution of diethyl ethylphosphonate (6.00 g, 36.1 mmol) in THF (50 mL) at −78 °C was added *n*-BuLi (24.8 mL, 1.6 M in hexane, 39.7 mmol). The mixture was stirred for 1 h, then EtOAc (3.62 mL, 36.8 mmol, freshly distilled from CaH_2) was added dropwise. After stirring for 1.5 h at −78 °C, the reaction was quenched with NH_4Cl (50 mL) and warmed to rt. The layers were separated and the aqueous extracted with EtOAc (5 × 50 mL). The combined organics were dried over $MgSO_4$ and concentrated *in vacuo*. The residue was purified by distillation under reduced pressure (0.42 Torr, 88 °C) to afford phosphonate **72** as a colourless oil (3.89 g, 62%).

R_f 0.13 (1:1 EtOAc/PE); **^{1}H NMR** (500 MHz, $CDCl_3$) δ_H 4.18-4.08 (4H, m, $P(OC\underline{H}_2CH_3)_2$), 3.20 (1H, dq, J = 25.6, 7.1 Hz, H_{14}), 2.34 (3H, s, Me_{12}), 1.38 (3H, dd, J = 21.3, 7.1 Hz, Me_{14}), 1.33 (6H, m, $P(OCH_2C\underline{H}_3)_2$).

These data are in agreement with those previously reported.[138]

6.4 Experimental procedures for Chapter 2

6.4.1 C_1–C_{14} northern fragment 36

Methyl (*R*)-3-((4-methoxybenzyl)oxy)-2-methylpropanoate, 59

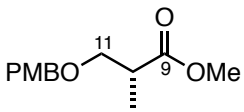

To a solution of methyl (*R*)-3-hydroxy-2-methylpropionate (4.00 g, 33.8 mmol) in CH_2Cl_2 (40 mL) was added freshly prepared PMBTCA (9.50 g, 37.2 mmol). PPTS (817 mg, 3.25 mmol) was added and the solution was stirred at rt for 2 h. The reaction was quenched with $NaHCO_3$ (75 mL) and the aqueous layer was extracted with CH_2Cl_2 (3 × 30 mL). The combined organics were dried ($MgSO_4$) and concentrated *in vacuo*. The crude mixture was triturated by solvating with the minimum volume of ice-cold petroleum ether (*ca*. 20 mL),

before being filtered through a plug of Celite and the filtrate was concentrated *in vacuo*. Purification by flash column chromatography (1:4 EtOAc/PE) afforded PMB-ether **59** as a colourless oil (6.99 g, 87%).

R_f 0.40 (1:4 EtOAc/PE); **^{1}H NMR** (500MHz, $CDCl_3$) δ_H 7.23 (2H, d, J = 8.5 Hz, ArH), 6.87 (2H, d, J = 8.5 Hz, ArH), 4.45 (2H, s, OCH_2Ar), 3.80 (3H, s, ArOMe), 3.69 (3H, s, OMe), 3.63 (1H, dd, J = 9.2, 7.3 Hz, H_{11a}), 3.46 (1H, dd, J = 9.3, 6.0 Hz, H_{11b}), 2.77 (1H, tq, J = 7.0, 6.0 Hz, H_{10}), 1.17 (3H, d, J = 7.3 Hz, Me_{10}).

These data are in agreement with those previously reported.[138]

(*R*)-*N*-methoxy-3-((4-methoxybenzyl)oxy)-*N*,2-dimethylpropanamide, 60

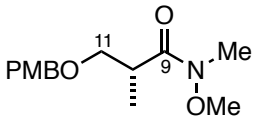

N,*O*-dimethylhydroxylamine hydrochloride (3.99 g, 41.0 mmol) was dried under vacuum for 3 h before being added to a stirred solution of methyl ester **59** (6.50 g, 27.3 mmol) in THF (55 mL). The resulting slurry was cooled to –20 °C and *i*-PrMgCl (41.0 mL, 2.0 M in THF, 81.8 mmol) was added dropwise over 30 min, ensuring that the internal temperature did not rise above –10 °C. The mixture was stirred at –20 °C for 2 h and quenched with NH_4Cl (100 mL). After warming to rt the mixture was extracted with Et_2O (3 × 75 mL) and the combined organic extracts were washed with brine (75 mL), dried ($MgSO_4$) and concentrated *in vacuo*. Purification by flash column chromatography (3:7 EtOAc/PE) afforded amide **60** as a colourless oil (6.43 g, 88%).

R_f 0.19 (3:7 EtOAc/PE) **^{1}H NMR** (500MHz, $CDCl_3$) δ_H 7.23 (2H, d, J = 8.8 Hz, ArH), 6.86 (2H, d, J = 8.8 Hz, ArH), 4.44 (2H, ABq, J = 11.5 Hz, OCH_2Ar), 3.80 (3H, s, ArOMe), 3.69 (3H, s, OMe), 3.68 (1H, dd, J = 8.8, 8.5 Hz, H_{11a}), 3.40 (1H, dd, J = 9.0, 6.0 Hz, H_{11b}), 3.20 (3H, s, NMe), 1.55 (1H, br s, H_{10}), 1.11 (3H, d, J = 6.8 Hz, Me_{10}).

These data are in agreement with those previously reported.[138]

(*R*)-1-((4-methoxybenzyl)oxy)-2-methylpentan-3-one, 42

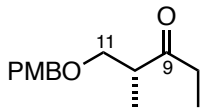

To a solution of amide **60** (6.00 g, 22.4 mmol) in Et_2O (75 mL) at 0 °C was added dropwise EtMgBr (25 mL, 3.0 M in Et_2O, 67.3 mmol). After stirring at 0 °C for 1 h, the reaction was carefully quenched by the slow addition of NH_4Cl (100 mL). The mixture was warmed to rt and extracted with Et_2O (3 × 50 mL), and the combined organic extracts were washed with brine (50 mL), dried ($MgSO_4$) and concentrated *in vacuo*. Purification by flash column chromatography (1:4 EtOAc/PE) afforded ketone **42** as a colourless oil (4.38 g, 82%).

$\mathbf{R_f}$ 0.32 (1:4 EtOAc/PE); ^{1}**H NMR** (500MHz, $CDCl_3$) $\boldsymbol{\delta}_H$ 7.21 (2H, d, J = 8.8 Hz, ArH), 6.87 (2H, d, J = 8.8 Hz, ArH), 4.41 (2H, ABq, J = 11.5 Hz, OCH_2Ar), 3.80 (3H, s, OMe), 3.59 (1H, dd, J = 9.0, 7.8 Hz, H_{11a}), 3.43 (1H, dd, J = 9.0, 5.5 Hz, H_{11b}), 2.92-2.82 (1H, m, H_{10}), 2.50 (2H, q, J = 7.3 Hz, H_8 × 2), 1.06 (3H, d, J = 7.0 Hz, Me_{10}), 1.03 (3H, t, J = 7.0 Hz, Me_8).

These data are in agreement with those previously reported.[138]

Methyl-7-oxohept-2-ynoate, 55

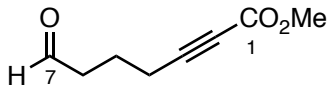

To a solution of alcohol **61** (3.00 g, 19.2 mmol) in CH_2Cl_2 (30 mL) was added DMSO (30 mL). The solution was cooled to 0 °C and NEt_3 (12.1 mL, 86.4 mmol) was added. Sulfur trioxide pyridine complex (13.7 g, 86.4 mmol) was added in small portions, ensuring that the temperature did not rise above 5 °C. Once addition was complete, the solution was stirred for 1 h and then quenched with NH_4Cl (50 mL). After warming to rt, the mixture was extracted with CH_2Cl_2 (3 × 30 mL). The combined organic layers were washed with brine (30 mL), dried ($MgSO_4$) and concentrated *in vacuo*. The crude product was purified by flash column chromatography (1:4 EtOAc/PE) to afford aldehyde **55** as a colourless oil (2.50 g, 86%).

R_f 0.25 (1:4 EtOAc/PE); **^{1}H NMR** (400MHz, $CDCl_3$) δ_H 9.80 (1H, t, J = 0.9 Hz, CHO), 3.76 (3H, s, OMe), 2.63 (2H, td, J = 6.9, 0.9 Hz, H_6 × 2), 2.43 (2H, t, J = 6.9 Hz, H_4 × 2), 1.91 (2H, tt, J = 6.9, 6.9 Hz, H_5 × 2).

These data are in agreement with those previously reported.[138]

(7*R*,8*R*,10*R*)-Methyl-7-hydroxy-11-((4-methoxybenzyl)oxy)-8,10-dimethyl-9-oxoundec-2-ynoate, 57

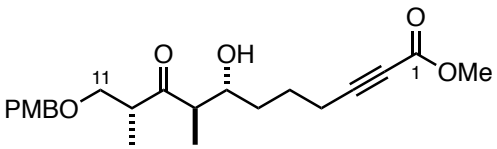

To a solution of dicyclohexylboron chloride (2.96 mL, 13.5 mmol) in Et_2O (20 mL) at –78 °C was added NEt_3 (2.74 mL, 19.7 mmol), followed by a solution of ketone **42** (2.90 g, 12.3 mmol) in Et_2O (10 mL) *via* cannula. The reaction mixture was warmed to –20 °C and stirred for 1.5 h, before being cooled to –78 °C and a solution of aldehyde **55** (1.14 g, 7.36 mmol) in Et_2O (10 mL) was added. The mixture was stirred at –78 °C for 3 h then left at –20 °C for 16 h. After warming to 0 °C, the reaction was quenched with MeOH (40 mL) and pH 7.0 buffer solution (40 mL), followed by hydrogen peroxide (20 mL, 30% aq.). The mixture was stirred for 1 h at rt then poured into H_2O (40 mL) and extracted with CH_2Cl_2 (3 × 40 mL). The combined organics were washed with $NaHCO_3$ (40 mL) and brine (40 mL), then dried ($MgSO_4$) and concentrated *in vacuo*. Purification by flash column chromatography (3:7 EtOAc/PE) gave aldol adduct **57** as a colourless oil (4.15 g, 88%, >95:5 *dr*).

R_f 0.20 (7:3 EtOAc/PE); **^{1}H NMR** (500MHz, $CDCl_3$) δ_H 7.20 (2H, d, J = 8.4 Hz, ArH), 6.86 (2H, d, J = 8.6 Hz, ArH), 4.40 (2H, ABq, J = 11.6 Hz, OCH_2Ar), 3.80 (3H, s, ArOMe), 3.75 (3H, s, CO_2Me), 3.70-3.64 (2H, m, H_7, H_{11a}), 3.39 (1H, dd, J = 8.9, 4.6 Hz, H_{11b}), 3.11-3.03 (1H, m, H_{10}), 2.66 (1H, dq, J = 7.1, 7.1 Hz, H_8), 2.34 (2H, t, J = 6.7 Hz, H_4 × 2), 1.80-1.71 (1H, m, H_{6a}), 1.69-1.57 (2H, m, H_5 × 2), 1.49-1.39 (1H, m, H_{6b}), 1.14 (3H, d, J = 6.7 Hz, Me_8), 1.03 (3H, d, J = 6.7 Hz, Me_{10}).

These data are in agreement with those previously reported.[138]

(7*R*,8*S*,9*R*,10*R*)-Methyl 9-hydroxy-11-((4-methoxybenzyl)oxy-8,10-dimethyl-7-(propionyl-oxy)undec -2-ynoate, 63

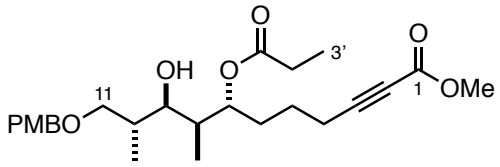

To a solution of propionaldehyde (freshly distilled from $CaCl_2$ 1.10 mL, 15.2 mmol) in THF (12 mL) at 0 °C was added freshly prepared SmI_2 (2.56 mL, 0.1 M in THF, 0.256 mmol). The solution was stirred for 5 min until the deep blue colouration had subsided. A solution of aldol adduct **57** (1.00 g, 2.56 mmol) in THF (5 mL) was then added *via* cannula. The reaction was stirred at 0 °C for 1 h, before being quenched with $NaHCO_3$ (10 mL) and extracted with Et_2O (3 × 10 mL). The combined organic layers were dried ($MgSO_4$), concentrated *in vacuo* and purified by flash column chromatography (3:7 EtOAc/PE) to give propionate ester **63** as a colourless oil (1.13 g, 98%, >95:5 *dr*).

R_f 0.33 (7:3 EtOAc/PE); **^{1}H NMR** (400MHz, $CDCl_3$) δ_H 7.23 (2H, d, J = 8.4 Hz, ArH), 6.87 (2H, d, J = 8.6 Hz, ArH), 4.94 (1H, td, J = 8.3, 3.2 Hz, H_7), 4.44 (2H, ABq, J = 11.6 Hz, OCH_2Ar), 3.80 (3H, s, ArOMe), 3.75 (3H, s, CO_2Me), 3.57-3.48 (2H, m, H_{11} × 2), 3.44 (1H, br d, J = 9.0 Hz, H_9), 3.28 (1H, br s, OH), 2.41-2.30 (4H, m, $H_{2'}$ × 2, H_4 × 2), 1.93-1.73 (3H, m, H_{6a}, H_8, H_{10}), 1.70-1.53 (3H, m, H_5 × 2, H_{6b}), 1.15 (3H, t, J = 7.4 Hz, $H_{3'}$ × 3), 0.88 (3H, d, J = 6.7 Hz, Me_{10}), 0.82 (3H, d, J = 6.7 Hz, Me_8).

These data are in agreement with those previously reported.[138]

(2*E*,4*E*,7*R*,8*S*,9*R*,10*R*)-Methyl-9-hydroxy-11-((4-methoxybenzyl)oxy)-8,10-dimethyl-7-(propionyloxy)undeca-2,4-dienoate, 65

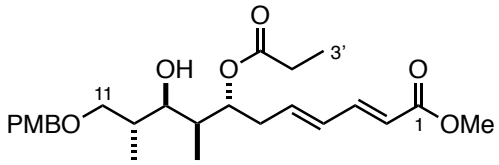

To a solution of alkyne ester **63** (3.98 g, 8.88 mmol) in benzene (32 mL) was added PPh_3 (4.66 g, 17.8 mmol) and PhOH (1.75 g, 18.7 mmol). The reaction mixture was stirred at rt for 48 h, then quenched by pouring into NaOH solution (35 mL, 10% aq.) and extracted

with Et_2O (3 × 30 mL). The combined organic layers were washed with brine (50 mL), dried ($MgSO_4$) and concentrated *in vacuo*. Purification by flash column chromatography (1:4 EtOAc/PE) yielded dienoate **65** as a colourless oil (3.71 g, 93%).

R_f 0.18 (1:4 EtOAc/PE); **^{1}H NMR** (500MHz, $CDCl_3$) δ_H 7.25 (1H, dd, *J* = 15.6, 10.7 Hz, H_3), 7.23 (2H, d, *J* = 8.6 Hz, ArH), 6.87 (2H, d, *J* = 8.6 Hz, ArH), 6.21 (1H, dd, *J* = 15.0, 11.1 Hz, H_4), 6.06 (1H, dt, *J* = 14.9, 8.1 Hz, H_5), 5.80 (1H, d, *J* = 15.0 Hz, H_2), 5.02 (1H, td, *J* = 8.1, 3.4 Hz, H_7), 4.44 (2H, ABq, *J* = 11.6 Hz, OCH_2Ar), 3.80 (3H, s, ArOMe), 3.74 (3H, s, CO_2Me), 3.54 (1H, dd, *J* = 9.0, 4.2 Hz, H_{11a}), 3.51-3.46 (2H, m, H_9, H_{11b}), 3.36 (1H, br s, OH), 2.64 (1H, ddd, *J* = 15.4, 5.1, 5.1 Hz, H_{6a}), 2.40 (1H, ddd, *J* = 15.4, 8.1, 8.1 Hz, H_{6b}), 2.31 (1H, q, *J* = 8.1 Hz, $H_{2'a}$), 2.31 (1H, q, *J* = 8.1 Hz, $H_{2'b}$), 1.93-1.85 (1H, m, H_{10}), 1.82-1.75 (1H, m, H_8), 1.12 (3H, t, *J* = 7.3 Hz, $H_{3'}$ × 3), 0.89 (3H, d, *J* = 6.8 Hz, Me_{10}), 0.80 (3H, d, *J* = 6.8 Hz, Me_8).

These data are in agreement with those previously reported.[138]

(2*E*,4*E*,7*R*,8*R*,9*R*,10*R*)-Methyl-7,9-dihydroxy-11-((4-methoxybenzyl)oxy-8,10-dimethylundeca-2,4-dienoate, 68

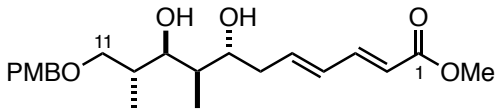

Potassium carbonate (2.85 g, 20.6 mmol) was added to a solution of ester **65** (3.70 g, 8.25 mmol) in MeOH (140 mL) and the solution was stirred at rt for 2 h. Once complete, the reaction mixture was poured into $NaHCO_3$ (100 mL) and extracted with EtOAc (4 × 100 mL). The combined organic extracts were dried (Na_2CO_3) and concentrated *in vacuo*. Purification by flash column chromatography (2:3 EtOAc/PE) gave diol **68** as a colourless oil (2.95 g, 93%).

R_f 0.33 (1:1 EtOAc/PE); **^{1}H NMR** (400MHz, $CDCl_3$) δ_H 7.27 (1H, dd, *J* = 15.4, 10.4 Hz, H_3), 7.24 (2H, d, *J* = 8.6 Hz, ArH), 6.87 (2H, d, *J* = 8.6 Hz, ArH), 6.26 (1H, dd, *J* = 15.7, 10.6 Hz, H_4), 6.19 (1H, dt, *J* = 15.4, 7.1 Hz, H_5), 5.80 (1H, d, *J* = 15.7 Hz, H_2), 4.45 (2H, ABq, *J* = 11.4 Hz, OCH_2Ar), 3.87 (1H, dd, *J* = 9.2, 7.1 Hz, H_9), 3.80 (3H, s, ArOMe), 3.74 (3H, s, CO_2Me), 3.70-3.64 (1H, m, H_7), 3.58 (1H, dd, *J* = 9.7, 3.6 Hz, H_{11a}), 3.44 (1H, t, *J* = 9.2 Hz, H_{11b}), 2.50 (1H, ddd, *J* = 14.6, 7.0, 7.0 Hz, H_{6a}), 2.44 (1H, ddd, *J* = 14.6, 6.5, 6.5

Hz, H_{6b}), 2.02-1.94 (1H, m, H_{10}), 1.63-1.57 (1H, m, H_8), 1.00 (3H, d, J = 7.1 Hz, Me_8), 0.70 (3H, d, J = 7.1 Hz, Me_{10}).

These data are in agreement with those previously reported.[138]

Methyl (2*E*,4*E*,7*R*,8*R*,9*R*,10*R*)-11-((4-methoxybenzyl)oxy)-8,10-dimethyl-7,9-bis((triethylsilyl)oxy)undeca-2,4-dienoate, 69

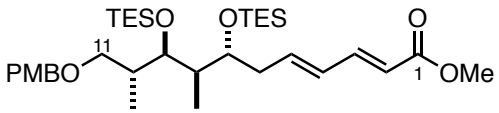

To a solution of diol **68** (900 mg, 2.30 mmol) in CH_2Cl_2 (25 mL) at –78 °C was added TESOTf (1.15 mL, 5.08 mmol) and 2,6-lutidine (0.67 mL, 5.75 mmol). The reaction was stirred for 1 h before being quenched with NH_4Cl (50 mL). The solution was warmed to rt and the layers were separated. The aqueous phase was extracted with CH_2Cl_2 (3 × 50 mL) and the combined organics were dried ($MgSO_4$) and concentrated *in vacuo*. The crude material was purified by flash column chromatography (1:15 EtOAc/PE) to give **69** as a colourless oil (1.31 g, 92%).

R_f 0.26 (1:15 EtOAc/PE); **^{1}H NMR** (400MHz, $CDCl_3$) δ_H 7.27 (1H, dd, J = 15.4, 10.4 Hz, H_3), 7.25 (2H, d, J = 8.8 Hz, ArH), 6.87 (2H, d, J = 8.8 Hz, ArH), 6.26 (1H, dd, J = 15.4, 10.5 Hz, H_4), 6.19 (1H, dt, J = 15.4, 7.0 Hz, H_5), 5.79 (1H, d, J = 15.4 Hz, H_2), 4.43 (2H, s, OCH_2Ar), 3.80 (3H, s, ArOMe), 3.74 (3H, s, CO_2Me), 3.73-3.68 (1H, m, H_7), 3.64 (1H, dd, J = 5.1, 3.7 Hz, H_{11a}), 3.48 (1H, dd, J = 9.2, 5.1 Hz, H_{11b}), 3.21 (1H, dd, J = 9.1, 7.5 Hz, H_9), 2.30-2.21 (2H, m, H_6 × 2), 2.00-1.93 (1H, m, H_{10}), 1.80-1.75 (1H, m, H_8), 0.99 (3H, d, J = 7.0 Hz, Me_{10}), 0.95 (9H, t, J = 7.7 Hz, $Si(CH_2C\underline{H}_3)_3$), 0.94 (9H, t, J = 7.7 Hz, $Si(CH_2C\underline{H}_3)_3$), 0.86 (3H, d, J = 7.1 Hz, Me_8), 0.60 (6H, q, J = 7.7 Hz, $Si(C\underline{H}_2CH_3)_3$), 0.56 (6H, q, J = 7.7 Hz, $Si(C\underline{H}_2CH_3)_3$).

These data are in agreement with those previously reported.[138]

Methyl (2*E*,4*E*,7*R*,8*R*,9*R*,10*R*)-11-hydroxy-8,10-dimethyl-7,9-bis((triethylsilyl)oxy) undeca-2,4-dienoate, 70

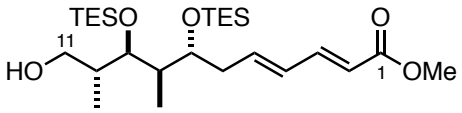

To a solution of PMB ether **69** (1.66 g, 2.00 mmol) in CH_2Cl_2 (32 mL) and pH 7.0 buffer (16 mL) was added DDQ (910 mg, 4.00 mmol). The resulting dark green solution was stirred for 2 h before $NaHCO_3$ (40 mL) was added. The mixture was diluted with H_2O (200 mL) and extracted with CH_2Cl_2 (3 × 100 mL). The combined organics were dried (Na_2SO_4), concentrated *in vacuo* and the crude purified by flash column chromatography (PhMe → 1:5 EtOAc/PE) to yield alcohol **70** as a colourless oil (1.19 g, 89%).

R_f 0.56 (1:4 EtOAc/PE); **^{1}H NMR** (500MHz, $CDCl_3$) δ_H 7.27 (1H, dd, J = 14.7, 10.0 Hz, H_3), 6.21 (1H, dd, J = 15.7, 10.6 Hz, H_4), 6.14 (1H, dt, J = 15.2, 6.9 Hz, H_5), 5.81 (1H, d, J = 15.2 Hz, H_2), 3.78-3.75 (2H, m, H_9, H_{11a}), 3.75 (3H, s, CO_2Me), 3.73-3.69 (1H, m, H_7), 3.55 (1H, ddd, J = 12.0, 6.1, 6.1 Hz, H_{11b}), 2.61 (1H, dd, J = 6.6, 5.3 Hz, OH), 2.34-2.22 (2H, H_6 × 2), 1.86-1.79 (1H, m, H_8), 1.78-1.72 (1H, m, H_{10}), 1.00 (3H, d, J = 7.6 Hz, Me_{10}), 0.98 (9H, t, J = 8.3 Hz, $Si(CH_2C\underline{H}_3)_3$), 0.95 (9H, t, J = 8.3 Hz, $Si(CH_2C\underline{H}_3)_3$), 0.89 (3H, d, J = 7.1 Hz, Me_8), 0.65 (6H, q, J = 7.9 Hz, $Si(C\underline{H}_2CH_3)_3$), 0.60 (6H, q, J = 7.9 Hz, $Si(C\underline{H}_2CH_3)_3$).

These data are in agreement with those previously reported.[138]

Methyl (2*E*,4*E*,7*R*,8*R*,9*S*,10*S*)-11-iodo-8,10-dimethyl-7,9-bis((triethylsilyl)oxy) undeca -2,4-dienoate, 71

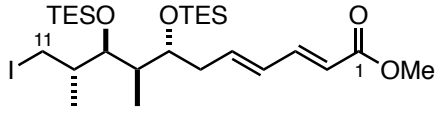

To a solution of alcohol **71** (1.19 g, 2.38 mmol) in Et_2O/MeCN (1:1 50 mL) at 0 °C was added PPh_3 (1.12 g, 4.28 mmol), imidazole (357 mg, 5.24 mmol) and, in small portions I_2 (1.08 g, 4.28 mmol). The reaction mixture was stirred at 0 °C for 1 h then warmed to rt and

stirred for 2 h, before being poured into $NaHCO_3$ (50 mL). The layers were separated, and the aqueous phase was extracted with Et_2O (3 × 50 mL). The combined organics were washed with brine (40 mL), dried ($MgSO_4$) and concentrated *in vacuo*. Purification by flash column chromatography (1:6 EtOAc/PE) gave iodide **71** as a colourless oil (1.14 g, 82%).

R_f 0.31 (1:4 EtOAc/PE); **^{1}H NMR** (500MHz, $CDCl_3$) δ_H 7.27 (1H, dd, J = 15.5, 10.6 Hz, H_3), 6.27-6.11 (2H, m, H_4, H_5), 5.81 (1H, d, J = 15.4 Hz, H_2), 3.75 (3H, s, CO_2Me), 3.72-3.68 (1H, m, H_7), 3.67-3.65 (1H, m, H_9), 3.29 (1H, dd, J = 9.3, 3.9 Hz, H_{11a}), 3.00 (1H, t, J = 9.6 Hz, H_{11b}), 2.34-2.25 (2H, m, H_6 × 2), 1.87-1.79 (1H, m, H_{10}), 1.74-1.65 (1H, m, H_8), 1.05 (3H, d, J = 6.6 Hz, Me_{10}), 0.96 (9H, t, J = 7.7 Hz, $Si(CH_2C\underline{H}_3)_3$), 0.95 (9H, t, J = 7.7 Hz, $Si(CH_2C\underline{H}_3)_3$), 0.85 (3H, d, J = 7.0 Hz, Me_8), 0.63 (6H, q, J = 7.7 Hz, $Si(C\underline{H}_2CH_3)_3$), 0.60 (6H, q, J = 7.7 Hz, $Si(C\underline{H}_2CH_3)_3$).

These data are in agreement with those previously reported.[138]

(2*E*,4*E*,7*R*,8*R*,9*S*,10*S*)-11-Iodo-8,10-dimethyl-7,9-bis((triethylsilyl)oxy)undeca-2,4-dien-1-ol, 160

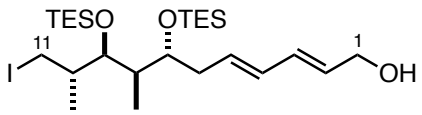

To a solution of ester **71** (1.14 g, 1.87 mmol) in CH_2Cl_2 (30 mL) was added DIBAL (5.59 mL, 5.59 mmol, 1.0 M in CH_2Cl_2) at –78 °C. Upon completion after 3 h, the reaction was quenched with Na^+/K^+ tartrate (60 mL) and allowed to warm to rt. The layers were separated and the aqueous was extracted with CH_2Cl_2 (4 × 50 mL). The combined organics were dried (Na_2SO_4) and concentrated *in vacuo*. The crude was purified by flash column chromatography (1:2 EtOAc/PE) to afford alcohol **160** as a colourless oil (1.05 g, 96%).

R_f 0.20 (1:2 EtOAc/PE); **^{1}H NMR** (500MHz, $CDCl_3$) δ_H 6.23 (1H, dd, J = 15.1, 10.4 Hz, H_3), 6.08 (1H, dd, J = 15.1, 10.4 Hz, H_4), 5.79-5.68 (2H, m, H_2, H_5), 4.18 (2H, t, J = 6.1 Hz, H_1 × 2), 3.69-3.63 (2H, m, H_7, H_9), 3.32 (1H, dd, J = 9.9, 4.1 Hz, H_{11a}), 2.99 (1H, t, J = 9.6 Hz, H_{11b}), 2.24-2.19 (2H, m, H_6 × 2), 1.89-1.78 (1H, m, H_{10}), 1.73-1.64 (1H, m, H_8), 1.33 (1H, t, J = 5.2 Hz, OH), 1.05 (3H, d, J = 6.7 Hz, Me_{10}), 0.96 (18H, t, J = 7.7 Hz, $Si(CH_2C\underline{H}_3)_3$), 0.85 (3H, d, J = 7.3 Hz, Me_8), 0.63 (6H, q, J = 7.7 Hz, $Si(C\underline{H}_2CH_3)_3$), 0.60 (6H, q, J = 7.7 Hz, $Si(C\underline{H}_2CH_3)_3$).

These data are in agreement with those previously reported.[138]

(6*E*,8*E*,11*R*,12*R*,13*S*)-15,15-Diethyl-13-((*S*)-1-iodopropan-2-yl)-2,2,3,3,12-pentamethyl-11-((triethylsilyl)oxy)-4,14-dioxa-3,15-disilaheptadeca-6,8-diene, 56

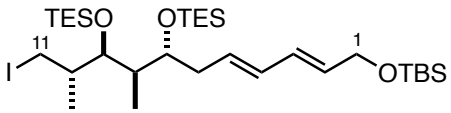

To a solution of alcohol **160** (3.57 g, 6.13 mmol) in CH_2Cl_2 (100 mL) was added TBSCl (1.38 g, 9.19 mmol) and imidazole (834 mg, 12.3 mmol). The reaction was stirred for 3 h before being quenched with NH_4Cl (100 mL). The layers were separated, the aqueous phase extracted with CH_2Cl_2 (3 × 70 mL) and the combined organics dried ($MgSO_4$) and concentrated *in vacuo*. The crude material was purified by flash column chromatography (1:20 EtOAc/PE) to give **56** as a colourless oil (4.27 g, 100%).

R_f 0.52 (1:20 EtOAc/PE); **^{1}H NMR** (500MHz, $CDCl_3$) δ_H 6.19 (1H, dd, *J* = 15.5, 10.5 Hz, H_3), 6.06 (1H, dd, *J* = 15.1, 10.5 Hz, H_4), 5.71-5.62 (2H, m, H_2, H_5), 4.21 (2H, d, *J* = 5.1 Hz, H_1 × 2), 3.68-3.62 (2H, m, H_7, H_9), 3.33 (1H, dd, *J* = 9.6, 3.8 Hz, H_{11a}), 2.98 (1H, t, *J* = 9.8 Hz, H_{11b}), 2.24-2.17 (2H, m, H_6 × 2), 1.88-1.79 (1H, m, H_{10}), 1.74-1.66 (1H, m, H_8), 1.05 (3H, d, *J* = 6.3 Hz, Me_{10}), 0.96 (18H, t, *J* = 7.8 Hz, $Si(CH_2C\underline{H}_3)_3$), 0.91 (9H, s, $SiC(C\underline{H}_3)_3$, 0.85 (3H, d, *J* = 6.7 Hz, Me_8), 0.63 (6H, q, *J* = 7.7 Hz, $Si(C\underline{H}_2CH_3)_3$), 0.60 (6H, q, *J* = 7.7 Hz, $Si(C\underline{H}_2CH_3)_3$), 0.07 (6H, s, $Si(C\underline{H}_3)_2$).

These data are in agreement with those previously reported.[138]

Diethyl ((6*R*,7*R*,8*R*,9*R*,11*E*,13*E*)-15-((*tert*-butyldimethylsilyl)oxy)-6,8-dimethyl-3-oxo-7,9-bis((triethylsilyl)oxy)pentadeca-11,13-dien-2-yl)phosphonate, 36

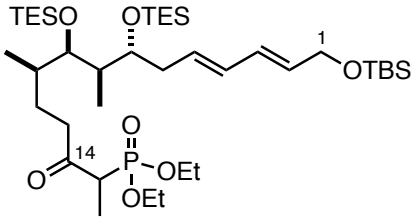

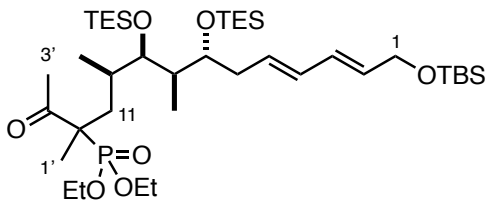

minor regioisomer

To sodium hydride (60% in mineral oil, 1.18 g, 29.5 mmol) was added THF (30 mL) and the suspension was cooled to 0 °C before a solution of phosphonate **72** (4.83 mL, 25.3 mmol) in THF (30 mL) was added *via* cannula. After stirring for 1 h, *n*-BuLi (15.8 mL, 1.6 M in hexanes, 25.3 mmol) was added dropwise and the mixture was stirred for a further 30 min. During this period of time the white slurry went into solution resulting in a yellow solution of dianion.

A solution of iodide **56** (2.94 g, 4.21 mmol) in THF (30 mL) was added dropwise to the above dianion solution at 0 °C over 15 min. The reaction was stirred for 2 h, before being quenched with NH_4Cl (100 mL) and warmed to rt. The aqueous phase was extracted with Et_2O (3 × 70 mL) and the combined organics were dried ($MgSO_4$) and concentrated *in vacuo*. Purification by flash column chromatography (1:9 → 1:1.5 EtOAc/PE) gave phosphonate **36** and the undesired regioisomer **77** (2.25 g, 68%) as a 3:1 inseparable mixture.

R_f 0.59 (1:1 EtOAc/PE); **^{1}H NMR** (500MHz, $CDCl_3$) δ_H 6.18 (1H, dd, J = 14.9, 10.7 Hz, H_3), 6.04 (1H, dd, J = 15.4, 11.8 Hz, H_4), 5.74-5.60 (2H, m, H_2, H_5), 4.20 (2H, d, J = 5.1 Hz, H_1 × 2), 4.17-4.06 (4H, m, $P(OC\underline{H}_2CH_3)_2$), 3.67-3.55 (1H, m, H_7), 3.55-3.50 (1H, m, H_9), 3.25 (0.4H, dq, J = 21.3, 7.2 Hz, H_{14}), 3.19 (0.4H, dq, J = 21.3, 7.2 Hz, H_{14}†), 2.87 (0.4H, ddd, J = 17.7, 10.1, 5.4 Hz, H_{12a}†), 2.78-2.58 (0.8H, m, H_{12a}, H_{12b}), 2.46 (0.4H, ddd, J = 18.4, 9.7, 6.1 Hz, H_{12b}†), [2.35] (0.7H, s, $Me_{3'}$*), 2.25-2.12 (2H, m, H_6 × 2), [1.88-1.80] (0.2H, m, H_{11a}*), 1.79-1.60 (2H, m, H_8, H_{11a}, H_{11b}*), 1.57-1.47 (1H, m, H_{10}), 1.42-1.28 (10H, m, H_{11b}, Me_{14}, $P(OCH_2C\underline{H}_3)_2$), 1.00-0.85 (33H, m, Me_{10}, Me_8, $Me_{1'}$*, $Si(CH_2C\underline{H}_3)_3$ × 2, $SiC(C\underline{H}_3)_3$), [0.72] (0.8H, d, J = 6.9 Hz, Me_8*), 0.65-0.54 (12H, m, $Si(C\underline{H}_2CH_3)_3$ × 2), 0.07 (6H, s, $Si(C\underline{H}_3)_2$).

Distinguishable resonances of the minor regioisomer **77** are given in brackets and marked with an asterisk (*). The diastereomeric ratio of **36** at C_{14} is approximately 1:1 and distinguishable resonances of the diastereoisomers are marked with a dagger (†).

These data are in agreement with those previously reported.[138]

6.4.2 C_{28}–C_{34} Side chain fragment 51

(2*R*,4*S*,5*R*)-5-Hydroxy-1-((4-methoxybenzyl)oxy)-2,4-dimethylhexan-3-one, 80

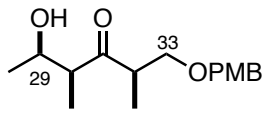

To a solution of $TiCl_4$ (175 μL, 1.78 mmol) in CH_2Cl_2 (8.4 mL) at 0 °C was added Ti(O-*i*Pr)$_4$ (175 μL, 0.59 mmol). The mixture was stirred at 0 °C for 10 min, then at rt for 20 min. The resulting colourless solution was added dropwise to a solution of ketone **42** (500 mg, 2.12 mmol, dried under vacuum for 2 h and stirred over CaH_2 immediately prior to use) in CH_2Cl_2 (13 mL) at −78 °C. To the yellow solution was added *i*-PrNEt$_2$ (0.41 mL) dropwise and the reaction mixture was allowed to enolise at −78 °C for 30 min. Acetaldehyde (1.12 mL, 21.2 mmol, distilled from $CaCl_2$ immediately prior to use) was dissolved in CH_2Cl_2 (10 mL) and added to the reaction mixture dropwise, causing the deep red solution to gradually turn pale orange. The mixture was stirred at −78 °C for 30 min before MeOH (8 mL) was added. After warming to rt Na^+/K^+ tartrate was added (20 mL) and the biphasic mixture was vigorously stirred overnight. The layers were separated, and the organic phase washed with brine (20 mL) and the combined aqueous layers were extracted with CH_2Cl_2 (3 × 20 mL). The combined organics were dried (Na_2SO_4) and concentrated *in vacuo* and purified by flash column chromatography (1:3 EtOAc/PE) to give aldol adduct **80** as a colourless oil (456 mg, 77%, 17:1 *dr*).

R_f 0.24 (3:1EtOAc/PE); **^{1}H NMR** (400 MHz, $CDCl_3$) δ_H 7.18 (2H, d, *J* = 8.6 Hz, ArH), 6.87 (2H, d, *J* = 8.9 Hz, ArH), 4.39 (2H, ABq, *J* = 8.6 Hz, OCH_2Ar), 4.19 (1H, qdd, *J* = 6.6, 4.1, 3.2 Hz, H_{29}), 3.80 (3H, s, OMe), 3.61 (1H, t, *J* = 9.1 Hz, H_{33a}), 3.42 (1H, dd, *J* = 8.7, 4.6 Hz, H_{33b}), 3.15 (1H, dqd, *J* = 9.4, 7.0, 4.7 Hz, H_{32}), 2.94 (1H, d, *J* = 4.2 Hz, OH), 2.73 (1H, qd, *J* = 7.1, 3.0 Hz, H_{30}), 1.12 (3H, d, *J* = 6.7 Hz, Me_{28}), 1.08 (3H, d, *J* = 7.1 Hz, Me_{30}), 1.00 (3H, d, *J* = 6.7 Hz, Me_{32}).

These data are in agreement with those previously reported.[165]

2*R*,3*R*,4*R*,5*R*)-4-hydroxy-6-((4-methoxybenzyl)oxy)-3,5-dimethylhexan-2-yl propionate, 82

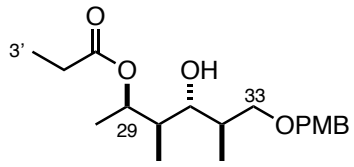

To a solution of propionaldehyde (freshly distilled from $CaCl_2$, 1.54 mL, 21.4 mmol) in THF (20 mL) at 0 °C was added freshly prepared SmI_2 (2.56 mL, 0.1 M in THF, 0.256 mmol). The solution was stirred for 5 min until the deep blue colouration had subsided. A solution of aldol adduct **80** (1.00 g, 3.57 mmol) in THF (10 mL) was then added *via* cannula. The reaction was stirred at 0 °C for 1 h, before being quenched with $NaHCO_3$ (10 mL) and extracted with Et_2O (3 × 10 mL). The combined organic layers were dried ($MgSO_4$), concentrated *in vacuo* and purified by flash column chromatography (1:4 EtOAc/PE) to give propionate ester **82** as a colourless oil (1.17 g, 97%, >95:5 *dr*).

R$_f$ 0.31 (1:4 EtOAc/PE); **^{1}H NMR** (400MHz, $CDCl_3$) δ_H 7.23 (2H, d, J = 8.4 Hz, ArH), 6.87 (2H, d, J = 8.7 Hz, ArH), 5.40 (1H, qd, J = 6.6, 2.1 Hz, H_{29}), 4.41 (2H, ABq, J = 11.6 Hz, OCH_2Ar), 3.80 (3H, s, OMe), 3.54-3.48 (2H, m, H_{33} × 2), 3.21-3.15 (2H, m, H_{31}, OH), 2.30 (2H, q, J = 7.7 Hz, $H_{2'}$ × 2), 2.03-1.94 (1H, m, H_{32}), 1.70-1.59 (1H, m, H_{30}), 1.22 (3H, d, J = 6.7 Hz, Me_{28}), 1.12 (3H, t, J = 7.5 Hz, $H_{3'}$ × 3), 1.08 (3H, d, J = 7.0 Hz, Me_{32}), 0.89 (3H, t, J = 6.9 Hz, Me_{30}).

These data are in agreement with those previously reported.[165]

(2*R*,3*S*,4*R*,5*R*)-4-methoxy-6-((4-methoxybenzyl)oxy)-3,5-dimethylhexan-2-yl propionate, 161

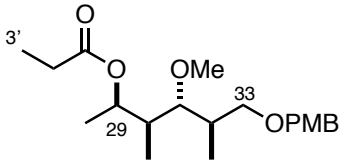

To a solution of Meerwein salt (Me_3OBF_4, 874 mg, 5.92 mmol) and proton sponge (1.90 g, 8.88 mmol) in CH_2Cl_2 (50 mL) was added alcohol **82** (1.00 g, 2.96 mmol). The reaction was stirred for 4 h before being quenched with NH_4Cl (100 mL). The layers were separated, and the aqueous phase extracted with CH_2Cl_2 (3 × 50 mL). The combined organic layers were dried ($MgSO_4$), concentrated *in vacuo* and purified by flash column chromatography (1:4 EtOAc/PE) to give methyl ether **161** as a colourless oil (0.939 g, 90%).

R_f 0.29 (1:3 EtOAc/PE); **^{1}H NMR** (400MHz, $CDCl_3$) δ_H 7.24 (2H, d, *J* = 8.6 Hz, ArH), 6.87 (2H, d, *J* = 8.6 Hz, ArH), 5.27-5.20 (1H, m, H_{29}), 4.41 (2H, ABq, *J* = 11.7 Hz, OCH_2Ar), 3.80 (3H, s, OMe), 3.54 (1H, dd, *J* = 9.1, 4.9 Hz, H_{33a}), 3.36 (3H, s, OMeAr), 3.31 (1H, dd, *J* = 8.7, 2.3 Hz, H_{33b}), 2.89 (1H, dd, J = 8.8, 3.2 Hz, H_{31}), 2.30 (2H, q, *J* = 7.8 Hz, $H_{2'}$ × 2), 2.12-2.03 (1H, m, H_{32}), 1.74-1.66 (1H, m, H_{30}), 1.21 (3H, d, *J* = 6.0 Hz, Me_{28}), 1.21 (3H, t, *J* = 7.6 Hz, $H_{3'}$ × 3), 1.10 (3H, d, *J* = 6.7 Hz, Me_{32}), 0.94 (3H, t, *J* = 7.4 Hz, Me_{30}).

These data are in agreement with those previously reported.[165]

(2*R*,3*S*,4*R*,5*R*)-6-hydroxy-4-methoxy-3,5-dimethylhexan-2-yl propionate, 162

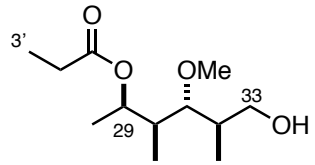

To a solution of PMB ether **161** (380 mg, 1.08 mmol) in CH_2Cl_2 (12 mL) was added pH 7.0 buffer (6 mL) and DDQ (490 mg, 2.16 mmol) at 0 °C. The reaction was warmed to rt and stirred for 1 h before being quenched with $NaHCO_3$ (15 mL). The layers were separated, and the aqueous phase was extracted with EtOAc (3 × 15 mL). The combined organics were dried (Na_2SO_4) and concentrated *in vacuo*. The crude material was purified by flash column chromatography (1:3 EtOAc/PE) to yield alcohol **162** as a colourless oil (245 mg, 93%).

R_f 0.21 (1:3 EtOAc/PE); **^{1}H NMR** (500MHz, $CDCl_3$) δ_H 5.24 (1H, dq, *J* = 6.5, 2.5 Hz, H_{29}), 3.84-3.78 (1H, m, H_{33a}), 3.58-3.52 (1H, m, H_{33b}), 3.47 (3H, s, OMe), 2.98 (1H, dd, *J* = 8.8, 3.2 Hz, H_{31}), 2.78 (1H, br s, OH), 2.32 (2H, q, *J* = 7.8 Hz, $H_{2'}$ × 2), 1.92-1.85 (1H, m, H_{32}), 1.82-1.75 (1H, m, H_{30}), 1.24 (3H, d, *J* = 6.5 Hz, Me_{28}), 1.15 (3H, d, *J* = 7.2 Hz, Me_{32}), 1.14 (3H, t, *J* = 7.5 Hz, $H_{3'}$ × 3), 0.92 (3H, d, *J* = 7.0 Hz, Me_{30}).

These data are in agreement with those previously reported.[165]

(2*R*,3*R*,4*S*,5*R*)-3-methoxy-2,4-dimethylhexane-1,5-diol, 83

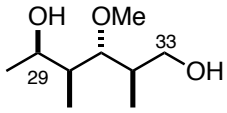

To a solution of ester **162** (233 mg, 1.00 mmol) in CH_2Cl_2 (10 mL) was added DIBAL (4 mL, 4.00 mmol, 1.0 M in CH_2Cl_2) at – 78 °C. Upon completion, the reaction was quenched with Na^+/K^+ tartrate (20 mL) and allowed to warm to rt. The layers were separated and the aqueous was extracted with CH_2Cl_2 (4 × 30 mL) and the combined organics were dried (Na_2SO_4) and concentrated *in vacuo*. The crude was purified by flash column chromatography (1:1 EtOAc/PE) to afford diol **83** as a colourless oil (153 mg, 87%).

R_f 0.20 (1:1 EtOAc/PE); **^{1}H NMR** (500MHz, $CDCl_3$) δ_H 4.19 (1H, q, *J* = 6.7 Hz, H_{29}), 3.76-3.64 (2H, m, H_{33} × 2), 3.56 (3H, s, OMe), 3.18 (1H, dd, *J* = 7.7, 4.5 Hz, H_{31}), 2.95 (1H, br s, OH), 2.27 (1H, br s, OH), 2.02-1.95 (1H, m, H_{32}), 1.71-1.64 (1H, m, H_{30}), 1.56 (3H, d, *J* = 6.4 Hz, Me_{28}), 1.03 (3H, d, *J* = 7.2 Hz, Me_{32}), 0.96 (3H, d, *J* = 6.7 Hz, Me_{30}); **^{13}C NMR** (125MHz, $CDCl_3$) δ_C 90.6, 66.6, 65.3, 61.8, 39.7, 37.6, 20.7, 14.9, 11.0; $[\alpha]_D^{20}$ +8.5 (*c* 1.00, $CHCl_3$); **IR** (thin film) ν_{max} (cm^{-1}) 3217, 2972, 2930, 1456, 1370, 1076, 1032, 1010, 998, 937, 900; **HRMS** calc. for $C_9H_{20}O_3Na$ $[M+Na]^+$ 199.1305, found 199.1299.

(2*S*,3*R*,4*R*)-3-Methoxy-2,4-dimethyl-5-oxohexanal, 78

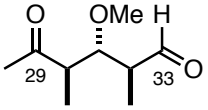

To a solution of DMSO (0.52 mL, 7.38 mmol) in CH_2Cl_2 (10 mL) at –78 °C was added oxalyl chloride (0.31 mL, 3.69 mmol). After stirring for 30 min, a solution of diol **83** (216 mg, 1.23 mmol) in CH_2Cl_2 (10 mL) was added. The mixture was stirred for 30 min and then triethylamine (2.06 mL, 14.7 mmol) was added. The reaction mixture was stirred at – 78 °C for 30 min, then warmed to rt for 1 h before being quenched with NH_4Cl solution (15 mL). The layers were separated, and the aqueous phase was extracted with Et_2O (3 × 15 mL). The combined organics were dried over $MgSO_4$ and concentrated *in vacuo* to afford aldehyde **78** (180 mg, 85%) which was used immediately crude in the subsequent Wittig reaction.

R_f 0.56 (1:1 EtOAc/PE); **^{1}H NMR** (500MHz, $CDCl_3$) δ_H 9.75 (1H, d, *J* = 1.7 Hz, CHO),

3.74 (1H, dd, J = 8.4, 3.9 Hz, H_{31}), 3.36 (3H, s, OMe), 2.94-2.83 (1H, m, H_{30}), 2.70-2.60 (1H, m, H_{32}), 2.21 (3H, s, Me_{28}), 1.17 (3H, d, J = 7.2 Hz, Me_{32}), 0.97 (3H, d, J = 6.8 Hz, Me_{30}).

_N_-((3_R_,4_R_,5_R_,_Z_)-4-methoxy-3,5-dimethyl-6-oxohept-1-en-1-yl)-_N_-methyl formamide, 86

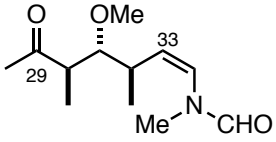

To a suspension of phosphonium salt **84 (**4.48 g, 11.3 mmol) in THF (25 mL) at –78 °C was added freshly prepared LiHMDS (12.5 mL, 1.0 M in THF, 12.5 mmol). The ylide solution was stirred at –78 °C for 30 min, warmed to –40 °C and stirred for 30 min, warmed to –20 °C and stirred for 30 min and finally warmed to 0 °C for 20 min after which the yellow suspension was cooled back down to –78 °C. A solution of aldehyde **78** (976 mg, 5.67 mmol, pre-dried over CaH_2 for 1 h) in THF (25 mL) was added slowly. The reaction mixture was stirred at –78 °C for 2 h before being quenched with pH 7.0 buffer (50 mL) and diluted with Et_2O (10 mL). The layers were separated and the aqueous layer extracted with EtOAc (3 × 50 mL). The combined organics were dried over $MgSO_4$ and concentrated *in vacuo*. The crude material was purified by flash column chromatography (1:1 EtOAc/PE) to afford enamide **86** as a pale yellow oil (800 mg, 62% over 2 steps, 3:1 *Z*/*E*).

R_f 0.27 (1:1 EtOAc/PE); **^{1}H NMR** (500MHz, $CDCl_3$) $\boldsymbol{\delta}_H$ 8.10 (0.85H, s, NCHO), [8.01] (0.1H, s, NCHO*), [6.19] (0.12H, d, J = 9.1 Hz, H_{34}*), 5.92 (0.81H, d, J = 8.7 Hz, H_{34}), 5.27 (0.84H, dd, J = 10.8, 8.7 Hz, H_{33}), [5.24-5.19] (0.13H, m, H_{33}*), 3.32 (3H, s, OMe), 3.20 (1H, dd, J = 9.4, 3.1 Hz, H_{31}), [2.98] (0.15H, s, NMe*), 2.95 (2.45H, s, NMe), [2.74-2.68] (0.16H, m, H_{32}*), 2.67-2.57 (2H, m, H_{32}, H_{30}), 2.14 (3H, s, Me_{28}), 1.09 (3H, d, J = 7.0 Hz, Me_{30}), [0.88] (0.67H, d, J = 7.0 Hz, Me_{32}*), 0.84 (2.40H, d, J = 7.0 Hz, Me_{32}); **^{13}C NMR** (125MHz, $CDCl_3$) $\boldsymbol{\delta}_C$ [212.4], 211.8, 162.5, [162.4], 127.7, 125.1, [124.5], [124.1], [87.2], 86.9, [61.2], 61.3, [49.7], 49.8, 36.2, [34.9], 33.8, 31.5, [31.1], 30.9, 19.0, [18.3], [13.4], 13.2; $[\boldsymbol{\alpha}]_D^{\mathbf{20}}$ +11.0 (*c* 1.00, $CHCl_3$); **IR** (thin film) ν_{max} (cm^{-1}) 2972, 2929, 1682, 1653, 1457, 1355, 1088, 1054; **HRMS** calc. for $C_{12}H_{21}NO_3Na$ $[M+Na]^+$ 250.1414, found 250.1412.

Distinguishable resonances of the minor rotamer (3:1 ratio) are given in brackets and assignments denoted with an asterisk.

_N_-((3_R_,4_R_,5_R_,_E_)-4-methoxy-3,5-dimethyl-6-oxohept-1-en-1-yl)-_N_-methyl formamide, 51

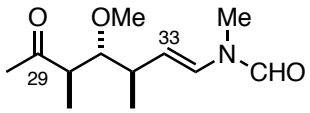

(*Z*)-Enamide **86** (810 mg, 3.56 mmol) was dissolved in CH_2Cl_2 (100 mL) and a solution of iodine (45 mg, 0.18 mmol) in CH_2Cl_2 (20 mL) was added. The reaction mixture was stirred in the dark at room temperature for 16 h before being quenched with sodium thiosulfate (100 mL, sat. aq.). The biphasic mixture was stirred rapidly for 2 h and the organic layer separated. The aqueous phase was extracted with CH_2Cl_2 (3 × 50 mL) and the combined organics dried ($MgSO_4$) and concentrated *in vacuo*. The crude was purified by flash column chromatography (1:1 EtOAc/PE) to afford (*E*)-enamide **51** as a pale-yellow oil (700 mg, 86%, >20:1 *E*/*Z*).

R_f 0.27 (1:1 EtOAc/PE); **^{1}H NMR** (500MHz, $CDCl_3$) δ_H 8.25 (0.59H, s, NCHO), [8.04] (0.33H, s, NCHO*), [7.09] (0.32H, d, J = 14.5 Hz, H_{34}*), 6.44 (0.59H, d, J = 14.5 Hz, H_{34}), 5.09 (1H, dd, J = 14.5, 8.5 Hz, H_{33}), 3.34 (3H, s, OMe), 3.26 (1H, dd, J = 10.5, 2.7 Hz, H_{31}), [3.04] (1H, s, NMe*), 3.00 (2H, s, NMe), 2.72-2.61 (1H, m, H_{32}), 2.44-2.31 (1H, m, H_{30}), 2.16 (3H, s, Me_{28}), 1.12 (3H, d, J = 6.7 Hz, Me_{32}), 0.92 (3H, d, J = 7.1 Hz, Me_{30}); **^{13}C NMR** (125MHz, $CDCl_3$) δ_C [212.4], 212.3, 162.1, 160.8, 128.7, 124.7, [113.1], 111.3, [87.4], 87.3, 61.2, 61.2, [49.7], 49.6, 37.6, 37.5, 33.0, [31.0], 30.9, 29.6, 27.5, 19.3, [13.4], 13.3; $[\alpha]_D^{20}$ –74.4 (*c* 0.84, $CHCl_3$); **IR** (thin film) ν_{max} (cm^{-1}) 2964, 2928, 1691, 1651, 1457, 1353, 1318, 1275, 1193, 1170, 1092, 1068, 956, 725; **HRMS** calc. for $C_{12}H_{21}NO_3Na$ $[M+Na]^+$ 250.1414, found 250.1412.

Distinguishable resonances of the minor rotamer (2:1 ratio) are given in brackets and assignments denoted with an asterisk.

(2*R*,3*S*,4*R*,5*R*)-6-((4-Methoxybenzyl)oxy)-3,5-dimethyl-4-((triethylsilyl)oxy)hexan-2-yl propionate, 92

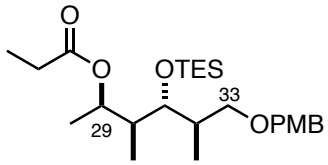

To a solution of alcohol **82** (1.17 g, 3.46 mmol) in CH_2Cl_2 (35 mL) at –78 °C was added TESOTf (1.20 mL, 5.2 mmol) and 2,6-lutidine (1.21 mL, 10.4 mmol). The reaction was stirred at this temperature for 2 h before being quenched with NH_4Cl (35 mL). The reaction mixture was warmed to rt and the layers were separated. The aqueous phase was extracted with CH_2Cl_2 (3 × 40 mL) and the combined organics were dried (Na_2SO_4) and concentrated *in vacuo*. Purification *via* flash column chromatography (1:19 EtOAc/PE) yielded TES ether **92** (1.55g, 99%) as a colourless oil.

R_f 0.60 (1:4 EtOAc/PE); **^{1}H NMR** (400MHz, $CDCl_3$) δ_H 7.25 (2H, d, J = 8.6 Hz, ArH), 6.87 (2H, d, J = 8.6 Hz, ArH), 5.05 (1H, qd, J = 6.5, 3.3 Hz, H_{29}), 4.41 (2H, s, OCH_2Ar), 3.80 (3H,s, OMe), 3.59-3.50 (2H, m, H_{31}, H_{33a}), 3.25 (1H, dd, J = 9.2, 8.1 Hz, H_{33b}), 2.28 (2H, q, J = 7.5 Hz, $H_{2'}$ × 2), 2.08-1.99 (1H, m, H_{30}), 1.72-1.62 (1H, m, H_{32}), 1.21 (3H, d, J = 7.8 Hz, Me_{28}), 1.12 (3H, t, J = 7.6 Hz, $H_{3'}$ × 3), 1.00 (3H, d, J = 7.0 Hz, Me_{32}), 1.00-0.93 (12H, m, Me_{30}, $Si(CH_2C\underline{H}_3)_3$), 0.59 (6H, q, J = 8.0 Hz, $Si(C\underline{H}_2CH_3)_3$).

These data are in agreement with those previously reported.[137]

(2*R*,3*S*,4*R*,5*R*)-6-hydroxy-3,5-dimethyl-4-((triethylsilyl)oxy)hexan-2-yl propionate, 163

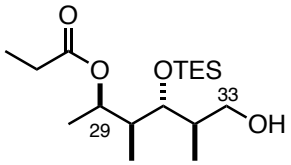

To a solution of PMB ether **92** (4.00 g, 8.84 mmol) in CH_2Cl_2 (90 mL) was added pH 9.2 buffer (22 mL) and DDQ (4.01 g, 17.7 mmol) at 0 °C. The reaction was warmed to rt and stirred for 2 h before being quenched with $NaHCO_3$ (100 mL). The layers were separated, and the aqueous phase was extracted with CH_2Cl_2 (8 × 50 mL), dried (Na_2SO_4) and concentrated *in vacuo*. The crude material was purified by flash column chromatography (1:19 EtOAc/PE) to yield alcohol **163** as a colourless oil (2.50 g, 85%).

R_f 0.18 (1:19 EtOAc/PE); **^{1}H NMR** (400MHz, $CDCl_3$) δ_H 5.00 (1H, dq, *J* = 6.4, 24.1 Hz, H_{29}), 3.78 (1H, ddd, *J* = 11.4, 4.1, 4.1 Hz, H_{33a}), 3.66 (1H, dd, *J* = 6.9, 4.3 Hz, H_{31}), 3.57 (1H, ddd, *J* = 11.8, 5.2, 4.9 Hz, H_{33b}), 2.64 (1H, dd, *J* = 6.9, 4.3 Hz, OH), 2.30 (2H, q, *J* = 7.6 Hz, $H_{2'}$ × 2), 1.91-1.82 (1H, m, H_{30}), 1.81-1.75 (1H, m, H_{32}), 1.25 (3H, d, *J* = 6.4 Hz, Me_{28}), 1.14 (3H, t, *J* = 6.8 Hz, $H_{3'}$ × 3), 1.06 (3H, d, *J* = 7.0 Hz, Me_{32}), 1.00-0.93 (12H, m, Me_{30}, $Si(CH_2C\underline{H}_3)_3$), 0.59 (6H, q, *J* = 8.0 Hz, $Si(C\underline{H}_2CH_3)_3$).

These data are in agreement with those previously reported.[137]

(2*R*,3*R*,4*S*,5*R*)-2,4-dimethyl-3-((triethylsilyl)oxy)hexane-1,5-diol, 93

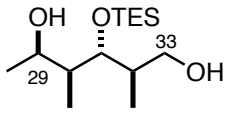

To a solution of ester **163** (5.00 g, 15.0 mmol) in CH_2Cl_2 (150 mL) was added DIBAL (60.2 mL, 60.2 mmol, 1.0 M in hexanes) at –78 °C. Upon completion, the reaction was quenched with Na^+/K^+ tartrate (240 mL) and allowed to warm to rt. The layers were separated and the aqueous was extracted with CH_2Cl_2 (3 × 60 mL) and the combined organics were dried (Na_2SO_4) and concentrated *in vacuo*. The crude was purified by flash column chromatography (1:3 EtOAc/PE) to afford diol **93** as a colourless oil (3.60 g, 87%).

R_f 0.22 (1:3 EtOAc/PE); **^{1}H NMR** (500MHz, $CDCl_3$) δ_H 4.23 (1H, qdd, *J* = 6.4, 1.7, 1.7 Hz, H_{29}), 3.72 (1H, dd, *J* = 7.0, 3.5 Hz, H_{31}), 3.66-3.62 (2H, m, H_{33} × 2), 2.97 (1H, br s, OH), 2.04-1.88 (2H, m, H_{32}, OH), 1.64-1.56 (1H, m, H_{30}), 1.13 (3H, d, *J* = 6.8 Hz, Me_{28}), 1.00 (3H, d, *J* = 6.8 Hz, Me_{30}), 0.98 (9H, t, *J* = 8.1 Hz, $Si(CH_2C\underline{H}_3)_3$), 0.96 (3H, d, *J* = 7.0 Hz, Me_{32}), 0.69 (6H, q, *J* = 8.1 Hz, $Si(C\underline{H}_2CH_3)_3$).

These data are in agreement with those previously reported.[137]

(2*S*,3*R*,4*R*)-2,4-dimethyl-5-oxo-3-((triethylsilyl)oxy)hexanal, 164

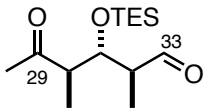

To a solution of oxalyl chloride (920 μL, 10.9 mmol) in CH_2Cl_2 (50 mL) at –78 °C was added DMSO (1.54 mL, 21.7 mmol). After stirring for 30 min, a solution of diol **93** (1.00 g, 3.62 mmol) in CH_2Cl_2 (20 mL) was added. The mixture was stirred for 30 min and then triethylamine (4.40 mL, 43.4 mmol) was added. The reaction mixture was stirred at –78 °C for 30 min, then warmed to rt for 1 h before being quenched with NH_4Cl solution (50 mL). The layers were separated, and the aqueous phase was extracted with Et_2O (3 × 50 mL). The combined organics were washed sequentially with 0.5 M HCl (25 mL) and brine (25 mL) then dried over $MgSO_4$ and concentrated *in vacuo* to afford aldehyde **164** (887 mg, 90% which was used immediately in the subsequent Wittig reaction.

R_f 0.63 (1:1 EtOAc/PE); **^{1}H NMR** (500MHz, $CDCl_3$) δ_H 9.75 (1H, d, *J* = 1.9 Hz, CHO), 4.29 (1H, dd, *J* = 8.0, 3.4 Hz, H_{31}), 2.88-2.81 (1H, m, H_{30}), 2.53-2.47 (1H, m, H_{32}), 2.18 (3H, s, Me_{28}), 1.14 (3H, d, *J* = 6.9 Hz, Me_{32}), 0.97 (3H, d, *J* = 6.9 Hz, Me_{30}), 0.93 (9H, t, *J* = 8.0 Hz, $Si(CH_2C\underline{H}_3)_3$), 0.59 (6H, q, *J* = 8.0 Hz, $Si(C\underline{H}_2CH_3)_3$).

These data are in agreement with those previously reported.[137]

***N*-((3*R*,4*R*,5*R*,*Z*)-3,5-dimethyl-6-oxo-4-((triethylsilyl)oxy)hept-1-en-1-yl)-*N*-methyl formamide, 94**

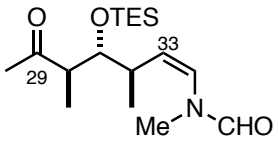

To a suspension of phosphonium salt **84** (5.21 g, 14.1 mmol) in THF (45 mL) at –78 °C was added freshly prepared LiHMDS (13.2 mL, 1.0 M in THF, 13.2 mmol). The ylide solution was warmed to 0 °C and stirred for 30 min, after which the yellow suspension was cooled back down to –78 °C. A solution of aldehyde **164** (2.56 g, 9.4 mmol, pre-dried over CaH_2 for 1 h) in THF (18 mL) was added slowly over 15 min. The reaction mixture was stirred at –78 °C for 1 h before being quenched with NH_4Cl (60 mL). The layers were

separated, and the aqueous layer extracted with EtOAc (3 × 50 mL), dried over $MgSO_4$ and concentrated *in vacuo*. The crude material was purified by flash column chromatography (1:1 EtOAc/PE) to afford enamide **94** as a colourless oil (2.00 g, 71% over 2 steps, 8:1 *Z*/*E*).

R_f 0.40 (1:1 EtOAc/PE); **^{1}H NMR** (500MHz, $CDCl_3$) δ_H 8.17 (0.9H, s, NCHO), [8.06] (0.1H, s, NCHO*), [6.26] (0.1H, d, *J* = 8.5 Hz, H_{34}*), 5.96 (0.9H, d, *J* = 8.6 Hz, H_{34}), 5.35 (0.9H, dd, *J* = 10.9, 8.5 Hz, H_{33}), [5.12] (0.1H, dd, *J* = 10.7, 8.8 Hz, H_{33}*), 3.82 (1H, dd, *J* = 7.8, 3.0 Hz, H_{31}), [3.19] (0.3H, s, NMe*), 3.00 (2.66H, s, NMe), 2.69-2.55 (2H, m, H_{30}, H_{32}), 2.15 (3H, s, Me_{28}), 1.05 (3H, d, *J* = 6.7 Hz, Me_{30}), 0.95 (9H, t, *J* = 7.8 Hz, $Si(CH_2C\underline{H}_3)_3$), 0.90 (3H, d, *J* = 7.0 Hz, Me_{32}), 0.60 (6H, q, *J* = 7.8 Hz, $Si(C\underline{H}_2CH_3)_3$).

Distinguishable resonances of the minor rotamer (2:1 ratio) are given in brackets and assignments denoted with an asterisk.
These data are in agreement with those previously reported.[137]

***N*-((3*R*,4*R*,5*R*,*Z*)-4-hydroxy-3,5-dimethyl-6-oxohept-1-en-1-yl)-*N*-methyl formamide, 95**

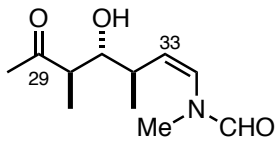

A solution of TBAF (55.6 mL, 1M in THF, 55.6 mmol) and glacial acetic acid (2.04 mL, 35.7 mmol) was stirred at 0 °C for 30 min before being added to TES ether **94** (2.61 g, 7.96 mmol) *via* cannula. The reaction mixture was stirred at rt for 16 h. Upon completion, the reaction was quenched by the addition of $NaHCO_3$ (100 mL) and then extracted with EtOAc (8 × 70 mL). The combined organics were dried ($MgSO_4$) and concentrated *in vacuo*. The crude residue was purified by flash column chromatography (1:1 EtOAc/PE) to afford alcohol **95** (1.68 g, 99%, 8:1 *Z*/*E*) as a pale-yellow oil.

R_f 0.12 (1:1 EtOAc/PE); **^{1}H NMR** (500MHz, $CDCl_3$) δ_H 8.17 (0.9H, s, NCHO), [8.04] (0.1H, s, NCHO*), [6.25] (0.1H, d, *J* = 8.6 Hz, H_{34}*), 6.00 (1H, d, *J* = 8.6 Hz, H_{34}), 5.32 (1H, dd, *J* = 10.9, 8.5 Hz, H_{33}), [5.11] (0.1H, dd, *J* = 10.5, 8.4 Hz, H_{33}*), 3.66-3.58 (1H, m, H_{31}), [3.13] (0.3H, s, NMe*), 3.00 (3H, s, NMe), 2.80-2.74 (1H, m, OH), 2.72-2.63 (1H, m, H_{32}), 2.63-2.55 (1H, m, H_{30}), 2.18 (3H, s, Me_{28}), 1.15 (3H, d, *J* = 6.7 Hz, Me_{30}), 1.05 (3H, d, *J* = 7.0 Hz, Me_{32}).

Distinguishable resonances of the minor rotamer (2:1 ratio) are given in brackets and assignments denoted with an asterisk.

These data are in agreement with those previously reported.[137]

6.5 Experimental procedures for Chapter 3

6.5.1 Alternative coupling strategy

(2*S*,3*S*,4*R*,5*S*)-13-((*tert*-butyldimethylsilyl)oxy)-1-hydroxy-3-methoxy-2,4-dimethyl tridecan-5-yl propionate, 165

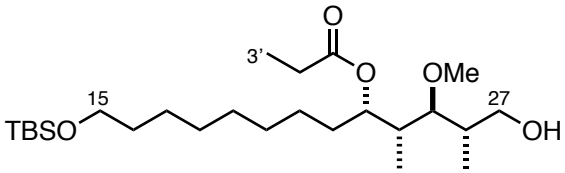

To a solution of PMB-ether **98** (500 mg, 0.86 mmol) in CH_2Cl_2 (16 mL) was added pH 7.0 buffer (8 mL) and the mixture was cooled to 0 °C. DDQ (390 mg, 1.72 mmol) was added, and the reaction was allowed to warm to rt. The biphasic mixture was vigorously stirred for 30 min, then quenched with $NaHCO_3$ (20 mL) and extracted with EtOAc (4 × 20 mL). The combined organic layers were dried ($MgSO_4$), concentrated *in vacuo* and purified by flash column chromatography (1:4 EtOAc/PE) to give alcohol **165** as a colourless oil (375 mg, 95%).

R_f 0.16 (1:4 EtOAc/PE); **^{1}H NMR** (500MHz, $CDCl_3$) δ_H 5.17 (1H, app td, J = 6.5, 2.4 Hz, H_{23}), 3.77 (1H, dd, J = 11.2, 3.0 Hz, H_{27a}), 3.57 (2H, t, J = 7.4 Hz, H_{15} × 2), 3.55-3.50 (1H, m, H_{27b}), 3.43 (3H, s, OMe), 2.93 (1H, dd, J = 8.6, 2.7 Hz, H_{25}), 2.86 (1H, br s, OH), 2.30 (2H, q, J = 7.4 Hz, $H_{2'}$ × 2), 1.90-1.85 (2H, m, H_{24}, H_{26}), 1.66-1.58 (1H, m, H_{22a}), 1.51-1.43 (3H, m, H_{16} × 2, H_{22b}), 1.32-1.22 (10H, m, $H_{17\text{-}21}$), 1.15-1.09 (6H, m, $H_{3'}$ × 3, Me_{26}), 0.90-0.84 (12H, m, SiC(C$\underline{H}_3$)$_3$, Me_{24}), 0.04 (6H, s, Si(C$\underline{H}_3$)$_2$); **^{13}C NMR** (125MHz, $CDCl_3$) δ_C 174.1, 125.3, 88.6, 73.0, 64.7, 63.3, 61.7, 39.3, 36.2, 32.8, 32.8, 29.5, 29.3, 28.0, 26.0, 25.8, 25.7, 18.4, 16.1, 10.6, 9.4, –5.2; $[\alpha]_D^{20}$ –2.7 (c 1.01, $CHCl_3$); **IR** (thin film) ν_{max} (cm^{-1}) 3300, 2933, 2853, 1732, 1465, 1255, 1189, 1090, 832, 775; **HRMS** calc. for $C_{25}H_{53}O_5Si$ $[M+H]^+$ 461.3657, found 461.3649.

(2*R*,3*R*,4*R*,5*S*)-13-((*tert*-butyldimethylsilyl)oxy)-3-methoxy-2,4-dimethyl-1-oxotridecan-5-yl propionate, 50

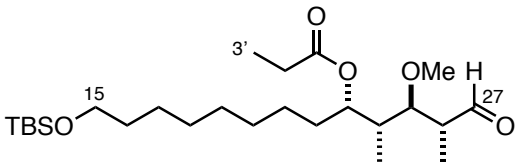

To a solution of oxalyl chloride (0.551 mL, 6.51 mmol) in CH_2Cl_2 (16 mL) at –78 °C was added DMSO (0.925 mL, 13.0 mmol) dropwise. After 30 min, a solution of alcohol **165** (1.00 g, 2.17 mmol) in CH_2Cl_2 (8 mL) was added and the solution stirred for a further 30 min. NEt_3 (2.72 mL, 19.5 mmol) was added and the solution stirred at –78 °C before being warmed to rt over 1 h. The reaction was quenched by addition of NH_4Cl (25 mL) and the layers were separated. The aqueous phase was extracted with Et_2O (3 × 5 mL) and the combined organics were dried ($MgSO_4$) and concentrated *in vacuo* to yield aldehyde **50** (930 mg, 93%) as a colourless oil which was used immediately crude in the subsequent aldol reaction.

R_f 0.80 (1:1 EtOAc/PE); **^{1}H NMR** (400MHz, $CDCl_3$) δ_H 9.75 (1H, d, J = 1.7 Hz, CHO), 5.26 (1H, dt, J = 5.8, 1.6 Hz, H_{23}), 3.59 (2H, t, J = 6.0 Hz, H_{15} × 2), 3.39 (3H, s, OMe), 3.24 (1H, dd, J = 8.8, 3.0 Hz, H_{25}), 2.73-2.65 (1H, m, H_{26}), 2.34 (2H, q, J = 6.7 Hz, $H_{2'}$ × 2), 1.86-1.77 (1H, m, H_{24}), 1.69-1.58 (1H, m, H_{22a}), 1.57-1.35 (3H, m, H_{16} × 2, H_{22b},), 1.30-1.24 (10H, m, H_{17-21}), 1.19-1.13 (6H, m, $H_{3'}$ × 3, Me_{26}), 0.89 (9H, s, $SiC(C\underline{H}_3)_3$), 0.82 (3H, d, J = 7.2 Hz, Me_{24}), 0.04 (6H, s, $Si(C\underline{H}_3)_2$).

9*S*,10*R*,11*S*,12*S*,13*E*,16*R*,17*R*,18*R*,19*E*)-1-((*tert*-butyldimethylsilyl)oxy)-11,17-dimethoxy-10,12,16,18-tetramethyl-20-(*N*-methylformamido)-15-oxoicosa-13,19-dien-9-yl propionate, 102

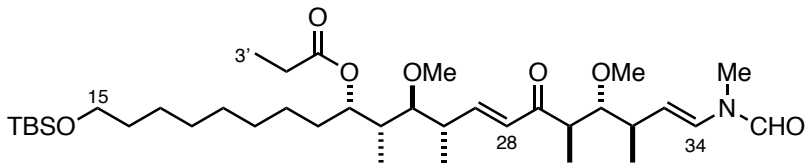

Ketone **51** and aldehyde **50** were each azetropically dried with benzene and placed under vacuum for 3 h. To a solution of ketone **51** (574 mg, 2.52 mmol) in Et_2O (6 mL) at 0 °C was added NEt_3 (0.39 mL, 2.78 mmol) and dicyclohexylboron chloride (0.60 mL, 2.78 mmol). The resulting cloudy yellow solution of enolate was stirred at 0 °C for 1 h before being cooled to –78 °C. A solution of aldehyde **50** (1.00 g, 2.18 mmol) in Et_2O (10 mL) was added and the reaction mixture was stirred at –78 °C for 2 h, then warmed to –10 °C over 1 h before being quenched with SiO_2 (*ca.* 5.00 g). The slurry was stirred for 1 h then filtered and rinsed with Et_2O (20 mL) before being concentrated *in vacuo.* The crude material was purified by flash column chromatography (1:1 EtOAc/PE). All fractions containing aldol adduct **101** and ketone **51** were combined and used subsequently in the elimination reaction.

To a solution of aldol adduct **101** and ketone **51** (*ca.* 1.40 g) in THF (12 mL) was added Burgess reagent (582 mg, 2.44 mmol). The reaction mixture was stirred at room temperature for 16 h then quenched with NH_4Cl (50 mL) and extracted with EtOAc (3 × 50 mL). The combined organic layers were washed with brine (25 mL), dried ($MgSO_4$) and concentrated *in vacuo*. The crude product was purified by flash column chromatography (1:1 EtOAc/PE) yielding enone **102** (1.17 g, 85% over 2 steps, >20:1 *E*/*Z*) and recovered ketone **51** (97 mg).

R_f 0.75 (1:1 EtOAc/PE); **^{1}H NMR** (500MHz, $CDCl_3$) δ_H 8.28 (0.68H, s, NCHO), [8.08] (0.39H, s, NCHO*), [7.14] (0.34H, d, J = 14.6 Hz, H_{34}*), 6.90-6.82 (1H, m, H_{27}), 6.47 (0.66H, d, J = 14.1 Hz, H_{34}), 6.16-6.10 (1H, m, H_{28}), 5.18-5.14 (1H, m, H_{23}), 5.13 (1H, dd, J = 14.1, 9.6 Hz, H_{33}), 3.57 (2H, t, J = 6.6 Hz, H_{15} × 2), 3.39 (3H, s, OMe), 3.27 (3H, s, OMe), 3.26-3.24 (1H, m, H_{31}), [3.09] (1H, s, NMe*), 3.05 (2H, s, NMe), 3.04-2.98 (1H, m, H_{30}), 2.86 (1H, m, H_{25}), 2.65-2.57 (1H, m, H_{26}), 2.49-2.36 (1H, m, H_{32}), 2.31 (2H, q, J = 7.7 Hz, $H_{2'}$ × 2), 1.65-1.56 (2H, m H_{22a}, H_{24}), 1.52-1.44 (2H, m, H_{16} × 2), 1.44-1.36 (1H, m, H_{22b}), 1.25 (10H, br s, $H_{17\text{-}21}$), 1.17-1.11 (9H, m, $H_{3'}$ × 3, Me_{26}, Me_{32}), 0.94 (3H, d, J = 6.7 Hz, Me_{30}), 0.88 (9H, s, SiC(C$\underline{H}_3$)$_3$), 0.80 (3H, d, J = 6.9 Hz, Me_{24}), 0.03 (6H, s,

Si(C<u>H</u>$_3$)$_2$); **^{13}C NMR** (125MHz, $CDCl_3$) δ_C [203.8], 203.6, 174.1, [174.0], 162.1, [160.8], 149.3, [149.1], 142.7, 131.0, [130.8], 128.8, [124.8], [113.3], 111.5, 87.8, [87.7], 86.1, [86.0], 73.1, 63.3, [61.2], 61.1, 45.6, 39.8, 39.4, 39.3, 38.0, [37.8], [33.0], 32.8, 32.5, 29.6, 29.5, 29.4, 28.0, 27.5, 25.8, 25.6, 20.0, 17.5, 13.8, 13.6, 9.7, 9.5, –5.3; $[\alpha]_D^{20}$ –12.0 (*c* 1.00, $CHCl_3$); **IR** (thin film) ν_{max} (cm^{-1}) 2930, 2853, 1732, 1696, 1659,1462, 1369, 1254, 1191, 1096, 1070, 835, 777; **HRMS** calc. for $C_{37}H_{73}N_2O_7Si$ $[M+NH_4]^+$ 685.5182, found 685.5173.

Distinguishable resonances of the minor rotamer (2:1 ratio) are given in brackets and assignments denoted with an asterisk.

(9*S*,10*R*,11*S*,12*S*,16*R*,17*R*,18*R*,*E*)-1-((*tert*-butyldimethylsilyl)oxy)-11,17-dimethoxy-10,12,16,18-tetramethyl-20-(*N*-methylformamido)-15-oxoicos-19-en-9-yl propionate, 105

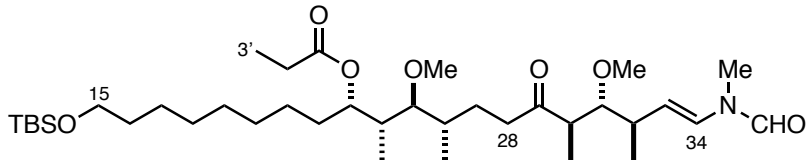

Stryker's reagent solution (3.50 mL, 0.087 mmol, 0.025 M in PhMe) was added to enone **102** (300 mg, 0.43 mmol) and the reaction mixture stirred at room temperature for 20 h. The solution was applied directly to a silica gel column and the product eluted with EtOAc/CH_2Cl_2 (3:17) to afford ketone **105** (268 mg, 93%) as a colourless oil.

R$_f$ 0.53 (3:17 EtOAc/PE); **^{1}H NMR** (500MHz, $CDCl_3$) δ_H 8.29 (0.63H, s, NCHO), [8.08] (0.35H, s, NCHO*), [7.11] (0.35H, d, *J* = 14.5 Hz, H_{34}*), 6.45 (0.61H, d, *J* = 14.2 Hz, H_{34}), 5.19 (1H, dt, *J* = 6.8, 1.8 Hz, H_{23}), 5.10 (1H, dd, *J* = 14.1, 8.9 Hz, H_{33}), 3.59 (2H, t, *J* = 6.5 Hz, H_{15} × 2), 3.39 (3H, s, OMe), 3.35 (3H, s, OMe), 3.30 (1H, dd, *J* = 9.2, 2.3 Hz, H_{31}), [3.08] (1H, s, NMe*), 3.04 (2H, s, NMe), 2.75 (1H, dd, *J* = 8.9, 2.4 Hz, H_{25}), 2.71-2.61 (1H, m, H_{30}), 2.61-2.50 (1H, m, H_{28a}), 2.50-2.35 (2H, m, H_{28b}, H_{32}), 2.32 (2H, q, *J* = 7.8 Hz, $H_{2'}$ × 2), 1.80-1.75 (1H, m, H_{24}), 1.69-1.61 (2H, m, H_{22a}, H_{26}), 1.54-1.44 (3H, m, H_{16} × 2, H_{22b}), 1.44-1.32 (2H, m, H_{27} × 2), 1.26 (10H, br s, $H_{17\text{-}21}$),1.16 (3H, d, *J* = 7.6Hz, Me_{32}), 1.14 (3H, t, *J* = 7.7 Hz, $H_{3'}$ × 3),0.97 (3H, d, *J* = 6.9 Hz, Me_{30}), 0.92 (3H, d, *J* = 6.6 Hz, Me_{26}), 0.89 (9H, s, SiC(C<u>H</u>$_3$)$_3$), 0.88 (3H, obs d, Me_{24}), 0.04 (6H, s, Si(C<u>H</u>$_3$)$_2$); **^{13}C NMR** (125MHz, $CDCl_3$) δ_C [214.2], 214.2, 174.1, 162.2, [160.9], 128.7, [124.7], [113.2], 111.4, [87.5], 87.4, 87.3, 73.4, 63.3, 61.5, 61.4, [49.2], 49.1, [42.0], 41.9, 38.8, 37.6, 37.5, 34.4,

[33.1], 32.9, 32.8, 29.9, 29.6, 29.5, 28.0, 27.6, 25.7, 23.2, 19.4, 17.4, 13.5, 10.2, 9.4, –5.3; $[\boldsymbol{\alpha}]_{\boldsymbol{D}}^{\mathbf{20}}$ –10.4 (*c* 1.00, $CHCl_3$); **IR** (thin film) ν_{max} (cm^{-1}) 2929, 2861, 1732, 1694, 1658, 1461, 1371, 1255, 1193, 1095, 834, 775; **HRMS** calc. for $C_{37}H_{75}N_2O_7Si$ $[M+NH_4]^+$ 687.5338, found 687.5330.

Distinguishable resonances of the minor rotamer (2:1 ratio) are given in brackets and assignments denoted with an asterisk.

(9*S*,10*R*,11*S*,12*S*,15*R*,16*S*,17*R*,18*R*,*E*)-1-((*tert*-butyldimethylsilyl)oxy)-15-hydroxy-11,17-dimethoxy-10,12,16,18-tetramethyl-20-(*N*-methylformamido)icos-19-en-9-yl propionate, 109

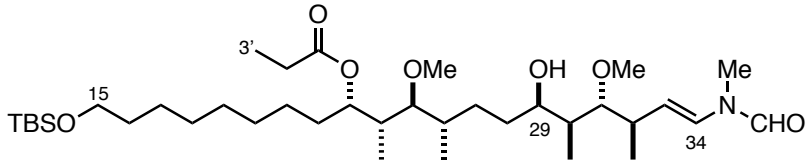

$Zn(BH_4)_2$ solution (10.1 mL, 0.175 M in Et_2O, 1.80 mmol) was added to ketone **105** (200 mg, 0.30 mmol) at 0 °C and the reaction stirred at this temperature for 2 h before being quenched with NH_4Cl (15 mL) and Na^+/K^+ tartrate solution (30 mL). The quenching mixture was stirred vigorously for 1 h and extracted with CH_2Cl_2 (3 × 30 mL). The combined organics were dried over $MgSO_4$ and concentrated *in vacuo*. The crude product was purified by flash chromatography (1:4 EtOAc/CH_2Cl_2) to yield alcohol **109** as a colourless oil (136 mg, 68%, 2:1 *dr*).

R_f 0.32 (1:4 EtOAc/CH_2Cl_2); **^{1}H NMR** (500MHz, $CDCl_3$) $\boldsymbol{\delta}_H$ 8.29 (0.60H, s, NCHO), [8.07] (0.28H, s, NCHO*), [7.15] (0.28H, d, *J* = 14.5 Hz, H_{34}*), 6.50 (0.56H, d, *J* = 14.5 Hz, H_{34}), 5.20 (1H, t, *J* = 7.3 Hz, H_{23}), [5.15] (0.32H, dd, *J* = 14.5, 8.6 Hz, H_{33}*), 5.07 (0.65H, dd, *J* = 14.2, 8.6 Hz, H_{33}), 3.90-3.84 (1H, m, H_{29}), 3.59 (2H, t, *J* = 6.6 Hz, H_{15} × 2), 3.48 (3H, s, OMe), 3.40 (3H, s, OMe), [3.06] (1H, s, NMe*), 3.03 (1H, obs dd, H_{31}), 3.02 (2H, s, NMe), 2.86 (1H, br s, OH), 2.76 (1H, dd, *J* = 9.1, 2.2 Hz, H_{25}), 2.58- 2.46 (1H, m, H_{32}), 2.32 (2H, q, *J* = 7.6 Hz, $H_{2'}$ × 2), 1.76-1.71 (1H, m, H_{24}), 1.70-1.65 (2H, m, H_{26}, H_{30}), 1.65-1.59 (2H, m, H_{22} × 2), 1.54-1.44 (6H, m, H_{16} × 2, H_{27} × 2, H_{28} × 2), 1.23-1.26 (10H, m, $H_{17\text{-}21}$), 1.15 (3H, t, *J* = 7.8 Hz, $H_{3'}$ × 3), [1.10] (1H, d, *J* = 7.0 Hz, Me_{32}*), 1.07 (3H, d, *J* = 7.0 Hz, Me_{32}), 1.01 (3H, d, *J* = 6.1 Hz, Me_{26}), 0.95 (3H, d, *J* = 7.0 Hz, Me_{30}), 0.90 (9H, s, $SiC(C\underline{H}_3)_3$), 0.85 (3H, d, *J* = 7.0 Hz, Me_{24}), 0.04 (6H, s, $Si(C\underline{H}_3)_2$); **^{13}C NMR** (125MHz, $CDCl_3$) $\boldsymbol{\delta}_C$ 174.1, 162.2, [160.8], 128.6, [124.5], 114.5, [113.0], 90.5, 90.1, 87.5, 73.4, 71.8,

[71.5], 63.3, 61.9, 61.8, 61.4, 39.4, 38.8, 38.7, 38.1, 38.0, 35.5, [33.1], 32.9, 29.6, 29.5, 29.4, 28.0, 27.5, 25.8, 18.8, 18.4, 17.7, 14.1, 10.9, 10.8, 10.4, 9.4, –5.3; $[\boldsymbol{\alpha}]_{\boldsymbol{D}}^{\boldsymbol{20}}$ +21.6 (*c* 0.454, $CHCl_3$); **IR** (thin film) ν_{max} (cm^{-1}) 3487, 2931,2857, 1734, 1690, 1657, 1462, 1379, 1193, 1093, 1072, 967, 878, 774, 712; **HRMS** calc. for $C_{37}H_{77}N_2O_7Si$ 689.5487, found 689.5495.

Distinguishable resonances of the minor rotamer (2:1 ratio) are given in brackets and assignments denoted with an asterisk.

(2*R*,3*S*,4*R*,5*R*,*E*)-4-methoxy-3,5-dimethyl-7-(*N*-methylformamido)hept-6-en-2-yl (*R*)-3,3,3-trifluoro-2-methoxy-2-phenylpropanoate, 107

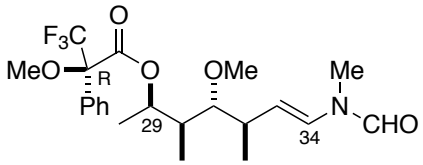

To a solution of alcohol **106** (3 mg, 0.013 mmol) in CH_2Cl_2 (0.10 mL) was added DMAP (1 crystal), DMAP hydrochloride (1 crystal), DCC (65 μL, 1M in CH_2Cl_2, 0.065 mmol) and (*R*)-(+)-MTPA OH (15 mg, 0.065 mmol) and the mixture was stirred at rt for 16 h. Once complete, the reaction mixture was filtered through a plug of silica (eluting with CH_2Cl_2) to give (*R*)-Mosher ester **107** as a colourless oil (4.7 mg, 81%).

R_f 0.60 (1:4 EtOAc/CH_2Cl_2); **^{1}H NMR** (500MHz, $CDCl_3$) $\boldsymbol{\delta}_H$ 8.27 (0.57H, s, NCHO), [8.05] (0.33H, s, NCHO*), 7.60-7.54 (2H, m, ArH), 7.45-7.38 (3H, m, ArH), [7.12] (0.32H, d, *J* = 14.8 Hz, H_{34}*), 6.44 (0.58H, d, *J* = 14.4 Hz, H_{34}), 5.48 (1H, dq, *J* = 6.4, 1.4 Hz, H_{29}), 5.06 (1H, dd, *J* = 14.4, 9.0 Hz, H_{33}), 3.51 (3H, s, OMe), 3.38 (3H, s, OMe), [3.04] (1H, s, NMe*), 3.00 (2H, s, NMe), 2.72 (1H, td, *J* = 9.8, 1.9 Hz, H_{31}), 2.42 (1H, dqd, *J* = 9.7, 7.4, 1.9 Hz, H_{32}), 1.49-1.46 (1H, m, H_{30}), 1.27 (3H, d, *J* = 6.7 Hz, Me_{28}), 1.13 (3H, d, *J* = 6.9 Hz, Me_{32}), 0.83 (3H, d, *J* = 6.9 Hz, Me_{30}).

Distinguishable resonances of the minor rotamer (2:1 ratio) are given in brackets and assignments denoted with an asterisk.

(2*R*,3*S*,4*R*,5*R*,*E*)-4-methoxy-3,5-dimethyl-7-(*N*-methylformamido)hept-6-en-2-yl (*S*)-3,3,3-trifluoro-2-methoxy-2-phenylpropanoate, 108

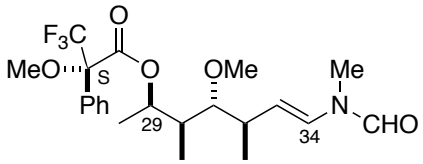

To a solution of alcohol **106** (3 mg, 0.013 mmol) in CH_2Cl_2 (0.10 mL) was added DMAP (1 crystal), DMAP hydrochloride (1 crystal), DCC (65 μL, 1M in CH_2Cl_2, 0.065 mmol) and (*S*)-(−)-MTPA OH (15 mg, 0.065 mmol) and the mixture was stirred at rt for 16 h. Once complete, the reaction was filtered through a plug of silica (eluting with CH_2Cl_2) to give (*S*)-Mosher ester **108** as a colourless oil (4.4 mg, 76%).

R_f 0.61 (1:4 EtOAc/CH_2Cl_2); **^{1}H NMR** (500MHz, $CDCl_3$) δ_H 8.26 (0.58H, s, NCHO), [8.05] (0.34H, s, NCHO*), 7.60-7.52 (2H, m, ArH), 7.43-7.37 (3H, m, ArH), [7.10] (0.33H, d, J = 14.6 Hz, H_{34}*), 6.42 (0.58H, d, J = 14.2 Hz, H_{34}), 5.48 (1H, dq, J = 6.3, 1.4 Hz, H_{29}), 5.05 (1H, dd, J = 14.4, 9.0 Hz, H_{33}), 3.56 (3H, s, OMe), 3.38 (3H, s, OMe), [3.03] (1H, s, NMe*), 3.00 (2H, s, NMe), 2.68 (1H, td, J = 9.8, 1.9 Hz, H_{31}), 2.38 (1H, dqd, J = 9.9, 7.6, 1.9 Hz, H_{32}), 1.49-1.46 (1H, m, H_{30}), 1.35 (3H, d, J = 6.7 Hz, Me_{28}), 1.11 (3H, d, J = 6.9 Hz, Me_{32}), 0.80 (3H, d, J = 6.9 Hz, Me_{30}).

Distinguishable resonances of the minor rotamer (2:1 ratio) are given in brackets and assignments denoted with an asterisk.

(3*R*,4*R*,5*S*,6*R*,9*S*,10*S*,11*R*,12*S*,*E*)-20-((*tert*-butyldimethylsilyl)oxy)-4,10-dimethoxy-3,5,9,11-tetramethyl-1-(*N*-methylformamido)-12-(propionyloxy)icos-1-en-6-yl-(*R*)-3,3,3-trifluoro-2-methoxy-2-phenylpropanoate, 111

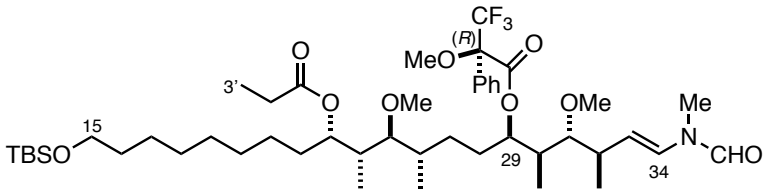

To a solution of alcohol **109** (2 mg, 2.98 μmol) in CH_2Cl_2 (0.10 mL) was added DMAP (1 crystal), DMAP hydrochloride (1 crystal), DCC (15 μL, 1M in CH_2Cl_2, 14.8 μmol) and

(*R*)-(+)-MTPA OH (3.5 mg, 14.8 μmol) and the mixture was stirred at 24 for 16 h. Once complete, the reaction was filtered through a plug of silica (eluting with CH_2Cl_2) then purified by flash column chromatography (1:4 EtOAc/CH_2Cl_2) to give (*R*)-Mosher ester **111** as a colourless oil (2.3 mg, 72%).

R_f 0.75 (1:4 EtOAc/CH_2Cl_2); **^{1}H NMR** (500MHz, $CDCl_3$) δ_H 8.26 (0.60H, s, NCHO), [8.05] (0.34H, s, NCHO*), 7.64-7.56 (2H, m, ArH), 7.45-7.36 (3H, m, ArH), [7.10] (0.30H, d, J = 15.2 Hz, H_{34}*), 6.44 (0.60H, d, J = 14.6 Hz, H_{34}), 5.38 (1H, app q, J = 6.1 Hz, H_{29}), 5.17 (1H, t, J = 6.9 Hz, H_{23}), 5.05 (1H, dd, J = 14.5, 9.7 Hz, H_{33}), 3.59 (2H, t, J = 6.6 Hz, H_{15} × 2), 3.50 (3H, s, OMe), 3.39 (3H, s, OMe), 3.37 (3H, s, OMe), [3.03] (1H, s, NMe*), 3.00 (2H, s, NMe), 2.72 (1H, dd, J = 9.6, 2.5 Hz, H_{25}), 2.66 (1H, td, J = 9.2, 2.2 Hz, H_{31}), 2.45-2.36 (1H, m, H_{32}), 2.32 (2H, q, J = 7.4 Hz, $H_{2'}$ × 2), 1.73-1.59 (7H, m, H_{22} × 2, H_{24}, H_{26}, H_{28} × 2, H_{30}), 1.52-1.37 (4H, m, H_{16} × 2, H_{27} × 2), 1.32-1.21 (10H, m, $H_{17\text{-}21}$), 1.14 (3H, t, J = 7.8 Hz, $H_{3'}$ × 3), 1.11 (3H, d, J = 7.1 Hz, Me_{32}), 0.99 (3H, d, J = 7.5 Hz, Me_{26}), 0.89 (9H, s, SiC($C\underline{H}_3$)$_3$), 0.81 (3H, d, J = 7.1 Hz, Me_{24}), 0.78 (3H, d, J = 7.1 Hz, Me_{30}), 0.04 (6H, s, Si($C\underline{H}_3$)$_2$).

Distinguishable resonances of the minor rotamer (2:1 ratio) are given in brackets and assignments denoted with an asterisk.

(3*R*,4*R*,5*S*,6*R*,9*S*,10*S*,11*R*,12*S*,*E*)-20-((*tert*-butyldimethylsilyl)oxy)-4,10-dimethoxy-3,5,9,11-tetramethyl-1-(*N*-methylformamido)-12-(propionyloxy)icos-1-en-6-yl-(*S*)-3,3,3-trifluoro-2-methoxy-2-phenylpropanoate, 112

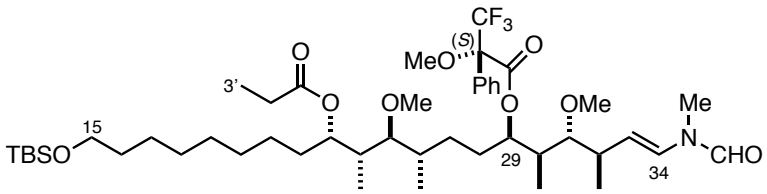

To a solution of alcohol **109** (2 mg, 2.98 μmol) in CH_2Cl_2 (0.10 mL) was added DMAP (1 crystal), DMAP hydrochloride (1 crystal), DCC (15 μL, 1M in CH_2Cl_2, 14.8 μmol) and (*S*)-(–)-MTPA OH (3.5 mg, 14.8 μmol) and the mixture was stirred at rt for 16 h. Once complete, the reaction was filtered through a plug of silica (eluting with CH_2Cl_2) then purified by flash column chromatography (1:4 EtOAc/CH_2Cl_2) to give (*S*)-Mosher ester **112** as a colourless oil (2.5 mg, 78%).

R_f 0.75 (1:4 EtOAc/CH_2Cl_2); **^{1}H NMR** (500MHz, $CDCl_3$) δ_H 8.26 (0.60H, s, NCHO), [8.05] (0.34H, s, NCHO*), 7.63-7.56 (2H, m, ArH), 7.44-7.37 (3H, m, ArH), [7.10] (0.30H, d, J = 15.0 Hz, H_{34}*), 6.41 (0.60H, d, J = 14.6 Hz, H_{34}), 5.36 (1H, app q, J = 6.2 Hz, H_{29}), 5.17 (1H, t, J = 6.9 Hz, H_{23}), 5.04 (1H, dd, J = 14.5, 9.7 Hz, H_{33}), 3.59 (2H, t, J = 6.7 Hz, H_{15} × 2), 3.50 (3H, s, OMe), 3.40 (3H, s, OMe), 3.37 (3H, s, OMe), [3.03] (1H, s, NMe*), 3.00 (2H, s, NMe), 2.72 (1H, dd, J = 8.8, 2.6 Hz, H_{25}), 2.64 (1H, td, J = 9.4, 1.9 Hz, H_{31}), 2.41-2.34 (1H, m, H_{32}), 2.32 (2H, q, J = 7.7 Hz, $H_{2'}$ × 2), 1.72-1.58 (7H, m, H_{22} × 2, H_{24}, H_{26}, H_{28} × 2, H_{30}), 1.52-1.45 (2H, m, H_{16} × 2), 1.44-1.32 (2H, m, H_{27} × 2), 1.30-1.19 (10H, m, $H_{17\text{-}21}$), 1.14 (3H, t, J = 7.2 Hz, $H_{3'}$ × 3), 1.09 (3H, d, J = 6.8 Hz, Me_{32}), 1.01 (3H, d, J = 7.2 Hz, Me_{26}), 0.89 (9H, s, SiC($C\underline{H}_3$)$_3$), 0.82 (3H, d, J = 7.6 Hz, Me_{24}), 0.76 (3H, d, J = 6.6 Hz, Me_{30}), 0.04 (6H, s, Si($C\underline{H}_3$)$_2$).

Distinguishable resonances of the minor rotamer (2:1 ratio) are given in brackets and assignments denoted with an asterisk.

(5*R*,8*S*,9*S*,10*R*,11*S*)-9-methoxy-5-((2*R*,3*R*,4*R*,*E*)-3-methoxy-4-methyl-6-(*N*-methyl formamido)hex-5-en-2-yl)-2,2,3,3,8,10,21,21,22,22-decamethyl-4,20-dioxa-3,21-disilatricosan-11-yl propionate, 113

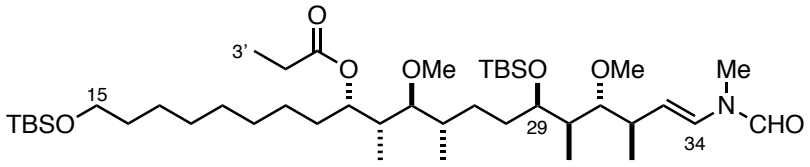

To a solution of alcohol **109** (84 mg, 0.12 mmol) in CH_2Cl_2 (2.00 mL) was added 2,6-lutidine (20 μL, 0.15 mmol) and TBSOTf (34 μL, 0.15 mmol) at –78 °C. After stirring at this temperature for 30 min, the solution was quenched with NH_4Cl (5 mL). The layers were separated and the aqueous was extracted with CH_2Cl_2 (3 × 5 mL). The combined organics were dried (Na_2SO_4) and concentrated *in vacuo.* The crude was purified by flash chromatography (CH_2Cl_2 → 1:4 EtOAc/CH_2Cl_2) to yield TBS ether **113** as a colourless oil (87 mg, 93%).

R_f 0.79 (1:4 EtOAc/CH_2Cl_2); **^{1}H NMR** (500MHz, $CDCl_3$) δ_H 8.27 (0.59H, s, NCHO), [8.05] (0.31H, s, NCHO*), [7.11] (0.29H, d, J = 14.6 Hz, H_{34}*), 6.43 (0.57H, d, J = 14.3 Hz, H_{34}), 5.19 (1H, t, J = 6.9 Hz, H_{23}), 5.12 (1H, dd, J = 14.3, 8.9 Hz, H_{33}), 3.99-3.93 (1H,

m, H_{29}), 3.59 (2H, t, J = 6.6 Hz, H_{15} × 2), 3.50 (3H, s, OMe), 3.38 (3H, s, OMe), 3.08 (1H, dd, J = 9.4, 1.8 Hz, H_{31}), [3.03] (1H, s, NMe*), 3.00 (2H, s, NMe), 2.73 (1H, dd, J = 9.1, 2.7 Hz, H_{25}), 2.54-2.41 (1H, m, H_{32}), 2.32 (2H, q, J = 7.6 Hz, $H_{2'}$ × 2), 1.75-1.66 (2H, m, H_{24}, H_{26}), 1.66-1.59 (2H, m, H_{22} × 2), 1.53-1.33 (7H, H_{16} × 2, H_{27} × 2, H_{28} × 2, H_{30}), 1.30-1.24 (10H, m, $H_{17\text{-}21}$), 1.16-1.14 (6H, m, $H_{3'}$ × 3, Me_{32}), 0.98 (3H, d, J = 7.2 Hz, Me_{26}), 0.89 (18H, s, SiC($C\underline{H}_3$)$_3$ × 2), 0.84 (3H, d, J = 7.2 Hz, Me_{24}), 0.72 (3H, d, J = 7.2 Hz, Me_{30}), 0.08 (6H, s, Si($C\underline{H}_3$)$_2$), 0.04 (6H, s, Si($C\underline{H}_3$)$_2$); **^{13}C NMR** (125MHz, $CDCl_3$) $\boldsymbol{\delta}_C$ 174.1, 162.2, [160.8], 128.3, [114.2], 112.4, [87.5], 86.4, 86.3, 73.4, 71.9, 63.3, 61.3, 61.2, 40.5, 38.8, 37.6, 37.3, 35.5, 35.4, 33.8, [33.1], 32.9, 32.8, 28.0, 27.7, 25.8, 20.1, 20.0, 18.4, 17.7, 17.6, 10.4, 9.4, 9.1, 9.0, –4.2, –5.3; $[\boldsymbol{\alpha}]_{\boldsymbol{D}}^{\boldsymbol{20}}$ –7.0 (*c* 0.410, $CHCl_3$); **IR** (thin film) ν_{max} (cm^{-1}) 2960, 2933, 2861, 1735, 1699,1660, 1462, 1453, 1364, 1274, 1255, 1192, 1059, 835, 774; **HRMS** calc. for $C_{43}H_{91}N_2O_7Si_2$ $[M+NH_4]^+$ 803.6357, found 803.6359.

Distinguishable resonances of the minor rotamer (2:1 ratio) are given in brackets and assignments denoted with an asterisk.

(9*S*,10*R*,11*S*,12*S*,15*R*,16*R*,17*R*,18*R*,*E*)-15-((*tert*-butyldimethylsilyl)oxy)-1-hydroxy-11,17-dimethoxy-10,12,16,18-tetramethyl-20-(*N*-methylformamido)icos-19-en-9-yl propionate, 114

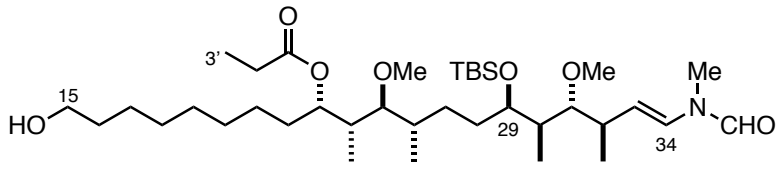

To a solution of *bis* TBS-ether **113** (87 mg, 0.11 mmol) in THF (1 mL) was added TBAF (120 µL, 0.12 mmol, 1M in THF). The reaction was stirred at rt for 8 h before being quenched with NH_4Cl (2 mL). The layers were separated, and the aqueous phase was extracted with EtOAc (3 × 3 mL). The combined organics were dried (Na_2SO_4) and concentrated *in vacuo*. The crude was filtered through a small plug of silica (eluting with CH_2Cl_2) to give alcohol **114** as a colourless oil (74 mg, 100%).

R_f 0.31 (1:4 EtOAc/CH_2Cl_2); **^{1}H NMR** (500MHz, $CDCl_3$) $\boldsymbol{\delta}_H$ 8.27 (0.56H, s, NCHO), [8.05] (0.27H, s, NCHO*), [7.11] (0.30H, d, J = 14.7 Hz, H_{34}*), 6.43 (0.57H, d, J = 14.2 Hz, H_{34}), 5.21-5.16 (1H, m, H_{23}), 5.15-5.10 (1H, m, H_{33}), 3.99-3.94 (1H, m, H_{29}), 3.63 (2H, t, J = 6.5 Hz, H_{15} × 2), 3.50 (3H, s, OMe), 3.38 (3H, s, OMe), 3.09 (1H, dd, J = 7.6, 2.0 Hz,

H_{31}), [3.04] (1H, s, NMe*), 3.00 (2H, s, NMe), 2.73 (1H, dd, J = 6.3, 2.7 Hz, H_{25}), 2.54-2.41 (1H, m, H_{32}), 2.32 (2H, q, J = 7.6 Hz, $H_{2'}$ × 2), 1.74-1.68 (1H, m, H_{24}), 1.66-1.59 (3H, m, H_{22} × 2, H_{26}), 1.51-1.38 (4H, m, H_{16} × 2, H_{28} × 2), 1.38-1.21 (13H, m, $H_{17\text{-}21}$, H_{27} × 2, H_{30}), 1.18-1.12 (6H, m, $H_{3'}$ × 3, Me_{32}), 0.99 (3H, d, J = 7.1 Hz, Me_{26}), 0.90 (9H, s, $SiC(C\underline{H}_3)_3$), 0.83 (3H, d, J = 7.1 Hz, Me_{24}), 0.72 (3H, d, J = 7.1 Hz, Me_{30}), 0.07 (6H, s, $Si(C\underline{H}_3)_2$); **^{13}C NMR** (125MHz, $CDCl_3$) δ_C 174.1, 162.2, [160.8], 135.5, 128.3, 124.8, [124.3], [114.1], 112.0, [87.5], 86.5, 73.4, 71.9, 63.1, 61.4, 61.3, 40.4, 38.7, 37.6, 37.3, 35.4, 33.8, [33.1], 32.8, 32.2, 31.0, 29.4, 29.2, 28.1, 27.6, 25.7, 23.4, 20.0, 18.4, 17.6, 10.3, 9.4, 9.1, 9.0, –4.1; $[\alpha]_D^{20}$ –4.6 (*c* 0.310, $CHCl_3$); **IR** (thin film) ν_{max} (cm^{-1}) 3476, 2948, 2932, 2857, 1732, 1694, 1655, 1462, 1250, 1189, 1090, 1066, 834, 786; **HRMS** calc. for $C_{37}H_{74}NO_7Si_1$ $[M+H]^+$ 672.5229, found 672.5224.

Distinguishable resonances of the minor rotamer (2:1 ratio) are given in brackets and assignments denoted with an asterisk.

(5*R*,8*S*,9*S*,10*R*,11*S*,19*E*,24*R*,25*R*,26*R*,27*R*,29*E*,31*E*)-9-methoxy-5-((2*R*,3*R*,4*R*,*E*)-3-methoxy-4-methyl-6-(*N*-methylformamido)hex-5-en-2-yl)- 2,2,3,3,8,10,20,24,26,35, 35, 36,36–tridecamethyl-21-oxo-25,27-bis((triethylsilyl)oxy)-4,34-dioxa-3,35-disila-heptatriaconta-19,29,31-trien-11-yl propionate, 116

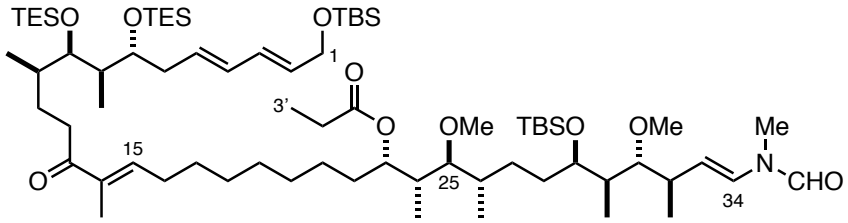

Alcohol **114** (100 mg, 0.15 mmol) was dissolved in CH_2Cl_2 (3 mL) before DMP (220 mg, 0.52 mmol) and $NaHCO_3$ (151 mg, 1.8 mmol) were added. The reaction was stirred at rt for 2 h before being quenched with $Na_2S_2O_3$ (10 mL) and $NaHCO_3$ (5 mL). The quenching mixture was stirred for 30 min and the layers were separated. The aqueous phase was extracted with CH_2Cl_2 (3 × 10 mL) and the combined organics were dried (Na_2SO_4) and concentrated *in vacuo* to an oily solid. Aldehyde **54** (*ca*. 100 mg) was used immediately crude in the subsequent olefination reaction.

To a suspension of $Ba(OH)_2$ (281 mg, 0.13 mmol) in THF (1 mL) was added phosphonate **36** (130 mg, 0.16 mmol) in THF (1 mL) and the mixture was stirred for 1 h. A solution of

aldehyde **54** (100 mg, 0.15 mmol) in THF/H_2O (40:1, 2 mL) was added and the reaction mixture was stirred for 72 h. Once complete, the solution was poured into NH_4Cl (5 mL) and extracted with Et_2O (3 × 5 mL). The combined organics were dried ($MgSO_4$) and concentrated *in vacuo*. Purification by flash column chromatography (1:4 EtOAc/PE) yielded **116** as a colourless oil (146 mg, 85%).

R_f 0.55 (1:3 EtOAc/PE); **^{1}H NMR** (500MHz, $CDCl_3$) δ_H 8.27 (0.67H, s, NCHO), [8.05] (0.33H, s, NCHO*), [7.11] (0.33H, d, *J* = 15.3 Hz, H_{34}*), 6.60 (1H, t, *J* = 7.1 Hz, H_{15}), 6.44 (0.67H, d, *J* = 15.3 Hz, H_{34}), 6.18 (1H, dd, *J* = 15.1, 10.5 Hz, H_3), 6.04 (1H, dd, *J* = 15.0, 10.1 Hz, H_4), 5.72-5.60 (2H, m, H_2, H_5), 5.20 (1H, t, *J* = 6.8 Hz, H_{23}), [5.13] (0.3H, dd, *J* = 14.7, 8.9 Hz, H_{33}*), 5.11 (0.6H, dd, *J* = 14.3, 8.6 Hz, H_{33}), 4.20 (2H, d, *J* = 5.2 Hz, H_1 × 2), 4.00-3.94 (1H, m, H_{29}), 3.63 (1H, app q, *J* = 5.8 Hz, H_7), 3.54 (1H, t, *J* = 4.3 Hz, H_9), 3.50 (3H, s, OMe), 3.38 (3H, s, OMe), 3.08 (1H, dd, *J* = 9.4, 1.8 Hz, H_{31}), [3.03] (1H, s, NMe*), 3.00 (2H, s, NMe), 2.77-2.70 (2H, m, H_{12a}, H_{25}), 2.60-2.51 (1H, m, H_{12b}), 2.51-2.42 (1H, m, H_{32}), 2.32 (2H, q, *J* = 7.8 Hz, $H_{2'}$ × 2), 2.21 (2H, app q, *J* = 7.4 Hz, H_{16} × 2), 2.18-2.13 (2H, m, H_6 × 2), 1.76 (3H, s, Me_{14}), 1.75-1.60 (6H, m, H_8, H_{10}, H_{11a}, H_{22a}, H_{24}, H_{26}), 1.54-1.48 (2H, m, H_{28} × 2), 1.48-1.35 (7H, m, H_{11b}, H_{17} × 2, H_{22b}, H_{27} × 2, H_{30},), 1.35-1.28 (8H, m, $H_{18\text{-}21}$), 1.16 (3H, t, *J* = 7.8 Hz, $H_{3'}$ × 3), 1.15 (3H, t, *J* = 7.5 Hz, Me_{32}), 0.99 (3H, d, *J* = 6.9 Hz, Me_{26}), 0.96 (9H, t, *J* = 8.0 Hz, $Si(CH_2C\underline{H}_3)_3$), 0.93 (9H, t, *J* = 8.0 Hz, $Si(CH_2C\underline{H}_3)_3$), 0.92-0.82 (27H, m, $SiC(C\underline{H}_3)_3$ × 2, Me_8, Me_{10}, Me_{24}), 0.72 (3H, d, *J* = 7.0 Hz, Me_{30}), 0.60 (6H, q, *J* = 8.2 Hz, $Si(C\underline{H}_2CH_3)_3$), 0.57 (6H, q, *J* = 8.2 Hz, $Si(C\underline{H}_2CH_3)_3$), 0.07 (12H, s, $Si(C\underline{H}_3)_2$); **^{13}C NMR** (125MHz, $CDCl_3$) δ_C 202.1, 174.1, 162.2, [160.8], 142.2, [142.1], 137.1, 131.4, 130.3, 130.2, 128.3, [124.3], [114.1], 112.3, [87.4], 86.4, 86.3, 74.4, 73.3, 72.0, 71.9, 63.7, 61.3, [61.2], 53.4, 41.8, 40.6, 38.8, 38.1, 37.6, [37.3], 36.0, 35.4, 33.8, [33.1], 32.8, 29.5, 29.4, 29.1, 28.7, 28.0, 27.6, 26.9, 25.9, 25.8, 20.0, 18.3, 17.7, 16.2, 11.4, 10.4, 10.3, 9.4, 9.1, 7.2, 7.0, 5.6, 5.2, –3.0, –4.1, –5.2; $[\alpha]_D^{20}$ –3.3 (*c* 1.00, $CHCl_3$); **IR** (thin film) ν_{max} (cm^{-1}) 2951, 2932, 2876, 1730, 1669, 1613, 1440, 1515, 1463, 1371, 1252, 1192, 1083, 1001, 992, 832, 775, 725; **HRMS** calc. for $C_{72}H_{145}N_2O_{10}Si_4$ $[M+NH_4]^+$ 1309.9971, found 1309.9978.

Distinguishable resonances of the minor rotamer (2:1 ratio) are given in brackets and assignments denoted with an asterisk.

_N_-((1_E_,3_R_,4_R_,5_R_,6_R_,9_S_,10_S_,11_R_,12_S_,20_E_,25_R_,26_R_,27_R_,28_R_,30_E_,32_E_)-6,34-bis((_tert_-butyldimethylsilyl)oxy)-12-hydroxy-4,10-dimethoxy-3,5,9,11,21,25,27-heptamethyl-22-oxo-26,28-bis((triethylsilyl)oxy)tetratriaconta-1,20,30,32-tetraen-1-yl)-_N_-methyl formamide, 119

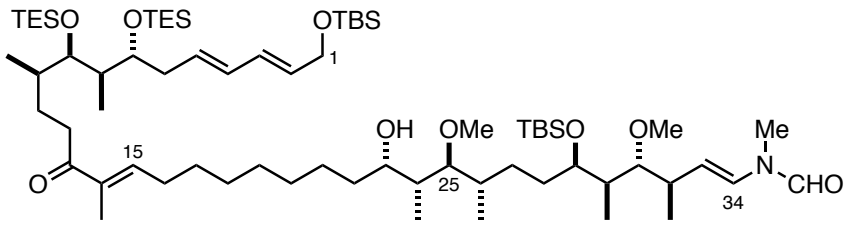

NaOH (45 mg, 0.89 mmol) was dissolved in MeOH (25 mL) and 3 mL of this stock solution was added to ester **116** (60 mg, 0.046 mmol). The solution was heated to 65 °C and stirred at this temperature for 1 h. The reaction was cooled to rt and quenched with NH_4Cl (3 mL) and brine (2 mL). The layers were separated, and the aqueous phase extracted with EtOAc (3 × 5 mL). The combined organics were dried (Na_2SO_4) and concentrated *in vacuo.* Purification *via* flash column chromatography (1:4 EtOAc/PE) yielded alcohol **119** as a colourless oil (25 mg, 50%, 87% brsm).

R_f 0.50 (1:2 EtOAc/PE); **^{1}H NMR** (500MHz, $CDCl_3$) δ_H 8.27 (0.67H, s, NCHO), [8.04] (0.33H, s, NCHO*), [7.11] (0.33H, d, J = 14.9 Hz, H_{34*}), 6.60 (1H, t, J = 7.0 Hz, H_{15}), 6.44 (0.67H, d, J = 14.1 Hz, H_{34}), 6.18 (1H, dd, J = 15.0, 10.7 Hz, H_3), 6.04 (1H, dd, J = 15.0, 10.7 Hz, H_4), 5.76-5.60 (2H, m, H_2, H_5), 5.13 (1H, dd, J = 14.1, 9.0 Hz, H_{33}), 4.20 (2H, d, J = 5.8 Hz, H_1 × 2), 4.00-3.95 (1H, m, H_{29}), 3.90-3.86 (1H, m, H_{23}), 3.65-3.59 (1H, m, H_7), 3.56-3.52 (1H, m, H_9), 3.50 (3H, s, OMe), 3.46 (3H, s, OMe), 3.07 (1H, d, J = 9.8 Hz, H_{31}), [3.03] (1H, s, NMe*), 2.99 (2H, s, NMe), 2.90 (1H, dd, J = 7.5, 3.2 Hz, H_{25}), 2.77-2.69 (1H, m, H_{12a}), 2.60-2.50 (1H, m, H_{12b}), 2.49-2.41 (1H, m, H_{32}), 2.22 (2H, app q, J = 7.4 Hz, H_{16} × 2), 2.18-2.13 (2H, m, H_6 × 2), 1.76 (3H, s, Me_{14}), 1.75-1.60 (5H, m, H_8, H_{11a}, H_{26}, H_{10}, H_{24}), 1.59-1.49 (4H, m, H_{22} × 2, H_{28a}, H_{11b}), 1.49-1.38 (6H, m, H_{17} × 2, H_{27} × 2, H_{28b}, H_{30}), 1.36-1.28 (8H, m, H_{18-21}), 1.17 (3H, d, J = 7.1 Hz, Me_{32}), 1.00 (3H, d, J = 6.9 Hz, Me_{26}), 0.95 (9H, t, J = 8.0 Hz, $Si(CH_2C\underline{H}_3)_3$), 0.93 (9H, t, J = 8.0 Hz, $Si(CH_2C\underline{H}_3)_3$), 0.92-0.82 (27H, m, $SiC(C\underline{H}_3)_3$ × 2), Me_{24}, Me_8, Me_{10}), 0.72 (3H, d, J = 6.7 Hz, Me_{30}), 0.60 (6H, q, J = 8.0 Hz, $Si(C\underline{H}_2CH_3)_3$), 0.58 (6H, q, J = 8.3 Hz, $Si(C\underline{H}_2CH_3)_3$), 0.07 (12H, s, $Si(C\underline{H}_3)_2$);**^{13}C NMR** (125MHz, $CDCl_3$) δ_C 202.1, 162.2, [160.8], 142.2, 137.1, 131.4, 130.2, 128.2, [124.5], [114.3], 112.5, 92.4, [86.4], 86.3, 74.5, 71.8, 71.0, 63.7, 61.9, 41.8, 40.4, 38.1, 37.6, 36.0, 35.4, 34.7, 33.4, [33.1], 29.7, 29.5, 29.1, 28.7, 27.6, 26.9, 25.9, 20.0, 18.4, 16.3, 11.7, 11.4, 10.5, 9.0, 7.2, 7.0, 5.6, 5.2, –3.0, –4.2, –5.2; $[\alpha]_D^{20}$ –2.8 (*c* 0.88,

$CHCl_3$); **IR** (thin film) ν_{max} (cm^{-1}) 3867, 2954, 2922, 2856, 1660, 1615, 1431, 1517, 1443, 1390, 1249, 1172, 1083, 1038, 991, 832, 778; **HRMS** calc. for $C_{69}H_{141}N_2O_9Si_4$ $[M+NH_4]^+$ 1253.9709, found 1253.9703.

Distinguishable resonances of the minor rotamer (2:1 ratio) are given in brackets and assignments denoted with an asterisk.

_N_-((1_E_,3_R_,4_R_,5_R_,6_R_,9_S_,10_S_,11_R_,12_S_,20_E_,25_R_,26_R_,27_R_,28_R_,30_E_,32_E_)-6-((_tert_-butyldimethylsilyl)oxy)-12-hydroxy-4,10-dimethoxy-3,5,9,11,21,25,27-heptamethyl-22,34-dioxo-26,28-bis((triethylsilyl)oxy)tetratriaconta-1,20,30,32-tetraen-1-yl)-_N_-methyl formamide, 120

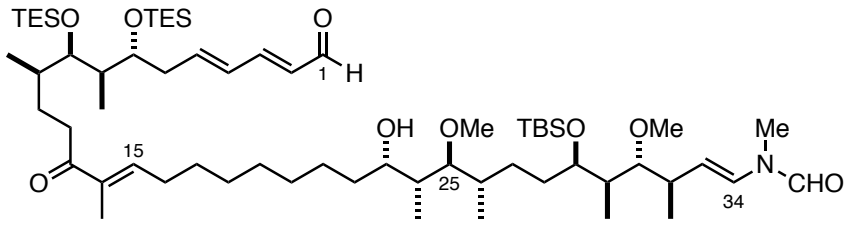

To a solution of **119** (30 mg, 24.3 μmol) in CH_2Cl_2 (1 mL) and pH 7 buffer solution (1.00 mL) at 0 °C was added DDQ (6.6 mg, 29 μmol). The mixture was warmed to rt and stirred in the dark for 2 h before being quenched with $NaHCO_3$ (2 mL). The solution was diluted with H_2O (5 mL) and extracted with CH_2Cl_2 (3 × 5 mL). The combined organics were dried (Na_2SO_3) and concentrated *in vacuo*. The crude material was purified by flash column chromatography (3:7 EtOAc/PE) to give aldehyde **120** as a colourless oil (20 mg, 74%).

R_f 0.28 (3:7 EtOAc/PE); **^{1}H NMR** (500MHz, $CDCl_3$) δ_H 9.55 (1H, d, J = 8.2 Hz, H_1), 8.27 (0.60H, s, NCHO), [8.04] (0.30H, s, NCHO*), 7.15-7.05 (1.3H, m, H_3, H_{34}*), 6.60 (1H, t, *J* = 6.5 Hz, H_{15}), 6.43 (0.6H, d, *J* = 14.4 Hz, H_{34}), 6.38-6.29 (2H, m, H_4, H_5), 6.08 (1H, dd, *J* = 14.9, 7.9 Hz, H_2), 5.13 (1H, dd, *J* = 14.1, 9.0 Hz, H_{33}), 4.00-3.94 (1H, m, H_{29}), 3.93-3.85 (1H, m, H_{23}), 3.76-3.70 (1H, m, H_7), 3.55 (1H, app t, *J* = 3.8 Hz, H_9), 3.50 (3H, s, OMe), 3.46 (3H, s, OMe), 3.07 (1H, d, *J* = 9.9 Hz, H_{31}), [3.03] (1H, s, NMe*), 2.99 (2H, s, NMe), 2.90 (1H, dd, *J* = 7.7, 3.5 Hz, H_{25}), 2.79-2.70 (1H, m, H_{12a}), 2.62-2.53 (1H, m, H_{12b}), 2.52-2.42 (1H, m, H_{32}), 2.38-2.26 (2H, m, H_6 × 2), 2.21 (2H, app q, *J* = 7.0 Hz, H_{16} × 2), 1.75 (3H, s, Me_{14}), 1.74-1.69 (2H, m, H_8, H_{11a}) 1.66-1.59 (3H, m, H_{24}, H_{26}, H_{28a}), 1.58-1.49 (4H, m, H_{10}, H_{22} × 2 H_{30},), 1.49-1.39 (6H, m, H_{11b}, H_{17} × 2, H_{27} × 2, H_{28b},), 1.36-1.28 (8H, m, $H_{18\text{-}21}$), 1.17 (3H, d, *J* = 8.0 Hz, Me_{32}), 1.02-0.82 (39H, m, $Si(CH_2C\underline{H}_3)_3$) × 2, $SiC(C\underline{H}_3)_3$, Me_8, Me_{10}, Me_{24}, Me_{26}), 0.72 (3H, d, *J* = 7.0 Hz, Me_{30}), 0.61 (6H, q, *J* = 7.5 Hz,

Si(C<u>H</u>$_2$CH$_3$)$_3$), 0.56 (6H, q, *J* = 7.5 Hz, Si(C<u>H</u>$_2$CH$_3$)$_3$), 0.09 (6H, s, Si(C<u>H</u>$_3$)$_2$); **^{13}C NMR** (125MHz, $CDCl_3$) δ_C 201.9, 194.0, 162.2, [160.7], 152.5, 144.5, 142.2, 137.1, 130.2, 128.2, [114.2], 112.4, 92.4, [86.3], 74.0, 71.8, 71.0, 61.8, 61.7, [61.3], 61.2, 53.4, 41.6, 40.4, 38.3, 37.6, 37.4, 36.6, 36.0, 35.1, 34.7, 33.3, [33.1], 29.7, 29.1, 28.7, 28.4, 27.5, 27.0, 23.8, 19.9, 18.3, 16.3, 16.0, 14.2, 11.7, 11.4, [10.3], 9.0, 7.1, 6.9, 5.6, 5.2, –3.0, –4.2; $[\alpha]_D^{20}$ –1.9 (*c* 0.72, $CHCl_3$); **IR** (thin film) ν_{max} (cm^{-1}) 3848, 2952, 2932, 2876, 1684, 1640, 1612, 1458, 1447, 1378, 1248, 1172, 1080, 1038, 995, 820; **HRMS** calc. for $C_{63}H_{121}NO_9Si_3$ $[M+H]^+$ 1120.8422, found 1120.8424.

Distinguishable resonances of the minor rotamer (2:1 ratio) are given in brackets and assignments denoted with an asterisk.

6.5.2 Established coupling strategy

(2*S*,3*S*,4*R*,5*S*)-13-hydroxy-3-methoxy-1-((4-methoxybenzyl)oxy)-2,4-dimethyl tridecan-5-yl propionate, 166

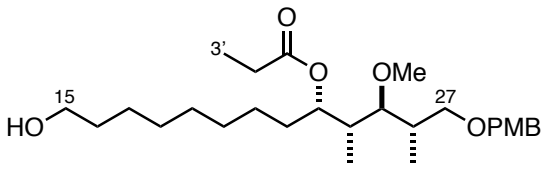

To a solution of TBS ether **98** (2.67 g, 4.60 mmol) in THF (62.5 mL) was added H_2O (25 mL) and HCl (3.0 M, 12.5 mL). The reaction was stirred for 2 h before being cooled to 0 °C and quenched with $NaHCO_3$ (100 mL, portionwise addition). The mixture was extracted with Et_2O (3 × 100 mL) and the combined organics were dried (Na_2SO_4) and concentrated *in vacuo*. Purification *via* flash column chromatography (1:3 EtOAc/PE) gave alcohol **166** (2.19 g, 100%) as a colourless oil.

R_f 0.17 (1:3 EtOAc/PE); **^{1}H NMR** (500MHz, $CDCl_3$) δ_H 7.24 (2H, d, *J* = 8.4 Hz, ArH), 6.86 (2H, d, *J* = 8.4 Hz, ArH), 5.18 (1H, t, *J* = 7.2 Hz, H_{23}), 4.41 (2H, ABq, *J* = 10.2 Hz, OCH_2Ar), 3.80 (3H, s, OMe), 3.63 (2H, q, *J* = 6.1 Hz, H_{15} × 2), 3.54 (1H, dd, *J* = 9.7, 5.2 Hz, H_{27a}), 3.38 (3H, s, OMe), 3.32 (1H, t, *J* = 8.5 Hz, H_{27b}), 2.86 (1H, dd, *J* = 8.9, 4.0 Hz, H_{25}), 2.31 (2H, q, *J* = 7.9 Hz, $H_{2'}$ × 2), 2.12-2.06 (1H, m, H_{26}), 1.78 (1H, dqd, *J* = 8.3, 7.9, 1.8 Hz, H_{24}), 1.66-1.59 (1H, m, H_{22a}), 1.55 (2H, app quint, *J* = 7.0 Hz, H_{16} × 2), 1.48-1.39 (1H, m, H_{22b}), 1.37-1.19 (10H, m, H_{17-21}), 1.14 (3H, t, *J* = 7.4 Hz, $H_{3'}$ × 3), 1.05 (3H, d, *J* = 7.1 Hz, Me_{26}), 0.90 (3H, d, *J* = 6.9 Hz, Me_{24}).

These data are in agreement with those previously reported.[165]

(2*S*,3*S*,4*R*,5*S*)-3-methoxy-1-((4-methoxybenzyl)oxy)-2,4-dimethyl-13-oxotridecan-5-yl propionate, 52

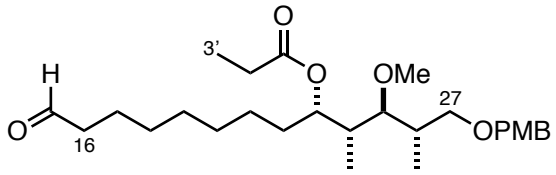

To a solution of oxalyl chloride (707 μL, 8.35 mmol) in CH_2Cl_2 (35 mL) at –78 °C was added DMSO (1.19 mL, 15.1 mmol) and the mixture stirred for 15 min. A solution of alcohol **166** (1.30 g, 2.79 mmol) in CH_2Cl_2 (20 mL) was added and the solution stirred for 30 min. Triethylamine (3.50 mL, 25.1 mmol) was added and the reaction was warmed to rt and stirred for 1.5 h before being quenched by the addition of NH_4Cl (75 mL). The layers were separated, and the aqueous phase was extracted with CH_2Cl_2 (2 × 50 mL) and the combined organics were concentrated *in vacuo*. The organic residue was dissolved in Et_2O (100 mL) and washed with brine (50 mL) before being dried (Na_2SO_4) and concentrated *in vacuo*. Flash column chromatography (1:3 EtOAc/PE) yielded aldehyde **52** (1.10 g, 85%) as a colourless oil.

R_f 0.35 (1:3 EtOAc/PE); **^{1}H NMR** (400MHz, $CDCl_3$) δ_H 9.75 (1H, t, J = 1.9 Hz, H_{15}), 7.24 (2H, d, J = 8.2 Hz, ArH), 6.86 (2H, d, J = 8.2 Hz, ArH), 5.17 (1H, t, J = 7.0 Hz, H_{23}), 4.42 (2H, ABq, J = 10.1 Hz, OCH_2Ar), 3.80 (3H, s, OMe), 3.53 (1H, dd, J = 9.5, 4.9 Hz, H_{27a}), 3.38 (3H, s, OMe), 3.32 (1H, dd, J = 9.0, 7.4 Hz, H_{27b}), 2.86 (1H, dd, J = 8.9, 3.9 Hz, H_{25}), 2.40 (2H, td, J = 7.4, 1.9 Hz, H_{16} × 2), 2.31 (2H, q, J = 7.6 Hz, $H_{2'}$ × 2), 2.12-2.06 (1H, m, H_{26}), 1.78 (1H, dqd, J = 8.8, 7.6, 1.9 Hz, H_{24}), 1.66-1.58 (3H, m, H_{22a}, H_{17} × 2), 1.47-1.40 (1H, m, H_{22b}), 1.34-1.20 (8H, m, $H_{18\text{-}21}$), 1.14 (3H, t, J = 7.5 Hz, $H_{3'}$ × 3), 1.05 (3H, d, J = 7.0 Hz, Me_{26}), 0.90 (3H, d, J = 7.0 Hz, Me_{24}).

These data are in agreement with those previously reported.[165]

(2*S*,3*S*,4*R*,5*S*,13*E*,18*R*,19*R*,20*R*,21*R*,23*E*,25*E*)-27-((*tert*-butyldimethylsilyl)oxy)-3-methoxy-1-((4-methoxybenzyl)oxy)-2,4,14,18,20-pentamethyl-15-oxo-19,21-bis ((triethylsilyl)oxy)heptacosa-13,23,25-trien-5-yl propionate, 121

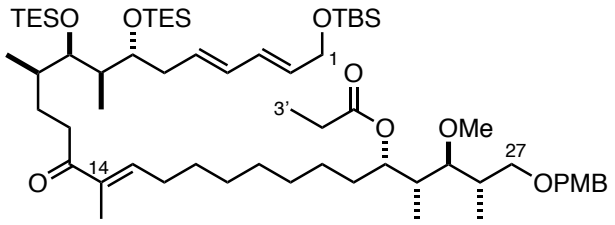

To $Ba(OH)_2$ (592 mg, 3.46 mmol) was added a solution of phosphonate **36** (2.24 g, 2.88 mmol, 3:1 mixture with regioisomer **77**) in THF (40 mL) and the suspension was stirred for 1 h at rt. Aldehyde **52** (1.10 g, 2.37 mmol) in THF/H_2O (40:1, 25 mL) was added and the reaction was stirred for 72 h. The reaction was quenched by the addition of NH_4Cl (75 mL) and the layers separated. The aqueous phase was extracted with EtOAc (3 × 100 mL) and the combined organics were dried ($MgSO_4$) and concentrated *in vacuo*. The crude material was purified by flash column chromatography (1:5 → 1:4 EtOAc/PE) to yield enone **121** (1.96 g, 85% >20:1) as a colourless oil.

R_f 0.76 (1:3 EtOAc/PE); **^{1}H NMR** (500MHz, $CDCl_3$) δ_H 7.24 (2H, d, *J* = 8.5 Hz, ArH), 6.86 (2H, d, *J* = 8.5 Hz, ArH), 6.59 (1H, t, *J* = 7.1 Hz, H_{15}), 6.18 (1H, dd, *J* = 14.9, 10.5 Hz, H_3), 6.04 (1H, dd, J = 15.2, 10.5 Hz, H_4), 5.68 (1H, dt, J = 14.7, 7.5 Hz, H_5), 5.64 (1H, dt, *J* = 14.7, 5.7 Hz, H_2), 5.18 (1H, td, *J* = 6.7, 2.0 Hz, H_{23}), 4.41 (2H, ABq, *J* = 11.0 Hz, OCH_2Ar), 4.20 (2H, d, *J* = 5.1 Hz, H_1 × 2), 3.80 (3H, s, OMe), 3.66-3.60 (1H, m, H_7), 3.56-3.51 (2H, m, H_9, H_{27a}), 3.38 (3H, s, OMe), 3.32 (1H, dd, *J* = 8.9, 7.2 Hz, H_{27b}), 2.87 (1H, dd, *J* = 8.8, 3.8 Hz, H_{25}), 2.73 (1H, ddd, *J* = 15.7, 9.7, 6.0 Hz, H_{12a}), 2.56 (1H, ddd, *J* = 15.7, 9.7, 6.0 Hz, H_{12b}), 2.31 (2H, q, *J* = 7.6 Hz, $H_{2'}$ × 2), 2.21 (2H, q, *J* = 7.4 Hz, H_{16} × 2), 2.18-2.14 (2H, m, H_6 × 2), 2.11-2.06 (1H, m, H_{26}), 1.81-1.70 (3H, m, H_8, H_{11a}, H_{24}), 1.76 (3H, s, Me_{14}), 1.67-1.58 (1H, m, H_{22a}), 1.48-1.37 (4H, m, H_{11b}, H_{22b}, H_{17} × 2), 1.34-1.20 (8H, m, $H_{18\text{-}21}$), 1.14 (3H, t, *J* = 7.6 Hz, $H_{3'}$ × 3), 1.06 (3H, d, *J* = 7.1 Hz, Me_{26}), 0.95 (9H, t, *J* = 8.2 Hz, $Si(CH_2C\underline{H}_3)_3$), 0.93 (9H, t, *J* = 8.2 Hz, $Si(CH_2C\underline{H}_3)_3$), 0.92-0.89 (15H, m, $SiC(C\underline{H}_3)_3$, Me_{24}, Me_{10}), 0.86 (3H, d, *J* = 6.9 Hz, Me_8), 0.61 (6H, q, *J* = 7.8 Hz, $Si(C\underline{H}_2CH_3)_3$), 0.56 (6H, q, *J* = 7.5 Hz, $Si(C\underline{H}_2CH_3)_3$), 0.07 (6H, s, $Si(C\underline{H}_3)_2$).

These data are in agreement with those previously reported.[165]

(2*S*,3*S*,4*R*,5*S*,13*E*,15*S*,18*R*,19*R*,20*R*,21*R*,23*E*,25*E*)-27-((*tert*-butyldimethylsilyl)oxy)-15-hydroxy-3-methoxy-1-((4-methoxybenzyl)oxy)-2,4,14,18,20-pentamethyl-19,21-bis((triethylsilyl)oxy)heptacosa-13,23,25-trien-5-yl propionate, 122

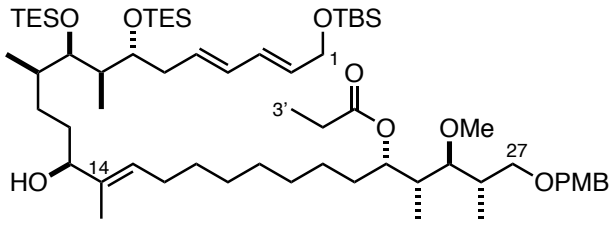

To a solution of enone **121** (1.96 g, 1.80 mmol) in THF (47 mL) was added (*R*)-Me-CBS catalyst (2.16 mL, 1 M in PhMe, 2.16 mmol) at –10 °C and the solution stirred for 5 min before dropwise addition of $BH_3{\cdot}SMe_2$ (188 μL, 1.98 mmol). The solution was stirred at –10 °C for 1.5 h then carefully quenched by the addition of MeOH (50 mL). The solution was warmed to rt and concentrated *in vacuo*. The residue was re-dissolved in MeOH (40 mL) and was again concentrated *in vacuo*. This process was repeated twice further. Purification *via* flash column chromatography (1:6 EtOAc/PE) gave alcohol **122** (1.79 g, 93%, >20:1 *dr*) as a colourless oil.

R_f 0.72 (1:3 EtOAc/PE); **^{1}H NMR** (500MHz, $CDCl_3$) δ_H 7.24 (2H, d, *J* = 8.5 Hz, ArH), 6.86 (2H, d, *J* = 8.5 Hz, ArH), 6.18 (1H, dd, *J* = 15.2, 10.4 Hz, H_3), 6.04 (1H, dd, *J* = 15.3, 10.2 Hz, H_4), 5.68 (1H, dt, *J* = 14.7, 7.4 Hz, H_5), 5.64 (1H, dt, *J* = 15.3, 5.6 Hz, H_2), 5.36 (1H, t, *J* = 6.4 Hz, H_{15}), 5.18 (1H, td, *J* = 7.2, 1.8 Hz, H_{23}), 4.41 (2H, ABq, *J* = 11.1 Hz, OCH_2Ar), 4.20 (2H, d, *J* = 5.2 Hz, $H_1 \times 2$), 3.94 (1H, td, *J* = 6.6, 2.5 Hz, H_{13}), 3.80 (3H, s, OMe), 3.62-3.58 (1H, m, H_7), 3.53 (1H, dd, *J* = 9.2, 4.8 Hz, H_{27a}), 3.50 (1H, dd, *J* = 5.1, 3.5 Hz, H_9), 3.38 (3H, s, OMe), 3.32 (1H, dd, *J* = 9.1, 7.4 Hz, H_{27b}), 2.87 (1H, dd, *J* = 8.6, 3.4 Hz, H_{25}), 2.31 (2H, q, *J* = 7.7 Hz, $H_{2'} \times 2$), 2.18-2.12 (2H, m, $H_6 \times 2$), 2.12-2.06 (1H, m, H_{26}), 2.03-1.94 (2H, m, $H_{16} \times 2$), 1.82-1.70 (2H, m, H_8, H_{24}), 1.66-1.60 (2H, m, H_{12a}, H_{22a}), 1.58 (3H, br s, Me_{14}), 1.54-1.48 (1H, m, H_{10}), 1.48-1.37 (4H, m, $H_{11} \times 2$, H_{12b}, H_{22b}), 1.35-1.29 (2H, m, $H_{17} \times 2$), 1.29-1.24 (8H, m, $H_{18\text{-}21}$), 1.14 (3H, t, *J* = 7.6 Hz, $H_{3'} \times 3$), 1.05 (3H, d, *J* = 7.0 Hz, Me_{26}), 0.96 (9H, t, *J* = 8.0 Hz, $Si(CH_2C\underline{H}_3)_3$), 0.93 (9H, t, *J* = 7.9 Hz, $Si(CH_2C\underline{H}_3)_3$), 0.91 (9H, s, $SiC(C\underline{H}_3)_3$), 0.90-0.84 (9H, m, Me_8, Me_{24}, Me_{10}), 0.60 (6H, q, *J* = 8.0 Hz, $Si(C\underline{H}_2CH_3)_3$), 0.57 (6H, q, *J* = 7.8 Hz, $Si(C\underline{H}_2CH_3)_3$), 0.07 (6H, s, $Si(C\underline{H}_3)_2$).

These data are in agreement with those previously reported.[165]

(2*S*,3*S*,4*R*,5*S*,13*E*,15*S*,18*R*,19*R*,20*R*,21*R*,23*E*,25*E*)-27-((*tert*-butyldimethylsilyl)oxy)-3,15-dimethoxy-1-((4-methoxybenzyl)oxy)-2,4,14,18,20-pentamethyl-19,21-bis((triethylsilyl)oxy)heptacosa-13,23,25-trien-5-yl propionate, 167

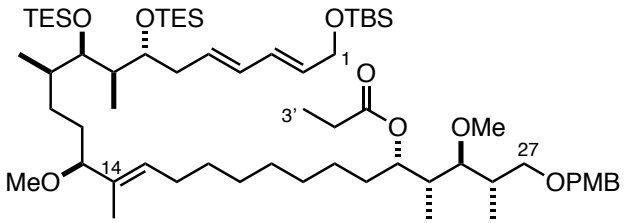

To a solution of Meerwein salt (143 mg, 0.96 mmol) and proton sponge (309 mg, 1.44 mmol) in CH_2Cl_2 (30 mL) was added alcohol **122** (525 mg, 0.48 mmol). The reaction was stirred for 4 h at rt before being quenched with NH_4Cl (50 mL). The layers were separated, and the aqueous phase extracted with CH_2Cl_2 (3 × 50 mL). The combined organic layers were dried ($MgSO_4$), concentrated *in vacuo* and purified by flash column chromatography (1:20 → 1:9 EtOAc/PE) to give methyl ether **167** as a colourless oil (445 mg, 87%).

R_f 0.79 (1:3 EtOAc/PE); **^{1}H NMR** (400MHz, $CDCl_3$) δ_H 7.24 (2H, d, J = 8.7 Hz, ArH), 6.86 (2H, d, J = 8.7 Hz, ArH), 6.18 (1H, dd, J = 14.9, 10.6 Hz, H_3), 6.03 (1H, dd, J = 15.3, 10.6 Hz, H_4), 5.68 (1H, dt, J = 14.8, 7.1 Hz, H_5), 5.64 (1H, dt, J = 14.8, 5.9 Hz, H_2), 5.31 (1H, t, J = 7.2 Hz, H_{15}), 5.18 (1H, td, J = 7.2, 1.7 Hz, H_{23}), 4.41 (2H, ABq, J = 11.6 Hz, OCH_2Ar), 4.20 (2H, d, J = 5.0 Hz, H_1 × 2), 3.80 (3H, s, OMe), 3.62-3.56 (1H, m, H_7), 3.53 (1H, dd, J = 8.9, 4.5 Hz, H_{27a}), 3.48 (1H, dd, J = 5.0, 3.2 Hz, H_9), 3.38 (3H, s, OMe), 3.36-3.30 (2H, m, H_{13}, H_{27b}), 3.14 (3H, s, OMe), 2.87 (1H, dd, J = 8.2, 3.9 Hz, H_{25}), 2.31 (2H, q, J = 7.6 Hz, $H_{2'}$ × 2), 2.19-2.12 (2H, m, H_6 × 2), 2.12-1.93 (3H, m, H_{16} × 2, H_{26}), 1.83-1.68 (2H, m, H_8, H_{24}), 1.68-1.57 (2H, m, H_{12a}, H_{22a}), 1.54-1.40 (4H, m, H_{10}, H_{12} × 2, H_{22b}), 1.49 (3H, s, Me_{14}), 1.39-1.31 (4H, m, H_{11} × 2, H_{17} × 2), 1.31-1.24 (8H, m, $H_{18\text{-}21}$), 1.14 (3H, t, J = 7.4 Hz, $H_{3'}$ × 3), 1.06 (3H, d, J = 7.1 Hz, Me_{26}), 0.94 (9H, t, J = 8.1 Hz, $Si(CH_2C\underline{H}_3)_3$), 0.93 (9H, t, J = 8.1 Hz, $Si(CH_2C\underline{H}_3)_3$), 0.91 (9H, s, $SiC(C\underline{H}_3)_3$), 0.90-0.83 (9H, m, Me_8, Me_{10}, Me_{24}), 0.60 (6H, q, J = 7.6 Hz, $Si(C\underline{H}_2CH_3)_3$), 0.57 (6H, q, J = 7.6 Hz, $Si(C\underline{H}_2CH_3)_3$), 0.07 (6H, s, $Si(C\underline{H}_3)_2$).

These data are in agreement with those previously reported.[165]

(2*S*,3*S*,4*R*,5*S*,13*E*,15*S*,18*R*,19*R*,20*R*,21*R*,23*E*,25*E*)-27-((*tert*-butyldimethylsilyl)oxy)-3,15-dimethoxy-1-((4-methoxybenzyl)oxy)-2,4,14,18,20-pentamethyl-19,21-bis((triethylsilyl)oxy)heptacosa-13,23,25-trien-5-ol, 123

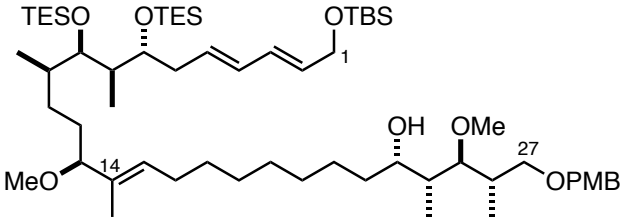

To a solution of ester **167** (1.58 g, 1.43 mmol) in CH_2Cl_2 (28 mL) was added DIBAL (2.86 mL, 2.86 mmol, 1.0 M in hexanes) at –78 °C. After 1.5 h, the reaction was quenched with NH_4Cl (25 mL) and Na^+/K^+ tartrate (25 mL) and allowed to warm to rt. The layers were separated and the aqueous was extracted with CH_2Cl_2 (3 × 25 mL) and the combined organics were dried (Na_2SO_4) and concentrated *in vacuo*. The crude was purified by flash column chromatography (1:4 EtOAc/PE) to afford alcohol **123** as a colourless oil (1.51 g, 99%).

R_f 0.62 (1:3 EtOAc/PE); **^{1}H NMR** (400MHz, $CDCl_3$) δ_H 7.26 (2H, d, J = 8.9 Hz, ArH), 6.88 (2H, d, J = 8.6 Hz, ArH), 6.18 (1H, dd, J = 15.2, 10.7 Hz, H_3), 6.04 (1H, dd, J = 15.2, 10.7 Hz, H_4), 5.68 (1H, dt, J = 14.4, 7.0 Hz, H_5), 5.64 (1H, dt, J = 15.2, 5.0 Hz, H_2), 5.31 (1H, t, J = 7.0 Hz, H_{15}), 4.44 (2H, s, OCH_2Ar), 4.20 (2H, d, J = 5.4 Hz, H_1 × 2), 3.89 (1H, t, J = 6.6 Hz, H_{23}), 3.80 (3H, s, OMe), 3.62-3.56 (1H, m, H_7), 3.54-3.50 (1H, m, H_{27a}), 3.50-3.46 (3H, m, H_9, H_{27b}, OH,), 3.44 (3H, s, OMe), 3.34 (1H, t, J = 7.1 Hz, H_{13}), 3.19 (1H, dd, J = 9.0, 3.0 Hz, H_{25}), 3.14 (3H, s, OMe), 2.19-2.10 (2H, m, H_6 × 2), 2.10-1.97 (3H, m, H_{26}, H_{16} × 2), 1.76-1.70 (2H, m, H_8, H_{24}), 1.55-1.44 (4H, m, H_{10}, H_{12} × 2, H_{22a}), 1.49 (3H, s, Me_{14}), 1.41-1.31 (5H, m, H_{11} × 2, H_{17} × 2, H_{22b}), 1.31-1.26 (8H, m, $H_{18\text{-}21}$), 1.04 (3H, d, J = 6.9 Hz, Me_{24}), 0.95 (9H, t, J = 8.1 Hz, $Si(CH_2C\underline{H}_3)_3$), 0.94 (9H, t, J = 8.1 Hz, $Si(CH_2C\underline{H}_3)_3$), 0.94-0.91 (3H, obs m, Me_{26}), 0.91 (9H, s, $SiC(C\underline{H}_3)_3$), 0.87 (3H, d, J = 7.5 Hz, Me_{10}), 0.85 (3H, d, J = 7.6 Hz, Me_8), 0.60 (6H, q, J = 8.0 Hz, $Si(C\underline{H}_2CH_3)_3$), 0.57 (6H, q, J = 8.1 Hz, $Si(C\underline{H}_2CH_3)_3$), 0.07 (6H, s, $Si(C\underline{H}_3)_2$).

These data are in agreement with those previously reported.[165]

(2*E*,4*E*,7*R*,8*R*,9*R*,10*R*,13*S*,14*E*,23*S*,24*R*,25*S*,26*S*)-23-hydroxy-13,25-dimethoxy-27-((4-methoxybenzyl)oxy)-8,10,14,24,26-pentamethyl-7,9-bis((triethylsilyl)oxy) heptacosa-2,4,14-trienal, 124

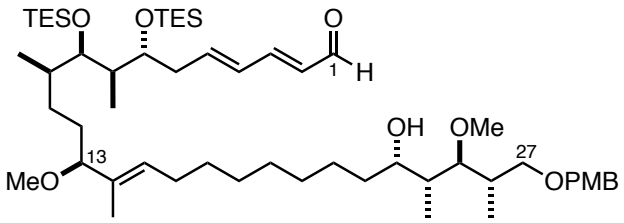

To a solution of TBS ether **123** (836 mg, 0.80 mmol) in CH_2Cl_2 (12 mL) and pH 9.2 buffer (3 mL) at 0 °C was added DDQ (200 mg, 0.88 mmol). The solution was stirred at this temperature for 15 min, then quenched with $NaHCO_3$ (60 mL) and warmed to rt. The mixture was extracted with CH_2Cl_2 (3 × 50 mL) and the combined organics were dried (Na_2SO_4) and concentrated *in vacuo*. Purification *via* flash column chromatography (1:6 EtOAc/PE) gave aldehyde **124** (560 mg, 75%, 91% brsm) as a colourless oil.

R_f 0.62 (1:3 EtOAc/PE); **^{1}H NMR** (500MHz, $CDCl_3$) δ_H 9.55 (1H, d, J = 7.9 Hz, H_1), 7.25 (2H, d, J = 7.8 Hz, ArH), 7.08 (1H, dd, J = 15.3, 10.1 Hz, H_3), 6.88 (2H, d, J = 8.5 Hz, ArH), 6.34-6.28 (2H, m, H_4, H_5), 6.08 (1H, dd, J = 15.4, 8.2 Hz, H_2), 5.31 (1H, t, J = 7.0 Hz, H_{15}), 4.43 (2H, s, OCH_2Ar), 3.90 (1H, app t, J = 6.6 Hz, H_{23}), 3.81 (3H, s, OMe), 3.70-3.63 (1H, m, H_7), 3.55-3.45 (4H, m, H_9, H_{27} × 2, OH), 3.44 (3H, s, OMe), 3.34 (1H, t, J = 6.1 Hz, H_{13}), 3.18 (1H, dd, J = 9.3, 3.7 Hz, H_{25}), 3.14 (3H, s, OMe), 2.37-2.24 (2H, m, H_6 × 2), 2.11-1.93 (3H, m, H_{16} × 2, H_{26}), 1.80-1.71 (1H, m, H_8), 1.71-1.64 (1H, m, H_{24}), 1.57-1.51 (4H, m, H_{10}, H_{22a}, H_{12} × 2), 1.49 (3H, s, Me_{14}), 1.45-1.33 (5H, m, H_{17} × 2, H_{11} × 2, H_{22b}), 1.33-1.25 (8H, m, H_{18-21}), 1.04 (3H, d, J = 7.1 Hz, Me_{24}), 0.95 (9H, t, J = 7.9 Hz, $Si(CH_2C\underline{H}_3)_3$), 0.94 (9H, t, J = 7.9 Hz, $Si(CH_2C\underline{H}_3)_3$), 0.93 (3H, obs d, J = 7.8 Hz, Me_{26}), 0.88 (3H, d, J = 6.8 Hz, Me_{10}), 0.87 (3H, d, J = 6.8 Hz, Me_8), 0.60 (6H, q, J = 7.8 Hz, $Si(C\underline{H}_2CH_3)_3$), 0.57 (6H, q, J = 7.8 Hz, $Si(C\underline{H}_2CH_3)_3$); **HRMS** calc. for $C_{54}H_{102}NO_8Si_2$ $[M+NH_4]^+$ 948.7138, found 948.7133.

These data are in agreement with those previously reported.[165]

(2*E*,4*E*,7*R*,8*R*,9*R*,10*R*,13*S*,14*E*,23*S*,24*R*,25*S*,26*S*)-23-hydroxy-13,25-dimethoxy-27-((4-methoxybenzyl)oxy)-8,10,14,24,26-pentamethyl-7,9-bis((triethylsilyl)oxy) heptacosa-2,4,14-trienoic acid, 125

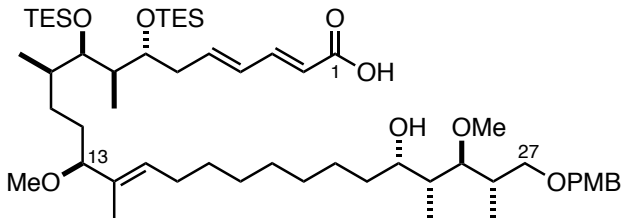

To aldehyde **124** (510 mg, 0.55 mmol) was added 2-methyl-2-butene (8.71 mL, 82.6 mmol) and the solution was cooled to 0 °C. $NaClO_2$ (1.86 g, 80% technical grade, 16.4 mmol) and $NaH_2PO_4{\cdot}H_2O$ (3.43 g, 22 mmol) were dissolved in H_2O/*t*-BuOH (34 mL, 1:1) and added to the reaction mixture. The reaction was warmed to rt and stirred for 16 h before being diluted with EtOAc (50 mL) and brine (50 mL). The mixture was extracted with EtOAc (3 × 10 mL) and the combined organics were dried (Na_2SO_4) and concentrated *in vacuo* to give *seco*-acid **125** (*ca*. 521 mg) as a pale-yellow oil. The crude material was used directly in the next reaction without further purification.

R_f 0.21 (1:4:1 EtOAc/PE/AcOH); **^{1}H NMR** (500MHz, $CDCl_3$) δ_H 7.32 (1H, dd, *J* = 15.2, 9.9 Hz, H_3), 7.25 (2H, d, *J* = 8.5 Hz, ArH), 6.88 (2H, d, *J* = 8.5 Hz, ArH), 6.27-6.12 (2H, m, H_4, H_5), 5.79 (1H, d, *J* = 15.5 Hz, H_2), 5.31 (1H, t, *J* = 7.0 Hz, H_{15}), 4.44 (2H, s, OCH_2Ar), 3.98-3.91 (1H, t, *J* = 7.1 Hz, H_{23}), 3.81 (3H, s, OMe), 3.67-3.60 (1H, m, H_7), 3.55-3.40 (2H, m, H_9, H_{27b}), 3.49-3.45 (1H, m, H_{27b}), 3.45 (3H, s, OMe), 3.35 (1H, t, *J* = 6.9 Hz, H_{13}), 3.19 (1H, dd, *J* = 8.8, 3.1 Hz, H_{25}), 3.14 (3H, s, OMe), 2.31-2.22 (2H, m, H_6 × 2), 2.12-2.06 (2H, m, H_{16a}, H_{26}), 2.01-1.93 (1H, m, H_{16b}), 1.76-1.70 (2H, m, H_8, H_{24}), 1.65-1.54 (4H, m, H_{10}, H_{12} × 2, H_{22a},), 1.50 (3H, s, Me_{14}), 1.40-1.20 (13H, m, H_{11} × 2, $H_{17\text{-}21}$, H_{22b}), 1.04 (3H, d, *J* = 7.3 Hz, Me_{24}), 0.95 (9H, t, *J* = 7.9 Hz, $Si(CH_2C\underline{H}_3)_3$), 0.94 (9H, t, *J* = 7.9 Hz, $Si(CH_2C\underline{H}_3)_3$), 0.94 (3H, obs d, *J* = 8.0 Hz, Me_{26}), 0.88 (3H, d, *J* = 6.8 Hz, Me_{10}), 0.84 (3H, d, *J* = 7.1 Hz, Me_8), 0.59 (6H, q, *J* = 7.1 Hz, $Si(C\underline{H}_2CH_3)_3$), 0.57 (6H, q, *J* = 7.8 Hz, $Si(C\underline{H}_2CH_3)_3$); **HRMS** calc. for $C_{54}H_{102}NO_9Si_2$ $[M+NH_4]^+$ 964.7081, found 964.7088.

These data are in agreement with those previously reported.[165]

(3*E*,5*E*,8*R*,9*R*,10*R*,11*R*,14*S*,15*E*,24*S*)-14-methoxy-24-((2*R*,3*S*,4*S*)-3-methoxy-5-((4-methoxybenzyl)oxy)-4-methylpentan-2-yl)-9,11,15-trimethyl-8,10-bis((triethylsilyl) oxy)oxacyclotetracosa-3,5,15-trien-2-one, 126

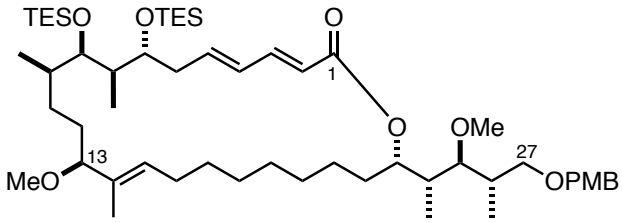

Crude *seco*-acid **125** (*ca*. 568 mg, 0.60 mmol) was dissolved in THF (15 mL) and NEt_3 (836 μL, 6.00 mmol) and TCBC (656 μL, 4.20 mmol) were added. The mixture was stirred at rt for 1 h, then diluted with PhMe (100 mL) and the resulting cloudy orange solution added to a solution of DMAP (733 mg, 6.00 mmol) in PhMe (50 mL) *via* syringe pump at a rate of 4.6 mL/h. Once complete the reaction was stirred for a further 16 h before being quenched with NH_4Cl (100 mL). The layers were separated, and the aqueous phase was extracted with EtOAc (3 × 100 mL) and the combined organics were dried (Na_2SO_4) and concentrated *in vacuo*. Flash column chromatography (1:50 → 1:9 EtOAc/PE) yielded macrocycle **126** (386 mg, 70%) as a colourless oil.

R_f 0.52 (1:5 EtOAc/PE); **^{1}H NMR** (500MHz, $CDCl_3$) δ_H 7.28 (1H, dd, *J* = 15.3, 10.0 Hz, H_3), 7.24 (2H, d, *J* = 8.9 Hz, ArH), 6.86 (2H, d, *J* = 8.5 Hz, ArH), 6.25-6.15 (2H, m, H_4, H_5), 5.83 (1H, d, *J* = 15.7 Hz, H_2), 5.38 (1H, dt, *J* = 10.8, 2.3 Hz, H_{23}), 5.24 (1H, dd, *J* = 8.0, 6.0 Hz, H_{15}), 4.41 (2H, ABq, *J* = 11.4 Hz, OCH_2Ar), 3.80 (3H, s, OMe), 3.67-3.61 (1H, m, H_7), 3.56-3.50 (2H, m, H_9, H_{27a}), 3.45 (3H, s, OMe), 3.32 (1H, dd, *J* = 9.2, 7.2 Hz, H_{27b}), 3.31 (1H, t, *J* = 8.7 Hz, H_{13}), 3.13 (3H, s, OMe), 2.90 (1H, dd, *J* = 8.3, 3.8 Hz, H_{25}), 2.35-2.26 (1H, m, H_{6a}), 2.18-2.03 (3H, m, H_{6b}, H_{16a}, H_{26}), 1.88-1.80 (1H, m, H_{16b}), 1.78-1.73 (1H, m, H_{24}), 1.73-1.64 (2H, m, H_8, H_{22a}), 1.62-1.57 (2H, m, H_{10}, H_{12a}), 1.53-1.48 (1H, m, H_{12b}), 1.48 (3H, s, Me_{14}), 1.43-1.33 (3H, m, H_{11a}, H_{21a}, H_{22b}), 1.33-1.20 (10H, m, H_{11b}, $H_{17\text{-}20}$, H_{21b},), 1.06 (3H, d, *J* = 7.1 Hz, Me_{26}), 0.96 (9H, t, *J* = 8.2 Hz, $Si(CH_2C\underline{H}_3)_3$), 0.95 (9H, t, *J* = 8.2 Hz, $Si(CH_2C\underline{H}_3)_3$), 0.94 (9H, m, Me_8, Me_{10}, Me_{24}), 0.61 (6H, q, *J* = 7.8 Hz, $Si(C\underline{H}_2CH_3)_3$), 0.58 (6H, q, *J* = 7.8 Hz, $Si(C\underline{H}_2CH_3)_3$); **^{13}C NMR** (125MHz, $CDCl_3$) δ_C 167.1, 158.9, 144.8, 141.8, 133.2, 130.8, 130.0, 129.9, 119.7, 113.6, 88.0, 85.6, 73.1, 72.6, 71.5, 61.0, 55.5, 55.1, 40.9, 40.7, 36.4, 35.9, 33.8, 31.3, 28.9, 28.5, 28.4, 28.2, 27.8, 27.7, 27.6, 24.5, 23.8, 20.7, 17.4, 17.2, 16.1, 14.6, 11.7, 11.1, 9.7, 7.0, 6.9, 5.3, 5.1; $[\boldsymbol{\alpha}]_{\boldsymbol{D}}^{\mathbf{20}}$ +10.9 (*c* 1.00, $CHCl_3$); **IR** (thin film) ν_{max} (cm^{-1}) 2930, 2876, 1711, 1643, 1614, 1580, 1513, 1458, 1367, 1300, 1245, 1171, 1134, 1091, 1038, 1001; **HRMS** calc. for $C_{54}H_{96}O_8Si_2Na$ $[M+Na]^+$ 951.6536, found 951.6541.

(3*E*,5*E*,8*R*,9*R*,10*R*,11*R*,14*S*,15*E*,24*S*)-24-((2*R*,3*S*,4*S*)-5-hydroxy-3-methoxy-4-methylpentan-2-yl)-14-methoxy-9,11,15-trimethyl-8,10-bis((triethylsilyl)oxy) oxacyclotetracosa-3,5,15-trien-2-one, 127

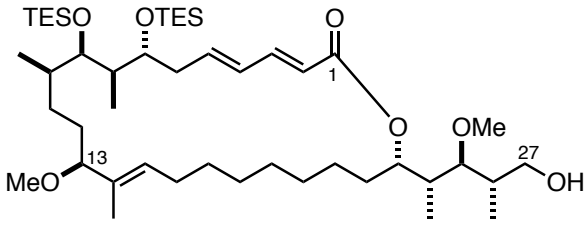

To a solution of PMB ether **126** (335 mg, 0.36 mmol) in CH_2Cl_2 (20 mL) and pH 7.0 buffer (10 mL) was added DDQ (164 mg, 0.72 mmol). The reaction was stirred for 2 h before being quenched with $NaHCO_3$ (50 mL). The solution was diluted with H_2O (100 mL) and the layers were separated. The aqueous phase was extracted with CH_2Cl_2 (3 × 100 mL) and the combined organics dried (Na_2SO_4) and concentrated *in vacuo*. The crude residue was purified by flash column chromatography (1:50 EtOAc/PhMe → 1:2 EtOAc/PE) to give alcohol **127** (238 mg, 82%) as a colourless oil.

R_f 0.21 (1:5 EtOAc/PE); **^{1}H NMR** (500MHz, $CDCl_3$) δ_H 7.28 (1H, dd, *J* = 15.1, 10.3 Hz, H_3), 6.23-6.18 (2H, m, H_4, H_5), 5.84 (1H, d, *J* = 14.8 Hz, H_2), 5.38 (1H, dt, *J* = 10.9, 2.6 Hz, H_{23}), 5.25 (1H, dd, *J* = 8.4, 5.7 Hz, H_{15}), 3.80 (1H, dd, *J* = 10.9, 3.5 Hz, H_{27a}), 3.68-3.62 (1H, m, H_7), 3.59-3.55 (2H, m, H_9, H_{27b}), 3.53 (3H, s, OMe), 3.31 (1H, dd, *J* = 8.4, 5.8 Hz, H_{13}), 3.14 (3H, s, OMe), 3.00 (1H, dd, *J* = 8.1, 3.5 Hz, H_{25}), 2.87 (1H, br s, OH), 2.35-2.27 (1H, m, H_{6a}), 2.23-2.06 (2H, m, H_{6b}, H_{16a}), 1.94-1.80 (3H, m, H_{16b}, H_{24}, H_{26}), 1.77-1.64 (2H, m, H_8, H_{22a}), 1.64-1.49 (4H, m, H_{10}, H_{12} × 2, H_{22b}), 1.47 (3H, s, Me_{14}), 1.45-1.36 (2H, m, H_{11a}, H_{21a}) 1.35-1.18 (10H, m, H_{11b}, $H_{17\text{-}20}$, H_{21b},), 1.13 (3H, d, *J* = 7.2 Hz, Me_{26}), 0.96 (9H, t, *J* = 7.9 Hz, $Si(CH_2C\underline{H}_3)_3$), 0.95 (9H, t, *J* = 7.9 Hz, $Si(CH_2C\underline{H}_3)_3$), 0.93 (3H, obs d, Me_{24}), 0.91 (3H, d, *J* = 7.6 Hz, Me_{10}), 0.89 (3H, d, *J* = 7.0 Hz, Me_8), 0.60 (6H, q, *J* = 7.8 Hz, $Si(C\underline{H}_2CH_3)_3$), 0.58 (6H, q, *J* = 7.8 Hz, $Si(C\underline{H}_2CH_3)_3$); **^{13}C NMR** (125MHz, $CDCl_3$) δ_C 167.3, 145.1, 141.8, 133.3, 130.1, 129.9, 129.1, 128.7, 119.6, 88.7, 88.1, 77.2, 73.4, 73.1, 65.1, 61.5, 41.7, 41.1, 39.6, 36.2, 36.2, 33.6, 31.4, 29.0, 28.6, 28.3, 27.9, 27.8, 27.7, 24.5, 16.2, 14.5, 11.7, 11.2, 9.8, 7.1, 7.0, 5.4, 5.2; $[\alpha]_D^{20}$ +19.2 (*c* 1.00, $CHCl_3$); **IR** (thin film) ν_{max} (cm^{-1}) 3452, 2935, 2876, 1712, 1642, 1458, 1415, 1367, 1300, 1238, 1134, 1092, 842, 739; **HRMS** calc. for $C_{46}H_{88}O_7Si_2Na$ $[M+Na]^+$ 831.5961, found 831.5957.

(2*R*,3*R*,4*R*)-3-methoxy-4-((2*S*,10*E*,12*S*,15*R*,16*R*,17*R*,18*R*,20*E*,22*E*)-12-methoxy-11,15,17-trimethyl-24-oxo-16,18-bis((triethylsilyl)oxy)oxacyclotetracosa-10,20,22-trien-2-yl)-2-methylpentanal, 53

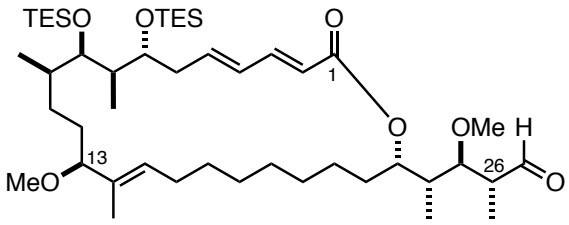

To a solution of alcohol **127** (144 mg, 0.18 mmol) in CH_2Cl_2 (17 ml) was added DMP (377 mg, 0.89 mmol) and $NaHCO_3$ (74 mg, 0.89 mmol). The mixture was stirred for 2 h before being quenched with $Na_2S_2O_3$ (50 mL). The quenching mixture was stirred for 1 h and the layers were separated. The aqueous phase was extracted with CH_2Cl_2 (3 × 50 mL) and the combined organics were dried (Na_2SO_4) and concentrated *in vacuo*. Aldehyde **53** was used immediately and crude subsequent aldol reaction.

R_f 0.68 (1:1 EtOAc/PE); **^{1}H NMR** (500MHz, $CDCl_3$) δ_H 9.74 (1H, d, J = 1.4 Hz, CHO), 7.29 (1H, dd, J = 15.0, 10.0 Hz, H_3), 6.27-6.15 (2H, m, H_4, H_5), 5.84 (1H, d, J = 14.4 Hz, H_2), 5.45 (1H, dt, J = 10.8, 2.2 Hz, H_{23}), 5.25 (1H, dd, J = 8.4, 5.7 Hz, H_{15}), 3.68-3.61 (1H, m, H_7), 3.56-3.49 (1H, m, H_9), 3.44 (3H, s, OMe), 3.34-3.26 (2H, m, H_{13}, H_{25}), 3.13 (3H, s, OMe), 2.74-2.64 (1H, m, H_{26}), 2.37-2.25 (1H, m, H_{6a}), 2.25-2.04 (2H, m, H_{6b}, H_{16a}), 1.90-1.78 (2H, m, H_{16b}, H_{24}), 1.78-1.65 (2H, m, H_8, H_{22a}), 1.65-1.49 (3H, m, H_{10}, H_{12} × 2,) 1.47 (3H, s, Me_{14}), 1.45-1.35 (3H, m, H_{11a}, H_{21a}, H_{22b}), 1.35-1.19 (10H, m, H_{11b}, $H_{17\text{-}20}$, H_{21b}), 1.16 (3H, d, J = 7.0 Hz, Me_{26}), 0.96 (18H, t, J = 7.6 Hz, $Si(CH_2C\underline{H}_3)_3$ × 2), 0.93 (3H, d, J = 7.2 Hz, Me_{10}), 0.89 (3H, d, J = 7.0 Hz, Me_8), 0.83 (3H, d, J = 7.0 Hz, Me_{24}), 0.61 (6H, q, J = 7.9 Hz, $Si(C\underline{H}_2CH_3)_3$), 0.57 (6H, q, J = 7.9 Hz, $Si(C\underline{H}_2CH_3)_3$).

These data are in agreement with those previously reported.[165]

***N*-((1*E*,3*R*,4*R*,5*R*,7*E*,9*S*,10*S*,11*R*)-4,10-dimethoxy-11-((2*S*,10*E*,12*S*,15*R*,16*R*,17*R*,18*R*,20*E*,22*E*)-12-methoxy-11,15,17-trimethyl-24-oxo-16,18-bis ((triethylsilyl)oxy) oxacyclotetracosa-10,20,22-trien-2-yl)-3,5,9-trimethyl-6-oxododeca-1,7-dien-1-yl)-*N*-methylformamide, 129**

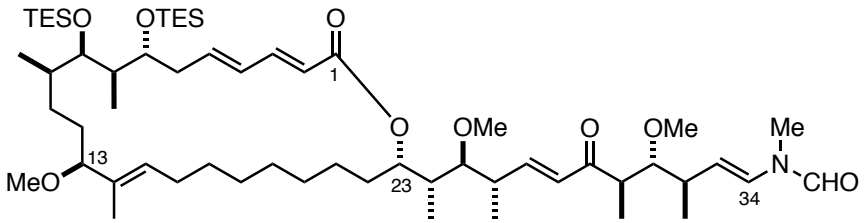

Ketone **51** was azeotropically dried with benzene and placed under vacuum for 16 h. To a solution of ketone **51** (125 mg, 0.55 mmol) in Et_2O (5 mL) at 0 °C was added a freshly prepared solution of $BCy_2Cl{\cdot}NEt_3$ (275 μL, 0.55 mmol, 2.0 M in Et_2O). The resulting cloudy yellow solution of enolate was stirred at 0 °C for 1 h before being cooled to –78 °C. A solution of crude aldehyde **53** (ca. 140 mg) in Et_2O (3 mL) was added and the reaction mixture was stirred at –78 °C for 2 h, then warmed to –10 °C over 1 h before being quenched with SiO_2 (*ca.* 1 g). The slurry was stirred for 1 h then filtered and rinsed with Et_2O (10 mL) before being concentrated *in vacuo.* The crude material was purified by flash column chromatography (3:1→1:1 EtOAc/PE). All fractions containing aldol adduct **128** and ketone **51** were combined and used subsequently in the elimination reaction.

To a solution of aldol adduct **128** and ketone **51** (*ca.* 184 mg) in THF (6 mL) was added Burgess reagent (83 mg, 0.36 mmol). The reaction mixture was stirred at room temperature for 16 h then quenched with NH_4Cl (10 mL) and extracted with EtOAc (3 × 10 mL). The combined organic layers were washed with brine (15 mL), dried ($MgSO_4$) and concentrated *in vacuo*. The crude product was purified by flash column chromatography (2:1→1:1 EtOAc/PE) yielding enone **129** (117 mg, 65% over 3 steps) and recovered ketone **51** (75 mg).

R_f 0.89 (1:1 EtOAc/PE); **^{1}H NMR** (500MHz, $CDCl_3$) δ_H 8.30 (0.60H, s, NCHO), [8.08] (0.30H, s, NCHO*), 7.30 (1H, dd, *J* = 15.4, 9.1 Hz, H_3), [7.15] (0.33H, d, *J* = 14.6 Hz, H_{34}*), 6.91 (1H, dd, *J* = 15.1, 8.1 Hz, H_{27}), 6.48 (0.67H, d, *J* = 14.3 Hz, H_{34}), 6.25-6.10 (3H, m, H_4, H_5, H_{28}), 5.83 (1H, d, *J* = 15.2 Hz, H_2), 5.40 (1H, br d, *J* = 10.7 Hz, H_{23}), 5.24 (1H, t, *J* = 6.0 Hz, H_{15}), 5.15 (1H, dd, *J* = 13.5, 9.9 Hz, H_{33}), 3.68-3.61 (1H, m, H_7), 3.56-3.51 (1H, m, H_9), 3.49 (3H, s, OMe), 3.33-3.27 (5H, m, H_{13}, H_{31}, OMe), 3.13 (3H, s, OMe), [3.10] (1H, s, NMe*), 3.06 (2H, s, NMe), 3.03-2.95 (1H, m, H_{30}), 2.95-2.89 (1H, m, H_{25}), 2.66-2.57 (1H, m, H_{26}), 2.50-2.37 (1H, m, H_{32}), 2.36-2.24 (1H, m, H_{6a}), 2.22-2.07 (2H, m,

H_{6b}, H_{16a}), 1.89-1.79 (1H, m, H_{16b}), 1.74-1.65 (2H, m, H_8, H_{22a}), 1.64-1.57 (3H, m, H_{10}, H_{12a}, H_{24},) 1.47 (3H, s, Me_{14}), 1.44-1.33 (2H, m, H_{11a}, H_{22b}), 1.32-1.19 (11H, m, H_{11b}, $H_{17\text{-}21}$), 1.18-1.12 (6H, m, Me_{26}, Me_{32}), 0.96 (18H, t, J = 7.7 Hz, $Si(CH_2C\underline{H}_3)_3$) × 2), 0.95 (3H, d, Me_{30}), 0.92 (3H, d, J = 7.1 Hz, Me_{10}), 0.89 (3H, d, J = 7.1 Hz, Me_8), 0.83 (3H, d, J = 7.4 Hz, Me_{24}), 0.60 (6H, q, J = 7.4 Hz, $Si(C\underline{H}_2CH_3)_3$), 0.58 (6H, q, J = 7.4 Hz, $Si(C\underline{H}_2CH_3)_3$); **^{13}C NMR** (125MHz, $CDCl_3$) δ_C [203.5], 203.4, [167.2], 162.2, [160.9], 149.3, [149.2], 145.1, 141.9, 133.2, [130.5], 130.1, 129.9, 128.8, [124.7], 119.5, [113.3], 111.4, 88.0, [87.6], 87.5, 86.0, 77.1, 73.4, 72.9, 61.2, 61.1, 55.4, [46.1], 46.0, 41.4, 39.6, 39.5, [37.9], 37.7, 36.5, 33.5, [33.0], 31.4, 29.0, 28.6, 28.3, 27.9, 27.8, 27.7, 27.5, 24.6, 19.5, 17.4, 14.5, 13.8, [13.7], 11.7, 10.4, [10.3], 9.8, 7.1, 7.0, 5.4, 5.2; $[\alpha]_D^{20}$ –39.7 (*c* 1.00, $CHCl_3$); **IR** (thin film) ν_{max} (cm^{-1}) 2924, 2875, 1696, 1656, 1458, 1370, 1237, 1134, 1095, 1069, 1003, 913; **HRMS** calc. for $C_{58}H_{105}NO_9Si_2Na$ $[M+Na]^+$ 1038.7220, found 1038.7230.

Distinguishable resonances of the minor rotamer (2:1 ratio) are given in brackets and assignments denoted with an asterisk.

_N_-((3_R_,4_R_,5_R_,9_S_,10_S_,11_R_,_E_)-4,10-dimethoxy-11-((2_S_,10_E_,12_S_,15_R_,16_R_,17_R_, 18_R_,20_E_,22_E_)-12-methoxy-11,15,17-trimethyl-24-oxo-16,18-bis((triethylsilyl)oxy) oxacyclotetracosa-10,20,22-trien-2-yl)-3,5,9-trimethyl-6-oxododec-1-en-1-yl)-_N_-methylformamide, 130

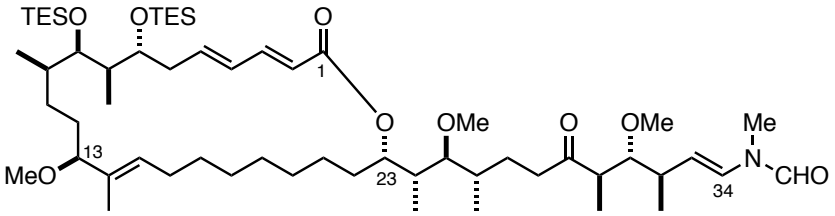

Stryker's reagent solution (104 μL, 0.0026 mmol, 0.025 M in PhMe) was added to enone **129** (54 mg, 0.052 mmol) and the reaction mixture stirred at room temperature for 1 h. Further aliquots of Stryker's reagent solution (100 μL) were added every hour for a further 4 h. The solution was applied directly to a silica gel column and the product eluted with EtOAc/CH_2Cl_2 (1:4) to afford ketone **130** (48 mg, 89%) as a colourless oil.

R_f 0.88 (1:1 EtOAc/PE); **^{1}H NMR** (500MHz, $CDCl_3$) δ_H 8.29 (0.67H, s, NCHO), [8.08] (0.33H, s, NCHO*), 7.28 (1H, dd, *J* = 15.4, 10.6 Hz, H_3), [7.15] (0.33H, d, *J* = 14.6 Hz, H_{34}*), 6.46 (0.67H, d, *J* = 14.6 Hz, H_{34}), 6.24-6.12 (2H, m, H_4, H_5), 5.83 (1H, d, *J* = 15.3 Hz, H_2), 5.42 (1H, d, *J* = 11.5 Hz, H_{23}), 5.23 (1H, t, *J* = 8.4 Hz, H_{15}), 5.15 (1H, dd, *J* = 14.6, 9.8 Hz, H_{33}), 3.67-3.59 (1H, m, H_7), 3.55-3.49 (1H, m, H_9), 3.47 (3H, s, OMe), 3.33 (3H, s, OMe), 3.23-3.27 (2H, m, H_{13}, H_{31}), 3.14 (3H, s, OMe), [3.07] (1H, s, NMe*), 3.03 (2H, s, NMe), 2.82-2.74 (1H, m, H_{25}), 2.72-2.62 (1H, m, H_{30}), 2.61-2.50 (1H, m, H_{28a}), 2.50-2.35 (2H, m, H_{28b}, H_{32}), 2.35-2.26 (1H, m, H_{6a}), 2.16-1.97 (2H, m, H_{6b}, H_{16a}), 1.88-1.79 (1H, m, H_{16b}), 1.78-1.49 (8H, m, H_8, H_{10}, H_{12} × 2, H_{22a}, H_{24}, H_{26}, H_{27a}), 1.47 (3H, s, Me_{14}), 1.43-1.33 (3H, m, H_{11a}, H_{22b}, H_{27b}), 1.32-1.19 (11H, m, $H_{17\text{-}21}$, H_{11b}), 1.15 (3H, d, *J* = 7.5 Hz, Me_{32}), 0.96-0.87 (33H, m, Me_8, Me_{10}, Me_{24}, Me_{26}, Me_{30}, $Si(CH_2C\underline{H}_3)_3$), 0.60 (6H, q, *J* = 7.7 Hz, $Si(C\underline{H}_2CH_3)_3$), 0.58 (6H, q, *J* = 7.7 Hz, $Si(C\underline{H}_2CH_3)_3$); **^{13}C NMR** (125MHz, $CDCl_3$) δ_C [214.3], 214.2, 167.2 162.1, [160.8], 144.9, 134.9, 133.2, 130.2, 130.0, 128.9, [124.5], 119.8, [113.2], 111.3, 88.0, 87.4, 87.3, 74.4, 73.4, 73.2, 61.4, 61.3, 55.5, [49.2], 49.1, 42.0, 41.0, 40.4, [37.7], 37.5, 36.5, 34.4, 33.7, [33.1], 31.4, 29.7, 29.0, 28.6, 28.3, 28.0, 27.8, 27.7, [27.4], 24.6, 23.4, [19.4], 19.3, 17.4, 14.5, 13.6, 13.5, 10.8, 9.8, 7.1, 7.0, 5.4, 5.2; $[\alpha]_D^{20}$ –22.5 (*c* 1.00, $CHCl_3$); **IR** (thin film) ν_{max} (cm^{-1}) 2934, 2869, 1706, 1657, 1458, 1369, 1238, 1068, 1004, 725; **HRMS** calc. for $C_{58}H_{107}NO_9Si_2Na$ $[M+Na]^+$ 1040.7377, found 1040.7353.

Distinguishable resonances of the minor rotamer (2:1 ratio) are given in brackets and assignments denoted with an asterisk.

6.5 Experimental procedures for Chapter 4

6.5.1 Analogue synthesis

_N_-((3_R_,4_R_,5_R_,9_S_,10_S_,11_R_,_E_)-11-((2_S_,10_E_,12_S_,15_R_,16_R_,17_R_,18_R_,20_E_,22_E_)-16,18-dihydroxy-12-methoxy-11,15,17-trimethyl-24-oxooxacyclotetracosa-10,20,22-trien-2-yl)-4,10-dimethoxy-3,5,9-trimethyl-6-oxododec-1-en-1-yl)-_N_-methylformamide, 132

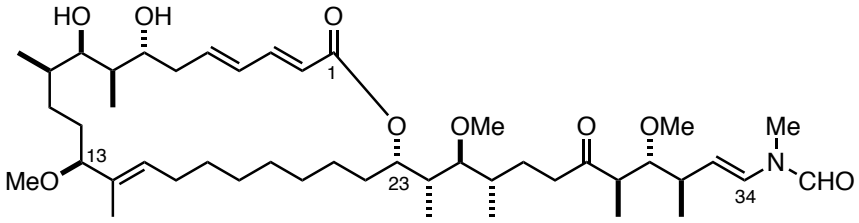

A stock solution of HF·pyridine was prepared by adding HF·pyridine (100 μL) to a solution of pyridine (200 μL) in THF (1 mL) at 0 °C before warming to rt and stirring for 30 min. This solution was added to *bis*-TES ether **130** (8 mg, 7.9 μmol) in a plastic reaction vessel at 0 °C and the reaction stirred at rt overnight. The reaction was quenched at 0 °C with $NaHCO_3$ solution (5 mL), stirred vigorously at rt for 30 min and the aqueous phase extracted with EtOAc (3 × 5 mL). The combined organics were dried (Na_2SO_4) and concentrated *in vacuo*. Purification *via* flash column chromatography (1:1:0 → 10:10:1 EtOAc/CH_2Cl_2/MeOH) yielded diol **132** (5.3 mg, 85%) as a colourless oil.

R_f 0.52 (5:5:1 EtOAc/CH_2Cl_2/MeOH); **^{1}H NMR** (500MHz, $CDCl_3$) δ_H 8.29 (0.67H, s, NCHO), [8.07] (0.33H, s, NCHO*), 7.27 (1H, obs dd, H_3), [7.13] (0.33H, d, J = 14.8 Hz, H_{34}*), 6.46 (0.67H, d, J = 13.6 Hz, H_{34}), 6.28 (1H, dd, J = 15.4, 11.1 Hz, H_4), 6.11 (1H, dt, J = 15.1, 7.4 Hz, H_5), 5.84 (1H, d, J = 15.0 Hz, H_2), 5.35 (1H, td, J = 10.2, 2.6 Hz, H_{23}), 5.30 (1H, t, J = 7.9 Hz, H_{15}), 5.11 (1H, dd, J = 14.3, 9.5 Hz, H_{33}), 3.89-3.82 (1H, m, H_7), 3.70-3.64 (1H, m, H_9), 3.46 (3H, s, OMe), 3.38-3.35 (1H, m, H_{13}), 3.34 (3H, s, OMe), 3.31 (1H, br d, J = 9.3 Hz, H_{31}), 3.15 (3H, s, OMe), [3.08] (1H, s, NMe*), 3.04 (2H, s, NMe), 2.82-2.74 (2H, m, H_{25}, OH), 2.71-2.62 (1H, m, H_{30}), 2.59-2.52 (3H, m, H_6 × 2, H_{28a}), 2.49-2.32 (3H, m, H_{28b}, H_{32}, OH), 2.09-1.94 (2H, m, H_{16} × 2), 1.80-1.54 (8H, m, H_8, H_{10}, H_{12} × 2, H_{22a}, H_{24}, H_{26}, H_{27a}), 1.53-1.47 (1H, m, H_{11a}), 1.47 (3H, s, Me_{14}), 1.47-1.33 (2H, m, H_{22b}, H_{27b}), 1.32-1.19 (11H, m, H_{11b}, $H_{17\text{-}21}$,), 1.16 (3H, d, J = 6.8 Hz, Me_{32}), 1.04 (3H, d, J = 7.1 Hz, Me_{24}), 0.97 (3H, d, J = 6.8 Hz, Me_8), 0.90 (3H, d, J = 7.1 Hz, Me_{30}), 0.90 (3H, d, J = 7.1 Hz, Me_{26}), 0.79 (3H, d, J = 7.2 Hz, Me_{10}); **^{13}C NMR** (125MHz, $CDCl_3$) δ_C [214.3], 214.2, 167.0 162.2, [160.9], 144.3, 138.9, 133.7, 131.0, 129.9, 128.8, [124.7], 120.6, [113.3], 111.4, 87.9, 87.5, 87.3, 75.3, 75.2, 73.8, 61.4, 61.3, 55.7, 49.1, 42.1, 40.7, 39.0,

[37.7], 37.5, 37.0, 34.5, 33.7, [33.1], 30.9, 29.7, 28.8, 28.7, 28.5, 27.8, 27.6, 27.3, 25.1, 23.5, 19.5, 17.4, 15.8, 13.5, 11.6, 10.9, 10.3; $[\boldsymbol{\alpha}]_{\boldsymbol{D}}^{\boldsymbol{20}}$ −46.8 (*c* 0.21, $CHCl_3$); **IR** (thin film) ν_{max} (cm^{-1}) 3349, 2939, 2853, 1703, 1655, 1461, 1360, 1277, 1134, 1065, 1002, 970, 800, 725; **HRMS** calc. for $C_{46}H_{79}NO_9Na$ $[M+Na]^+$ 812.5647, found 812.5643.

Distinguishable resonances of the minor rotamer (2:1 ratio) are given in brackets and assignments denoted with an asterisk.

(3*E*,5*E*,8*R*,9*S*,10*R*,11*R*,14*S*,15*E*,24*S*)-24-((2*R*,3*S*,4*S*,8*R*,9*R*,10*R*,*E*)-3,9-dimethoxy-4,8,10-trimethyl-12-(*N*-methylformamido)-7-oxododec-11-en-2-yl)-10-hydroxy-14-methoxy-9,11,15-trimethyl-2-oxooxacyclotetracosa-3,5,15-trien-8-yl *N*,*N*,*O*-trimethyl-*L*-serinate, 133

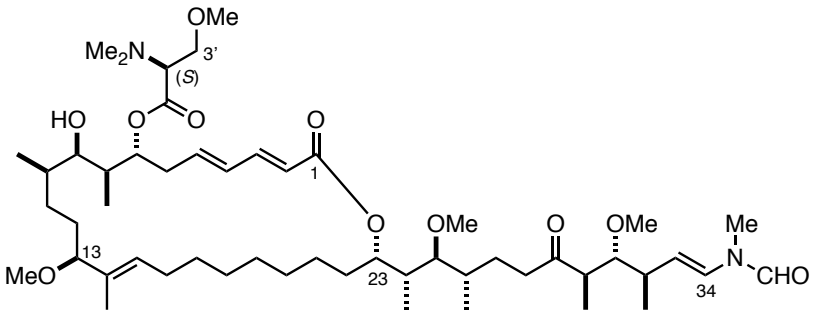

(*S*)-Trimethyl serine (3.9 mg, 26.5 μmol) and DMAP (3.2 mg, 26.3 μmol) were dissolved in CH_2Cl_2 (3 mL), then TCBC (8 μL, 51.1 μmol) and NEt_3 (11 μL, 78.9 μmol) were added to form a stock solution of mixed anhydride. Diol **132 (**2 mg, 2.65 μmol) was dissolved in benzene (0.30 mL) and an aliquot of the stock solution (0.30 mL) was added at 0 °C. Further aliquots of stock solution (0.15 mL) were added hourly for 4 h. The reaction was then quenched with MeOH (0.5 mL) and concentrated *in vacuo*. The crude residue was purified by preparative thin layer chromatography (4:4:1 EtOAc/CH_2Cl_2/MeOH) to give ester **133** as a colourless oil (1.5 mg, 62%).

R_f 0.57 (4:4:1 EtOAc/CH_2Cl_2/MeOH); **^{1}H NMR** (500MHz, $CDCl_3$) $\boldsymbol{\delta}_H$ 8.29 (0.67H, s, NCHO), [8.07] (0.33H, s, NCHO*), 7.23 (1H, obs dd, H_3), [7.12] (0.33H, d, *J* = 14.8 Hz, H_{34}*), 6.45 (0.67H, d, *J* = 14.2 Hz, H_{34}), 6.26 (1H, dd, *J* = 14.7, 11.2 Hz, H_4), 6.04 (1H, dt, *J* = 14.7, 6.7 Hz, H_5), 5.86 (1H, d, *J* = 15.1 Hz, H_2), 5.38 (1H, br d, *J* = 10.8 Hz, H_{23}), 5.28 (1H, t, *J* = 7.5 Hz, H_{15}), 5.11 (1H, dd, *J* = 14.5, 9.6 Hz, H_{33}), 5.00-4.95 (1H, m, H_7), 3.67 (1H, dd, *J* = 9.9, 2.8 Hz, $H_{3'a}$), 3.64 (1H, dd, *J* = 8.3, 4.0 Hz, $H_{3'b}$), 3.61-3.58 (1H, m, H_9), 3.46 (3H, s, OMe), 3.42-3.39 (1H, m, $H_{2'}$), 3.38-3.35 (4H, m, H_{13}, OMe), 3.34 (3H, s,

OMe), 3.31 (1H, br d, J = 9.1 Hz, H_{31}), 3.14 (3H, s, OMe), [3.08] (1H, s, NMe*), 3.04 (2H, s, NMe), 2.78 (1H, dt, J = 9.1, 2.5 Hz, H_{25}), 2.72-2.61 (1H, m, H_{30}), 2.61-2.51 (2H, m, H_{6a}, H_{28a}), 2.50-2.40 (3H, m, H_{6b}, H_{28b}, H_{32}), 2.40-2.35 (7H, m, OH, $C_{2'}NMe_2$), 1.95-1.90 (2H, m, H_{16} × 2), 1.80-1.70 (3H, m, H_{24}, H_{26}, H_{27a}) 1.65-1.58 (3H, m, H_{10}, H_{12} × 2), 1.50 (3H, s, Me_{14}), 1.46-1.35 (4H, m, H_{11a}, H_{22} × 2, H_{27b}), 1.35-1.19 (11H, m, H_{11b}, $H_{17\text{-}21}$,), 1.16 (3H, d, J = 6.9 Hz, Me_{32}), 0.99-0.95 (6H, m, Me_8, Me_{10}), 0.92 (3H, d, J = 6.5 Hz, Me_{30}), 0.90 (3H, d, J = 6.1 Hz, Me_{24}), 0.88 (3H, d, J = 6.9 Hz, Me_{26}); **^{13}C NMR** (125MHz, $CDCl_3$) $\boldsymbol{\delta}_C$ [214.3], 214.2, 170.2, 167.0, 162.2, [160.9], 144.0, 137.8, 133.8, 131.4, 129.9, 128.7, 128.2, [124.7], 121.2, [113.2], 111.4, 87.8, 87.4, 87.4, 87.3, 74.0, 73.7, 70.5, 67.6, 67.4, 61.4, [61.3], 59.2, 55.6, [49.2], 49.1, 42.5, 42.4, 42.1, [40.8], 40.8, [37.7], 37.5, 36.7, 36.4, 34.6, 34.5, 33.8, [33.1], 31.6, 29.7, 29.4, 28.9, 28.4, 28.1, 27.7, 27.6, 27.4, 22.7, [22.7], [19.4], 19.4, 17.4, 15.5, 13.5, 11.8, 10.9, 10.1; $[\boldsymbol{\alpha}]_{\boldsymbol{D}}^{\boldsymbol{20}}$ –22.1 (c 0.032, $CHCl_3$); **IR** (thin film) ν_{max} (cm^{-1}) 3390, 2451, 2896, 2853, 1711, 1678, 1651, 1462, 1360, 1272, 1220, 1079, 1002, 957, 891, 829, 701; **HRMS** calc. for $C_{52}H_{90}N_2O_{11}K$ $[M+K]^+$ 957.6176, found 957.6189.

Distinguishable resonances of the minor rotamer (2:1 ratio) are given in brackets and assignments denoted with an asterisk.

(3*E*,5*E*,8*R*,9*S*,10*R*,11*R*,14*S*,15*E*,24*S*)-24-((2*R*,3*S*,4*S*,8*R*,9*R*,10*R*,*E*)-3,9-dimethoxy-4,8,10-trimethyl-12-(*N*-methylformamido)-7-oxododec-11-en-2-yl)-10-hydroxy-14-methoxy-9,11,15-trimethyl-2-oxooxacyclotetracosa-3,5,15-trien-8-yl *N*,*N*,*O*-trimethyl-*D*-serinate, 134

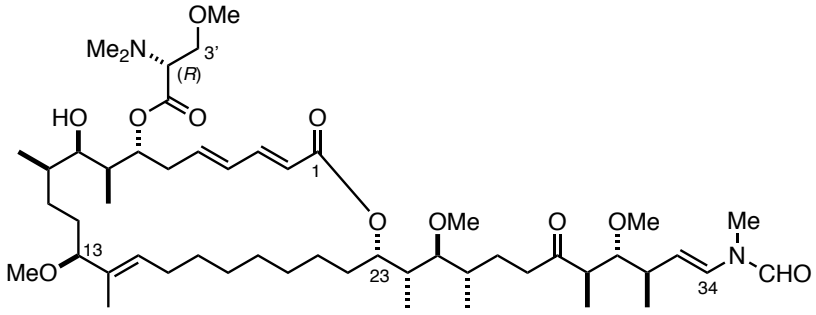

(*R*)-Trimethyl serine (3.9 mg, 26.5 μmol) and DMAP (3.2 mg, 26.3 μmol) were dissolved in CH_2Cl_2 (3 mL), then TCBC (8 μL, 51.1 μmol) and NEt_3 (11 μL, 78.9 μmol) were added to form a stock solution of mixed anhydride. Diol **132** (2.1 mg, 2.67 μmol) was dissolved in benzene (0.30 mL) and an aliquot of the stock solution (0.30 mL) was added at 0 °C. Further aliquots of stock solution (0.30 mL) were added every 30 min for 1.5 h. The

reaction was then quenched with MeOH (1.00 mL) and concentrated *in vacuo*. The crude residue was purified by flash column chromatography (1:1:0 → 4:4:1 EtOAc/CH_2Cl_2 /MeOH) to give ester **134** as a colourless oil (1.8 mg, 73%).

R_f 0.42 (5:5:1 EtOAc/CH_2Cl_2/MeOH); **^{1}H NMR** (500MHz, $CDCl_3$) δ_H 8.29 (0.67H, s, NCHO), [8.07] (0.33H, s, NCHO*), 7.26 (1H, obs dd, H_3), [7.13] (0.33H, d, J = 14.0 Hz, H_{34}*), 6.46 (0.67H, d, J = 14.1 Hz, H_{34}), 6.26 (1H, dd, J = 14.6, 11.9 Hz, H_4), 6.06-6.00 (1H, m, H_5), 5.86 (1H, d, J = 15.5 Hz, H_2), 5.38 (1H, br d, J = 10.7 Hz, H_{23}), 5.32-5.26 (1H, m, H_{15}), 5.09 (1H, dd, J = 14.3, 9.1 Hz, H_{33}), 4.99-4.95 (1H, m, H_7), 3.69 (2H, app d, J = 6.4 Hz, $H_{3'}$ × 2), 3.59-3.56 (1H, m, H_9), 3.46 (3H, s, OMe), 3.46-3.40 (1H, m, $H_{2'}$), 3.37-3.35 (4H, m, H_{13}, OMe), 3.34 (3H, s, OMe), 3.31 (1H, br d, J = 10.9 Hz, H_{31}), 3.14 (2H, s, OMe), [3.12] (1H, s, OMe*), [3.08] (1H, s, NMe*), 3.04 (2H, s, NMe), 2.78 (1H, dt, J = 8.2, 3.1 Hz, H_{25}), 2.72-2.62 (1H, m, H_{30}), 2.61-2.42 (5H, m, H_6 × 2, H_{28} × 2, H_{32}), 2.40-2.35 (7H, m, OH, $C_{2'}NMe_2$), 1.96-1.90 (2H, m, H_{16} × 2), 1.82-1.71 (3H, m, H_{24}, H_{26}, H_{27a}) 1.65-1.59 (3H, m, H_{10}, H_{12} × 2), 1.51 (3H, s, Me_{14}), 1.43-1.35 (4H, m, H_{11a}, H_{22} × 2, H_{27b}), 1.35-1.17 (11H, m, H_{11b}, H_{17-21},), 1.15 (3H, d, J = 7.0 Hz, Me_{32}), 0.99-0.95 (6H, m, Me_8, Me_{10}), 0.92 (3H, d, J = 6.6 Hz, Me_{30}), 0.90 (3H, d, J = 6.4 Hz, Me_{24}), 0.88 (3H, d, J = 7.0 Hz, Me_{26}); **^{13}C NMR** (125MHz, $CDCl_3$) δ_C [214.3], 214.2, 169.9, 166.9, 162.2, [160.8], 143.8, 138.8, 137.6, 133.8, 132.1, 131.5, 129.9, 128.7, 128.5, 127.7, 125.0, [124.7], 121.2, [113.2], 111.4, 87.8, 87.4, 87.4, 87.3, 74.0, 73.7, 71.3, 67.2, 61.4, [61.4], 61.3, 59.1, 55.6, [49.2], 49.1, 42.3, 42.1, 40.8, [37.7], 37.5, 36.6, 36.3, 34.6, 34.5, 33.8, [33.1], 30.5, 29.7, 29.4, 29.0, 28.4, 28.2, 27.7, 27.6, 27.5, 22.7, [19.4], 19.4, 17.4, 15.5, [13.6], 13.5, 11.6, 10.9, [10.9], 10.1; $[\alpha]_D^{20}$ −7.1 (*c* 0.028, $CHCl_3$); **IR** (thin film) ν_{max} (cm^{-1}) 3392, 2896, 2846, 1710, 1675, 1651, 1461, 1343, 1288, 1221, 1082, 1003, 960, 892, 829, 700; **HRMS** calc. for $C_{52}H_{90}N_2O_{11}Na$ $[M+Na]^+$ 941.6442, found 941.6402.

Distinguishable resonances of the minor rotamer (2:1 ratio) are given in brackets and assignments denoted with an asterisk.

_N_-((3_R_,4_R_,5_S_,6_R_,9_S_,10_S_,11_R_,_E_)-6-hydroxy-4,10-dimethoxy-11-((2_S_,10_E_,12_S_,15_R_, 16_R_,17_R_,18_R_,20_E_,22_E_)-12-methoxy-11,15,17-trimethyl-24-oxo-16,18-bis((triethyl silyl)oxy)oxacyclotetracosa-10,20,22-trien-2-yl)-3,5,9-trimethyldodec-1-en-1-yl)-_N_-methylformamide, 135

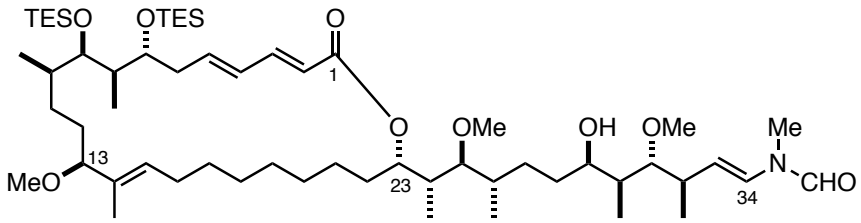

$Zn(BH_4)_2$ solution (1.12 mL, 0.175 M in Et_2O, 0.196 mmol) was added to ketone **130** (20 mg, 0.0196 mmol) at 0 °C and the reaction stirred at this temperature for 5 h before being quenched with NH_4Cl (5 mL) and Na^+/K^+ tartrate solution (10 mL). The quenching mixture was stirred vigorously for 3 h then extracted with CH_2Cl_2 (3 × 10 mL). The combined organics were dried over Na_2SO_4 and concentrated *in vacuo*. The crude product was purified by flash chromatography (1:0 → 4:1 → 1:1 CH_2Cl_2/EtOAc) to yield alcohol **135** as a colourless oil (11.5 mg, 58%, 2:1 *dr*).

R_f 0.45 (1:2 EtOAc/CH_2Cl_2); **^{1}H NMR** (500MHz, $CDCl_3$) δ_H 8.29 (0.66H, s, NCHO), [8.07] (0.33H, s, NCHO*), 7.28 (1H, dd, *J* = 15.2, 9.8 Hz, H_3), [7.15] (0.33H, d, *J* = 14.7 Hz, H_{34}*), 6.49 (0.66H, d, *J* = 14.3 Hz, H_{34}), 6.24-6.14 (2H, m, H_4, H_5), 5.84 (1H, d, *J* = 15.1 Hz, H_2), 5.42 (1H, dd, *J* = 10.9, 2.0 Hz, H_{23}), 5.24 (1H, t, *J* = 7.8 Hz, H_{15}), [5.15] (0.37H, dd, *J* = 15.2, 8.8 Hz, H_{33}*), 5.07 (0.60H, dd, *J* = 14.2, 8.3 Hz, H_{33}), 3.90-3.83 (1H, m, H_{29}), 3.67-3.61 (1H, m, H_7), 3.55-3.40 (1H, m, H_9), 3.48 (3H, s, OMe), 3.46 (3H, s, OMe), 3.30 (1H, dd, *J* = 8.1, 5.9 Hz, H_{13}), [3.06] (1H, s, NMe*), 3.02 (2H, s, NMe), 3.01 (1H, obs dd, H_{31}), 2.79 (1H, dd, *J* = 11.0, 2.1 Hz, H_{25}), 2.60-2.46 (1H, m, H_{32}), 2.38-2.27 (1H, m, H_{6a}), 2.17-2.00 (3H, m, H_{6b}, H_{16} × 2), 1.88-1.77 (1H, m, H_{22a}), 1.75-1.61 (4H, m, H_8, H_{22b}, H_{24}, H_{26}), 1.61-1.55 (4H, m, H_{10}, H_{12} × 2, H_{30}), 1.51-1.48 (2H, m, H_{28} × 2), 1.47 (3H, s, Me_{14}), 1.43-1.33 (4H, m, H_{11} × 2, H_{27} × 2), 1.31-1.20 (10H, m, $H_{17\text{-}21}$), [1.10] (1H, d, *J* = 6.7 Hz, Me_{32}*), 1.07 (2H, d, *J* = 6.7 Hz, Me_{32}), 1.00 (3H, d, *J* = 6.7 Hz, Me_{26}), 0.97 (3H, obs d, Me_8), 0.96 (9H, t, *J* = 8.3 Hz, $Si(CH_2C\underline{H}_3)_3$), 0.95 (9H, t, *J* = 8.3 Hz, $Si(CH_2C\underline{H}_3)_3$), 0.92-0.86 (9H, m, Me_{10}, Me_{24}, Me_{30}), 0.60 (6H, q, *J* = 8.0 Hz, $Si(C\underline{H}_2CH_3)_3$), 0.58 (6H, q, *J* = 8.0 Hz, $Si(C\underline{H}_2CH_3)_3$); **^{13}C NMR** (125MHz, $CDCl_3$) δ_C 167.3, 162.2, [160.8], 144.9, 135.2, 134.5, 133.1, 132.1, 131.9, 130.1, 129.9, 128.5, 125.0, [124.5], 122.3, 119.8, 114.5, [113.0], 90.5, 90.1, 88.0, [87.6], 87.5, 74.3, 73.6, 73.3, 71.8, 71.5, 61.9, [61.2], 55.4, [40.9], 40.4, 40.1, 39.3, 38.8, 38.1, 35.5, 33.7, [33.1], 31.9, 31.4, 30.7, 29.7,

29.6, 29.1, 28.9, 28.7, 28.3, 27.9, 27.7, 27.5, 26.6, 25.7, 24.6, 23.4, 22.7, 18.8, 17.7, 14.5, 14.1, [10.9], 10.8, 9.8, 9.7, 7.1, 7.0, 5.4, 5.2; $[\boldsymbol{\alpha}]_{\boldsymbol{D}}^{\boldsymbol{20}}$ −15.1 (*c* 0.46, $CHCl_3$); **IR** (thin film) ν_{max} (cm^{-1}) 3445, 2933, 2876, 1698, 1657, 1461, 1240, 1225, 1006, 727, 669; **HRMS** calc. for $C_{58}H_{109}NO_9Si_2Na$ $[M+Na]^+$ 1042.7533, found 1042.7539.

Distinguishable resonances of the minor rotamer (2:1 ratio) are given in brackets and assignments denoted with an asterisk.

(3*R*,4*R*,5*S*,6*R*,9*S*,10*S*,11*R*,*E*)-4,10-dimethoxy-11-((2*S*,10*E*,12*S*,15*R*,16*R*,17*R*,18*R*, 20*E*,22*E*)-12-methoxy-11,15,17-trimethyl-24-oxo-16,18-bis((triethylsilyl)oxy) oxacyclotetracosa-10,20,22-trien-2-yl)-3,5,9-trimethyl-1-(*N*-methylformamido) dodec-1-en-6-yl-(*R*)-3,3,3-trifluoro-2-methoxy-2-phenyl propanoate, 136

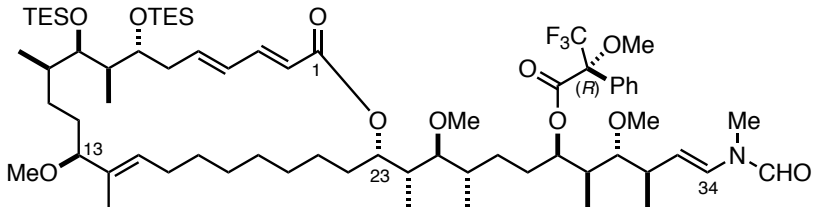

To a solution of alcohol **135** (2 mg, 1.96 μmol) in CH_2Cl_2 (0.10 mL) was added DMAP (1 crystal), DMAP hydrochloride (1 crystal), DCC (7 μL, 1M in CH_2Cl_2, 9.82 μmol) and (*R*)-(-)-MTPA OH (2 mg, 9.82 μmol) and the mixture was stirred for 16 h. Once complete, the reaction was purified by flash column chromatography (1:4 EtOAc/CH_2Cl_2) to give (*R*)-Mosher ester **136** as a colourless oil (1.5 mg, 63%).

R_f 0.78 (1:3 EtOAc/CH_2Cl_2); **^{1}H NMR** (500MHz, $CDCl_3$) $\boldsymbol{\delta}_H$ 8.27 (0.66H, s, NCHO), [8.05] (0.33H, s, NCHO*), 7.61-7.56 (2H, m, ArH), 7.44-7.37 (3H, m, ArH), 7.30 (1H, obs dd, H_3), [7.11] (0.33H, d, *J* = 14.7 Hz, H_{34*}), 6.43 (0.66H, d, *J* = 14.5 Hz, H_{34}), 6.24-6.14 (2H, m, H_4, H_5), 5.84 (1H, d, *J* = 15.1 Hz, H_2), 5.38 (1H, dd, *J* = 10.9, 2.1 Hz, H_{23}), 5.36 (1H, app q, *J* = 8.4 Hz, H_{29}), 5.24 (1H, t, *J* = 7.4 Hz, H_{15}), [5.13] (0.47H, dd, *J* = 15.2, 8.8 Hz, H_{33*}), 5.06 (1H, dd, *J* = 13.9, 7.9 Hz, H_{33}), 3.68-3.61 (1H, m, H_7), 3.56-3.51 (1H, m, H_9), 3.49 (3H, s, OMe), 3.47 (3H, s, OMe), 3.38 (3H, s, OMe), 3.31 (1H, dd, *J* = 8.2, 5.9 Hz, H_{13}), 3.15 (3H, s, OMe), [3.04] (1H, s, NMe*), 3.00 (2H, s, NMe), 2.74 (1H, dt, *J* = 8.8, 2.7 Hz, H_{25}), 2.65 (1H, td, *J* = 9.6, 1.7 Hz, H_{31}), 2.43-2.22 (3H, m, $H_6 \times 2$, H_{32}), 2.15-2.08 (2H, m, $H_{16} \times 2$), 1.91-1.71 (2H, m, H_8, H_{22a}), 1.65-1.55 (7H, m, H_{10}, $H_{12} \times 2$, H_{22b}, H_{24}, H_{26}, H_{30}), 1.54-1.43 (4H, m, $H_{28} \times 2$, Me_{14}), 1.42-1.36 (4H, m, $H_{11} \times 2$, $H_{27} \times 2$), 1.32-

1.22 (10H, m, $H_{17\text{-}21}$,), 1.10 (3H, d, J = 6.8 Hz, Me_{32}), 0.99 (3H, d, J = 7.0 Hz, Me_{26}), 0.97 (3H, obs d, Me_8), 0.96 (9H, t, J = 8.0 Hz, $Si(CH_2C\underline{H}_3)_3$), 0.95 (9H, t, J = 8.0 Hz, $Si(CH_2C\underline{H}_3)_3$), 0.87 (3H, d, J = 6.6 Hz, Me_{24}), 0.84 (3H, d, J = 6.6 Hz, Me_{10}), 0.78 (3H, d, J = 6.6 Hz, Me_{30}), 0.60 (6H, q, J = 8.1 Hz, $Si(C\underline{H}_2CH_3)_3$), 0.58 (6H, q, J = 8.1 Hz, $Si(C\underline{H}_2CH_3)_3$).

Distinguishable resonances of the minor rotamer (2:1 ratio) are given in brackets and assignments denoted with an asterisk.

(3*R*,4*R*,5*S*,6*R*,9*S*,10*S*,11*R*,*E*)-4,10-dimethoxy-11-((2*S*,10*E*,12*S*,15*R*,16*R*,17*R*,18*R*,20*E*,22*E*)-12-methoxy-11,15,17-trimethyl-24-oxo-16,18-bis((triethylsilyl)oxy)oxacyclotetracosa-10,20,22-trien-2-yl)-3,5,9-trimethyl-1-(*N*-methylformamido)dodec-1-en-6-yl (*S*)-3,3,3-trifluoro-2-methoxy-2-phenylpropanoate, 137

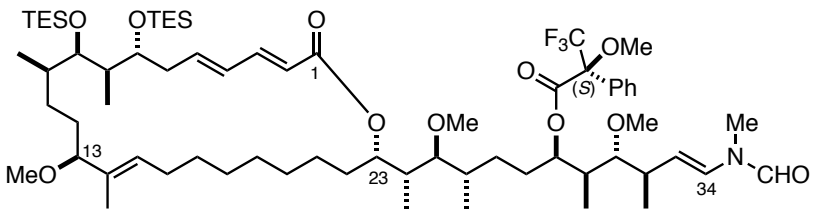

To a solution of alcohol **135** (1.8 mg, 1.77 μmol) in CH_2Cl_2 (0.10 mL) was added DMAP (1 crystal), DMAP hydrochloride (1 crystal), DCC (7 μL, 1M in CH_2Cl_2, 9.82 μmol) and (*S*)-(-)-MTPA OH (2 mg, 9.82 μmol) and the mixture was stirred for 16 h. Once complete, the reaction was purified by flash column chromatography (1:4 EtOAc/CH_2Cl_2) to give (*S*)-Mosher ester **137** as a colourless oil (1.6 mg, 72%).

R_f 0.78 (1:3 EtOAc/CH_2Cl_2); **^{1}H NMR** (500MHz, $CDCl_3$) δ_H 8.27 (0.66H, s, NCHO), [8.05] (0.33H, s, NCHO*), 7.62-7.56 (2H, m, ArH), 7.43-7.37 (3H, m, ArH), 7.29 (1H, obs dd, H_3), [7.10] (0.33H, d, J = 14.5 Hz, H_{34*}), 6.41 (0.66H, d, J = 14.5 Hz, H_{34}), 6.24-6.14 (2H, m, H_4, H_5), 5.83 (1H, d, J = 15.5 Hz, H_2), 5.39 (1H, dd, J = 10.7, 2.4 Hz, H_{23}), 5.35 (1H, app q, J = 8.4 Hz, H_{29}), 5.24 (1H, t, J = 8.2 Hz, H_{15}), [5.10] (0.37H, dd, J = 14.3, 8.2 Hz, H_{33*}), 5.04 (0.6H, dd, J = 14.7, 8.2 Hz, H_{33}), 3.67-3.59 (1H, m, H_7), 3.57 (3H, s, OMe), 3.55-3.40 (1H, m, H_9), 3.45 (3H, s, OMe), 3.39 (3H, s, OMe), 3.31 (1H, dd, J = 8.4, 5.7 Hz, H_{13}), 3.15 (3H, s, OMe), [3.03] (1H, s, NMe*), 3.00 (2H, s, NMe), 2.75 (1H, dt, J = 8.9, 2.2 Hz, H_{25}), 2.64 (1H, td, J = 9.6, 1.7 Hz, H_{31}), 2.41-2.24 (3H, m, $H_6 \times 2$, H_{32}), 2.17-2.08 (2H, m, $H_{16} \times 2$), 1.90-1.72 (2H, m, H_8, H_{22a}), 1.65-1.55 (7H, m, H_{10}, $H_{12} \times 2$, H_{22b}, H_{24}, H_{26}, H_{30}), 1.51-1.44 (5H, m, $H_{28} \times 2$, Me_{14}), 1.43-1.35 (4H, m, $H_{11} \times 2$, $H_{27} \times 2$), 1.32-

1.22 (10H, m, $H_{17\text{-}21}$,), 1.09 (3H, d, J = 6.8 Hz, Me_{32}), 1.00 (3H, d, J = 7.0 Hz, Me_{26}), 0.97 (3H, obs d, Me_8), 0.96 (9H, t, J = 8.2 Hz, $Si(CH_2C\underline{H}_3)_3$), 0.95 (9H, t, J = 8.2 Hz, $Si(CH_2C\underline{H}_3)_3$), 0.89 (3H, d, J = 6.6 Hz, Me_{24}), 0.84 (3H, d, J = 6.6 Hz, Me_{10}), 0.76 (3H, d, J = 6.6 Hz, Me_{30}), 0.60 (6H, q, J = 8.2 Hz, $Si(C\underline{H}_2CH_3)_3$), 0.58 (6H, q, J = 8.2 Hz, $Si(C\underline{H}_2CH_3)_3$).

Distinguishable resonances of the minor rotamer (2:1 ratio) are given in brackets and assignments denoted with an asterisk.

_N_-((3_R_,4_R_,5_S_,6_R_,9_S_,10_S_,11_R_,_E_)-6-hydroxy-4,10-dimethoxy-11-((2_S_,10_E_,12_S_,15_R_, 16_R_,17_R_,18_R_,20_E_,22_E_)-12-methoxy-11,15,17-trimethyl-24-oxo-16,18-bis((triethyl silyl)oxy)oxacyclotetracosa-10,20,22-trien-2-yl)-3,5,9-trimethyldodec-1-en-1-yl)-_N_-methylformamide, 138

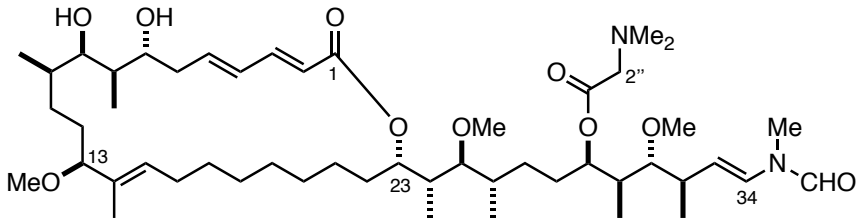

DMAP (11 mg, 8.8 μmol), DMAP hydrochloride (14 mg, 8.8 μmol), dimethylglycine (9 mg, 8.8 μmmol) and alcohol **135** (9 mg, 8.8 μmmol) were dissolved in CH_2Cl_2 (0.50 mL). DCC (88 μL, 8.8 μmol, 1M in CH_2Cl_2) was added and the reaction stirred for 16 h before being quenched with $NaHCO_3$ (2 mL). The layers were separated, and the aqueous phase extracted with CH_2Cl_2 (3 × 5 mL). The combined organics were dried (Na_2SO_4), concentrated *in vacuo* and the crude material transferred to a plastic reaction vessel.

A stock solution of HF·pyridine was prepared by adding HF·pyridine (100 μL) to a solution of pyridine (200 μL) in THF (1 mL) at 0 °C before warming to rt and stirring for 30 min. This solution was added the crude material 0 °C and the reaction stirred at rt overnight. The reaction was quenched at 0 °C with $NaHCO_3$ solution (5 mL), stirred vigorously at rt for 30 min and the aqueous phase extracted with EtOAc (3 × 5 mL). The combined organics were dried (Na_2SO_4) and concentrated *in vacuo*. Purification *via* flash column chromatography (1:1:0 → 4:4:1 EtOAc/CH_2Cl_2/MeOH) yielded diol **138** (5.3 mg, 69%) as a colourless oil.

R_f 0.45 (4:4:1 EtOAc/CH_2Cl_2/MeOH); **^{1}H NMR** (500MHz, $CDCl_3$) δ_H 8.28 (0.66H, s, NCHO), [8.06] (0.33H, s, NCHO*), 7.27 (1H, obs dd, H_3), [7.12] (0.33H, d, J = 14.5 Hz,

H_{34*}), 6.45 (0.66H, d, J = 14.5 Hz, H_{34}), 6.28 (1H, dd, J = 15.3, 11.0 Hz, H_4), 6.12 (1H, dt, J = 15.2, 7.8 Hz, H_5), 5.84 (1H, d, J = 15.7 Hz, H_2), 5.35-5.27 (2H, m, H_{23}, H_{29}), 5.24 (1H, t, J = 6.9 Hz, H_{15}), 5.11 (1H, dd, J = 14.5, 10.0 Hz, H_{33}), 3.88-3.80 (1H, m, H_7), 3.70-3.59 (1H, m, H_9), 3.53-3.46 (2H, m, $H_{2''}$ × 2), 3.44 (3H, s, OMe), 3.43 (3H, s, OMe), 3.41 (1H, obs dd, H_{13}), 3.15 (3H, s, OMe), [3.05] (1H, s, NMe*), 3.00 (2H, s, NMe), 2.81 (1H, dd, J = 9.8, 2.1 Hz, H_{25}), 2.75 (1H, dd, J = 8.4, 2.4 Hz, H_{31}), 2.59-2.42 (3H, m, H_6 × 2, H_{32}), 2.39 (6H, s, $C_{2''}NMe_2$), 2.10-1.99 (2H, m, H_{16} × 2), 1.73-1.65 (6H, m, H_8, H_{22a}, H_{24}, H_{26}, H_{28} × 2), 1.64-1.51 (5H, m, H_{10}, H_{12} × 2, H_{22b}, H_{30}), 1.38-1.31 (4H, m, H_{11} × 2, H_{27} × 2), 1.48 (3H, s, Me_{14}), 1.30-1.19 (10H, m, $H_{17\text{-}21}$,), 1.16 (3H, d, J = 6.6 Hz, Me_{32}), 1.04 (3H, d, J = 6.6 Hz, Me_8), 0.97 (3H, d, J = 7.4 Hz, Me_{26}), 0.88-0.82 (6H, m, Me_{10}, Me_{24}), 0.79 (3H, d, J = 7.4 Hz, Me_{30}); **^{13}C NMR** (125MHz, $CDCl_3$) δ_C 170.2, 167.0, 162.2, [160.9], 156.7, 144.3, 139.0, 133.7, 130.9, 129.9, 128.8, 128.6, [124.6], 120.5, [113.4], 111.7, 87.9, 87.3, 86.6, 75.3, 74.0, 73.9, 61.3, [61.1], 60.3, 55.6, 49.1, 45.2, 40.6, [39.3], 39.1, 39.0, 38.1, [37.8], 37.0, 36.9, 35.2, 33.9, 33.6, [33.1], 30.9, 29.7, 28.8, 28.7, 28.5, 27.8, 27.6, 27.3, 24.9, 20.3, [17.4], 17.3, 15.7, [11.6], 11.1, 10.3, 9.8, 9.7; $[\alpha]_D^{20}$ −13.9 (*c* 0.16, $CHCl_3$); **IR** (thin film) ν_{max} (cm^{-1}) 3325, 2952, 2853, 1708, 1690, 1656, 1635, 1559, 1448, 1254, 1159, 1091 975; **HRMS** calc. for $C_{50}H_{88}N_2O_{10}Na$ $[M+Na]^+$ 899.6337, found 899.6324.

Distinguishable resonances of the minor rotamer (2:1 ratio) are given in brackets and assignments denoted with an asterisk.

(3*E*,5*E*,8*R*,9*S*,10*R*,11*R*,14*S*,15*E*,24*S*)-24-((2*R*,3*S*,4*S*,7*R*,8*S*,9*R*,10*R*,*E*)-7-((dimethylglycyl)oxy)-3,9-dimethoxy-4,8,10-trimethyl-12-(*N*-methylformamido)dodec-11-en-2-yl)-10-hydroxy-14-methoxy-9,11,15-trimethyl-2-oxooxacyclotetracosa-3,5,15-trien-8-yl *N*,*N*,*O*-trimethyl-*L*-serinate, 44

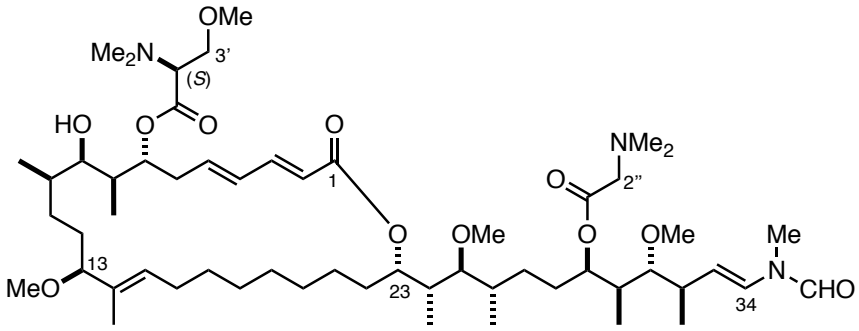

(*S*)-Trimethyl serine (6.7 mg, 46.1 μmol) and DMAP (5.6 mg, 46.1 μmol) were dissolved in CH_2Cl_2 (3 mL) and TCBC (15 μL, 92.3 μmol) and NEt_3 (13 μL, 92.3 μmol) were added to form a stock solution of mixed anhydride. Diol **138** (2 mg, 46.1 μmol) was dissolved in

benzene (0.30 mL) and an aliquot of the stock solution (0.40 mL) was added at 0 °C. Further aliquots of stock solution (0.40 mL) were added every 30 min for 2 h. The reaction was then quenched with MeOH (1.5 mL) and concentrated *in vacuo*. The crude residue was purified by flash column chromatography (1:0:0 → 1:1:0 → 4:4:1CH_2Cl_2/EtOAc/MeOH) to give ester **44** as a colourless oil (1.4 mg, 65%).

R_f 0.31 (4:4:1 EtOAc/CH_2Cl_2/MeOH); **^{1}H NMR** (500MHz, $CDCl_3$) δ_H 8.28 (0.66H, s, NCHO), [8.06] (0.33H, s, NCHO*), 7.24 (1H, obs dd, H_3), [7.12] (0.33H, d, J = 14.4 Hz, H_{34*}), 6.46 (0.66H, d, J = 14.2 Hz, H_{34}), 6.28 (1H, dd, J = 14.8, 11.1 Hz, H_4), 6.03 (1H, dt, J = 15.2, 7.8 Hz, H_5), 5.86 (1H, d, J = 15.4 Hz, H_2), 5.34 (1H, dt, J = 9.5, 2.4 Hz, H_{15}), 5.31-5.25 (2H, m, H_{23}, H_{29}), 5.08 (1H, dd, J = 14.6, 9.4 Hz, H_{33}), 5.01-4.95 (1H, m, H_7), 3.82-3.68 (2H, m, $H_{3'}$ × 2, $H_{2''}$ × 2), 3.60-3.55 (1H, m, H_9), 3.44 (3H, s, OMe), 3.43 (3H, s, OMe), 3.37 (3H, s, OMe) 3.42-3.38 (1H, m, $H_{2'}$), 3.35 (1H, br d, J = 6.4 Hz, H_{13}), 3.15 (3H, s, OMe), [3.05] (1H, s, NMe*), 3.00 (2H, s, NMe), 2.81 (1H, dd, J = 9.1, 2.5 Hz, H_{25}), 2.76 (1H, dd, J = 8.4, 2.7 Hz, H_{31}), 2.58 (6H, s, $C_{2'}$ NMe_2), 2.52 (7H, s, $C_{2''}NMe_2$, H_{32}), 2.50-2.41 (2H, m, H_6 × 2), 1.96-1.86 (2H, m, H_{16} × 2), 1.72-1.66 (4H, m, H_8, H_{22a}, H_{24}, H_{26},), 1.64-1.53 (7H, m, H_{10}, H_{12} × 2, H_{22b}, H_{28} × 2, H_{30}), 1.38-1.29 (4H, m, H_{11} × 2, H_{27} × 2), 1.50 (3H, s, Me_{14}), 1.28-1.19 (10H, m, $H_{17\text{-}21}$,), 1.15 (3H, d, J = 6.6 Hz, Me_{32}), 0.98 (6H, d, J = 7.4 Hz, Me_8, Me_{26}), 0.88 (3H, d, J = 6.8 Hz, Me_{10}), 0.86 (3H, d, J = 6.8 Hz, Me_{24}), 0.83 (3H, d, J = 7.0 Hz, Me_{30}); **^{13}C NMR** (125MHz, $CDCl_3$) δ_C 169.1, [168.5], 166.9, 162.2, 160.9, 143.9, 137.7, 135.2, 133.8, 131.4, 129.9, 128.7, 127.6, 125.0, [124.7], 121.1, [113.6], 111.7, 87.7, [87.3], 86.6, 74.1, 73.7, 70.3, 67.0, 61.9, 61.3, [61.3], 59.2, 55.6, 49.2, 45.2, 42.2, 40.8, 39.2, 39.0, 38.1, 37.8, 36.5, 35.2, 34.3, 33.9, 33.7, [33.1], 30.4, 29.7, 29.4, 29.0, 28.4, 28.1, 27.8, 27.6, 27.5, 26.4, 25.9, 23.4, 22.7, 20.1, 17.6, [17.5], 15.5, 14.1, [11.6], 11.1, 10.2, 9.9, 9.8; $[\alpha]_D^{20}$ –4.5 (*c* 0.056, $CHCl_3$); **IR** (thin film) ν_{max} (cm^{-1}) 3456, 2940, 2925, 2912, 1714, 1692, 1649, 1613, 1546, 1454, 1368, 1258, 1218, 1129, 1094, 852, 820, 780, 731; **HRMS** calc. for $C_{55}H_{98}N_3O_{11}$ $[M+H]^+$ 992.7151 found 992.7126.

Distinguishable resonances of the minor rotamer (2:1 ratio) are given in brackets and assignments denoted with an asterisk.

6.5.2 Linker synthesis

2,5-dioxopyrrolidin-1-yl (((9*H*-fluoren-9-yl)methoxy)carbonyl)-*L*-valinate, 148

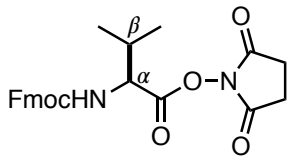

Fmoc-Val-OSuc

To a solution of Fmoc-Val-OH **147** (500 mg, 1.47 mmol) in THF (4 mL) at 0 °C was added *N*-hydroxysuccinimide (254 mg, 2.21 mmol) and DCC (303 mg, 1.47 mmol). The reaction was stirred at this temperature for 2 h before warming to rt for 16 h. The suspension was filtered and the solid was washed with THF (3 × 4 mL). The filtrate was concentrated *in vacuo* to produce Fmoc-Val-OSuc **148** as a glassy solid (580 mg, 90%) which was used in the next reaction without further purification.

^{1}H NMR (400 MHz, DMSO-d_6) δ_H 8.14 (1H, d, J = 8.5 Hz, CONHVal), 7.89 (2H, d, J = 7.8 Hz, ArH), 7.74 (2H, t, J = 8.8 Hz, ArH), 7.42 (2H, t, J = 7.8 Hz, ArH), 7.33 (2H, t, J = 8.3 Hz, ArH), 4.39-4.20 (4H, m, Fmoc CH_2, Fmoc CH, H_αVal), 2.82 (4H, s, $NCOCH_2$), 2.28-2.15 (1H, m, H_βVal), 1.03 (6H, d, J = 6.1 Hz, CH_3 × 2 Val); **^{13}C NMR** (101 MHz, DMSO-d_6) δ_C 170.0, 167.9, 156.3, 143.8, 143.6, 140.7, 127.7, 127.1, 125.3, 125.3, 120.1, 66.1, 58.0, 46.6, 30.1, 25.5, 25.2, 18.6, 18.0.

These data are in agreement with those previously reported.[252]

(*S*)-2-((*S*)-2-((((9*H*-fluoren-9-yl)methoxy)carbonyl)amino)-3-methylbutanamido)-5-ureidopentanoic acid, 149

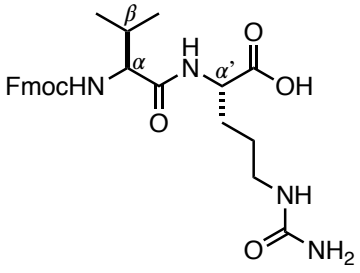

Fmoc-Val-Cit-OH

To a solution of Fmoc-Val-OSuc **148** (3.50 g, 8.02 mmol) in DME (26 mL) at 0 °C was added a solution of *L*-citrulline (1.96 g, 11.2 mmol) and $NaHCO_3$ (944 mg, 11.2 mmol) in H_2O (26 mL) slowly. THF (13 mL) was added to aid solubility. The resulting solution was

warmed to rt and stirred for 48 h. K_2CO_3 (20 ml, sat. aq.) was added and the aqueous layer extracted with EtOAc (2 × 40 mL). The aqueous phase was then acidified to pH 3-4 with 10% HCl (30 mL) upon which a gelatinous material formed. The material was extracted with 10% IPA/EtOAc (7 × 300 mL) and the organics were dried ($MgSO_4$) and concentrated *in vacuo*. The resulting white solid was washed with MTBE (3 × 50 mL) and dried under vacuum at 40 °C for 72 h to give Fmoc-Val-Cit-OH **149** as a free-flowing white solid (3.55 g, 89%).

^{1}H NMR (400 MHz, DMSO-d_6) δ_H 12.5 (1H, br s, COOH), 8.17 (1H, d, J = 7.4 Hz, CONHCit), 7.89 (2H, d, J = 8.1 Hz, ArH), 7.75 (2H, t, J = 8.1 Hz, ArH), 7.41 (3H, q, J = 7.4 Hz, ArH, CONHVal), 7.35-7.29 (2H, m, ArH), 5.94 (1H, t, J = 5.7 Hz, NHCit), 5.37 (2H, s, NH_2Cit), 4.32-4.18 (3H, m, Fmoc CH_2, Fmoc CH), 4.18-4.11 (1H, m, $H_{\alpha'}$Cit), 3.92 (1H, dd, J = 9.0, 7.2 Hz, H_αVal), 2.99-2.90 (2H, m, NCH_2Cit), 2.03-1.93 (1H, m, H_βVal), 1.74-1.64 (1H, m, CH_2Cit), 1.62-1.50 (1H, m, CH_2Cit), 1.45-1.33 (2H, m, CH_2Cit), 0.89 (3H, d, J = 6.7 Hz, CH_3Val), 0.86 (3H, d, J = 6.7 Hz, CH_3Val); **^{13}C NMR** (101 MHz, DMSO-d_6) δ_C 173.4, 171.3, 158.7, 156.0, 143.9, 143.8, 140.7, 127.6, 127.0, 125.4, 120.1, 65.7, 59.8, 51.9, 46.7, 38.7, 30.5, 28.3, 26.7, 19.2, 18.2.

These data are in agreement with those previously reported.[252]

(9*H*-fluoren-9-yl)methyl ((*S*)-1-(((*S*)-1-((4-(hydroxymethyl)phenyl)amino)-1-oxo-5-ureidopentan-2-yl)amino)-3-methyl-1-oxobutan-2-yl)carbamate, 153

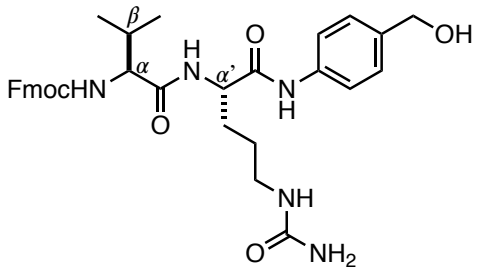

Fmoc-Val-Cit-PABOH

Fmoc-Val-Cit-OH **149** (630 mg, 1.27 mmol), PABOH (250 mg, 2.02 mmol) and EEDQ (500 mg, 2.02 mmol) were dissolved in CH_2Cl_2/MeOH (2:1, 24 mL) and stirred in the dark for 72 h. The reaction was concentrated *in vacuo* and the residue suspended in MTBE (50 mL) before being filtered to yield Fmoc-Val-Cit-PABOH **153** as a yellow solid (565 mg, 74%).

^{1}H NMR (400 MHz, DMSO-d_6) δ_H 9.97 (1H, s, PABNH), 8.09 (1H, d, J = 7.2 Hz, CONHCit), 7.89 (2H, d, J = 7.8 Hz, ArHFmoc), 7.74 (2H, t, J = 8.8 Hz, ArHFmoc), 7.54

(2H, d, J = 8.8 Hz, ArHPAB), 7.41 (3H, t, J = 7.2 Hz, ArHFmoc, CONHVal), 7.32 (2H, t, J = 8.0 Hz, ArHFmoc), 7.23 (2H, d, J = 8.8 Hz, ArHPAB), 5.97 (1H, t, J = 5.7 Hz, NHCit), 5.40 (2H, s, NH_2Cit), 5.08 (1H, t, J = 5.5 Hz, PABOH), 4.43 (2H, d, J = 5.5 Hz, $ArCH_2PAB$), 4.35-4.19 (4H, m, Fmoc CH_2, Fmoc CH, H_αCit), 3.93 (1H, t, J = 7.2 Hz, H_αVal), 3.08-2.88 (2H, m, NCH_2Cit), 2.07-1.92 (1H, m, H_βVal), 1.76-1.64 (1H, m, CH_2Cit), 1.64-1.51 (1H, m, CH_2Cit), 1.50-1.30 (2H, m, CH_2Cit), 0.92-0.81 (6H, m, 2 × CH_3Val); **^{13}C NMR** (101 MHz, DMSO-d_6) δ_C 171.2, 170.4, 158.9, 156.1, 143.9, 143.8, 140.7, 137.5, 137.4, 127.6, 127.1, 126.9, 125.4, 120.1, 118.8, 65.7, 62.6, 60.1, 53.0, 46.7, 38.6, 30.4, 29.5, 26.8, 19.2, 18.3.

These data are in agreement with those previously reported.[252]

(*S*)-2-amino-*N*-((*S*)-1-((4-(hydroxymethyl)phenyl)amino)-1-oxopropan-2-yl)-3-methylbutanamide, 155

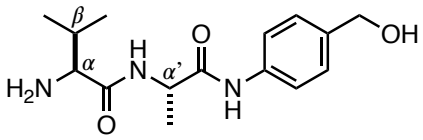

Val-Ala-PABOH

To a solution of Alloc-Val-Ala-PABOH **154** (3.00 g, 7.95 mmol) in MeOH (78 mL) was added $Pd(PPh_3)_4$ (92 mg, 0.0795 mmol) and the mixture was stirred for 5 min. K_2CO_3 (6.59 g, 47.7 mmol) was added and the reaction stirred for 30 min before being concentrated *in vacuo*. The residue was dissolved in H_2O (50 mL) and the aqueous extracted with EtOAc (6 × 100 mL). The combined organics were dried ($MgSO_4$) and concentrated *in vacuo* to yield Val-Ala-PABOH **155** as a pale yellow solid (2.00 g, 85%).

^{1}H NMR (400 MHz, DMSO-d_6): δ_H 10.03 (1H, s, PABNH), 8.20 (1H, br s, NHAla), 7.54 (2H, d, J = 8.3 Hz, ArH), 7.24 (2H, d, J = 8.3 Hz, ArH), 4.51-4.45 (1H, m, $H_{\alpha'}$Ala), 4.43 (2H, s, $ArCH_2PAB$), 3.03 (1H, d, J = 5.0 Hz, H_αVal), 1.97-1.88 (1H, m, H_βVal), 1.30 (3H, d, J = 6.8 Hz, CH_3Ala), 0.89 (3H, d, J = 6.8 Hz, CH_3Val), 0.79 (3H, d, J = 6.8 Hz, CH_3Val); **^{13}C NMR** (101 MHz, DMSO-d_6): δ_C 174.1, 171.0, 137.5, 137.5, 126.9, 119.0, 62.6, 59.6, 48.6, 31.4, 19.5, 18.7, 16.9.

These data are in agreement with those previously reported.[261]

6-(2,5-dioxo-2,5-dihydro-1*H*-pyrrol-1-yl)-*N*-((*S*)-1-(((*S*)-1-((4-(hydroxymethyl) phenyl)amino)-1-oxopropan-2-yl)amino)-3-methyl-1-oxobutan-2-yl)hexanamide, 156

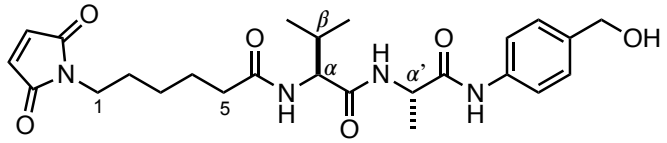

Mc-Val-Ala-PABOH

HATU (373 mg, 0.98 mmol) and 6-maleimidohexanoic acid (190 mg, 0.98 mmol) were dissolved in DMF (8 mL) before the addition of *i*-Pr_2NEt (5.00 mL, 0.98 mmol). The solution was stirred for 1 h. Amine **155** (240 mg, 0.82 mmol) was dissolved in DMF (3 mL) and added to the reaction mixture, which was left to stir for a further 16 h. The reaction was quenched with 5% aq. LiCl (20 mL) and extracted with EtOAc (6 × 50 mL). The combined organics were washed with H_2O (100 mL) and brine (100 mL), dried ($MgSO_4$) and concentrated *in vacuo*. Purification *via* flash column chromatography (1:19 MeOH/CH_2Cl_2) gave Mc-Val-Ala-PABOH **156** as a pale orange solid (300 mg, 78%).

^{1}H NMR (500 MHz, DMSO-d_6) δ_H 9.85 (1H, s, PABNH), 8.14 (1H, d, J = 7.0 Hz, NHAla), 7.82 (1H, d, J = 8.2 Hz, NHVal), 7.54 (2H, d, J = 8.6 Hz, ArH), 7.23 (2H, d, J = 8.6 Hz, ArH), 7.00 (2H, s, CH-Mal), 5.10 (1H, br s, PABOH), 4.43 (2H, s, $ArCH_2PAB$), 4.39 (1H, t, J = 7.3 Hz, $H_{\alpha'}$Ala), 4.17 (1H, dd, J = 8.6, 7.0 Hz, H_αVal), 3.40-3.34 (2H, m, H_1 × 2), 2.25-2.09 (2H, m, H_5 × 2), 2.01-1.92 (1H, m, H_βVal), 1.57-1.43 (4H, m, H_2 × 2, H_4 × 2), 1.31 (3H, d, J = 7.0 Hz, CH_3Ala), 1.23-1.15 (2H, m, H_3 × 2), 0.86 (3H, d, J = 7.0 Hz, CH_3Val), 0.82 (3H, d, J = 7.0 Hz, CH_3Val); **^{13}C NMR** (126 MHz, DMSO-d_6) δ_C 172.4, 171.1, 171.0, 171.0, 137.6, 137.4, 134.5, 126.9, 119.9, 62.6, 57.6, 49.0, 37.1, 35.0, 30.4, 27.8, 25.8, 24.9, 19.3, 18.2, 18.0.

These data are in agreement with those previously reported.[261]

_N_-((_S_)-1-(((_S_)-1-((4-(chloromethyl)phenyl)amino)-1-oxopropan-2-yl)amino)-3-methyl -1-oxobutan-2-yl)-6-(2,5-dioxo-2,5-dihydro-1_H_-pyrrol-1-yl)hexanamide, 157

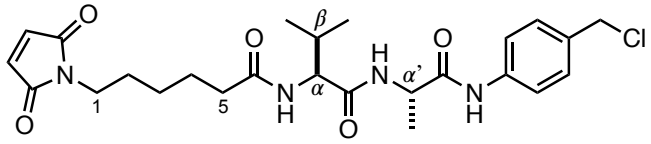

Mc-Val-Ala-PABCl

To a solution of Mc-Val-Ala-PABOH **156** (50 mg, 0.11 mmol) in DMF (500 μL) at 0 °C was added $SOCl_2$ (9 μL, 0.12μmol). The reaction was stirred at this temperature for 5 min before being quenched by the addition of H_2O (1 mL). The resulting precipitated solid was collected by filtration and washed with H_2O (2 mL) and MTBE (2 mL), then dried under vacuum for 2 h to yield Mc-Val-Ala-PABCl **157** as a brown solid (30 mg, 61%).

^{1}H NMR (500 MHz, DMSO-d_6) δ_H 10.00 (1H, s, PABNH), 8.16 (1H, d, J = 6.7 Hz, NHAla), 7.81 (1H, d, J = 8.0 Hz, NHVal), 7.60 (2H, d, J = 8.0 Hz, ArH), 7.36 (2H, d, J = 8.3 Hz, ArH), 7.00 (2H, s, CH-Mal), 4.71 (2H, s, $ArCH_2PAB$), 4.38 (1H, t, J = 7.4 Hz, $H_{\alpha'}$Ala), 4.16 (1H, dd, J = 8.5, 7.0 Hz, H_αVal), 3.36 (2H, t, J = 7.4 Hz, $H_1 \times 2$), 2.22-2.10 (2H, m, $H_5 \times 2$), 2.03-1.94 (1H, m, H_βVal), 1.53-1.42 (4H, m, $H_2 \times 2$, $H_4 \times 2$), 1.30 (3H, d, J = 7.5 Hz, CH_3Ala), 1.22-1.14 (2H, m, $H_3 \times 2$), 0.86 (3H, d, J = 6.9 Hz, CH_3Val), 0.82 (3H, d, J = 6.9 Hz, CH_3Val); **^{13}C NMR** (126 MHz, DMSO-d_6) δ_C 172.2, 171.1, 171.0, 171.0, 139.0, 134.4, 129.4, 119.1, 63.3, 57.5, 52.3, 49.0, 37.0, 34.9, 30.3, 27.7, 25.7, 24.8, 19.2, 18.2, 17.9; $[\alpha]_D^{20}$ +18.2 (c 1.00, $CHCl_3$); **IR** (thin film) ν_{max} (cm^{-1}) 3285, 2940, 1701, 1655, 1604, 1515, 1441, 1409, 1371, 1318, 1247, 1181, 1140, 1098, 1022, 946, 826; **HRMS** calc. for $C_{25}H_{33}ClN_4O_5Na$ $[M+Na]^+$ 527.2037 found, 527.2010; **m.p.** 133-135 °C.

References

(1) Masamune, S.; Ali, S. A.; Snitman, D. L.; Garvey, D. S. *Angew. Chemie Int. Ed. Engl.* **1980**, *19*, 557.

(2) Yamada, K.; Ojika, M.; Ishigaki, T.; Yoshida, Y.; Ekimoto, H.; Arakawa, M. *J. Am. Chem. Soc.* **1993**, *115*, 11020.

(3) Cragg, G. M.; Newman, D. J. *Biochim. Biophys. Acta* **2013**, *1830*, 3670.

(4) Li, F.; Wang, Y.; Li, D.; Chen, Y.; Dou, Q. P. *Expert Opin. Drug Discov.* **2019**, *14*, 417.

(5) Cragg, G. M.; Newman, D. J. *Biochim. Biophys. Acta - Gen. Subj.* **2013**, *1830*, 3670.

(6) Butler, M. S. *J. Nat. Prod.* **2004**, *67*, 2141.

(7) Dias, D. A.; Urban, S.; Roessner, U. *Metabolites* **2012**, *2*, 303.

(8) Newman, D. J.; Cragg, G. M. *J. Nat. Prod.* **2016**, *79*, 3

(9) Cragg, G. M.; Newman, D. J.; Weiss, R. B. *Semin. Oncol.* **1997**, *24*, 156.

(10) Kong, D.-X.; Jiang, Y.-Y.; Zhang, H.-Y. *Drug Discov. Today* **2010**, *15*, 884.

(11) Faulkner, D. J. *Nat. Prod. Rep.* **2001**, *18*, 1.

(12) Dias, D. A.; Urban, S. *Phytochemistry* **2011**, *72*, 2081.

(13) Kimura, J.; Kamada, N.; Tsujimoto, Y. *Bull. Chem. Soc. Jpn.* **1999**, *72*, 289.

(14) San-Martín, A.; Darias, J.; Soto, H.; Contreras, C.; Herrera, J. S.; Rovirosa, J. *Nat. Prod. Lett.* **1997**, *10*, 303.

(15) Leal, M. C.; Puga, J.; Serôdio, J.; Gomes, N. C. M.; Calado, R. *PLoS One* **2012**, *7*, 1

(16) Martins, A.; Vieira, H.; Gaspar, H.; Santos, S. *Mar. Drugs* **2014**, *12*, 1066.

(17) Piel, J. *Nat. Prod. Rep.* **2009**, *26*, 338.

(18) Penesyan, A.; Kjelleberg, S.; Egan, S. *Mar. Drugs* **2010**, *8*, 438.

(19) Waters, A. L.; Hill, R. T.; Place, A. R.; Hamann, M. T. *Curr. Opin. Biotechnol.* **2010**, *21*, 780.

(20) Butler, M. S. *Nat. Prod. Rep.* **2008**, *25*, 475.

(21) Ahmad, B.; Shah, M.; Choi, S. *Mar. Drugs* **2019**, *17*, 282.

(22) Schwartsmann, G. *Ann. Oncol.* **2000**, *11,* 235.

(23) Bergman, W.; Feeney, R. J. *J. Org. Chem.* **1951**, *16*, 981.

(24) Nicolaou, K. C.; Vourloumis, D.; Winssinger, N.; Baran, P. S. *Angew. Chem. Int. Ed. Engl.* **2000**, *39*, 44.

(25) Baran, P. S. *J. Am. Chem. Soc.* **2018**, *140*, 4751.

(26) Mickel, S. J.; Sedelmeier, G. H.; Niederer, D.; Daeffler, R.; Osmani, A.; Schreiner, K.; Seeger-Weibel, M.; Bérod, B.; Schaer, K.; Gamboni, R.; Chen, S.; Chen, W.; Jagoe, C. T.; Kinder, F. R.; Loo, M.; Prasad, K.; Repič, O.; Shieh, W.-C.; Wang, R.-M.; Waykole, L.; Xu, D. D.; Xue, S. *Org. Process Res. Dev.* **2004**, *8*, 92.

(27) Mickel, S. J.; Sedelmeier, G. H.; Niederer, D.; Schuerch, F.; Grimler, D.; Koch, G.; Daeffler, R.; Osmani, A.; Hirni, A.; Schaer, K.; Gamboni, R.; Bach, A.; Chaudhary, A.; Chen, S.; Chen, W.; Hu, B.; Jagoe, C. T.; Kim, H.-Y.; Kinder, F. R.; Liu, Y.; Lu, Y.; McKenna, J.; Prashad, M.; Ramsey, T. M.; Repič, O.; Rogers, L.; Shieh, W.-C.; Wang, R.-M.; Waykole, L. *Org. Process Res. Dev.* **2004**, *8*, 101.

(28) Mickel, S. J.; Sedelmeier, G. H.; Niederer, D.; Schuerch, F.; Koch, G.; Kuesters, E.; Daeffler, R.; Osmani, A.; Seeger-Weibel, M.; Schmid, E.; Hirni, A.; Schaer, K.; Gamboni, R.; Bach, A.; Chen, S.; Chen, W.; Geng, P.; Jagoe, C. T.; Kinder, F. R.; Lee, G. T.; McKenna, J.; Ramsey, T. M.; Repič, O.; Rogers, L.; Shieh, W.-C.; Wang, R.-M.; Waykole, L. *Org. Process Res. Dev.* **2004**, *8*, 107.

(29) Mickel, S. J.; Sedelmeier, G. H.; Niederer, D.; Schuerch, F.; Seger, M.; Schreiner, K.; Daeffler, R.; Osmani, A.; Bixel, D.; Loiseleur, O.; Cercus, J.; Stettler, H.; Schaer, K.; Gamboni, R.; Bach, A.; Chen, G.-P.; Chen, W.; Geng, P.; Lee, G. T.; Loeser, E.; McKenna, J.; Kinder, F. R.; Konigsberger, K.; Prasad, K.; Ramsey, T. M.; Reel, N.; Repič, O.; Rogers, L.; Shieh, W.-C.; Wang, R.-M.; Waykole, L.; Xue, S.; Florence, G.; Paterson, I. *Org. Process Res. Dev.* **2004**, *8*, 113.

(30) Mickel, S. J.; Niederer, D.; Daeffler, R.; Osmani, A.; Kuesters, E.; Schmid, E.; Schaer, K.; Gamboni, R.; Chen, W.; Loeser, E.; Kinder, F. R.; Konigsberger, K.; Prasad, K.; Ramsey, T. M.; Repič, O.; Wang, R.-M.; Florence, G.; Lyothier, I.; Paterson, I. *Org. Process Res. Dev.* **2004**, *8*, 122.

(31) Mita, A.; Lockhart, A. C.; Chen, T.-L.; Bochinski, K.; Curtright, J.; Cooper, W.; Hammond, L.; Rothenberg, M.; Rowinsky, E.; Sharma, S. *J. Clin. Oncol.* **2004**, *22* 2025.

(32) Crane, E. A.; Gademann, K. *Angew. Chem. Int. Ed. Engl.* **2016**, *55*, 3882.

(33) Wender, P. A.; Quiroz, R. V.; Stevens, M. C. *Acc. Chem. Res.* **2015**, *48*, 752.

(34) Nicolaou, K. C.; Rhoades, D.; Wang, Y.; Bai, R.; Hamel, E.; Aujay, M.; Sandoval, J.; Gavrilyuk, J. *J. Am. Chem. Soc.* **2017**, *139*, 7318.

(35) Nicolaou, K. C.; Rigol, S. *Acc. Chem. Res.* **2019**, *52*, 127.

(36) Suen, L. M.; Tekle-Smith, M. A.; Williamson, K. S.; Infantine, J. R.; Reznik, S. K.; Tanis, P. S.; Casselman, T. D.; Sackett, D. L.; Leighton, J. L. *Nat. Comm*. **2018**, 9, 4710.

(37) Wender, P. A. *Nat. Prod. Rep.* **2014**, *31*, 433.

(38) Wender, P. A.; Baryza, J. L.; Bennett, C. E.; Bi, F. C.; Brenner, S. E.; Clarke, M. O.; Horan, J. C.; Kan, C.; Lacôte, E.; Lippa, B.; Nell, P. G.; Turner, T. M. *J. Am. Chem. Soc.* **2002**, *124*, 13648.

(39) Wender, P. A.; Hardman, C. T.; Ho, S.; Jeffreys, M. S.; Maclaren, J. K.; Quiroz, R. V.; Ryckbosch, S. M.; Shimizu, A. J.; Sloane, J. L.; Stevens, M. C. *Science* **2017**, *358*, 218.

(40) Gaul, C.; Njardarson, J. T.; Shan, D.; Dorn, D. C.; Wu, K.-D.; Tong, W. P.; Huang, X.-Y.; Moore, M. A. S.; Danishefsky, S. J. *J. Am. Chem. Soc.* **2004**, *126*, 11326.

(41) Bonazzi, S.; Eidam, O.; Güttinger, S.; Wach, J.-Y.; Zemp, I.; Kutay, U.; Gademann, K. *J. Am. Chem. Soc.* **2010**, *132*, 1432.

(42) Aicher, T. D.; Buszek, K. R.; Fang, F. G.; Forsyth, C. J.; Jung, S. H.; Kishi, Y.; Matelich, M. C.; Scola, P. M.; Spero, D. M.; Yoon, S. K. *J. Am. Chem. Soc.* **1992**, *114*, 3162.

(43) Towle, M. J.; Salvato, K. A.; Budrow, J.; Wels, B. F.; Kuznetsov, G.; Aalfs, K. K.; Welsh, S.; Zheng, W.; Seletsky, B. M.; Palme, M. H.; Habgood, G. J.; Singer, L. A.; Dipietro, L. V; Wang, Y.; Chen, J. J.; Quincy, D. A.; Davis, A.; Yoshimatsu, K.; Kishi, Y.; Yu, M. J.; Littlefield, B. A. *Cancer Res.* **2001**, *61*, 1013.

(44) Yu, M. J.; Zheng, W.; Seletsky, B. M. *Nat. Prod. Rep.* **2013**, *30*, 1158.

(45) Chari, R. V. J. *Acc. Chem. Res.* **2008**, *41*, 98.

(46) Chari, R. V. J.; Miller, M. L.; Widdison, W. C. *Angew. Chemie Int. Ed.* **2014**, *53*, 3796.

(47) Mellman, I.; Coukos, G.; Dranoff, G. *Nature* **2011**, *480*, 480.

(48) Vanneman, M.; Dranoff, G. *Nat. Rev. Cancer* **2012**, *12*, 237.

(49) Zhang, J.; Yang, P. L.; Gray, N. S. *Nat. Rev. Cancer* **2009**, *9*, 28.

(50) Druker, B. J. *J. Clin. Oncol.* **2003**, *21*, 239.

(51) Vlahov, I. R.; Leamon, C. P. *Bioconjug. Chem.* **2012**, *23*, 1357.

(52) Govindan, S. V; Cardillo, T. M.; Rossi, E. A.; Trisal, P.; McBride, W. J.; Sharkey, R. M.; Goldenberg, D. M. *Mol. Pharm.* **2015**, *12*, 1836.

(53) Beck, A.; Goetsch, L.; Dumontet, C.; Corvaïa, N. *Nat. Rev. Drug Discov.* **2017**, *16*, 315.

(54) Shor, B.; Gerber, H.-P.; Sapra, P. *Mol. Immunol.* **2015**, *67*, 107.

(55) Godwin, C. D.; Gale, R. P.; Walter, R. B. *Leukemia* **2017**, *31*, 1855.

(56) Lambert, J. M.; Chari, R. V. J. *J. Med. Chem.* **2014**, *57*, 6949.

(57) Senter, P. D.; Sievers, E. L. *Nat. Biotechnol.* **2012**, *30*, 631.

(58) Kovtun, Y. V; Audette, C. A.; Ye, Y.; Xie, H.; Ruberti, M. F.; Phinney, S. J.; Leece, B. A.; Chittenden, T.; Blättler, W. A.; Goldmacher, V. S. *Cancer Res.* **2006**, *66*, 3214.

(59) Novakovic, B. J. *Radiol. Oncol.* **2015**, *49*, 315.

(60) Sela-Culang, I.; Kunik, V.; Ofran, Y. *Front. Immunol.* **2013**, *4*, 302.

(61) Thurber, G. M.; Schmidt, M. M.; Wittrup, K. D. *Adv. Drug Deliv. Rev.* **2008**, *60*, 1421.

(62) Adams, G. P.; Schier, R.; McCall, A. M.; Simmons, H. H.; Horak, E. M.; Alpaugh, R. K.; Marks, J. D.; Weiner, L. M. *Cancer Res.* **2001**, *61*, 4750.

(63) Kyriakos, R. J.; Shih, L. B.; Ong, G. L.; Patel, K.; Goldenberg, D. M.; Mattes, M. J.; Marks, J. D.; Adams, G. P. *Cancer Res.* **1992**, *52*, 835.

(64) Nadler, L. M.; Stashenko, P.; Hardy, R.; Kaplan, W. D.; Button, L. N.; Kufe, D. W.; Antman, K. H.; Schlossman, S. F. *Cancer Res.* **1980**, *40*, 3147.

(65) Almagro, J. C.; Fransson, J. *Front. Biosci.* **2008**, *13*, 1619.

(66) Tsuchikama, K.; An, Z. *Protein Cell* **2018**, *9*, 33.

(67) Jackson, D.; Atkinson, J.; Guevara, C. I.; Zhang, C.; Kery, V.; Moon, S.-J.; Virata, C.; Yang, P.; Lowe, C.; Pinkstaff, J.; Cho, H.; Knudsen, N.; Manibusan, A.; Tian, F.; Sun, Y.; Lu, Y.; Sellers, A.; Jia, X.-C.; Joseph, I.; Anand, B.; Morrison, K.; Pereira, D. S.; Stover, D. *PLoS One* **2014**, *9*, 1

(68) Hamblett, K. J.; Senter, P. D.; Chace, D. F.; Sun, M. M. C.; Lenox, J.; Cerveny, C. G.; Kissler, K. M.; Bernhardt, S. X.; Kopcha, A. K.; Zabinski, R. F.; Meyer, D. L.; Francisco, J. A. *Clin. Cancer Res.* **2004**, *10*, 7063.

(69) Agarwal, P.; Bertozzi, C. R. *Bioconjug. Chem.* **2015**, *26*, 176.

(70) Boylan, N. J.; Zhou, W.; Proos, R. J.; Tolbert, T. J.; Wolfe, J. L.; Laurence, J. S. *Bioconjug. Chem.* **2013**, *24*, 1008.

(71) Acchione, M.; Kwon, H.; Jochheim, C. M.; Atkins, W. M. *MAbs* **2012**, *4*, 362.

(72) Chari, R. V. J. *ACS Med. Chem. Lett*. **2016**, *7*, 974.

(73) Axup, J. Y.; Bajjuri, K. M.; Ritland, M.; Hutchins, B. M.; Kim, C. H.; Kazane, S. A.; Halder, R.; Forsyth, J. S.; Santidrian, A. F.; Stafin, K.; Lu, Y.; Tran, H.; Seller, A. J.; Biroc, S. L.; Szydlik, A.; Pinkstaff, J. K.; Tian, F.; Sinha, S. C.; Felding-Habermann, B.; Smider, V. V; Schultz, P. G. *Proc. Natl. Acad. Sci. U. S. A.* **2012**, *109*, 16101.

(74) Zimmerman, E. S.; Heibeck, T. H.; Gill, A.; Li, X.; Murray, C. J.; Madlansacay, M. R.; Tran, C.; Uter, N. T.; Yin, G.; Rivers, P. J.; Yam, A. Y.; Wang, W. D.; Steiner, A. R.; Bajad, S. U.; Penta, K.; Yang, W.; Hallam, T. J.; Thanos, C. D.; Sato, A. K. *Bioconjug. Chem.* **2014**, *25*, 351.

(75) Junutula, J. R.; Gerber, H.-P. *ACS Med. Chem. Lett.* **2016**, *11*, 972.

(76) Lyon, R. P.; Setter, J. R.; Bovee, T. D.; Doronina, S. O.; Hunter, J. H.; Anderson, M. E.; Balasubramanian, C. L.; Duniho, S. M.; Leiske, C. I.; Li, F.; Senter, P. D. *Nat. Biotechnol.* **2014**, *32*, 1059.

(77) Walsh, S. J.; Omarjee, S.; J D Galloway, W. R.; T-L Kwan, T.; Sore, H. F.; Parker, J. S.; HyvönenHyv, M.; Carroll, J. S.; Spring, D. R. *Chem. Sci.* **2019**, *10,* 694.

(78) Badescu, G.; Bryant, P.; Bird, M.; Henseleit, K.; Swierkosz, J.; Parekh, V.;

Tommasi, R.; Pawlisz, E.; Jurlewicz, K.; Farys, M.; Camper, N.; Sheng, X.; Fisher, M.; Grygorash, R.; Kyle, A.; Abhilash, A.; Frigerio, M.; Edwards, J.; Godwin, A. *Bioconjug. Chem.* **2014**, *25*, 1124.

(79) Gébleux, R.; Casi, G. *Pharmacol. Ther.* **2016**, *167*, 48.

(80) Francisco, J. A.; Cerveny, C. G.; Meyer, D. L.; Mixan, B. J.; Klussman, K.; Chace, D. F.; Rejniak, S. X.; Gordon, K. A.; DeBlanc, R.; Toki, B. E.; Law, C.-L.; Doronina, S. O.; Siegall, C. B.; Senter, P. D.; Wahl, A. F. *Blood* **2003**, *102*, 1458.

(81) Doronina, S. O.; Toki, B. E.; Torgov, M. Y.; Mendelsohn, B. A.; Cerveny, C. G.; Chace, D. F.; DeBlanc, R. L.; Gearing, R. P.; Bovee, T. D.; Siegall, C. B.; Francisco, J. A.; Wahl, A. F.; Meyer, D. L.; Senter, P. D. *Nat. Biotechnol.* **2003**, *21*, 778.

(82) Verma, S.; Miles, D.; Gianni, L.; Krop, I. E.; Welslau, M.; Baselga, J.; Pegram, M.; Oh, D.-Y.; Diéras, V.; Guardino, E.; Fang, L.; Lu, M. W.; Olsen, S.; Blackwell, K. *N. Engl. J. Med*. **2012**, *367*, 1783.

(83) Maiese, W. M.; Lechevalier, M. P.; Lechevalier, H. A.; Korshalla, J.; Kuck, N.; Fantini, A.; Wildey, M. J.; Thomas, J.; Greenstein, M. *J. Antibiot.* **1989**, *42*, 558.

(84) Lee, M. D.; Manning, J. K.; Williams, D. R.; Kuck, N. A.; Testa, R. T.; Borders, D. B. *J. Antibiot.* **1989**, *42*, 1070.

(85) Ricart, A. D. *Clin. Cancer Res.* **2011**, *17*, 6417.

(86) Casi, G.; Neri, D. *J. Med. Chem.* **2015**, *58*, 8751.

(87) Yamamura, S.; Hirata, Y. *Tetrahedron* **1963**, *19*, 1485.

(88) Kigoshi, H.; Imamura, Y.; Yoshikawa, K.; Yamada, K. *Tetrahedron Lett.* **1990**, *31*, 4911.

(89) Kawamura, A.; Kita, M.; Kigoshi, H. *Angew. Chemie Int. Ed.* **2015**, *54*, 7073.

(90) Ojika, M.; Kigoshi, H.; Suenaga, K.; Imamura, Y.; Yoshikawa, K.; Ishigaki, T.; Sakakura, A.; Mutou, T.; Yamada, K. *Tetrahedron* **2012**, *68*, 982.

(91) Yamada, K.; Ojika, M.; Kigoshi, H.; Suenaga, K. *Nat. Prod. Rep.* **2009**, *26*, 27.

(92) Kigoshi, H.; Ojika, M.; Ishigaki, T.; Suenaga, K.; Mutou, T.; Sakakura, A.; Ogawa, T.; Yamada, K. *J. Am. Chem. Soc.* **1994**, *116*, 7443.

(93) Ojika, M.; Kigoshi, H.; Ishigaki, T.; Tsukada, I.; Tsuboi, T.; Ogawa, T.; Yamada, K. *J. Am. Chem. Soc.* **1994**, *116*, 7441.

(94) Ojika, M.; Kigoshi, H.; Ishigaki, T.; Nisiwaki, M.; Tsukada, I.; Mizuta, K.; Yamada, K. *Tetrahedron Lett.* **1993**, *34*, 8505.

(95) Ojika, M.; Kigoshi, H.; Ishigaki, T.; Yamada, K. *Tetrahedron Lett.* **1993**, *34*, 8501.

(96) Kigoshi, H.; Ojika, M.; Suenaga, K.; Mutou, T.; Hirano, J.; Sakakura, A.; Ogawa, T.; Nisiwaki, M.; Yamada, K. *Tetrahedron Lett.* **1994**, *35*, 1247.

(97) Suenaga, K.; Ishigaki, T.; Sakakura, A.; Kigoshi, H.; Yamada, K. *Tetrahedron Lett.* **1995**, *36*, 5053.

(98) Ciavatta, M. L.; Lefranc, F.; Carbone, M.; Mollo, E.; Gavagnin, M.; Betancourt, T.; Dasari, R.; Kornienko, A.; Kiss, R. *Med. Res. Rev.* **2017**, *37*, 702.

(99) Shoemaker, R. H. *Nat. Rev. Cancer* **2006**, *6*, 813.

(100) Crews, P.; Gerwick, W.; Schmitz, F.; France, D.; Bair, K.; Wright, A.; Hallock, Y. *Pharm. Biol.* **2003**, *41*, 39.

(101) Saito, S.-Y.; Watabe, S.; Ozaki, H.; Kigoshi, H.; Yamada, K.; Fusetani, N.; Karaki, H. *J. Biochem.* **1996**, *120*, 552.

(102) Dominguez, R.; Holmes, K. C. *Annu. Rev. Biophys.* **2011**, *40*, 169.

(103) Allingham, J. S.; Klenchin, V. A.; Rayment, I. *Cell. Mol. Life Sci.* **2006**, *63*, 2119.

(104) Otterbein, L. R.; Graceffa, P.; Dominguez, R. *Science* **2001**, *293*, 708.

(105) Narita, A. *Bioarchitecture* **2011**, *1*, 205.

(106) Pantaloni, D.; Le Clainche, C.; Carlier, M.-F. *Science* **2001**, *292*, 1502.

(107) Yeung, K.-S.; Paterson, I. *Angew. Chemie Int. Ed.* **2002**, *41*, 4632.

(108) Hirata, K.; Muraoka, S.; Suenaga, K.; Kuroda, T.; Kato, K.; Tanaka, H.; Yamamoto, M.; Takata, M.; Yamada, K.; Kigoshi, H. *J. Mol. Biol.* **2006**, *356*, 945.

(109) Smith, C. D.; Carmeli, S.; Moore, R. M.; Patterson, G. M. L. *Cancer Res* **1993***, 53 1343*

(110) Fusetani, N.; Yasumuro, K.; Matsunaga, S.; Hashimoto, K. *Tetrahedron Lett.* **1989**, *30*, 2809.

(111) Jansen, R.; Steinmetz, H.; Sasse, F.; Schubert, W.-D.; Hagelüken, G.; Albrecht, S. C.; Müller, R. *Tetrahedron Lett.* **2008**, *49*, 5796.

(112) D'Auria, M. V.; Paloma, L. G.; Minale, L.; Zampella, A.; Verbist, J.-F.; Roussakis, C.; Debitus, C.; Patissou, J. *Tetrahedron* **1994**, *50*, 4829.

(113) Ueoka, R.; Uria, A. R.; Reiter, S.; Mori, T.; Karbaum, P.; Peters, E. E.; Helfrich, E. J. N.; Morinaka, B. I.; Gugger, M.; Takeyama, H.; Matsunaga, S.; Piel, J. *Nat. Chem. Biol.* **2015**, *11*, 705.

(114) Kita, M.; Hirayama, Y.; Sugiyama, M.; Kigoshi, H. *Angew. Chemie Int. Ed.* **2011**, *50*, 9871.

(115) Ohno, O.; Morita, M.; Kitamura, K.; Teruya, T.; Yoneda, K.; Kita, M.; Kigoshi, H.; Suenaga, K. *Bioorg. Med. Chem. Lett.* **2013**, *23*, 1467.

(116) Suenaga, K.; Kamei, N.; Okugawa, Y.; Takagi, M.; Akao, A.; Kigoshi, H.; Yamada, K. *Bioorg. Med. Chem. Lett.* **1997**, *7*, 269.

(117) Kigoshi, H.; Suenaga, K.; Takagi, M.; Akao, A.; Kanematsu, K.; Kamei, N.; Okugawa, Y.; Yamada, K. *Tetrahedron* **2002**, *58*, 1075.

(118) Pereira, J. H.; Petchprayoon, C.; Hoepker, A. C.; Moriarty, N. W.; Fink, S. J.; Cecere, G.; Paterson, I.; Adams, P. D.; Marriott, G. *ChemMedChem* **2014**, *9*, 2286.

(119) Perrins, R. D.; Cecere, G.; Paterson, I.; Marriott, G. *Chem. Biol.* **2008**, *15*, 287.

(120) Fink, S. J. *PhD Thesis*, University of Cambridge, 2012.

(121) Williams, S. *PhD thesis*, University of Cambridge, 2015

(122) Kigoshi, H.; Suenaga, K.; Mutou, T.; Ishigaki, T.; Atsumi, T.; Ishiwata, H.; Sakakura, A.; Ogawa, T.; Ojika, M.; Yamada, K. *J. Org. Chem.* **1996**, *61*, 5326.

(123) Kobayashi, K.; Fujii, Y.; Hirayama, Y.; Kobayashi, S.; Hayakawa, I.; Kigoshi, H. *Org. Lett.* **2012**, *14*, 1290.

(124) Kita, M.; Hirayama, Y.; Yoneda, K.; Yamagishi, K.; Chinen, T.; Usui, T.; Sumiya, E.; Uesugi, M.; Kigoshi, H. *J. Am. Chem. Soc.* **2013**, *135*, 18089.

(125) Hirayama, Y.; Yamagishi, K.; Suzuki, T.; Kawagishi, H.; Kita, M.; Kigoshi, H. *Bioorg. Med. Chem.* **2016**, *24*, 2809.

(126) Jordan, M. A.; Wendell, K.; Gardiner, S.; Derry, W. B.; Copp, H.; Wilson, L. *Cancer Res.* **1996**, *56*, 816.

(127) Jordan, M. A.; Thrower, D.; Wilson, L. *Cancer Res.* **1991**, *51*, 2212.

(128) Kita, M.; Kigoshi, H. *Nat. Prod. Rep.* **2015**, *32*, 534.

(129) Liu, J.; Farmer, J. D.; Lane, W. S.; Friedman, J.; Weissman, I.; Schreiber, S. L. *Cell* **1991**, *66*, 807.

(130) Kigoshi, H.; Suenaga, K.; Takagi, M.; Akao, A.; Kanematsu, K.; Kamei, N.; Okugawa, Y.; Yamada, K. *Tetrahedron* **2002**, *58*, 1075.

(131) Hayakawa, I.; Saito, K.; Matsumoto, S.; Kobayashi, S.; Taniguchi, A.; Kobayashi, K.; Fujii, Y.; Kaneko, T.; Kigoshi, H. *Org. Biomol. Chem.* **2017**, *15*, 124.

(132) Hong, W. P.; Noshi, M. N.; El-Awa, A.; Fuchs, P. L. *Org. Lett.* **2011**, *13*, 6342.

(133) El-Awa, A.; Fuchs, P. *Org. Lett.* **2006**, *8*, 2905.

(134) Calter, M. A.; Zhou, J. *Tetrahedron Lett.* **2004**, *45*, 4847.

(135) Calter, M. A.; Guo, X. *Tetrahedron* **2002**, *58*, 7093.

(136) Marshall, J. A.; Johns, B. A. *J. Org. Chem.* **2000**, *65*, 1501.

(137) Paterson, I.; Fink, S. J.; Lee, L. Y. W.; Atkinson, S. J.; Blakey, S. B. *Org. Lett.* **2013**, *15*, 3118.

(138) Anžiček, N.; Williams, S.; Housden, M. P.; Paterson, I. *Org. Biomol. Chem.* **2018**, *16*, 1343.

(139) Paterson, I.; Cowden, C.; Watson, C. *Synlett* **1996**, *3*, 209.

(140) Weissman, K. J. *Beilstein J. Org. Chem.* **2017**, *13*, 348.

(141) Zimmerman, H. E.; Traxler, M. D. *J. Am. Chem. Soc.* **1957**, *79*, 1920.

(142) Goodman, J. M.; Paterson, I. *Tetrahedron Lett.* **1992**, *33*, 7223.

(143) Evans, D. A.; Vogel, E.; Nelson, J. V. *J. Am. Chem. Soc.* **1979**, *101*, 6120.

(144) Evans, D. A.; Nelson, J. V.; Vogel, E.; Taber, T. R. *J. Am. Chem. Soc.* **1981**, *103*, 3099.

(145) Cowden, C. J.; Paterson, I. *Organic Reactions*; John Wiley & Sons, NJ, USA, 1997; pp 1–200.

(146) Masamune, S.; Choy, W.; Francis A. J. K.; Imperiali, B. *J. Am. Chem. Soc.* **1981**, *103*, 1566.

(147) Brown, H. C.; Dhar, R. K.; Ganesan, K.; Singaram, B. *J. Org. Chem.* **1992**, *57*, 499.

(148) Paton, R. S.; Goodman, J. M. *J. Org. Chem.* **2008**, *73*, 1253.

(149) Paterson, I.; Woodrow, M. D.; Cowden, C. J. *Tetrahedron Lett.* **1998**, *39*, 6041.

(150) Bubb, M. R.; Spector, I.; Bershadsky, A. D.; Korn, E. D. *J. Biol. Chem.* **1995**, *270*, 3463.

(151) Ohyoshi, T.; Takano, A.; Namiki, M.; Ogura, T.; Miyazaki, Y.; Ebihara, Y.; Takeno, K.; Hayakawa, I.; Kigoshi, H. *Chem. Commun.* **2018**, *54*, 9537.

(152) Futaki, K.; Takahashi, M.; Tanabe, K.; Fujieda, A.; Kigoshi, H.; Kita, M. *ACS Omega* **2019**, *4*, 8598.

(153) Suenaga, K.; Kamei, N.; Okugawa, Y.; Takagi, M.; Akao, A.; Kigoshi, H.; Yamada, K. *Bioorg. Med. Chem. Lett.* **1997**, *7*, 269.

(154) Goodman, J. M.; Paton, R. S. *Chem. Commun.* **2007**, *21*, 2124.

(155) Paton, R. S.; Goodman, J. M. *Org. Lett.* **2006**, *8*, 4299.

(156) Evans, D. A.; Hoveyda, A. H. *J. Am. Chem. Soc.* **1990**, *112*, 6447.

(157) Lee, L. Y. W. *PhD Thesis*, University of Cambridge, 2010

(158) Rychnovsky, S. D.; Kim, J. *J. Org. Chem.* **1994**, *59*, 2659.

(159) Woodrow, M. D. *PhD Thesis*, University of Cambridge, 1998.

(160) Horita, K.; Yoshioka, T.; Tanaka, T.; Oikawa, Y.; Yonemitsu, O. *Tetrahedron* **1986**, *42*, 3021.

(161) Appel, R. *Angew. Chemie Int. Ed. Engl.* **1975**, *14*, 801.

(162) Garegg, P. J.; Regberg, T.; Stawiński, J.; Strömberg, R. *J. Chem. Soc., Perkin Trans. 2* **1987**, *3*, 271.

(163) Grieco, P. A.; Pogonowski, C. S. *J. Am. Chem. Soc.* **1973**, *95*, 3071.

(164) Anžiček, N. *PhD Thesis*, University of Cambridge, 2017.

(165) Pettigrew, T. R. *PhD Thesis*, University of Cambridge, 2018.

(166) Esteve, C.; Ferreró, M.; Romea, P.; Urpí, F.; Vilarrasa, J. *Tetrahedron Lett.* **1999**, *40*, 5079.

(167) Figueras, S.; Martín, R.; Romea, P.; Urpí, F.; Vilarrasa, J. *Tetrahedron Lett.* **1997**, *38*, 1637.

(168) Paterson, I.; Tillyer, R. D. *Tetrahedron Lett.* **1992**, *33*, 4233.

(169) Paterson, I.; Ashton, K.; Britton, R.; Cecere, G.; Chouraqui, G.; Florence, G. J.; Stafford, J. *Angew. Chem. Int. Ed. Engl.* **2007**, *46*, 6167.

(170) Couture, A.; Deniau, E.; Woisel, P.; Grandclaudon, P. *Tetrahedron Lett.* **1995**, *36*, 2483.

(171) Böhme, H.; Raude, E. *Chem. Ber.* **1981**, *114*, 3421.

(172) Paterson, I.; Watson, C.; Yeung, K. S.; Wallace, P. A.; Ward, R. A. *J. Org. Chem.* **1997**, *62*, 452.

(173) Schwartz, J.; Labinger, J. A. *Angew. Chemie Int. Ed. Engl.* **1976**, *15*, 333.

(174) Takai, K.; Nitta, K.; Utimoto, K. *J. Am. Chem. Soc.* **1986**, *108*, 7408.

(175) Shen, R.; Porco, J. A. *Org. Lett.* **2000**, *2*, 1333.

(176) Klapars, A.; Antilla, J. C.; Huang, X.; Buchwald, S. L. *J. Am. Chem. Soc.* **2001**, *123*, 7727.

(177) Nakamura, R.; Tanino, K.; Miyashita, M. *Org. Lett.* **2003**, *5*, 3583.

(178) Williamson, A. *London, Edinburgh, Dublin Philos. Mag. J. Sci.* **1850**, *37*, 350.

(179) Evans, D. A.; Ratz, A. M.; Huff, B. E.; Sheppard, G. S. *Tetrahedron Lett.* **1994**, *35*, 7171.

(180) Walker, H. G.; Gee, M.; McCready, R. M. *J. Org. Chem.* **1962**, *27*, 2100.

(181) Kuhn, R.; Trieschmann, H.; Löw, I. *Angew. Chemie* **1955**, *67*, 32.

(182) Blakey, S. B. *PhD Thesis*, University of Cambridge, 2002.

(183) Atkins, G. M.; Burgess, E. M. *J. Am. Chem. Soc.* **1968**, *90*, 4744.

(184) Dalby, S. M.; Goodwin-Tindall, J.; Paterson, I. *Angew. Chemie Int. Ed.* **2013**, *52*, 6517.

(185) Paterson, I.; Chen, D. Y.-K.; Coster, M. J.; Aceña, J. L.; Bach, J.; Wallace, D. J. *Org. Biomol. Chem.* **2005**, *3*, 2431.

(186) Burgess, E. M.; Penton, H. R.; Taylor, E. A. *J. Org. Chem.* **1973**, *38*, 26.

(187) Smith, A. B.; Kanoh, N.; Ishiyama, H.; Minakawa, N.; Rainier, J. D.; Hartz, R. A.; Cho, Y. S.; Cui, H.; Moser, W. H. *J. Am. Chem. Soc*. **2003**, *125*, 8228.

(188) Smith, B. R.; Njardarson, J. T. *Org. Lett.* **2018**, *20*, 2993.

(189) Evans, D. A.; Carter, P. H.; Carreira, E. M.; Prunet, J. A.; Charette, A. B.; Lautens, M. *Angew. Chemie Int. Ed.* **1998**, *37*, 2354.

(190) Holton, R. A.; Kim, H. B.; Somoza, C.; Liang, F.; Biediger, R. J.; Boatman, P. D.; Shindo, M.; Smith, C. C.; Kim, S. *J. Am. Chem. Soc.* **1994**, *116*, 1599.

(191) Smith, A. B.; Nolen, E. G.; Shirai, R.; Blase, F. R.; Ohta, M.; Chida, N.; Hartz, R. A.; Fitch, D. M.; Clark, W. M.; Sprengeler, P. A. *J. Org. Chem.* **1995**, *60*, 7837.

(192) Mahoney, W. S.; Brestensky, D. M.; Stryker, J. M. *J. Am. Chem. Soc.* **1988**, *110*, 291.

(193) Chiu, P.; Li, Z.; Fung, K. C. M. *Tetrahedron Lett.* **2003**, *44*, 455.

(194) Deutsch, C.; Krause, N.; Lipshutz, B. H. *Chem. Rev*. **2008**, *8*, 2916 .

(195) Lee, D.; Yun, J. *Tetrahedron Lett.* **2004**, *45*, 5415.

(196) Lipshutz, B. H.; Keith, J.; Papa, P.; Vivian, R. *Tetrahedron Lett.* **1998**, *39*, 4627.

(197) Rendler, S.; Oestreich, M. *Angew. Chemie Int. Ed.* **2007**, *46*, 498.

(198) Lee, D. W.; Yun, J. *Tetrahedron Lett.* **2005**, *46*, 2037.

(199) Oishi, T.; Nakata, T. *Acc. Chem. Res.* **1984**, *17*, 338.

(200) Dale, J. A.; Dull, D. L.; Mosher, H. S. *J. Org. Chem.* **1969**, *34*, 2543.

(201) Dale, J. A.; Mosher, H. S. *J. Am. Chem. Soc.* **1973**, *95*, 512.

(202) Boden, E. P.; Keck, G. E. *J. Org. Chem.* **1985**, *50*, 2394.

(203) Hoye, T. R.; Jeffrey, C. S.; Shao, F. *Nat. Protoc.* **2007**, *2*, 2451.

(204) Narasimhan, S.; Balakumar, R. *Aldrichimica Acta* **1998**, *31*, 19.

(205) Wadsworth, W. S.; Emmons, W. D. *J. Am. Chem. Soc.* **1961**, *83*, 1733.

(206) Wadsworth, D. H.; Schupp, O. E.; Seus, E. J.; Ford, J. A. *J. Org. Chem.* **1965**, *30*, 680.

(207) Kobayashi, K.; Tanaka, K.; Kogen, H. *Tetrahedron Lett.* **2018**, *59*, 568.

(208) Boutagy, J.; Thomas, R. *Chem. Rev.* **1974**, *74*, 87.

(209) Ando, K. *J. Org. Chem.* **1999**, *64*, 6815.

(210) Vedejs, E.; Peterson, M. J.; John Wiley & Sons Ltd, 2007; pp 1–157.

(211) Paterson, I.; Yeung, K. S.; Smaill, J. *Synlett* **1993**, *10*, 774.

(212) Nicolaou, K. C.; Heretsch, P.; Nakamura, T.; Rudo, A.; Murata, M.; Konoki, K. *J. Am. Chem. Soc.* **2014**, *136*, 16444.

(213) Crimmins, M. T.; Shamszad, M.; Mattson, A. E. *Org. Lett.* **2010**, *12*, 2614.

(214) Winbush, S. M.; Mergott, D. J.; Roush, R. W. *J. Org. Chem* **2008**, *73*, 1818.

(215) Rodríguez, A.; Nomen, M.; Spur, B. W.; Godfroid, J.-J. *European J. Org. Chem.* **1999**, *10*, 2655.

(216) Corey, E. J.; Link, J. O. *Tetrahedron Lett.* **1989**, *30*, 6275.

(217) Hashiguchi, S.; Fujii, A.; Takehara, J.; Ikariya, T.; Noyori, R. *J. Am. Chem. Soc.* **1995**, *117*, 7562.

(218) Noyori, R.; Hashiguchi, S. *Acc. Chem. Res* **1997**, *30*, 97.

(219) Han, B. Y.; Lam, N. Y. S.; MacGregor, C. I.; Goodman, J. M.; Paterson, I. *Chem. Commun.* **2018**, *54*, 3247.

(220) Paterson, I.; Smith, J. D.; Ward, R. A.; Gumming, J. G.; Yeung, K.-S.; Richter, J. P. *J. Chem. Soc. Perkin Trans. I* **1994**, *116*, 1147.

(221) Paterson, I.; Cowden, C.; Rahn, V. S.; Woodrow, M. D. *Synlett* **1998**, *8*, 915.

(222) Inanaga, J.; Hirata, K.; Saeki, H.; Katsuki, T.; Yamaguchi, M. *Bull. Chem. Soc. Jpn.* **1979**, *52*, 1989.

(223) Lindgren, B. O.; Nilsson, T. *Acta Chem. Scand.* **1973**, *27*, 888.

(224) Kraus, G. A.; Taschner, M. J. *J. Org. Chem.* **1980**, *45*, 1175.

(225) Kraus, G. A.; Roth, B. *J. Org. Chem.* **1980**, *45*, 4825.

(226) Bal, B. S.; Childers, W. E.; Pinnick, H. W. *Tetrahedron* **1981**, *37*, 2091.

(227) Tsakos, M.; Schaffert, E. S.; Clement, L. L.; Villadsen, N. L.; Poulsen, T. B. *Nat. Prod. Rep.* **2015**, *32*, 605.

(228) Dhimitruka, I.; SantaLucia, J. *Org. Lett.* **2006**, *8*, 47.

(229) Baker, B. A; Bošković, Z. V. A.; Lipshutz, B. H. *Org. Lett.* **2007**, *10*, 289.

(230) Hikota, M.; Sakurai, Y.; Horita, K.; Yonemitsu, O. *Tetrahedron Lett.* **1990**, *31*, 6367.

(231) Sato, G.; Fisher, H. W.; Puck, T. T. *Science* **1957**, *126*, 961.

(232) Puck, T. T.; Marcus, P. I. *Proc. Natl. Acad. Sci. U. S. A.* **1955**, *41*, 432.

(233) Puck, T. T.; Marcus, P. I.; Cieciura, S. J. *J. Exp. Med.* **1956**, *103*, 273.

(234) Puck, T. T.; Fisher, H. W. *J. Exp. Med.* **1956**, *104*, 427.

(235) Kita, M.; Yoneda, K.; Hirayama, Y.; Yamagishi, K.; Saito, Y.; Sugiyama, Y.; Miwa, Y.; Ohno, O.; Morita, M.; Suenaga, K.; Kigoshi, H. *ChemBioChem* **2012**, *13*, 1754.

(236) Kita, M.; Hirayama, Y.; Yamagishi, K.; Yoneda, K.; Fujisawa, R.; Kigoshi, H. *J. Am. Chem. Soc.* **2012**, *134*, 20314.

(237) Pillow, T. H.; Tien, J.; Parsons-Reponte, K. L.; Bhakta, S.; Li, H.; Staben, L. R.; Li, G.; Chuh, J.; Fourie-O'Donohue, A.; Darwish, M.; Yip, V.; Liu, L.; Leipold, D. D.; Su, D.; Wu, E.; Spencer, S. D.; Shen, B.-Q.; Xu, K.; Kozak, K. R.; Raab, H.; Vandlen, R.; Lewis-Phillips, G. D.; Scheller, R. H.; Polakis, P.; Sliwkowski, M. X.; Flygare, J. A.; Junutula, J. R. *J. Med. Chem.* **2014**, *57*, 7890.

(238) Ducry, L.; Stump, B. *Bioconjug. Chem.* **2010**, *21*, 5.

(239) Nani, R. R.; Gorka, A. P.; Nagaya, T.; Kobayashi, H.; Schnermann, M. J. *Angew. Chemie Int. Ed.* **2015**, *54*, 13635.

(240) Ho, S.; Sackett, D. L.; Leighton, J. L. *J. Am. Chem. Soc.* **2015**, *137*, 14047.

(241) Jain, N.; Smith, S. W.; Ghone, S.; Tomczuk, B. *Pharm. Res.* **2015**, *32*, 3526.

(242) Burke, P. J.; Hamilton, J. Z.; Pires, T. A.; Setter, J. R.; Hunter, J. H.; Cochran, J. H.; Waight, A. B.; Gordon, K. A.; Toki, B. E.; Emmerton, K. K.; Zeng, W.; Stone, I. J.; Senter, P. D.; Lyon, R. P.; Jeffrey, S. C. *Mol. Cancer Ther.* **2016**, *15*, 938.

(243) Staben, L. R.; Koenig, S. G.; Lehar, S. M.; Vandlen, R.; Zhang, D.; Chuh, J.; Yu, S.-F.; Ng, C.; Guo, J.; Liu, Y.; Fourie-O'Donohue, A.; Go, M.; Linghu, X.; Segraves, N. L.; Wang, T.; Chen, J.; Wei, B.; Phillips, G. D. L.; Xu, K.; Kozak, K. R.; Mariathasan, S.; Flygare, J. A.; Pillow, T. H. *Nat. Chem.* **2016**, *8*, 1112.

(244) Carl, P. L.; Chakravarty, P. K.; Katzenellenbogen, J. A. *J. Med. Chem.* **1981**, *24*, 479.

(245) Dubowchik, G. M.; Firestone, R. A. *Bioorg. Med. Chem. Lett.* **1998**, *8*, 3341.

(246) Adem, Y. T.; Schwarz, K. A.; Duenas, E.; Patapoff, T. W.; Galush, W. J.; Esue, O. *Bioconjug. Chem.* **2014**, *25*, 656.

(247) Zhao, R. Y.; Wilhelm, S. D.; Audette, C.; Jones, G.; Leece, B. A.; Lazar, A. C.; Goldmacher, V. S.; Singh, R.; Kovtun, Y.; Widdison, W. C.; Lambert, J. M.; Chari, R. V. J. *J. Med. Chem.* **2011**, *54*, 3606.

(248) Chennamsetty, N.; Voynov, V.; Kayser, V.; Helk, B.; Trout, B. L. *Proc. Natl. Acad. Sci. U. S. A.* **2009**, *106*, 11937.

(249) Burke, P. J.; Senter, P. D.; Meyer, D. W.; Miyamoto, J. B.; Anderson, M.; Toki, B. E.; Manikumar, G.; Wani, M. C.; Kroll, D. J.; Jeffrey, S. C. *Bioconjug. Chem.* **2009**, *20*, 1242.

(250) Verma, V. A.; Pillow, T. H.; DePalatis, L.; Li, G.; Phillips, G. L.; Polson, A. G.; Raab, H. E.; Spencer, S.; Zheng, B. *Bioorg. Med. Chem. Lett.* **2015**, *25*, 864.

(251) Zhang, D.; Le, H.; Cruz-Chuh, J.; Bobba, S.; Guo, J.; Staben, L.; Zhang, C.; Ma, Y.; Kozak, K. R.; Lewis Phillips, G. D.; Vollmar, B. S.; Sadowsky, J. D.; Vandlen, R.; Wei, B.; Su, D.; Fan, P.; Dragovich, P. S.; Khojasteh, S. C.; Hop, C. E. C. A.; Pillow, T. H. *Bioconjug. Chem.* **2018**, *29*, 267.

(252) Dubowchik, G. M.; Firestone, R. A.; Padilla, L.; Willner, D.; Hofstead, S. J.; Mosure, K.; Knipe, J. O.; Lasch, S. J.; Trail, P. A. *Bioconjug. Chem.* **2002**, *13*, 855.

(253) Mondal, D.; Ford, J.; Pinney, K. G. *Tetrahedron Lett.* **2018**, *59*, 3594.

(254) Wei, B.; Gunzner-Toste, J.; Yao, H.; Wang, T.; Wang, J.; Xu, Z.; Chen, J.; Wai, J.; Nonomiya, J.; Tsai, S. P.; Chuh, J.; Kozak, K. R.; Liu, Y.; Yu, S.-F.; Lau, J.; Li, G.; Phillips, G. D.; Leipold, D.; Kamath, A.; Su, D.; Xu, K.; Eigenbrot, C.; Steinbacher, S.; Ohri, R.; Raab, H.; Staben, L. R.; Zhao, G.; Flygare, J. A.; Pillow, T. H.; Verma, V.; Masterson, L. A.; Howard, P. W.; Safina, B. *J. Med. Chem.* **2018**, *61*, 989.

(255) Belleau, B.; Malek, G. *J. Am. Chem. Soc.* **1968**, *90*, 1651.

(256) Belleau, B.; Martel, R. R.; Lacasse, G.; Menard, M.; Weinberg, N. L.; Perron, Y. G. *J. Am. Chem. Soc.* **1968**, *90*, 823.

(257) Cremin, D. J.; Hegarty, A. F.; Begley, M. J. *J. Chem. Soc. Perkin Trans. 2* **1980**, *2*, 412.

(258) Tiberghien, A. C.; Levy, J.-N.; Masterson, L. A.; Patel, N. V.; Adams, L. R.; Corbett, S.; Williams, D. G.; Hartley, J. A.; Howard, P. W. *ACS Med. Chem. Lett.* **2016**, *7*, 983.

(259) Jeffrey, S. C.; Nguyen, M. T.; Andreyka, J. B.; Meyer, D. L.; Doronina, S. O.; Senter, P. D. *Bioorg. Med. Chem. Lett.* **2006**, *16*, 358.

(260) Cazzamalli, S.; Corso, A. D.; Neri, D. *J. Control. Release* **2017**, *246*, 39.

(261) Wang, Y.; Fan, S.; Zhong, W.; Zhou, X.; Li, S.; Wang, Y.; Fan, S.; Zhong, W.; Zhou, X.; Li, S. *Int. J. Mol. Sci.* **2017**, *18*, 1860.

(262) Deziel, R. *Tetrahedron Lett.* **1987**, *28*, 4371.

(263) Mitsunobu, O.; Yamada, M. *Bull. Chem. Soc. Jpn.* **1967**, *40*, 2380.

(264) Bargh, J. *CPGS*, University of Cambridge, 2017.

(265) Gaynord, J. *CPGS*, Univeristy of Cambridge, 2017.

(266) Armarego W.L.F, *Purification of Laboratory Chemicals*, 4th edition; Butterworth-Heinemann, 1996.

(267) Patil, V. J. *Tetrahedron Lett.* **1996**, *37*, 1481.

(268) Couture, A.; Deniau, E.; Grandclaudon, P.; Woisel, P. *Tetrahedron* **1996**, *52*, 4433.

Appendix: *Selected ^{1}H and ^{13}C NMR spectra*

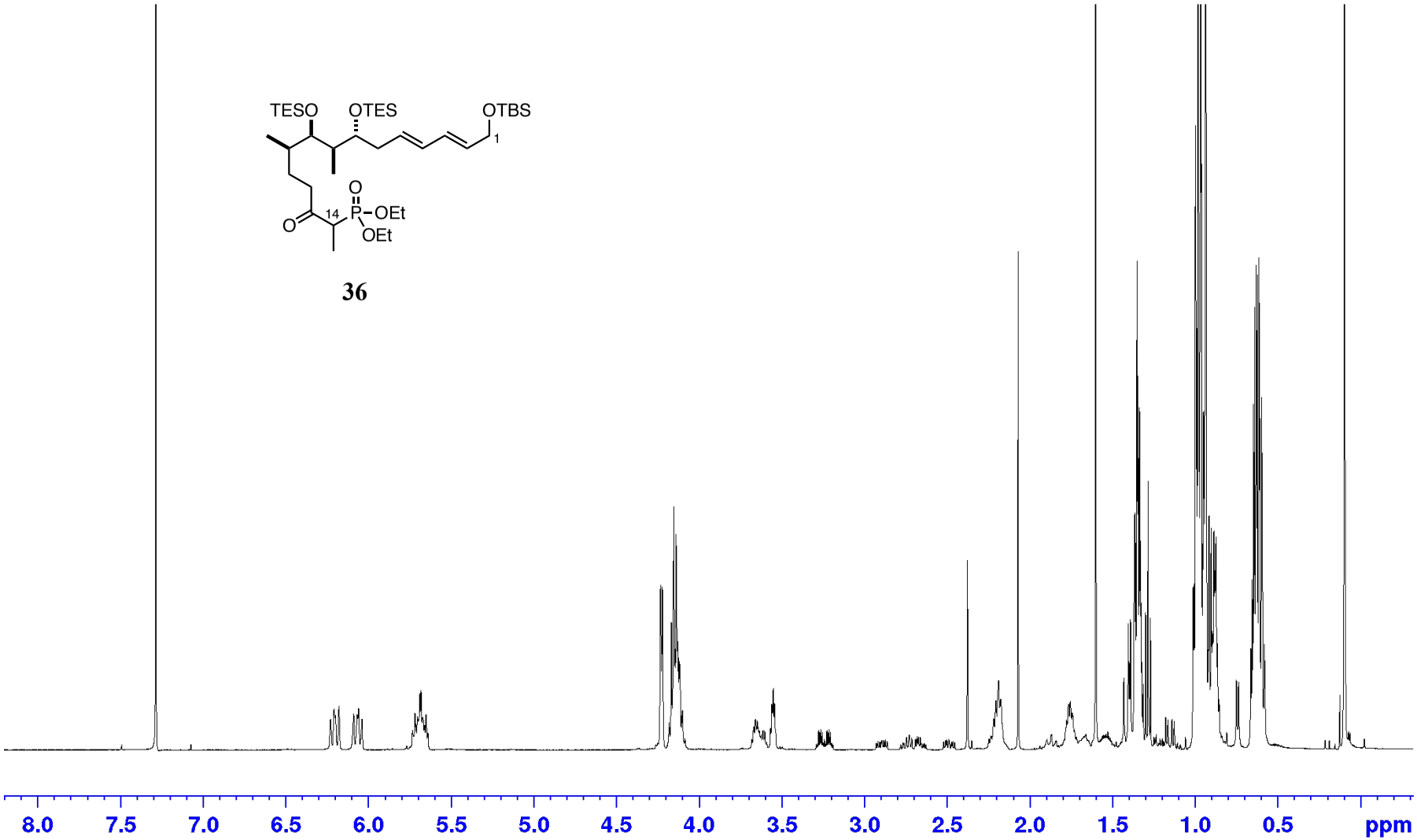
TESO
OTES
OTBS
1
O
14
P
OEt
OEt
O
8.0
7.5
7.0
6.5
6.0
5.5
5.0
4.5
4.0
3.5
3.0
2.5
2.0
1.5
1.0
0.5
ppm

36

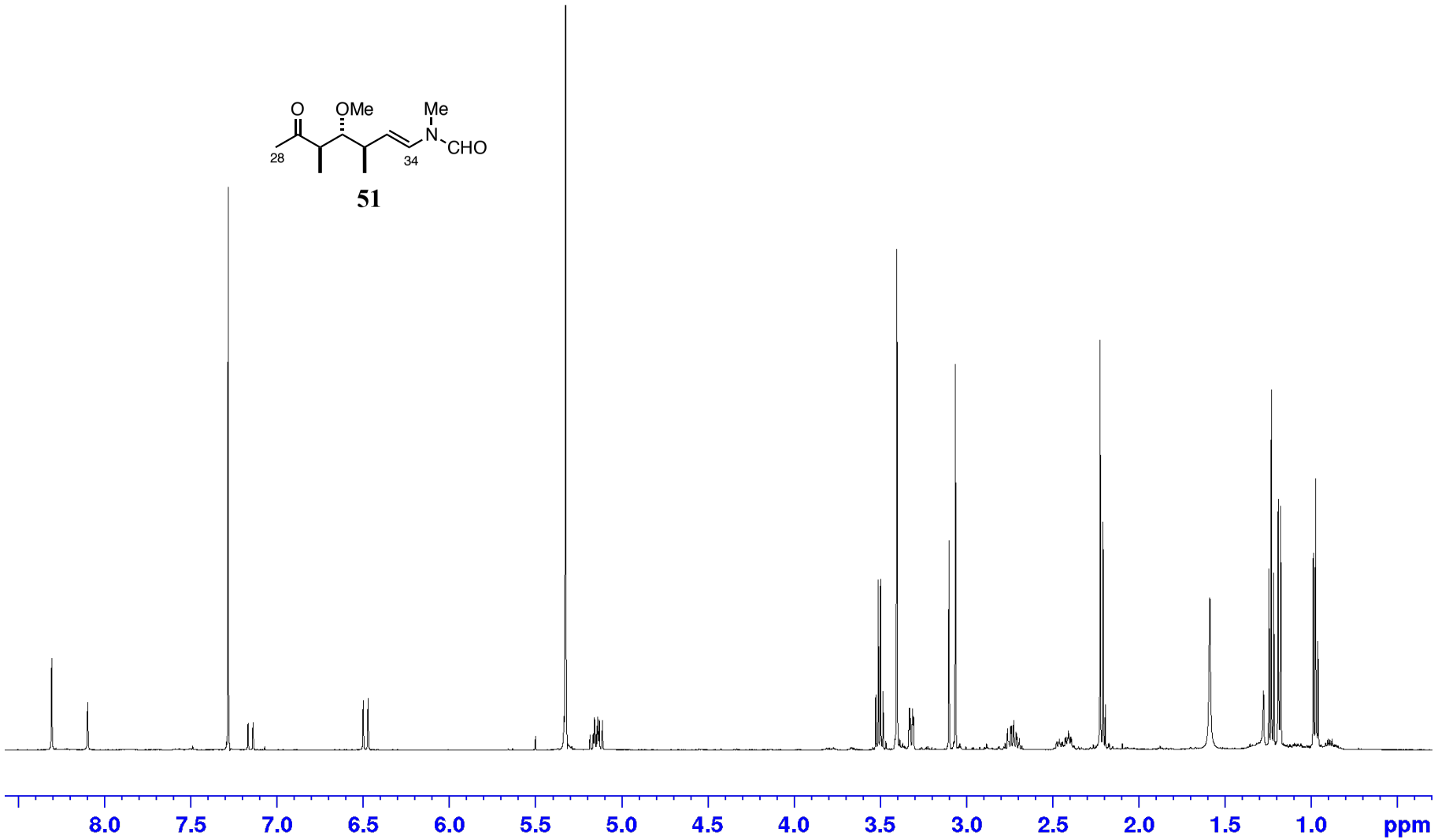

51

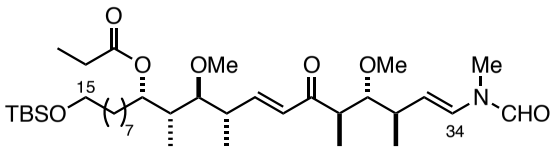
O
O
OMe
O
OMe
Me
N
CHO
TBSO
15
7
34

102

8.0
7.5
7.0
6.5
6.0
5.5
5.0
4.5
4.0
3.5
3.0
2.5
2.0
1.5
1.0
0.5
ppm

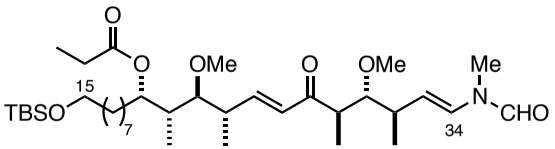
O
O
OMe
O
OMe
Me
15
TBSO
7
N
CHO
34

102

200
190
180
170
160
150
140
130
120
110
100
90
80
70
60
50
40
30
20
10
0
ppm

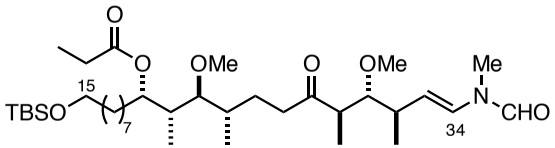
O
O
OMe
O
OMe
Me
15
TBSO
7
N
CHO
34

105

8.5
8.0
7.5
7.0
6.5
6.0
5.5
5.0
4.5
4.0
3.5
3.0
2.5
2.0
1.5
1.0
0.5
ppm

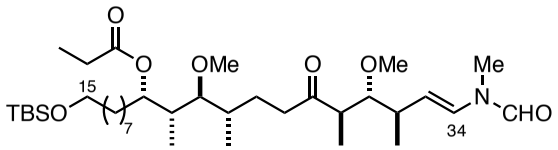
O
O
OMe
O
OMe
Me
15
TBSO
7
N
CHO
34

105

210
200
190
180
170
160
150
140
130
120
110
100
90
80
70
60
50
40
30
20
10
0
ppm

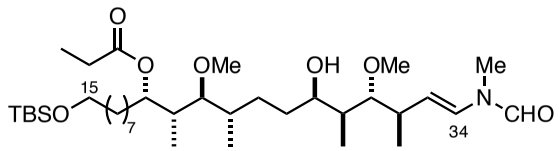
O
O
OMe
OH
OMe
Me
15
TBSO
7
N
CHO
34

109

8.5
8.0
7.5
7.0
6.5
6.0
5.5
5.0
4.5
4.0
3.5
3.0
2.5
2.0
1.5
1.0
0.5
0.0
ppm

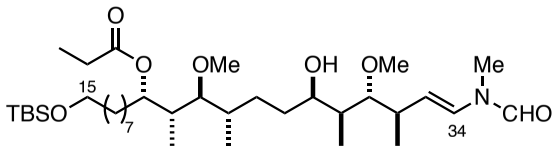
O
O
OMe
OH
OMe
Me
15
TBSO
7
N
CHO
34

109

200
190
180
170
160
150
140
130
120
110
100
90
80
70
60
50
40
30
20
10
0
ppm

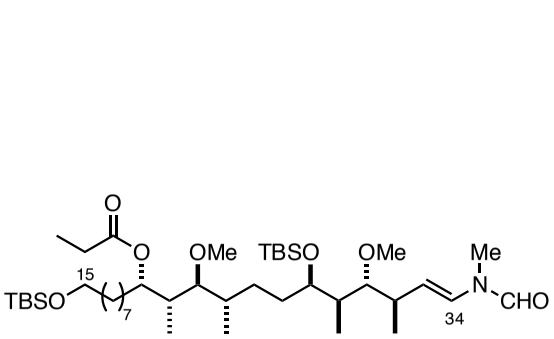
O
O
OMe
TBSO
OMe
Me
15
TBSO
7
N
CHO
34

113

8.5
8.0
7.5
7.0
6.5
6.0
5.5
5.0
4.5
4.0
3.5
3.0
2.5
2.0
1.5
1.0
0.5
0.0
-0.5
ppm

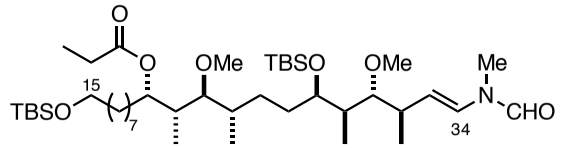
O
O
OMe
TBSO
OMe
Me
15
TBSO
7
N
CHO
34

113

180
170
160
150
140
130
120
110
100
90
80
70
60
50
40
30
20
10
0
ppm

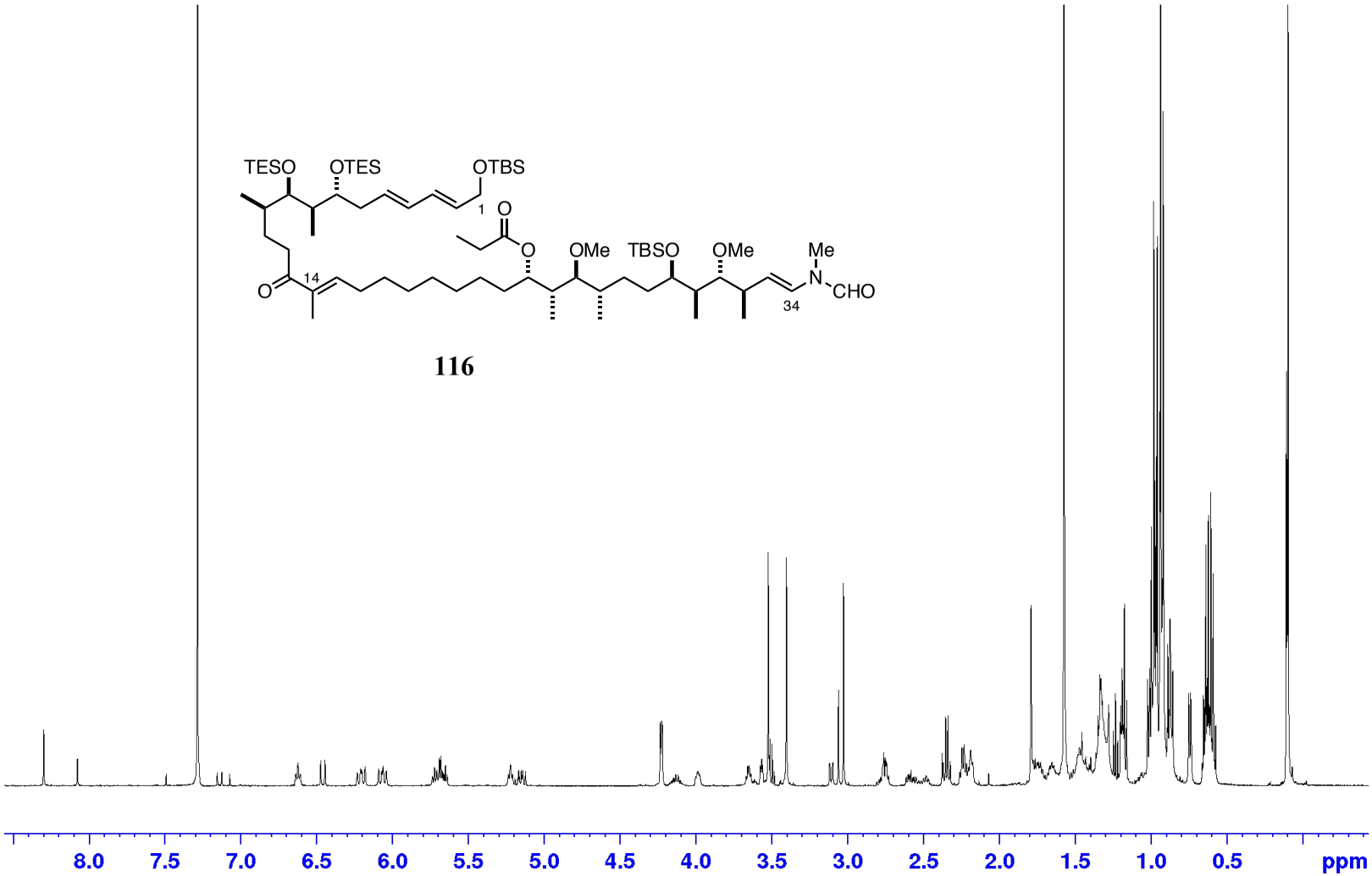
TESO
OTES
OTBS
1
O
O
OMe
TBSO
OMe
Me
N
CHO
34
14
O
8.0
7.5
7.0
6.5
6.0
5.5
5.0
4.5
4.0
3.5
3.0
2.5
2.0
1.5
1.0
0.5
ppm

116

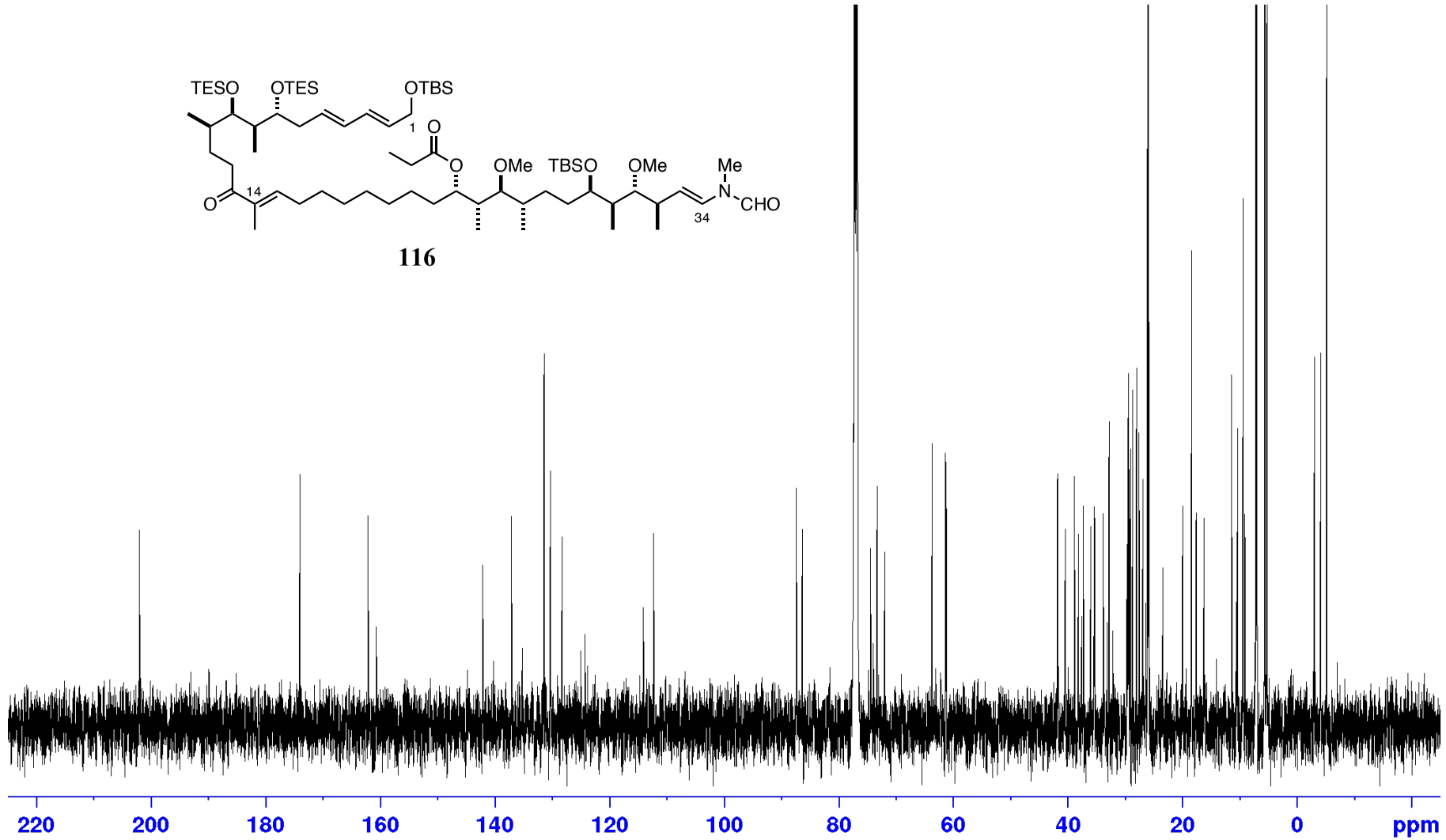
TESO
OTES
OTBS
1
O
O
OMe
TBSO
OMe
Me
N
CHO
O
14
34
220
200
180
160
140
120
100
80
60
40
20
0
ppm

116

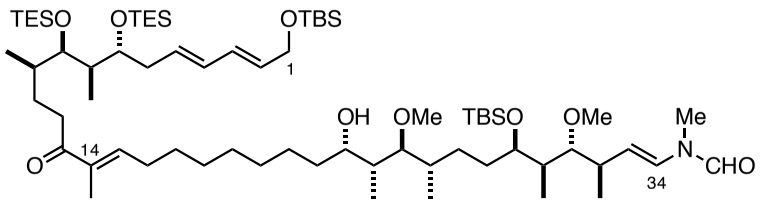
TESO
OTES
OTBS
1
OH
OMe
TBSO
OMe
Me
N
CHO
O
14
34

119

8.0
7.5
7.0
6.5
6.0
5.5
5.0
4.5
4.0
3.5
3.0
2.5
2.0
1.5
1.0
0.5
0.0
ppm

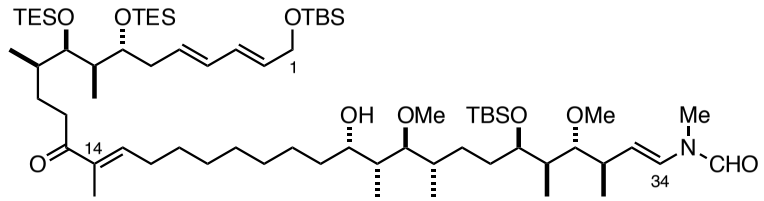
TESO
OTES
OTBS
1
OH
OMe
TBSO
OMe
Me
N
CHO
O
14
34

119

200
190
180
170
160
150
140
130
120
110
100
90
80
70
60
50
40
30
20
10
0
ppm

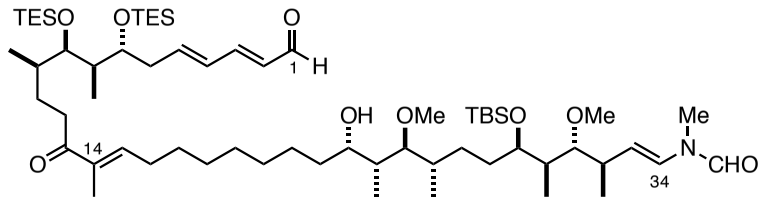
TESO
OTES
O
1
H
OH
OMe
TBSO
OMe
Me
N
CHO
O
14
34

120

9.5
9.0
8.5
8.0
7.5
7.0
6.5
6.0
5.5
5.0
4.5
4.0
3.5
3.0
2.5
2.0
1.5
1.0
0.5
ppm

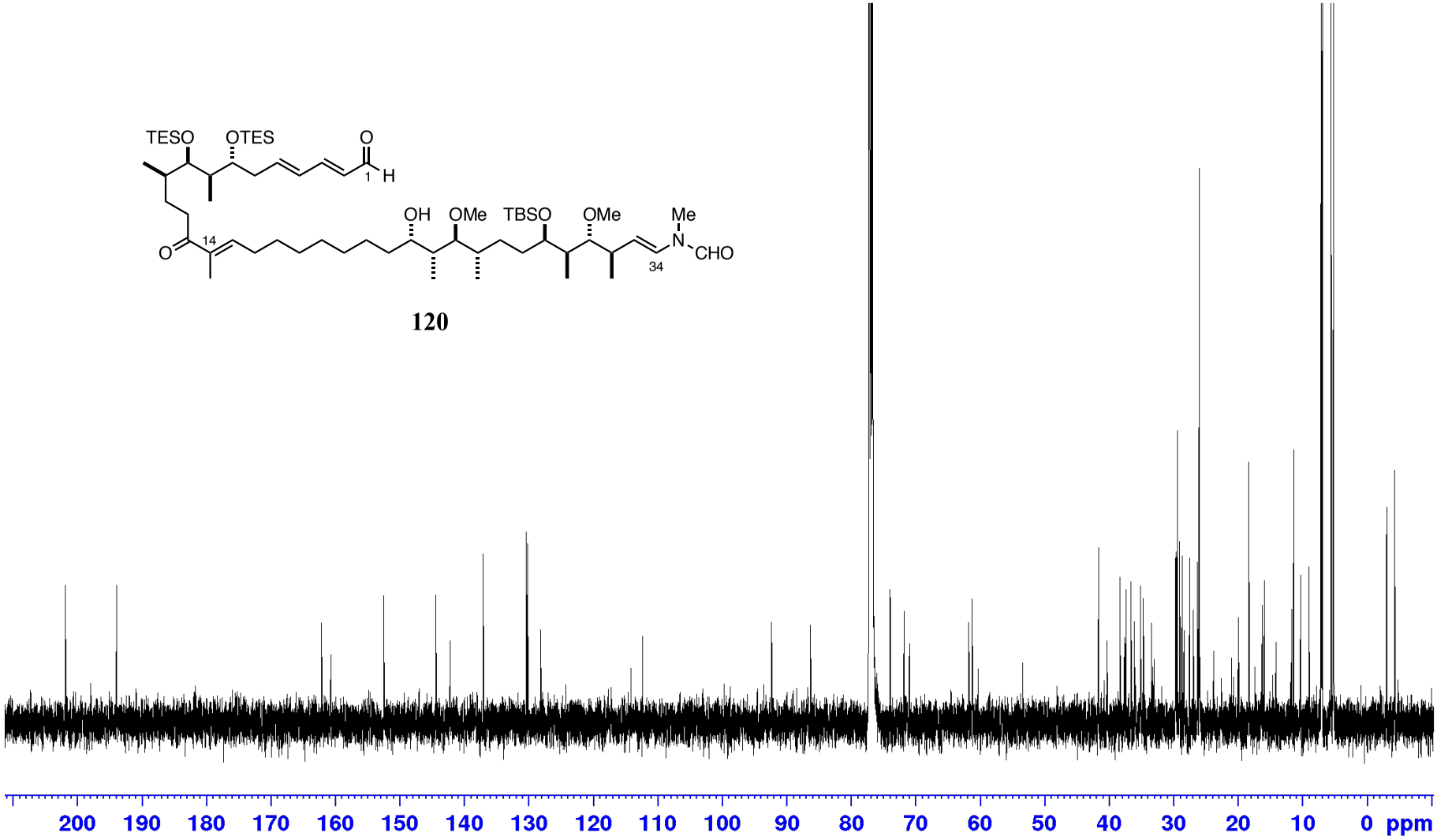
TESO
OTES
O
1
H
OH
OMe
TBSO
OMe
Me
N
CHO
14
O
34
200
190
180
170
160
150
140
130
120
110
100
90
80
70
60
50
40
30
20
10
0
ppm

120

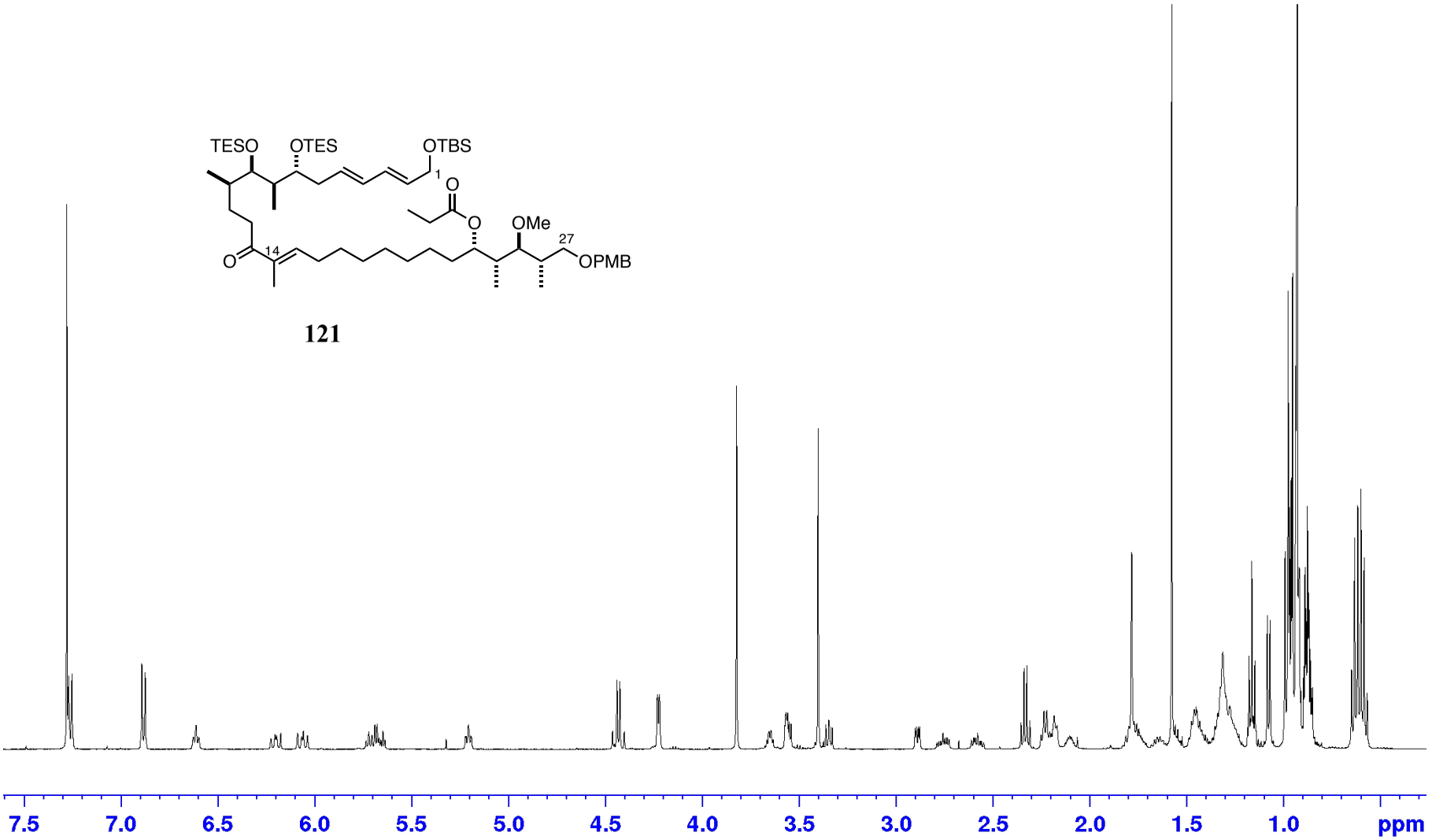
TESO
OTES
OTBS
1
O
O
OMe
27
14
O
OPMB
7.5
7.0
6.5
6.0
5.5
5.0
4.5
4.0
3.5
3.0
2.5
2.0
1.5
1.0
ppm

121

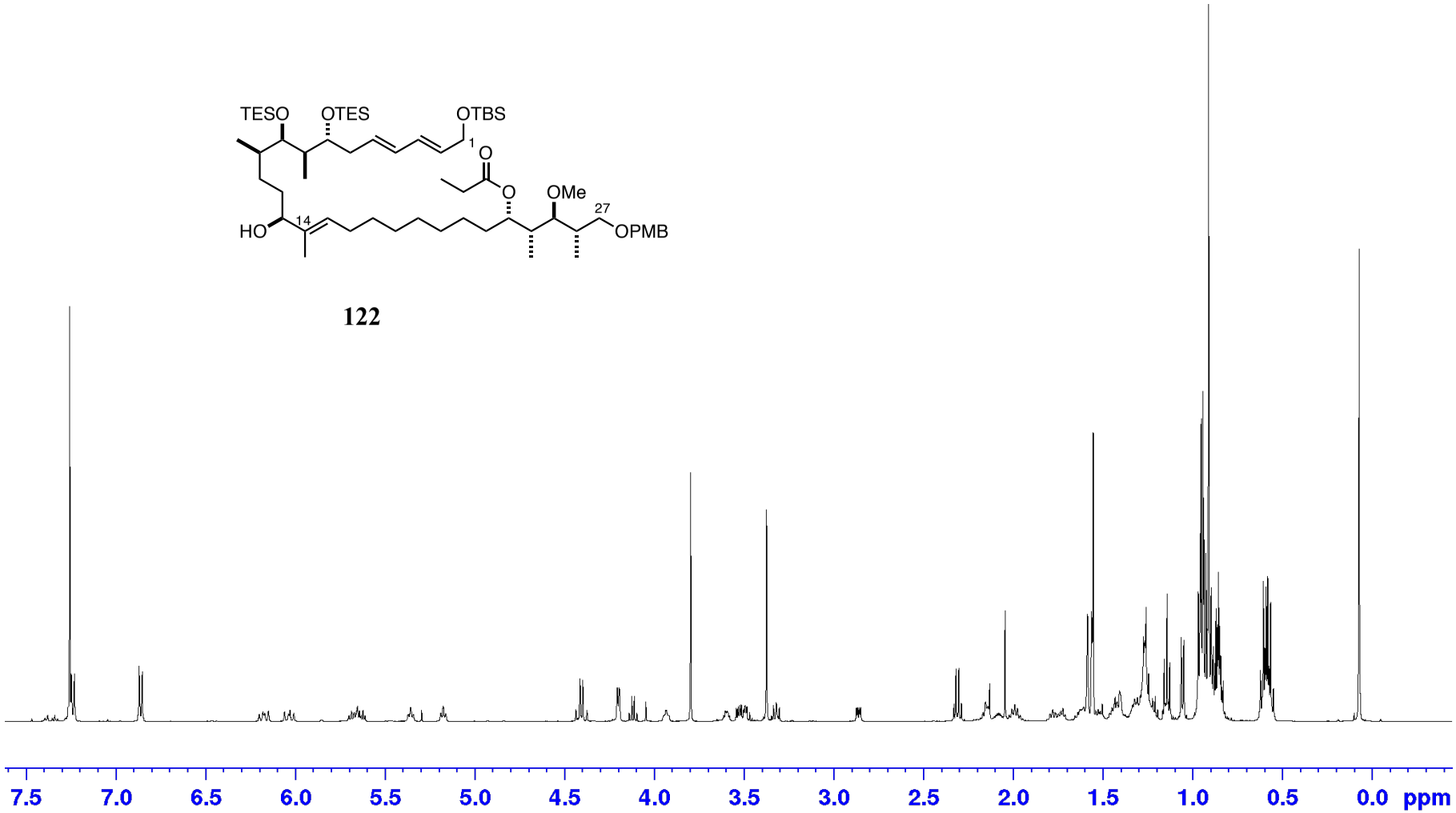
TESO
OTES
OTBS
1
O
O
OMe
27
HO
14
OPMB
7.5
7.0
6.5
6.0
5.5
5.0
4.5
4.0
3.5
3.0
2.5
2.0
1.5
1.0
0.5
0.0
ppm

122

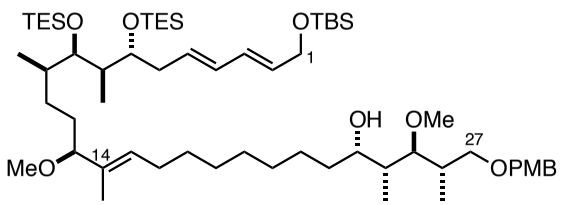
TESO
OTES
OTBS
1
OH
OMe
27
MeO
14
OPMB

123

7.0
6.5
6.0
5.5
5.0
4.5
4.0
3.5
3.0
2.5
2.0
1.5
1.0
0.5
ppm

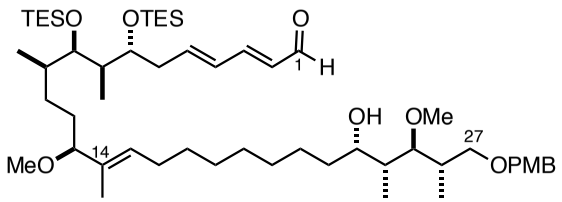
TESO
OTES
O
1
H
OH
OMe
27
MeO
14
OPMB

124

9.5
9.0
8.5
8.0
7.5
7.0
6.5
6.0
5.5
5.0
4.5
4.0
3.5
3.0
2.5
2.0
1.5
1.0
ppm

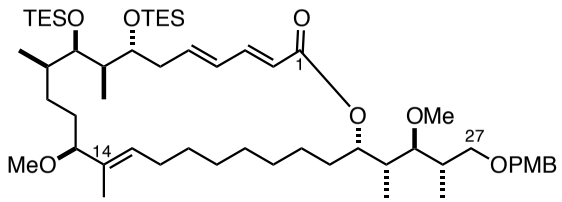
TESO
OTES
O
1
O
OMe
27
MeO
14
OPMB

126

7.0
6.5
6.0
5.5
5.0
4.5
4.0
3.5
3.0
2.5
2.0
1.5
1.0
ppm

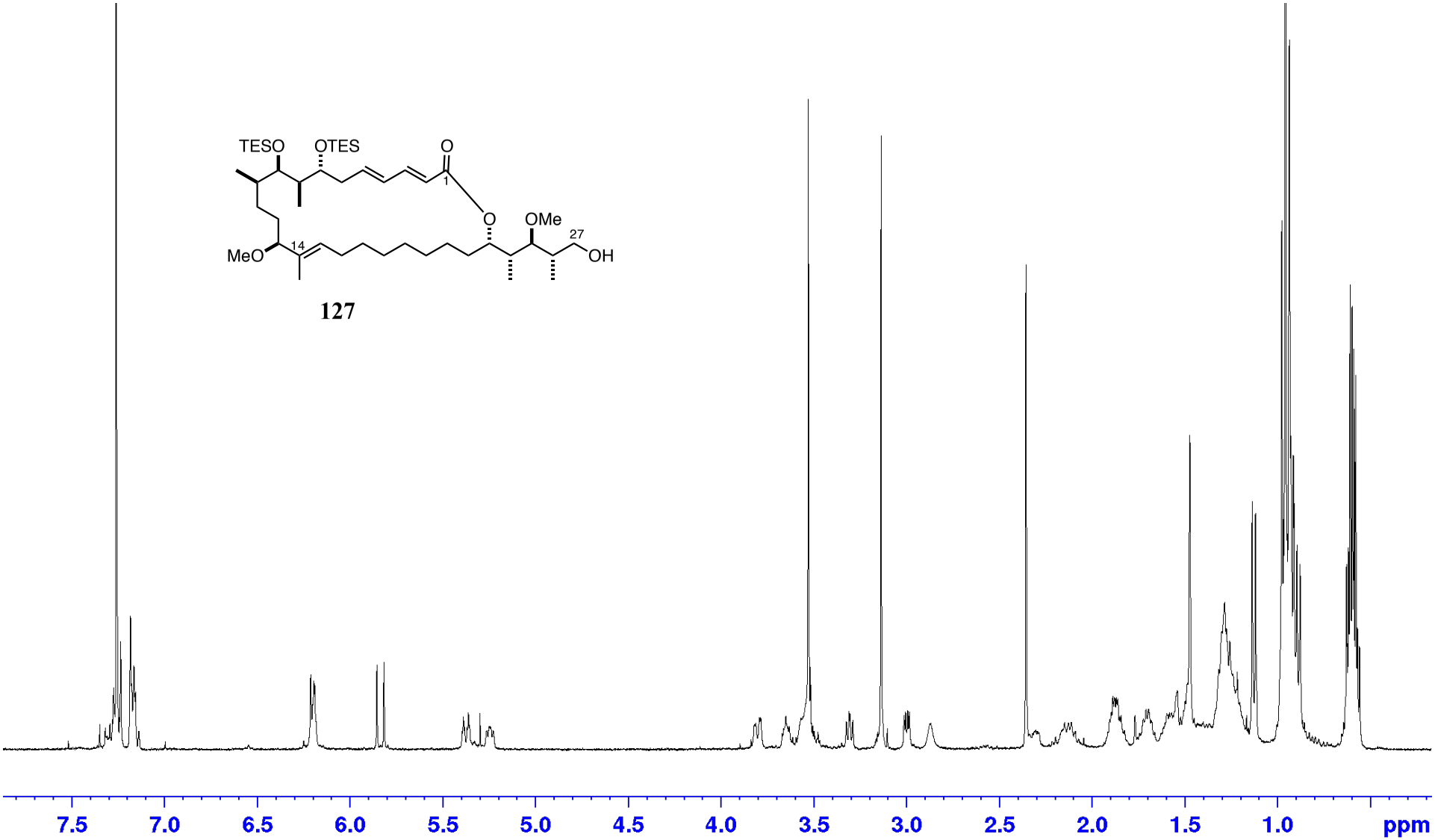
TESO
OTES
O
1
O
OMe
27
MeO
14
OH
7.5
7.0
6.5
6.0
5.5
5.0
4.5
4.0
3.5
3.0
2.5
2.0
1.5
1.0
ppm

127

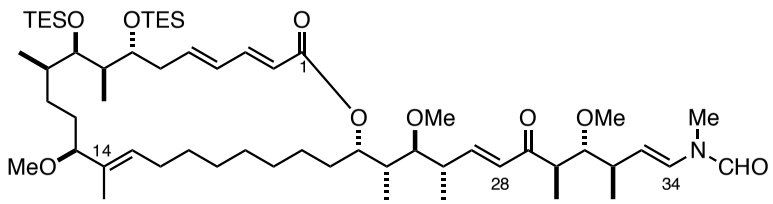
TESO
OTES
O
1
O
OMe
O
OMe
Me
N
CHO
MeO
14
28
34

129

8.0
7.5
7.0
6.5
6.0
5.5
5.0
4.5
4.0
3.5
3.0
2.5
2.0
1.5
1.0
0.5
ppm

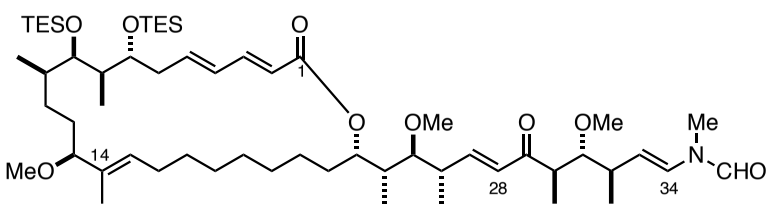
TESO
OTES
O
1
O
OMe
O
OMe
Me
N
CHO
MeO
14
28
34

129

200
190
180
170
160
150
140
130
120
110
100
90
80
70
60
50
40
30
20
10
ppm

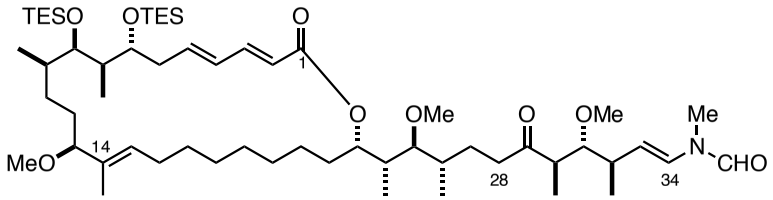
TESO
OTES
O
1
O
OMe
O
OMe
Me
N
CHO
MeO
14
28
34

130

8.5
8.0
7.5
7.0
6.5
6.0
5.5
5.0
4.5
4.0
3.5
3.0
2.5
2.0
1.5
1.0
ppm

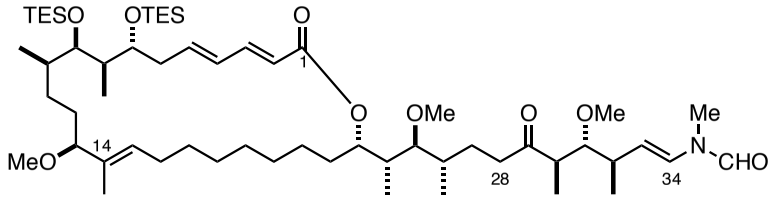
TESO
OTES
O
1
O
OMe
O
OMe
Me
N
CHO
MeO
14
28
34

130

220
210
200
190
180
170
160
150
140
130
120
110
100
90
80
70
60
50
40
30
20
ppm

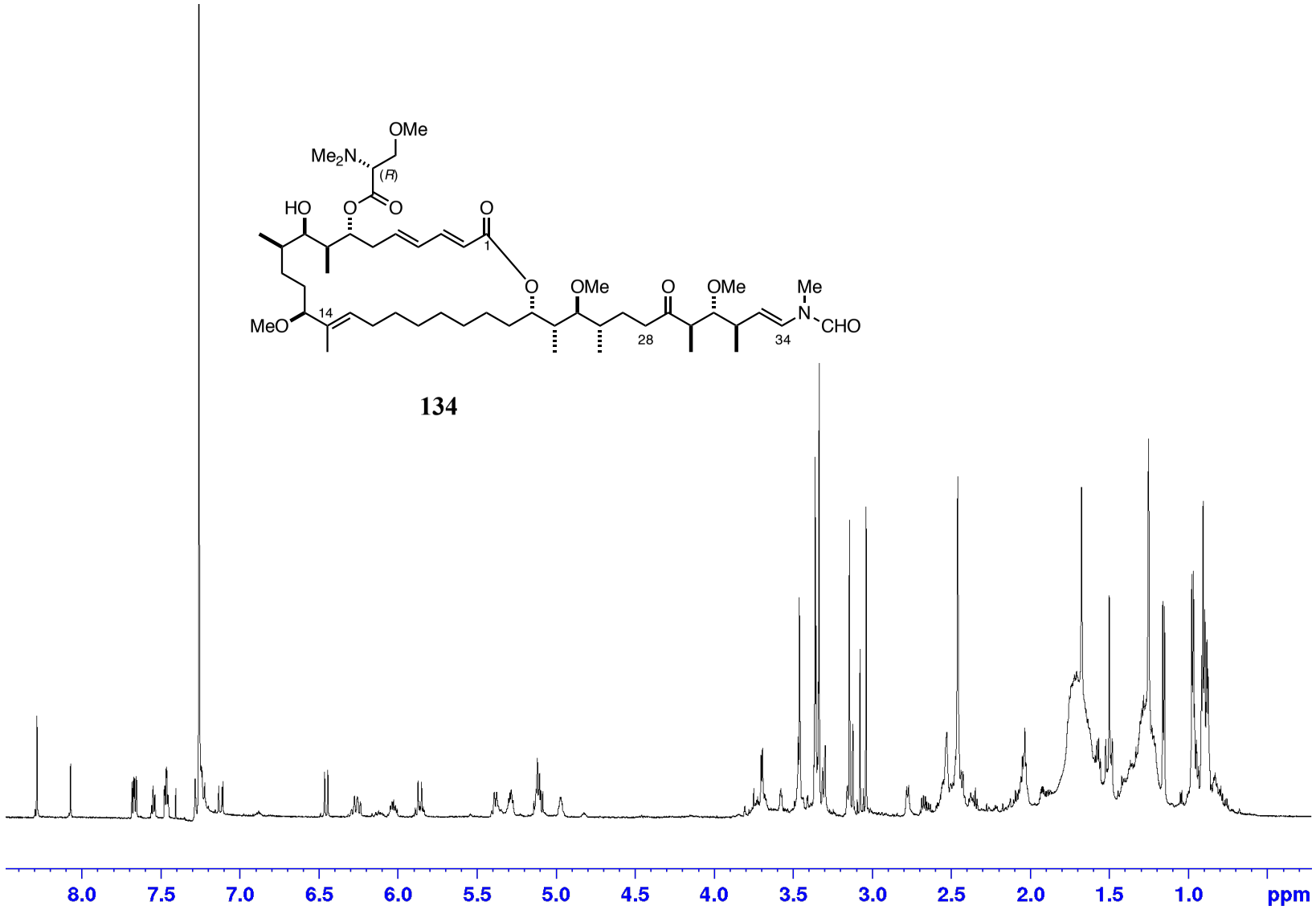
OMe
Me2N
(R)
HO
O
O
O
1
O
OMe
O
OMe
Me
N
CHO
MeO
14
28
34
8.0
7.5
7.0
6.5
6.0
5.5
5.0
4.5
4.0
3.5
3.0
2.5
2.0
1.5
1.0
ppm

134

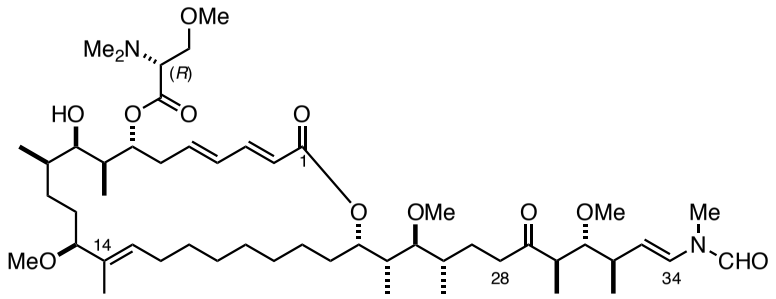
OMe
Me2N
(R)
HO
O
O
O
1
O
OMe
O
OMe
Me
N
CHO
MeO
14
28
34

134

210
200
190
180
170
160
150
140
130
120
110
100
90
80
70
60
50
40
30
20
ppm

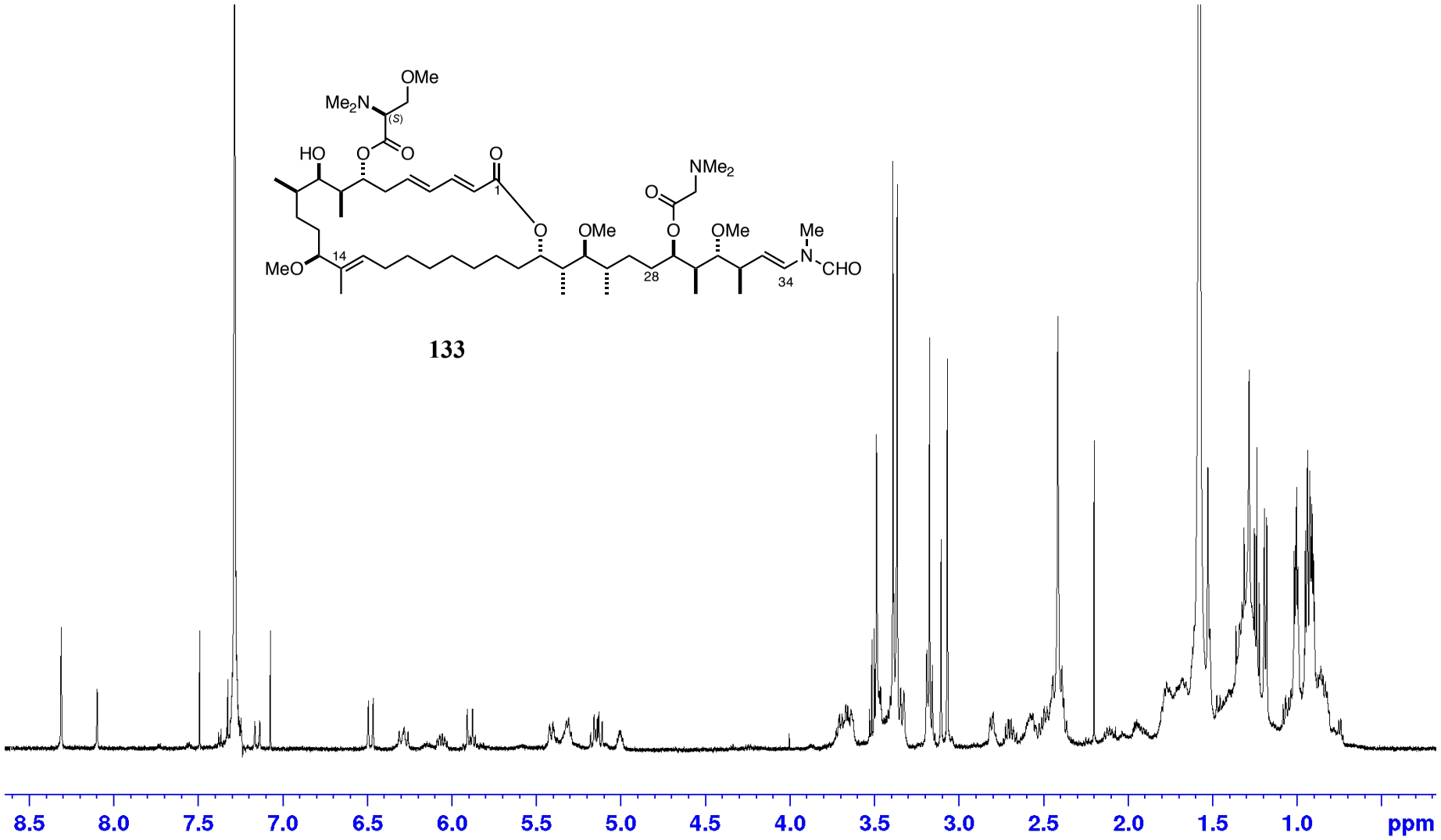
OMe
Me2N
(S)
HO
O
O
O
1
NMe2
O
O
OMe
O
OMe
Me
N
CHO
MeO
14
28
34
8.5
8.0
7.5
7.0
6.5
6.0
5.5
5.0
4.5
4.0
3.5
3.0
2.5
2.0
1.5
1.0
ppm

133

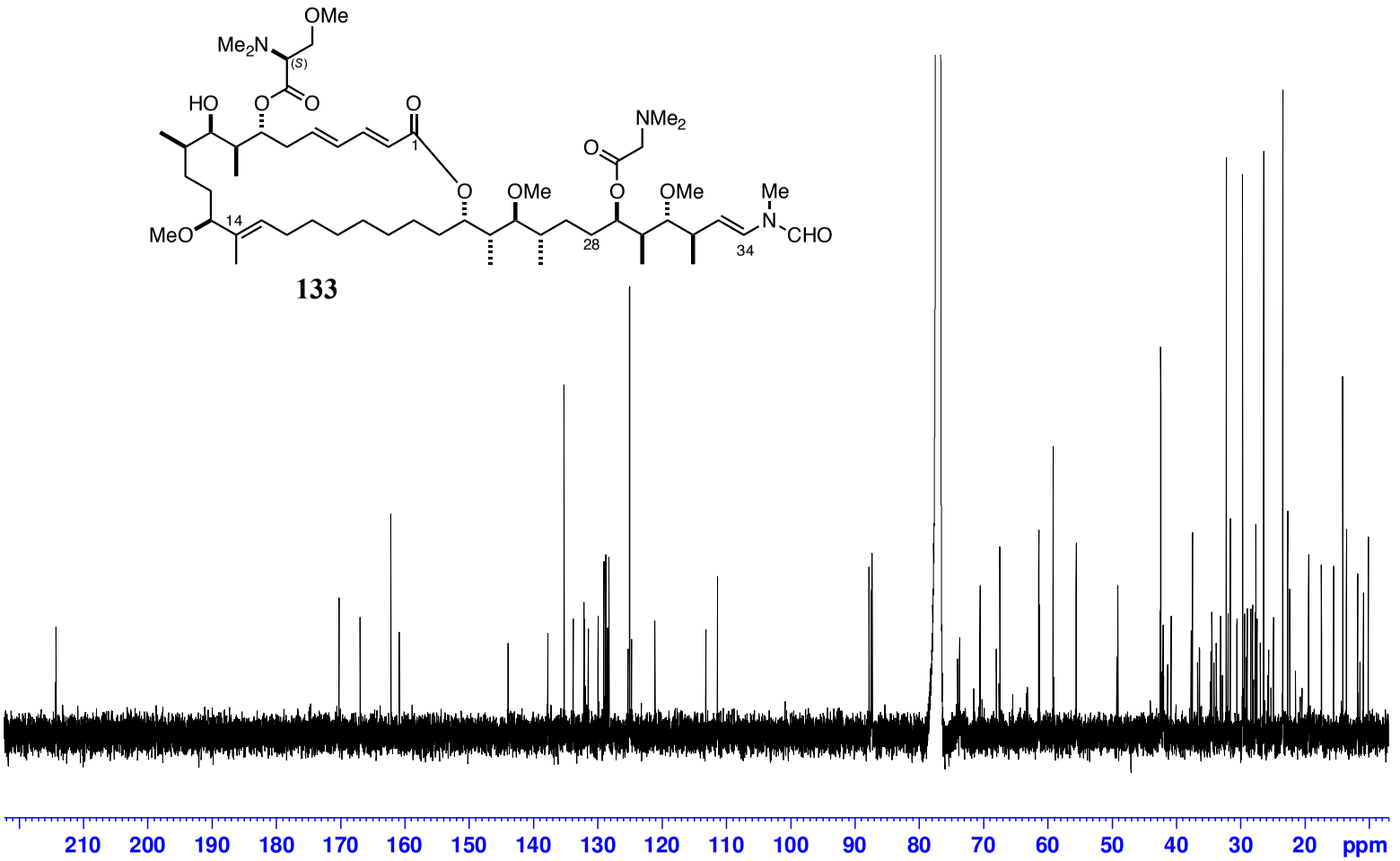
OMe
Me2N
(S)
HO
O
O
O
1
NMe2
O
O
OMe
O
OMe
Me
N
CHO
MeO
14
28
34
210
200
190
180
170
160
150
140
130
120
110
100
90
80
70
60
50
40
30
20
ppm

133

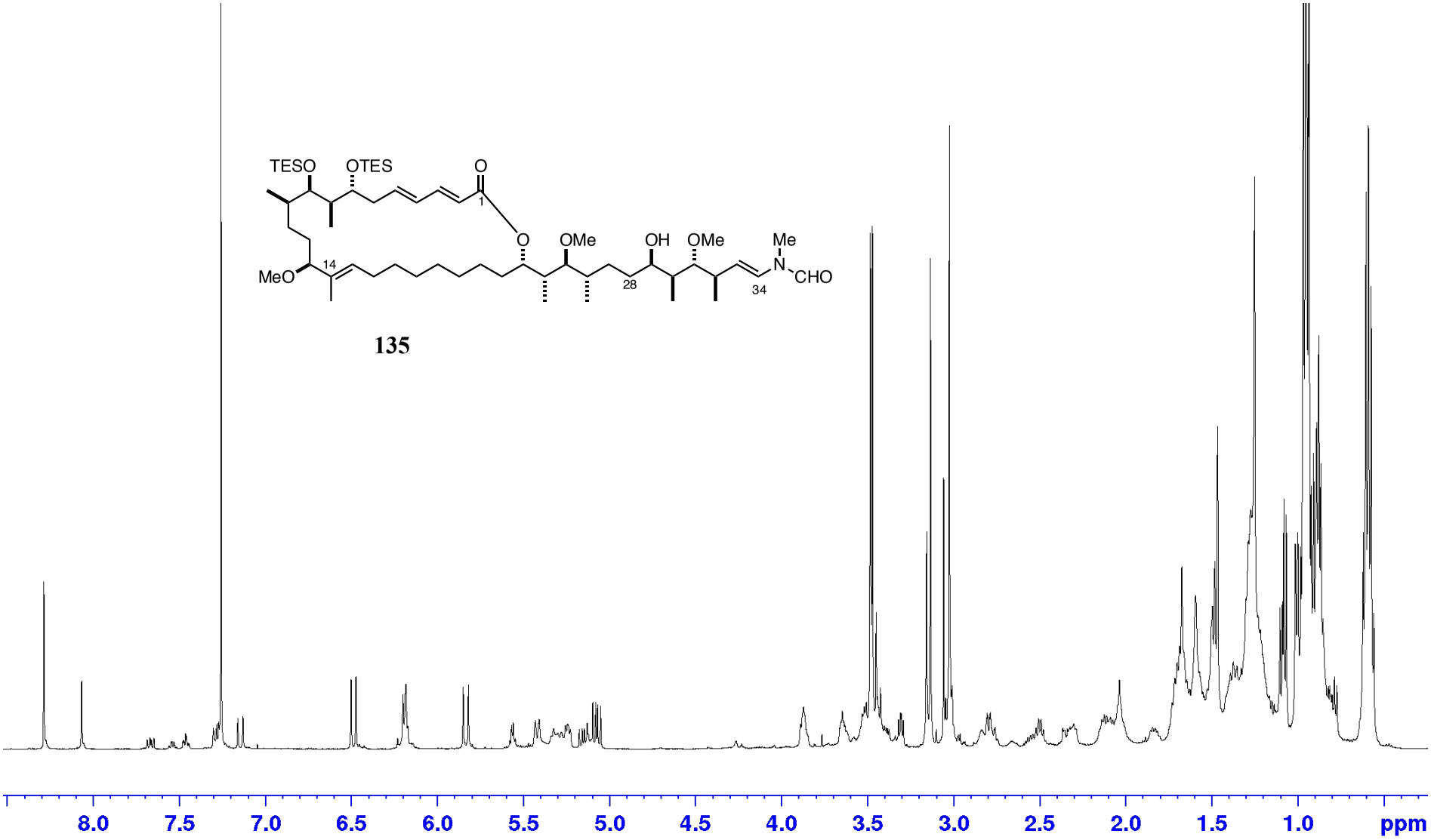
TESO
OTES
O
1
O
OMe
OH
OMe
Me
N
CHO
MeO
14
28
34
8.0
7.5
7.0
6.5
6.0
5.5
5.0
4.5
4.0
3.5
3.0
2.5
2.0
1.5
1.0
ppm

135

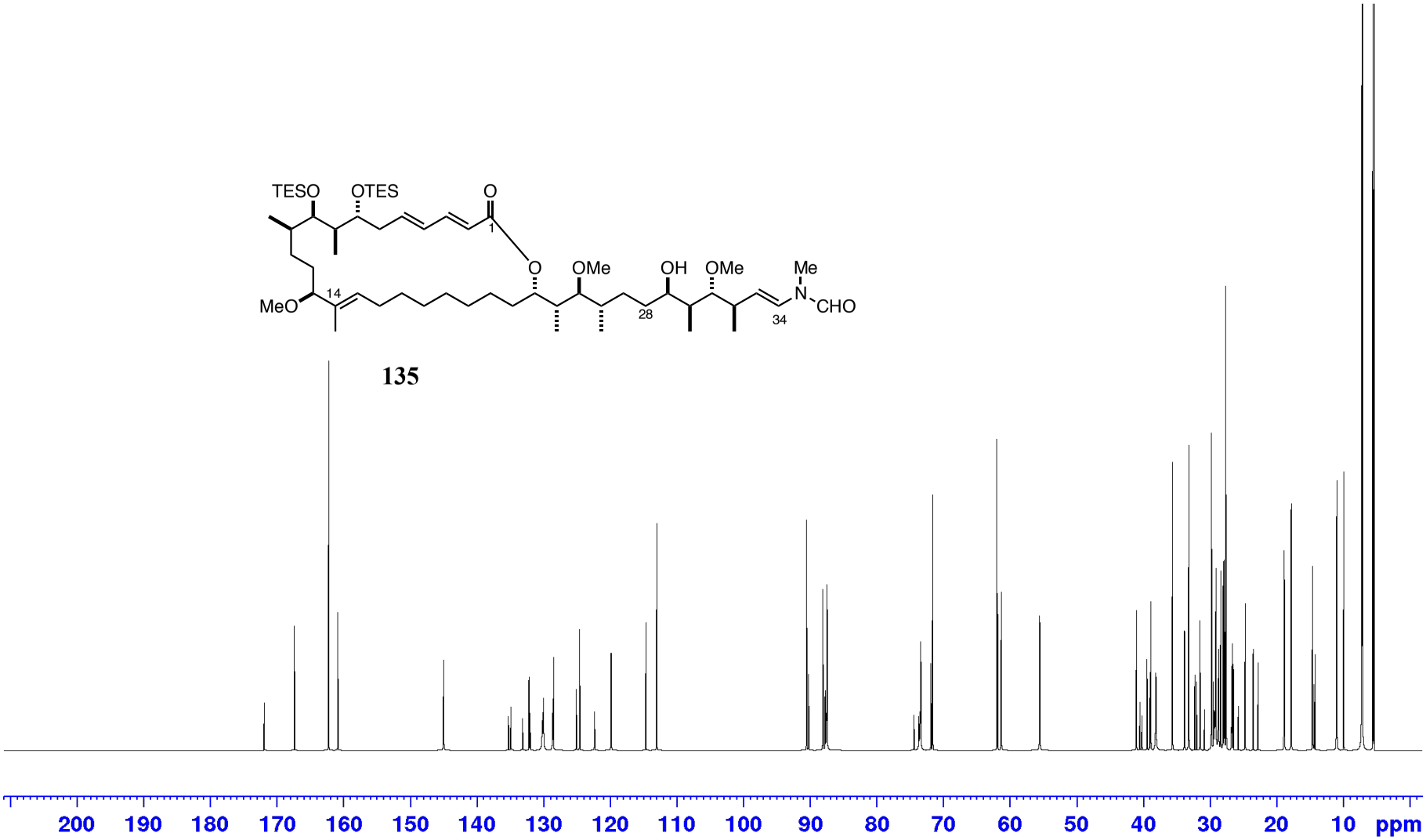
TESO
OTES
O
1
O
OMe
OH
OMe
Me
N
CHO
MeO
14
28
34
200
190
180
170
160
150
140
130
120
110
100
90
80
70
60
50
40
30
20
10
ppm

135

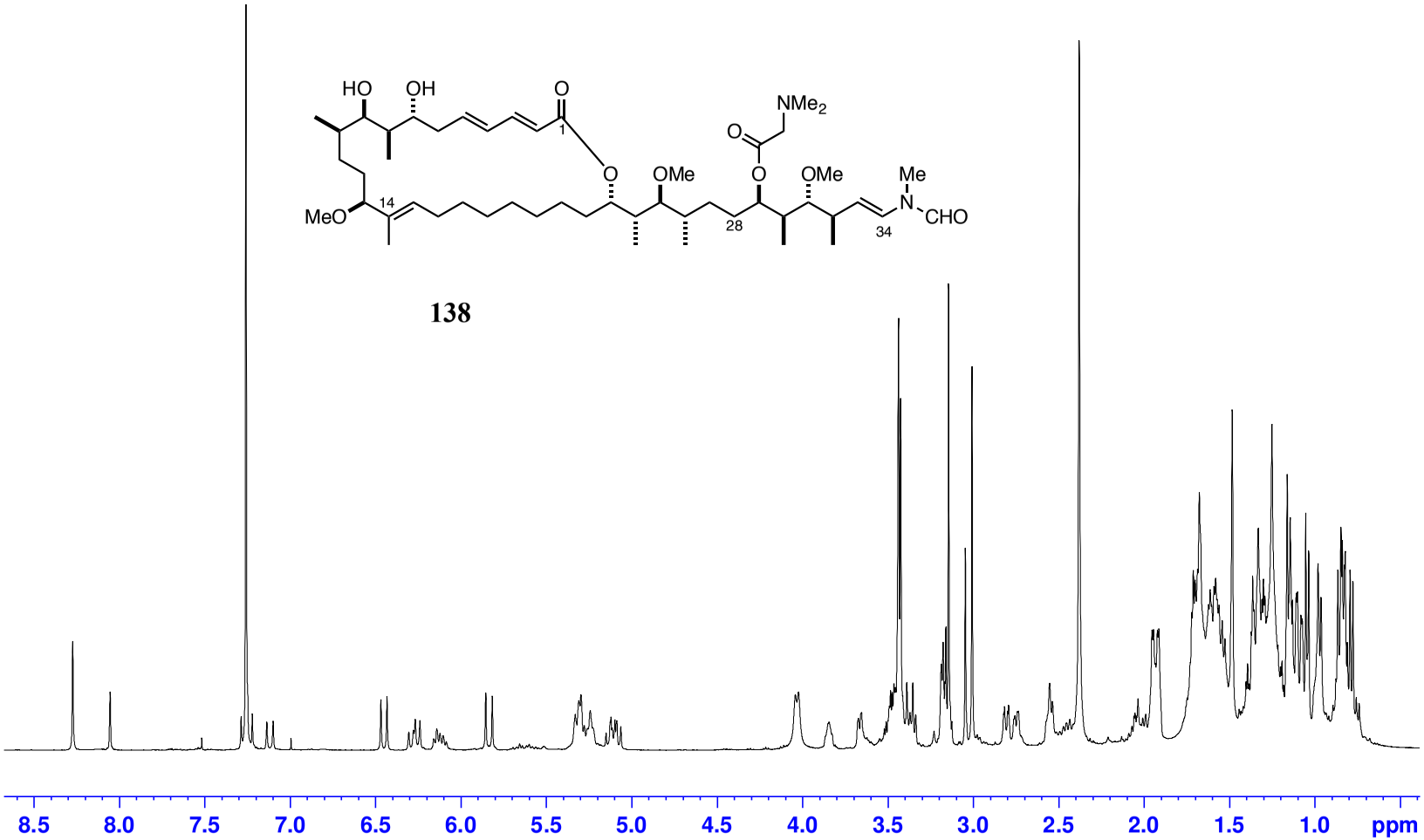
HO
OH
O
1
NMe2
O
O
OMe
O
OMe
Me
N
CHO
MeO
14
28
34
8.5
8.0
7.5
7.0
6.5
6.0
5.5
5.0
4.5
4.0
3.5
3.0
2.5
2.0
1.5
1.0
ppm

138

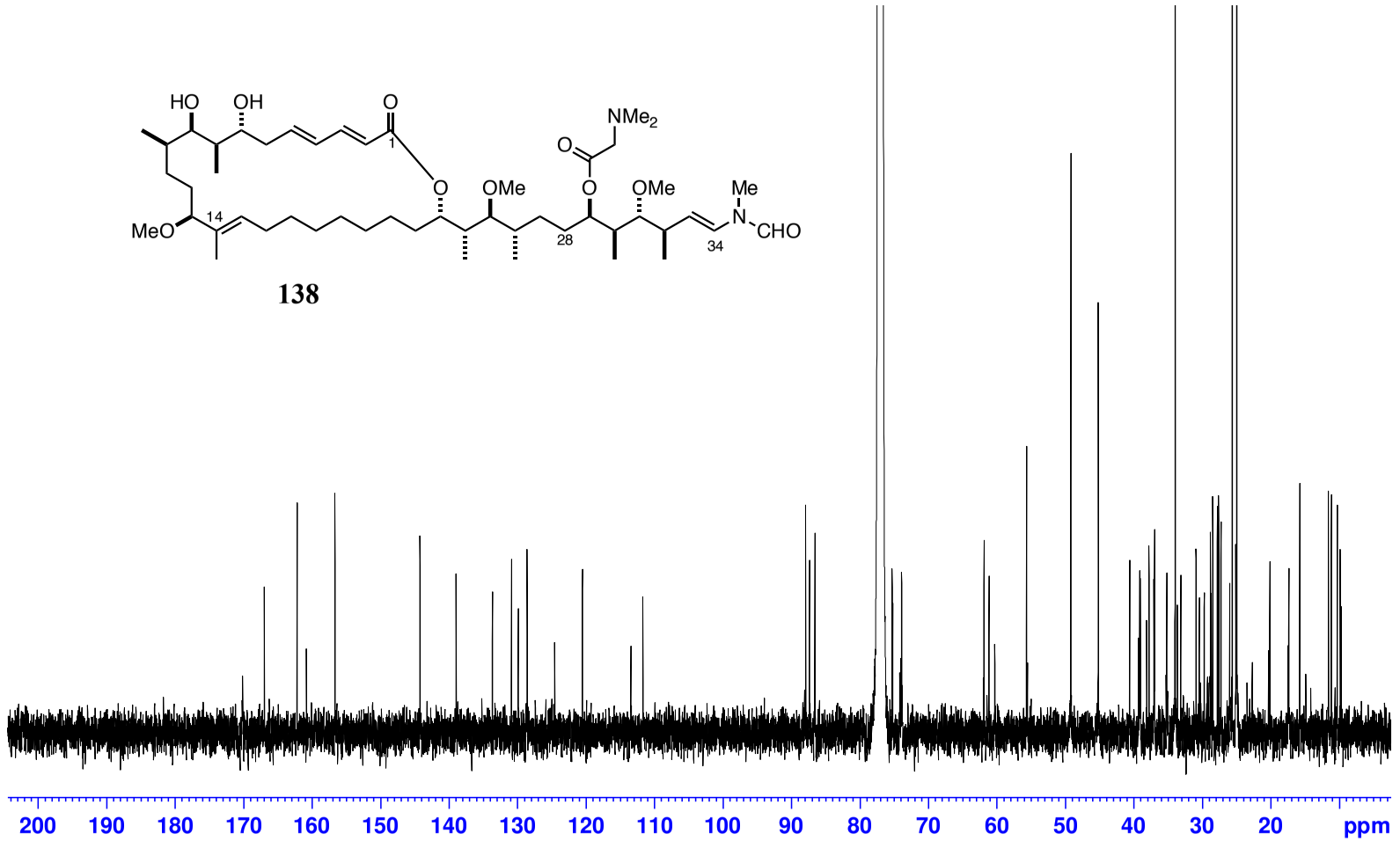
HO
OH
O
1
NMe2
O
O
OMe
O
OMe
Me
N
CHO
MeO
14
28
34
200
190
180
170
160
150
140
130
120
110
100
90
80
70
60
50
40
30
20
ppm

138

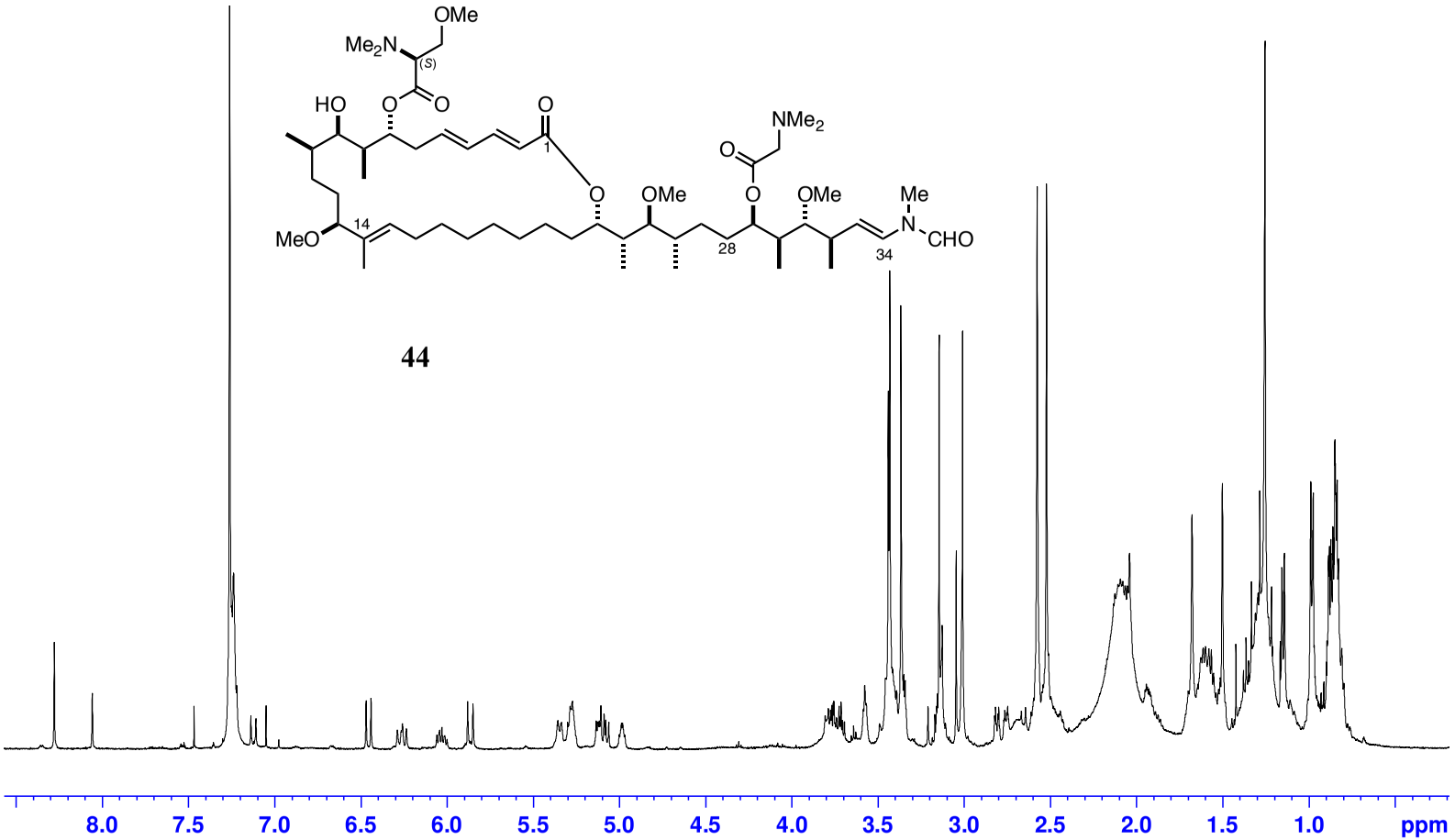
OMe
Me2N
(S)
HO
O
O
O
1
NMe2
O
O
OMe
O
OMe
Me
N
CHO
MeO
14
28
34
8.0
7.5
7.0
6.5
6.0
5.5
5.0
4.5
4.0
3.5
3.0
2.5
2.0
1.5
1.0
ppm

44

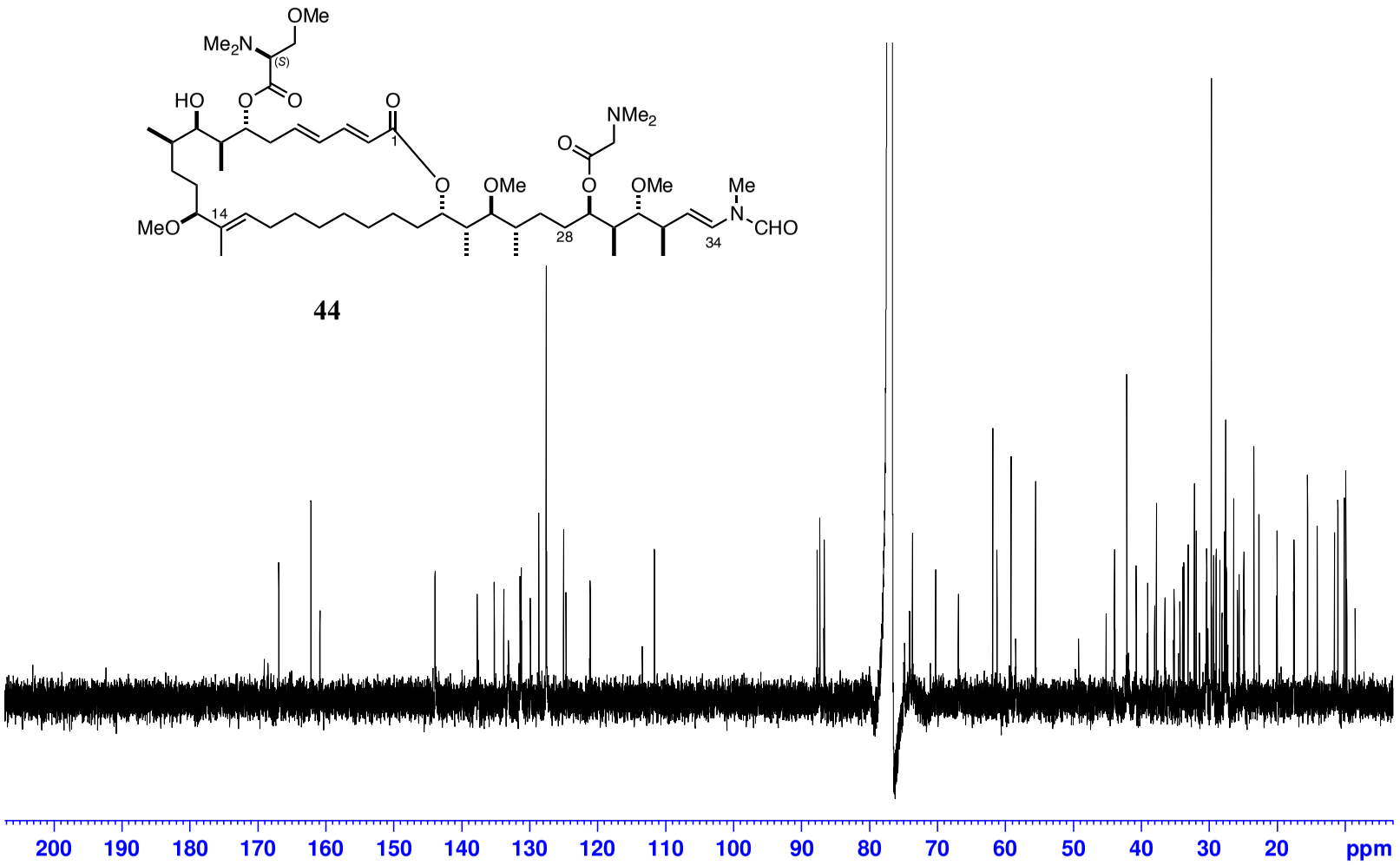
OMe
Me2N
(S)
HO
O
O
O
1
NMe2
O
O
OMe
O
OMe
Me
N
CHO
MeO
14
28
34
200
190
180
170
160
150
140
130
120
110
100
90
80
70
60
50
40
30
20
ppm

44

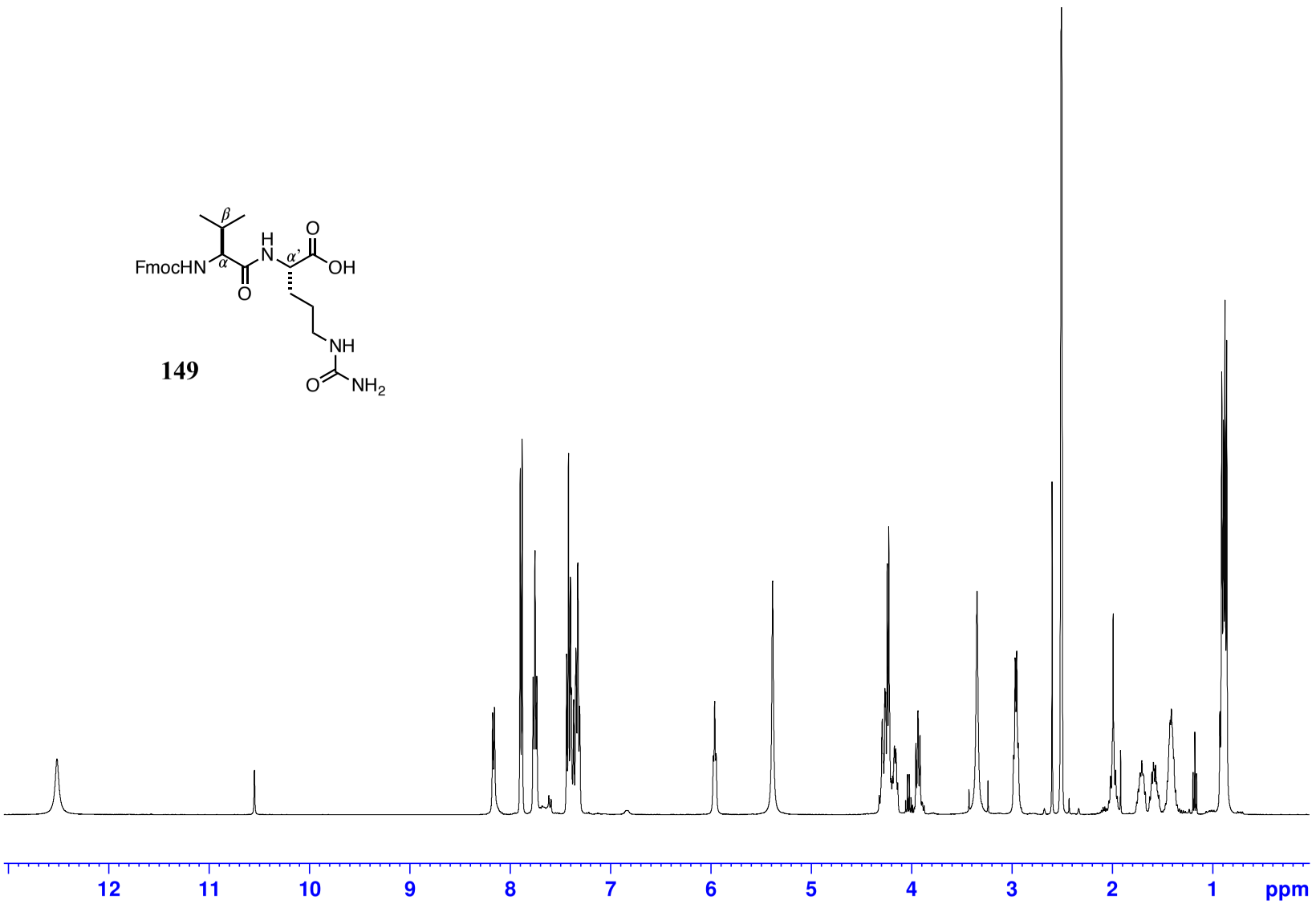

149

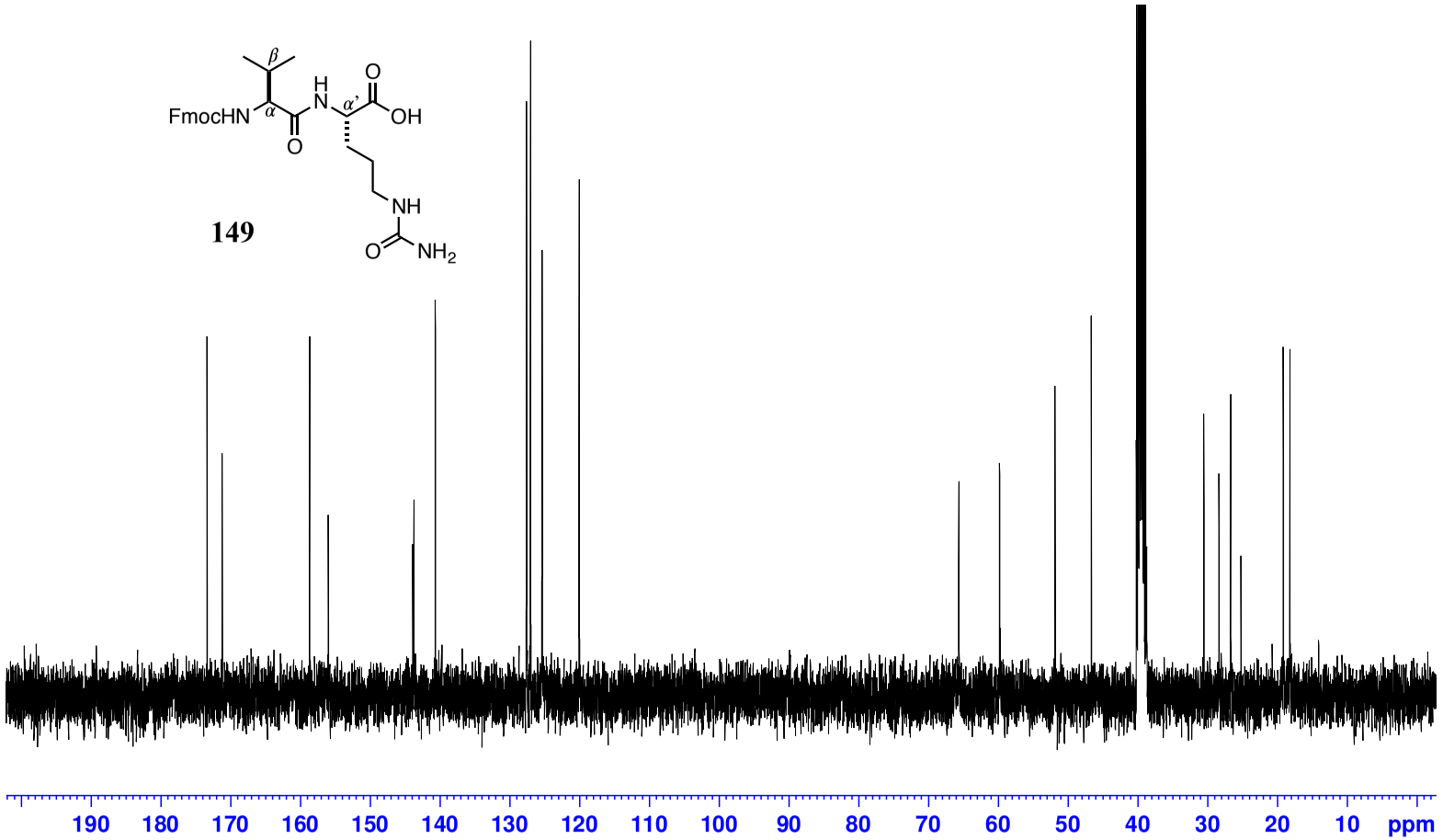
FmocHN
β
α
α'
H
N
O
O
OH
O
NH
O
NH2
149
190
180
170
160
150
140
130
120
110
100
90
80
70
60
50
40
30
20
10
ppm

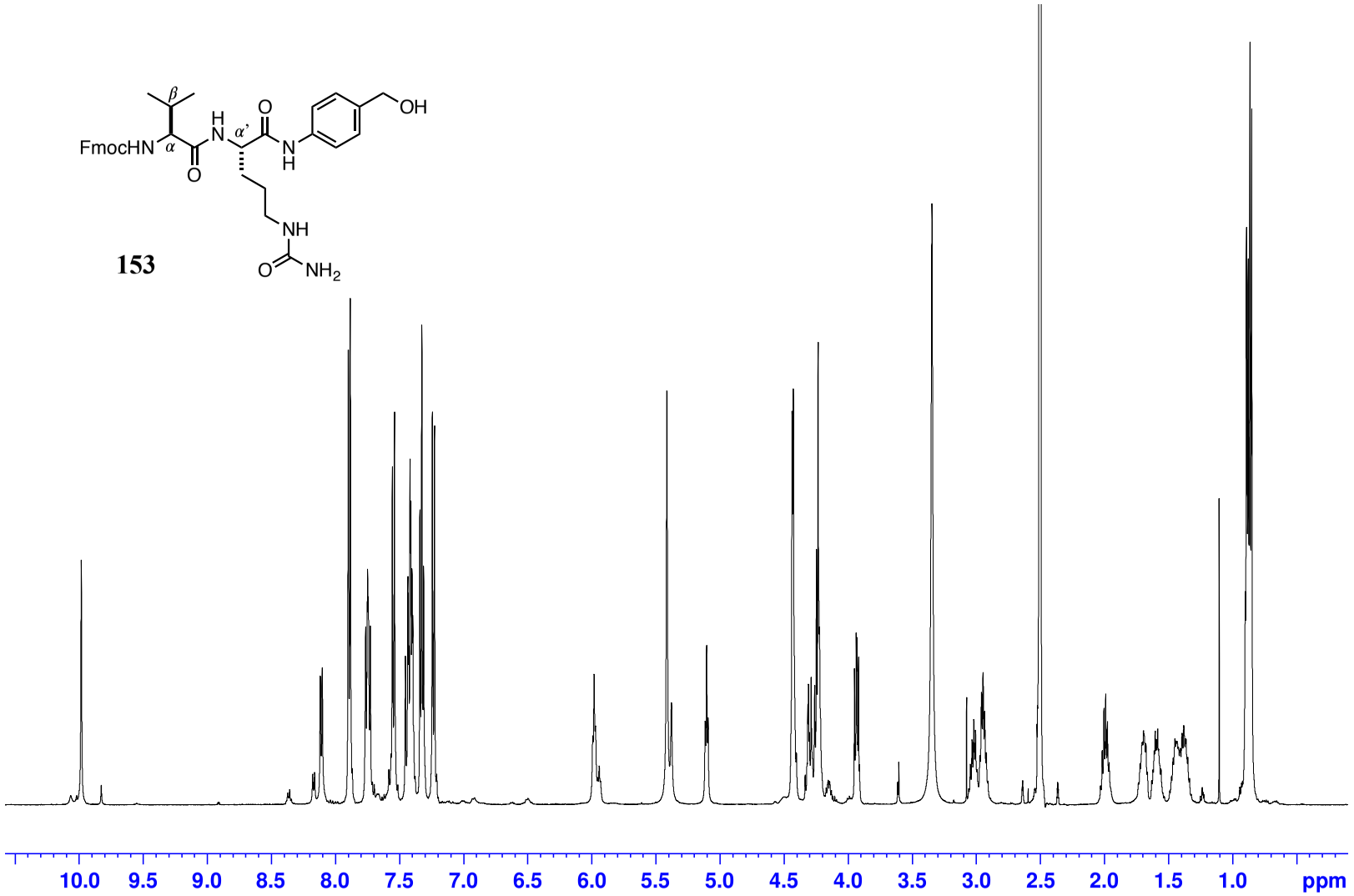
FmocHN
β
α
α'
H
N
O
O
N
H
OH
NH
O
NH2
153
10.0
9.5
9.0
8.5
8.0
7.5
7.0
6.5
6.0
5.5
5.0
4.5
4.0
3.5
3.0
2.5
2.0
1.5
1.0
ppm

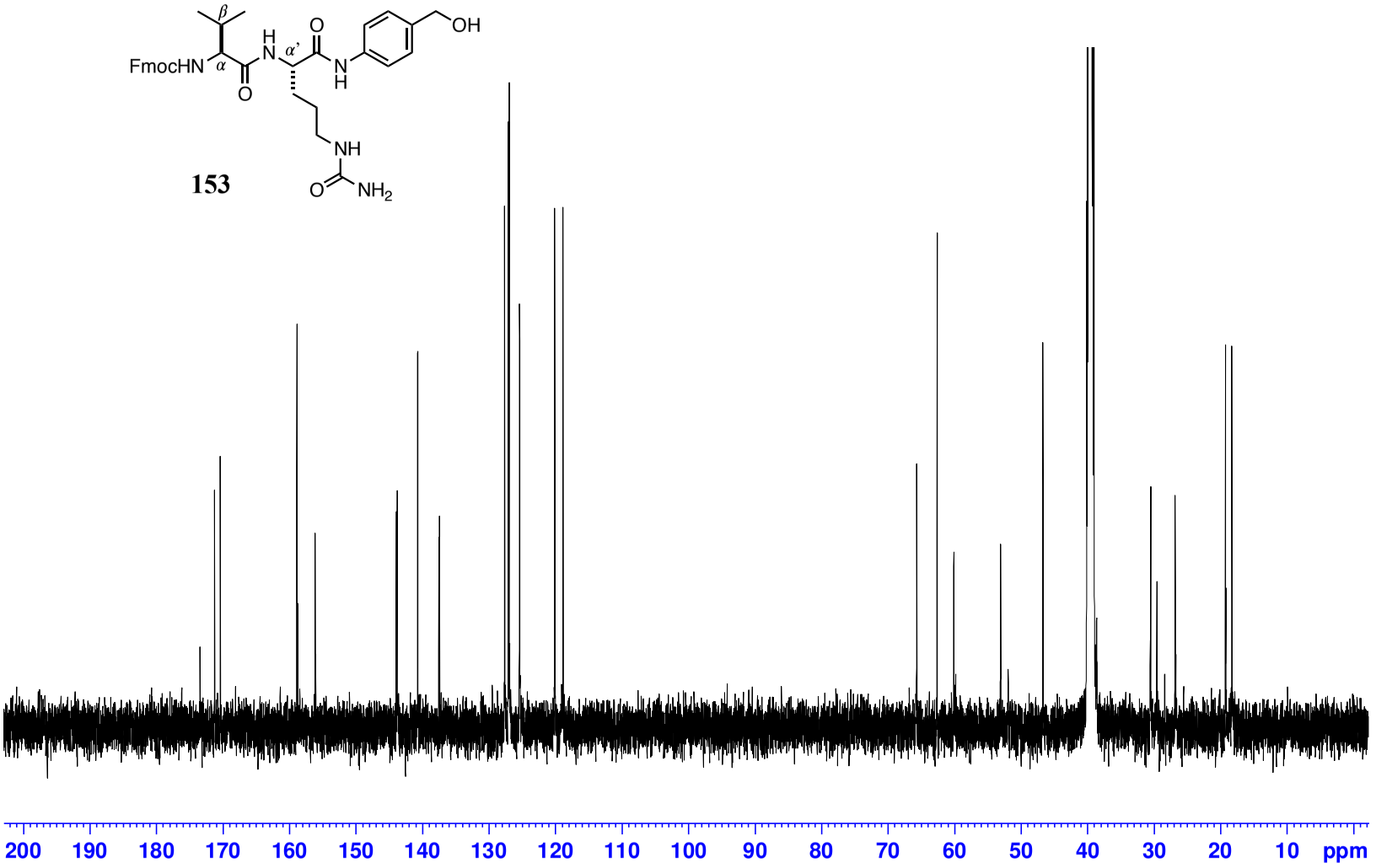
FmocHN
β
α
α'
H
N
O
O
N
H
OH
NH
O
NH2
153
200
190
180
170
160
150
140
130
120
110
100
90
80
70
60
50
40
30
20
10
ppm

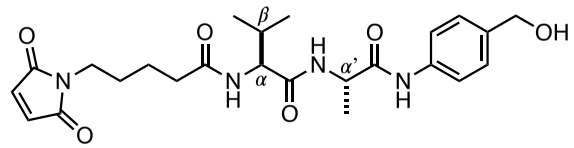

156

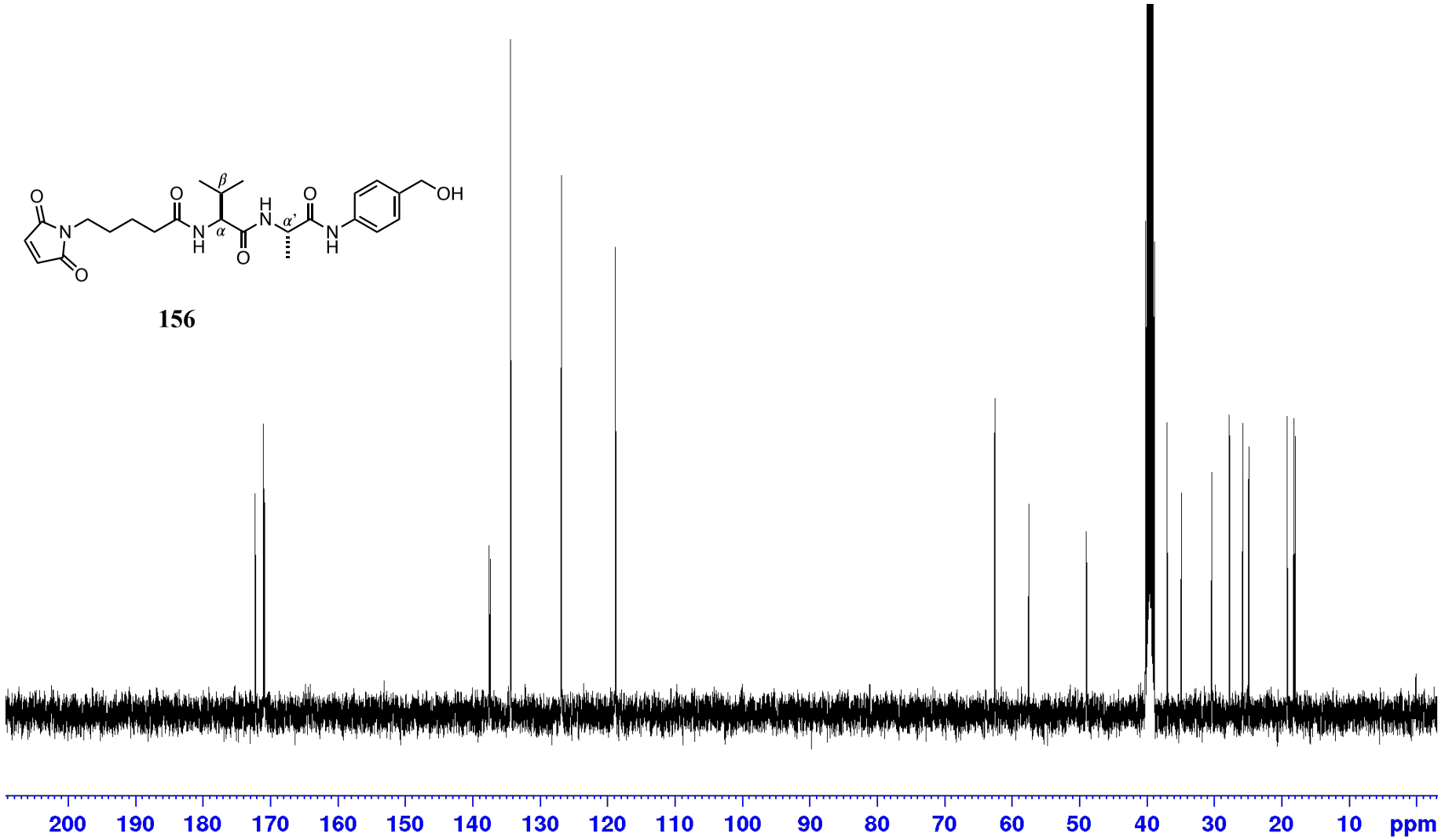
O
N
O
O
O
N
H
α
β
O
N
H
α'
O
N
H
OH
200
190
180
170
160
150
140
130
120
110
100
90
80
70
60
50
40
30
20
10
ppm

156

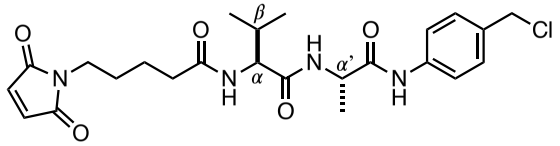
O
N
O
O
O
N
H
α
β
O
N
H
α'
O
N
H
Cl

157

9.5
9.0
8.5
8.0
7.5
7.0
6.5
6.0
5.5
5.0
4.5
4.0
3.5
3.0
2.5
2.0
1.5
1.0
ppm

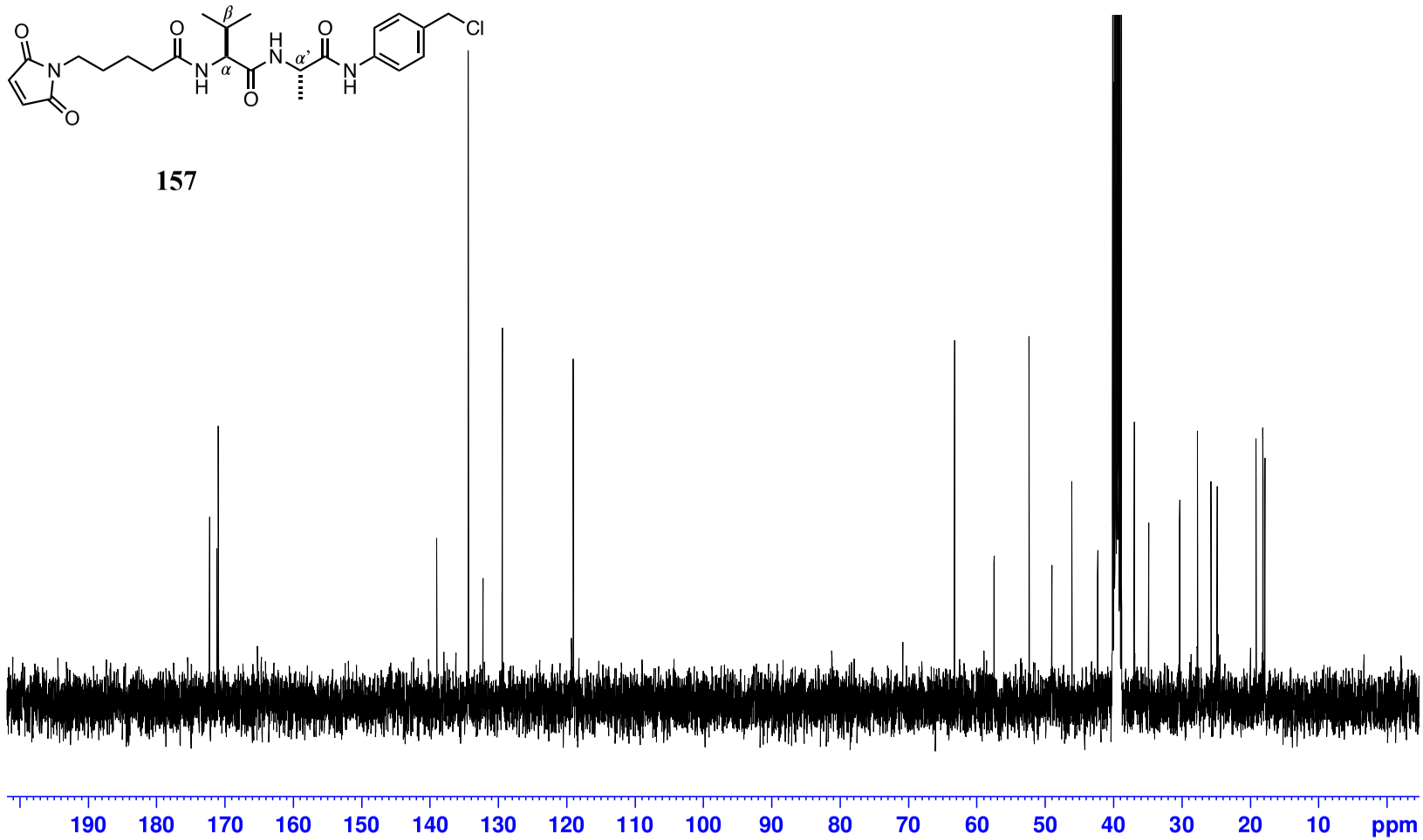
O
N
O
O
O
N
H
α
β
O
H
N
α'
O
N
H
Cl
190
180
170
160
150
140
130
120
110
100
90
80
70
60
50
40
30
20
10
ppm

157